

Continuous Blending of Dry Pharmaceutical Powders

by

Lakshman Pernenkil

B. Tech & M.Tech, Chemical Engineering, IIT Madras, India, 2003

Submitted to the Department of Chemical Engineering
in partial fulfillment of the requirements for the degree of

Doctor of Philosophy in Chemical Engineering Practice

at the

MASSACHUSETTS INSTITUTE OF TECHNOLOGY

May 2008

© Massachusetts Institute of Technology 2008. All rights reserved.

Author
Department of Chemical Engineering
May 8, 2008

Certified by
Charles L. Cooney
Robert T. Haslam (1911) Professor of Chemical Engineering
Thesis Supervisor

Accepted by
William M. Deen
Carbon P. Dubbs Professor
Chairman, Department Committee on Graduate Students

Continuous Blending of Dry Pharmaceutical Powders

by

Lakshman Pernenkil

B. Tech & M.Tech, Chemical Engineering, IIT Madras, India, 2003

Submitted to the Department of Chemical Engineering
on May 8, 2008, in partial fulfillment of the
requirements for the degree of
Doctor of Philosophy in Chemical Engineering Practice

Abstract

Conventional batch blending of pharmaceutical powders coupled with long quality analysis times increases the production cycle time leading to strained cash flows. Also, scale-up issues faced in process development causes delays in transforming a drug in research to a drug under commercial production. Continuous blending is as an attractive alternative design choice to batch process and is examined in this work. This work proposes to examine the feasibility of applying continuous blending in pharmaceutical manufacturing.

Two kinds of blenders, a double helical ribbon blender and a Zigzag[®] blender were chosen as experimental systems representing high shear and moderate shear equipment. This work first focuses on developing a process understanding of continuous blending by examining the flow behavior of powders in experimental blenders using impulse stimulus response experiments and subsequent residence time distribution analysis.

Powder flow behavior was modeled using an residence time distribution models like axial dispersion models. These flow behavior studies were followed by blender performance studies. The dependence of the mixing performance of the continuous blending system on different operational variables like rotation rates of mixing elements and raw material properties like particle size, shape and cohesion were studied.

Mean residence time and time period of fluctuation in the concentration of active ingredient coming at the inlet were the two most important operational variables that affected blender performance. Larger particles and particles with less cohesion were seen to mix well with higher dispersion coefficients in a ribbon blender.

A residence time distribution based process model for continuous blending was investigated and shown to depict the process well within experimental errors in determining the parameters of the residence time distribution model. The predictive capability of the process model was found to dependent on the scale of scrutiny of the powder mixture in the blender. Choosing the correct scale of scrutiny was demonstrated to be of critical importance in determination of blend quality.

Growing pressures on pharmaceutical industry due to patent expirations has forced manufacturers to look beyond the US and EU for potential manufacturing locations

in addition to invest in novel manufacturing methods and technologies. The capstone work in this thesis proposes a framework that managers of pharmaceutical and biologics manufacturing can utilize to identify critical issues in globalization of manufacturing and in making strategic manufacturing location decisions.

Thesis Supervisor: Charles L. Cooney

Title: Robert T. Haslam (1911) Professor of Chemical Engineering

*Dedicated to Amma and Pappa,
the beacons of light in my life . . .*

0.1 Acknowledgments

I would like to thank Professor Cooney whose staunch support, cheerful optimism and constant encouragement has been a catalyst in the successful completion of my thesis work. I believe that the emphasis he placed on asking the right questions and on employing creativity and structured thinking in solving problems has prepared me well for my professional career. I am very grateful to him for the exposure he gave me to the pharmaceutical industry through his teachings, interactions and introductions. The right mix of scientific understanding and pragmatic thinking he has imparted in me has been immensely helpful in the construction of my perspectives and thoughts.

I would like to extend my gratitude to my thesis committee - Professors Jeff Tester and Alan Hatton - for their critical and valuable feedback on my thesis progress from time to time. I thank all my teachers who taught me in the graduate core curriculum in my first year and showed me the importance of diligence, hard work and intelligence. I specially thank my Professors at MIT Sloan for imparting a sense of pragmatism towards my engineering thinking. I would like to specially thank Professor Don Lessard of MIT Sloan School of Management for his inputs, feedback and encouragement towards my capstone paper.

Without the financial support of and constant feedback from the Consortium for the Advancement of Manufacturing of Pharmaceuticals (CAMP), this work would not have been realized. I thank CAMP and it's member companies - Abbott, Bristol-Myers Squibb, GlaxoSmithKline, Johnson and Johnson, Novartis, Roche, Sanofi-Aventis and Wyeth - for extending their support for this work. In particular, I would like to express my gratitude to Dr. Rajeev Garg, Dr. Steve Laurenz, Dr. John Levins, Dr. Keith Hill, Dr. G.K. Raju and Dr. Michael Hoffmann for sharing their views and opinions from time to time on the project. I would also like to thank Dr. Tom Chirkot and Patterson-Kelley & Co. for their help in the pilot plant scale experiments. Andy Gallant of the Central Machine Shop at MIT was very instrumental in designing the lab-scale blender used in this work and I would like to thank him and his team for their support.

I would like to specially thank Dr. Samuel Ngai, my labmate, friend and mentor who constantly encouraged me to push my boundaries and think outside the box. I also would like to thank my labmates Dr. Reuben Domike, Dr. Steven Hu, Daniel Webere, Yu Pu, Matt Abel, Mridula Pore for engaging me in discussions within and outside of research work. I would like to specially thank my UROPs (undergraduate researchers) - Farzad Jalali Yazdi, Jason Whittaker, Sohrab Singh Virk, Louis Perna and Yiqun Bai - for their patient and dedicated hard work in helping me complete many critical parts of my experimental work. Also, I would like to thank Professor Cooney's administrative assistants over the years, Brett, Karen and Rosangela for their support. I also would like to thank all my friends and classmates who have made my graduate student life very memorable.

I want to end with some personal notes of acknowledgment. First, I want to thank my dear brother who has been a source of joy in my life. I want to thank my best friend, beloved fiancée and wife-to-be, for all her love and affection. Finally, no words of gratitude can match what my parents have sacrificed to give me a chance to complete my education and succeed in my endeavors. It is in humble reverence, that I have dedicated this Thesis to them.

Contents

| | | |
|----------|---|-----------|
| 0.1 | Acknowledgments | 7 |
| 1 | Introduction | 25 |
| 1.1 | Secondary Pharmaceutical Manufacturing | 25 |
| 1.2 | Challenges in Batch Manufacturing | 27 |
| 1.3 | Continuous Manufacturing of Pharmaceuticals | 27 |
| 1.3.1 | Definition of Continuous Processing | 28 |
| 1.3.2 | Benefits of Continuous Processing | 28 |
| 1.4 | Powder Blending | 32 |
| 1.5 | Thesis Outline | 33 |
| 2 | Literature Review | 35 |
| 2.1 | Prior Reviews | 36 |
| 2.2 | Theoretical Developments | 37 |
| 2.2.1 | Ideal Continuous Blender | 37 |
| 2.2.2 | Non-Ideal Continuous Blender | 38 |
| 2.3 | Studies on Continuous Powder Blending | 48 |
| 2.3.1 | Powders in Continuous Blending Studies | 48 |
| 2.3.2 | Feeding in Continuous Blending Systems | 49 |
| 2.3.3 | Process Monitoring of Continuous Blending | 54 |
| 2.3.4 | Process Control of Continuous Blending | 58 |
| 2.3.5 | Experimental Studies on Continuous Blending | 58 |
| 2.4 | Research on Continuous and Batch Blending | 71 |
| 2.4.1 | Powder Kinematics and Dynamics | 77 |

| | | |
|----------|--|-----------|
| 2.4.2 | General Monitoring Techniques | 80 |
| 2.5 | Conclusion | 88 |
| 3 | Thesis Objectives | 91 |
| 3.1 | Specific Objectives | 91 |
| 3.1.1 | Investigation of powder flow behavior | 92 |
| 3.1.2 | Understanding macroscopic blending behavior | 92 |
| 3.1.3 | Analyzing economics of continuous blending | 92 |
| 3.1.4 | Framework for Globalization of Manufacturing | 93 |
| 4 | Method of Approach | 95 |
| 4.1 | Choice of Continuous Blender | 95 |
| 4.1.1 | Patterson Kelley ZigZag Blender | 95 |
| 4.1.2 | Double Helical Ribbon Blender | 97 |
| 4.2 | Powder Feeders | 98 |
| 4.3 | Sampling and Analytical Techniques | 99 |
| 4.3.1 | Light Induced Fluorescence, LIF | 99 |
| 4.3.2 | Near Infra-red (NIR) Spectroscopy | 101 |
| 4.3.3 | Ultra-Violet Absorption Spectroscopy | 105 |
| 4.4 | API and Excipients | 106 |
| 4.4.1 | Caffeine | 107 |
| 4.4.2 | Acetaminophen | 109 |
| 4.4.3 | Lactose | 109 |
| 4.4.4 | Microcrystalline cellulose | 110 |
| 4.4.5 | Magnesium Stearate, MgSt | 111 |
| 4.5 | Flow Behavior Experiments | 114 |
| 4.5.1 | Axial Dispersion Model | 114 |
| 4.5.1.1 | Closed-Closed Boundary Condition | 115 |
| 4.5.1.2 | Open-Open Boundary Condition | 115 |
| 4.5.2 | Determination of Residence Time Distribution | 116 |
| 4.5.3 | Summary | 117 |

| | | |
|----------|--|------------|
| 4.6 | Blending Experiments | 117 |
| 4.6.1 | Theoretical Variance Reduction Ratio | 117 |
| 4.6.2 | The Random Mixture Limit | 119 |
| 4.6.3 | Summary | 120 |
| 5 | Patterson Kelley Zigzag Blender | 121 |
| 5.1 | Flow Behavior Experiments | 123 |
| 5.1.1 | Confirmation of Steady State | 123 |
| 5.1.2 | RTD Experiments | 123 |
| 5.1.3 | Analysis of Data | 124 |
| 5.2 | Blending Experiments | 125 |
| 5.2.1 | Two Component Blending | 126 |
| 5.2.1.1 | Varying Rotation Rates | 126 |
| 5.2.1.2 | Varying Throughput | 127 |
| 5.2.2 | Three Component Experiments | 127 |
| 5.2.3 | Analysis of Data | 129 |
| 5.2.3.1 | Two Component Blending - Varying Rotation Rates | 129 |
| 5.2.3.2 | Two Component Blending - Varying Throughput . . | 131 |
| 5.2.3.3 | Three-component Blending | 131 |
| 6 | Zigzag Blender Performance | 135 |
| 6.1 | Results of Flow Behavior Experiments | 135 |
| 6.1.1 | Confirmation of Steady State | 135 |
| 6.1.2 | RTD of API in Zigzag Blender | 136 |
| 6.1.2.1 | Effect of Intensifier Bar Rotation Rate | 136 |
| 6.1.2.2 | Effect of External Shell Rotation Rate | 137 |
| 6.1.2.3 | Effect of Caffeine Content | 138 |
| 6.1.2.4 | Artefacts of the LIF Data Collection Method | 139 |
| 6.2 | Results of Blending Experiments | 140 |
| 6.2.1 | Varying Rotation Rates in Two Component Blending | 140 |
| 6.2.1.1 | Response Surface Analysis of VRR | 141 |

| | | |
|----------|--|------------|
| 6.2.1.2 | Effect of Intensifier Bar Rotation Rate | 143 |
| 6.2.1.3 | Effect of External Shell Rotation Rate | 143 |
| 6.2.1.4 | Effect of Caffeine Content | 144 |
| 6.2.2 | Varying Throughput in Two Component Blending | 144 |
| 6.2.2.1 | PCA of RSD and Operational Variables | 146 |
| 6.2.2.2 | Effect of External Shell Rotation Rate | 148 |
| 6.2.2.3 | Effect of Total Throughput | 149 |
| 6.2.3 | Three Component Blending | 149 |
| 6.2.3.1 | PCA of Spectral RSD with Shell Rotation Rate . . . | 150 |
| 6.2.3.2 | Effect of MgSt on Caffeine RSD | 150 |
| 6.2.3.3 | Effect of MgSt on MgSt RSD | 152 |
| 6.2.3.4 | Effect of MgSt RSD on Caffeine RSD | 153 |
| 6.3 | Summary of Results | 153 |
| 7 | Double Helical Ribbon Blender | 155 |
| 7.1 | Flow Behavior Experiments | 156 |
| 7.1.1 | Fill Weight Experiments | 156 |
| 7.1.2 | RTD Experiments | 158 |
| 7.1.3 | Analysis of Data | 159 |
| 7.1.3.1 | Fill Weight Experiments | 159 |
| 7.1.3.2 | Residence Time Distribution | 160 |
| 7.2 | Blending Experiments | 160 |
| 7.2.1 | Two Component Experiments | 161 |
| 7.2.2 | Three Component Experiments | 163 |
| 7.2.3 | Analysis of Data | 164 |
| 7.2.3.1 | Two Component Blending | 164 |
| 7.2.3.2 | Three Component Blending | 165 |
| 8 | Ribbon Blender Performance | 167 |
| 8.1 | Results on Flow Behavior Experiments | 167 |
| 8.1.1 | Fill Weight Experiments | 167 |

| | | |
|----------|---|------------|
| 8.1.1.1 | Effect of Initial Fill Weight | 168 |
| 8.1.1.2 | Effect of Flow Rate on Fill Weight | 171 |
| 8.1.1.3 | Effect of Shaft Rotation Rate on Fill Weight | 172 |
| 8.1.1.4 | Effect of Angle of Incline on Fill Weight | 172 |
| 8.1.2 | RTD of API in Ribon Blender | 173 |
| 8.1.2.1 | Effect Shaft Rotation Rate on Mean Residence Time | 174 |
| 8.1.2.2 | Effect of Angle of Incline on Mean Residence Time . | 174 |
| 8.1.2.3 | Effect of Flow Rate on Mean Residence Time | 177 |
| 8.1.2.4 | Effect Shaft Rotation Rate on Dispersion Coefficient | 177 |
| 8.1.2.5 | Effect of Flow Rate on Dispersion Coefficient | 178 |
| 8.1.2.6 | Effect of Angle of Incline on Dispersion Coefficient . | 178 |
| 8.2 | Results of Blending Experiments | 180 |
| 8.2.1 | Two Component Experiments | 180 |
| 8.2.1.1 | PCA of VRR | 180 |
| 8.2.1.2 | Effect of Dispersion Coefficient | 180 |
| 8.2.1.3 | Effect of Shaft Rotation Rate | 181 |
| 8.2.1.4 | Effect of Flow Rate | 182 |
| 8.2.1.5 | Effect of Mean Residence Time | 183 |
| 8.2.1.6 | Effect of Disturance Time Period | 184 |
| 8.2.2 | Three Component Blending | 184 |
| 8.2.2.1 | Effect of MgSt on API RSD | 185 |
| 8.2.2.2 | Effect of Residence Time on API RSD and MgSt RSD | 186 |
| 8.3 | Summary of Results | 187 |
| 9 | The Effect of Microscale Properties on Macroscopic Phenomena | 189 |
| 9.1 | Effect of Particle Size | 189 |
| 9.1.1 | Effect of Size on Bodenstein Number | 190 |
| 9.1.2 | Effect of Size on Dispersion Coefficient | 190 |
| 9.1.3 | Effect of Size on Variance Reduction Ratio | 191 |
| 9.2 | Effect of Microscale Properties | 192 |

| | | |
|-----------|--|------------|
| 9.2.1 | Effect of Cohesion and Adhesion Surface Energy | 194 |
| 9.2.2 | Effect of Particle Shape | 196 |
| 9.2.3 | Effect of Lubricant | 196 |
| 9.3 | Theoretical and Experimental Performance | 197 |
| 9.3.1 | Prediction of VRR from Axial Dispersion RTD Model | 198 |
| 9.3.2 | Theoretical prediction of VRR from Experimental RTD | 202 |
| 9.3.3 | Comparing of Theoretical Predictions with Experimental VRR | 202 |
| 9.3.4 | Sources of Error in Theoretical Prediction | 202 |
| 9.4 | Effect of Scale of Scrutiny | 204 |
| 9.4.1 | Theoretical Calculation of Scale of Scrutiny | 205 |
| 9.4.2 | RSD from Moving Averages | 205 |
| 10 | Path for Future Research | 209 |
| 10.1 | Path for Continuous Blending Research | 209 |
| 10.1.1 | Blender Design | 210 |
| 10.1.2 | Material Properties | 211 |
| 10.1.3 | Environmental Variables | 212 |
| 10.1.4 | Analytical Techniques | 212 |
| 10.2 | Transforming Batch to Continuous | 213 |
| 10.2.1 | Crystallization | 214 |
| 10.2.2 | Granulation | 214 |
| 10.2.3 | Drying | 214 |
| 10.2.4 | Milling | 215 |
| 10.3 | Economic Analysis of Continuous Blending | 215 |
| 11 | A Framework for Global Pharmaceutical Manufacturing Strategy | 217 |
| 11.1 | Overview of Manufacturing | 218 |
| 11.1.1 | Differences between Pharmaceuticals and Biologics | 218 |
| 11.1.2 | Pharmaceutical Manufacturing Output | 219 |
| 11.1.3 | Asia and Eastern Europe Manufacturing Output | 222 |
| 11.2 | Prior Literature | 226 |

| | | |
|-----------|---|------------|
| 11.2.1 | Determinants of Manufacturing Location | 226 |
| 11.2.2 | Frameworks for Global Strategy | 227 |
| 11.3 | Objectives and Scope | 232 |
| 11.4 | The Growing Influence of Emerging Economies | 232 |
| 11.4.1 | Factor Cost Advantages | 235 |
| 11.4.2 | Labor Productivity | 238 |
| 11.5 | A Life-cycle Model for Globalization of Manufacturing | 239 |
| 11.5.1 | Model for Pharmaceuticals | 240 |
| 11.5.2 | Model for Biologics | 242 |
| 11.6 | A Framework for Global Manufacturing Strategy | 243 |
| 11.6.1 | Industry Level Framework | 243 |
| 11.6.1.1 | Scale | 243 |
| 11.6.1.2 | Scope | 244 |
| 11.6.1.3 | Risk | 245 |
| 11.6.1.4 | Regulations | 246 |
| 11.6.2 | Geographic Region Level Framework | 247 |
| 11.6.2.1 | Factor Cost Advantages | 247 |
| 11.6.2.2 | Tax Policy and Regulations | 248 |
| 11.6.2.3 | Country risk profile | 251 |
| 11.6.2.4 | Infrastructure | 251 |
| 11.6.2.5 | Knowledge and Skills of Local Population | 252 |
| 11.6.3 | Deriving Implications of the Framework on Biologics Companies | 252 |
| 11.7 | Case Studies on Applying the Framework | 257 |
| 11.7.1 | Location Decision for Amgen | 257 |
| 11.7.2 | Location Decision for Novo Nordisk | 258 |
| 11.8 | Impact and Summary | 259 |
| 11.9 | Acknowledgments | 261 |
| 12 | Conclusion | 263 |
| A | Nomenclature | 267 |

List of Figures

| | | |
|------|---|-----|
| 1-1 | A Schematic of Secondary Pharmaceutical Manufacturing | 26 |
| 1-2 | Challenges in Pharmaceutical Manufacturing | 26 |
| 1-3 | Powder Blending at the Interface | 32 |
| 2-1 | Scale and Intensity of Segregation | 39 |
| 2-2 | Perfect and Random Mixtures | 39 |
| 2-3 | Structurally Different Powder Blends | 40 |
| 4-1 | Picture of Zigzag Blender | 96 |
| 4-2 | Double Helical Ribbon Blender | 97 |
| 4-3 | Logarithmic LIF Calibration Curve | 100 |
| 4-4 | Exponential LIF Calibration Curve | 100 |
| 4-5 | LIF Signal Ratio Calibration Curve | 101 |
| 4-6 | PLS Calibration Plot for Caffeine and Lactose DCL14 Mixture | 103 |
| 4-7 | Three Component PLS Calibration Plot for Caffeine | 104 |
| 4-8 | Three Component PLS Calibration Plot for MgSt | 105 |
| 4-9 | UV Calibration of Caffeine in Water (272 nm) | 106 |
| 4-10 | Mass Volume Curve for Caffeine | 108 |
| 4-11 | ESEM of Avicel MCC PH102 | 111 |
| 4-12 | Effect of Input Fluctuation | 119 |
| 5-1 | Zigzag Blender with LIF Sensors | 121 |
| 5-2 | Schematic of NIR on Zigzag Blender | 122 |
| 5-3 | NIR Setup on the Zigzag Blender | 123 |

| | | |
|------|---|-----|
| 5-4 | RTD of Plug Flow and Ideal Mixer in Series | 125 |
| 5-5 | Three component mixing | 128 |
| 5-6 | LIF Linear Calibration on Zigzag Blender | 129 |
| 5-7 | Spectral RSD from PCA | 132 |
| 6-1 | Mean Residence Times in the Zigzag Blender | 136 |
| 6-2 | Effect of Intensifer Bar Rotation Rate on RTD | 137 |
| 6-3 | Effect of Shell Rotation Rate on RTD | 138 |
| 6-4 | Effect of Caffeine Content on RTD | 138 |
| 6-5 | Experimental and Fitted RTD | 140 |
| 6-6 | VRR in Zigzag Blender from LIF data | 141 |
| 6-7 | VRR in Zigzag Blender from Solution UV Analysis | 143 |
| 6-8 | RSD of Caffeine from LIF - Throughput Experiments | 145 |
| 6-9 | RSD of Caffeine from Solution Analysis for Throughput Experiments | 145 |
| 6-10 | Mean Caffeine Content: from LIF vs from Solution Analysis | 146 |
| 6-11 | RSD of Caffeine: from LIF vs from Solution Analysis | 147 |
| 6-12 | PCA of RPM, Throughput and LIF Caffeine RSD | 147 |
| 6-13 | Loading Plot with Residence Times, Flow Rate and RPM | 148 |
| 6-14 | Loading plot for Caffeine RSD, MgSt Content and Shell Rotation Rate | 151 |
| 6-15 | Loadings plot for MgSt RSD, MgSt Content, Caffeine RSD and Shell Rotation Rate | 151 |
| 7-1 | Schematic of Ribbon Blender Experimental Set-up | 155 |
| 7-2 | Input Fluctuations of API Content to the Ribbon Blender | 162 |
| 8-1 | Time Evolution of Flow Rate in Ribbon Blender | 168 |
| 8-2 | Maximum and Minimum Fill Weight at 10 RPM (Manual Feeding) | 169 |
| 8-3 | Dependence of Fill Weight on Initial Conditions - Manual Feeding | 169 |
| 8-4 | Dependence of Fill Weight on Initial Conditions - Automatic Feeder | 170 |
| 8-5 | Repeatability of Fill Weights | 170 |
| 8-6 | Steady State Fill Weights at Zero Degree Incline | 171 |

| | | |
|------|---|-----|
| 8-7 | Steady State Fill Weights at -5 Degree Incline | 172 |
| 8-8 | Steady State Fill Weights at +5 Degree Incline | 173 |
| 8-9 | Non-linear Regression of Dispersion Model | 174 |
| 8-10 | Mean Residence Times from NIR Data | 175 |
| 8-11 | Mean Residence Time: 0 Degree Incline | 175 |
| 8-12 | Mean Residence Time: -5 Degree Incline | 176 |
| 8-13 | Mean Residence Time: +5 Degree Incline | 177 |
| 8-14 | Dispersion Coefficients at Zero Degree Incline | 178 |
| 8-15 | Dispersion Coefficients at -5 Degree Incline | 179 |
| 8-16 | Dispersion Coefficients at +5 Degree Incline | 179 |
| 8-17 | Loadings Plot of VRR, Mean Residence Time and Dispersion Coefficient | 181 |
| 8-18 | Loadings Plot of VRR and Operational Variables | 182 |
| 8-19 | Variance Reduction Ratio vs Mean Residence Time | 183 |
| 8-20 | VRR vs Residence Time to Fluctuation Time Period Ratio | 184 |
| 8-21 | Effect of MgSt on Caffeine RSD in Ribbon Blender | 185 |
| 8-22 | Effect of MgSt on Acetaminophen RSD in Ribbon Blender | 186 |
| 8-23 | Effect of MgSt on MgSt RSD in Ribbon Blender | 187 |
| | | |
| 9-1 | Effect of Particle Size on Bodenstein Number | 190 |
| 9-2 | Effect of Particle Size on Dispersion Coefficient | 191 |
| 9-3 | Effect of Particle Size on VRR, $T_f=30s$ | 192 |
| 9-4 | Effect of Particle Size on VRR, $T_f=50s$ | 193 |
| 9-5 | Effect of Time Period of Fluctuation on Theoretical VRR, $45 \leq D \leq$ $150 \mu m$ | 193 |
| 9-6 | Effect of Time Period of Fluctuation on Theoretical VRR, $150 \leq D \leq$ $250 \mu m$ | 194 |
| 9-7 | Loadings Plot of Effect of Excipients and APIs | 195 |
| 9-8 | Non-linear Regression of Axial Dispersion Model with NIR Data . . . | 198 |
| 9-9 | Over-prediction of Variance Reduction Ratio | 199 |
| 9-10 | Axial Dispersion RTD with Magnitude Dependent Gaussian Noise . . | 200 |

| | | |
|-------|--|-----|
| 9-11 | Predicted Blender Response Without Noise Addition in the RTD Model | 201 |
| 9-12 | Predicted Blender Response With Noise Added to the Dispersion Model | 201 |
| 9-13 | Theoretical and Experimental Variance Reduction Ratio $T_f = 25s$ | 203 |
| 9-14 | Theoretical and Experimental Variance Reduction Ratio $T_f = 60s$ | 204 |
| 9-15 | RSD from Moving Average Model | 206 |
| 9-16 | Comparison of Offline vs Online VRR | 207 |
| | | |
| 11-1 | Schematic of Pharmaceutical Manufacturing | 219 |
| 11-2 | Schematic of Biologics Manufacturing | 219 |
| 11-3 | Pharmaceutical Output and Value Added for OECD Countries | 221 |
| 11-4 | PPP-Adjusted Output and Value Added for OECD Countries | 221 |
| 11-5 | Pharmaceutical Output for US, EU and Japan | 222 |
| 11-6 | PPP-Adjusted Output for US, EU and Japan | 223 |
| 11-7 | Pharmaceutical Output for Asia | 223 |
| 11-8 | PPP-Adjusted Output for Asia | 224 |
| 11-9 | Pharmaceutical Output for Eastern Europe | 225 |
| 11-10 | PPP-Adjusted Output for Eastern Europe | 225 |
| 11-11 | Ferdows [30] Model for Organizing Manufacturing Plants | 229 |
| 11-12 | Shi and Gregory [92] Model for Organizing Manufacturing Plants | 230 |
| 11-13 | Output and In-Country Market Demand for 2002 | 233 |
| 11-14 | Output and In-Country Market Demand Growth for 2002 | 234 |
| 11-15 | Pharmaceutical Manufacturing Establishments | 235 |
| 11-16 | Employees in Pharmaceutical Manufacturing | 236 |
| 11-17 | Factor Cost Percentages on a PPP basis for Eastern Europe | 237 |
| 11-18 | Factor Cost Percentages on a PPP basis for Asia | 237 |
| 11-19 | PPP-Adjusted Value Added Per Employee as a Percentage of that in the US | 238 |
| 11-20 | Global Expansion Model for Pharmaceutical Manufacturing | 241 |
| 11-21 | Global Expansion Model for Biologics Manufacturing | 241 |

| | |
|--|-----|
| 11-22An Industry-Level Framework for Global Manufacturing Strategy, Ex- tension from [59] | 244 |
| 11-23A Geographic Region Level Framework for Global Manufacturing Strat- egy | 247 |
| 11-24Strategic Implications Based on Proposed Framework | 254 |
| 11-25Application of the Proposed Framework for Amgen Inc. | 259 |
| 11-26Application of the Proposed Framework for Novo Nordisk A/S | 260 |

List of Tables

| | | |
|------|--|-----|
| 2.1 | Theoretical Models from Literature | 43 |
| 2.2 | Powders in Continuous Blending | 51 |
| 2.3 | Feeding in Continuous Blending Work | 55 |
| 2.4 | Continuous Blending Work from Literature | 61 |
| 2.5 | Past reviews on Powder Blending | 72 |
| 2.6 | Monitoring Techniques in Literature | 82 |
| 4.1 | LIF Calibration Parameters | 101 |
| 4.2 | PLS Calibration of NIR Spectra | 103 |
| 4.3 | Properties of APIs and Excipients Used | 113 |
| 6.1 | ANOVA of Response Model | 142 |
| 6.2 | Statistics of Individual Effects on VRR | 142 |
| 7.1 | Excipient Massing for Manual Feeding | 157 |
| 7.2 | API and Lubricant Feeding Profile Masses | 161 |
| 7.3 | API Feeding Time Profiles | 162 |
| 11.1 | Average PPP Conversion Factors, 1997-2002 [2] | 220 |
| 11.2 | Characteristics of Ferdows Factory Model [30] | 231 |
| 11.3 | Tax Savings Calculations | 249 |
| 11.4 | Top Revenue Generating Biologics Companies of 2007 | 255 |

Chapter 1

Introduction

Conventional batch processing compels pharmaceutical manufacturers to carry large inventories and to install huge equipment. This increased capital and operational cost reduces bottom-line returns on the product. With an increased pressure on pharmaceutical production, there is a desire to cut manufacturing costs. Continuous processes are known to operate with minimal capital and operating cost. The PAT guidance issued by the FDA clearly states the development of continuous processing as an avenue for improving efficiency and managing variability.

1.1 Secondary Pharmaceutical Manufacturing

Secondary Pharmaceutical Manufacturing refers to all the processing steps after the active pharmaceutical ingredient (or API), that delivers the requisite therapeutic effect on the human body, has been chemically synthesized. Most often, the API is crystallized into a dry powder that is then sent to the secondary manufacturing facility, where it is formulated with other ingredients, broadly called excipients, and manufactured in a form that is consumed by the end user, the patient.

Oral solid dosage forms, like tablets and capsules are the most popular forms of delivery of a pharmaceutical product because of a number of advantages. Solid dosage forms are easy to pack, store, transport, deliver, and consume. Moreover, the integrity of the dose (quality and quantity) can be preserved in its intended form, if

the formulation (or mixing API with excipients and synthesizing the product) is done properly. The stability of the API can be enhanced as the API can be prevented from coming in contact with the atmosphere by the presence of excipients. The availability and delivery of the API can also be enhanced if the excipients dissolve and/or disintegrate in the human body very quickly and efficiently. Clearly, solid dosage forms are the most popular choice for delivering pharmaceutical products.



Figure 1-1: A Schematic of Secondary Pharmaceutical Manufacturing

Secondary pharmaceutical manufacturing involves many steps in the process. These steps generally include, crystallization, drying, milling, blending, compaction, coating and packaging and are schematically represented in figure 1-1. Pharmaceutical products are manufactured in batches or lots that can vary in size from 100 kg for special pharmaceutical products with very small market size to 10 tons for blockbuster drugs. Batch processing is a good process choice if the size of the batch is below a certain critical value. Over this critical size of the batch, the cost of batch manufacturing tends to be higher and efficiency tends to be lower than the alternative choice of continuous manufacturing. There are many other challenges that batch manufacturing faces and is the described below and depicted in figure 1-2.

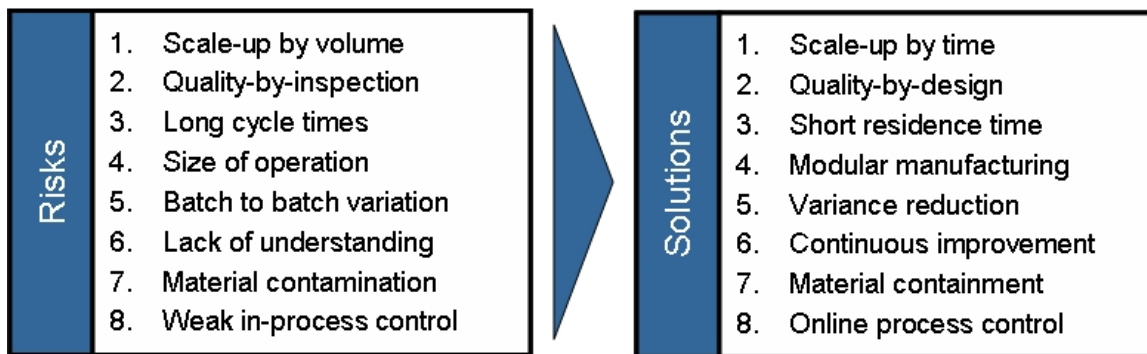


Figure 1-2: Challenges in Pharmaceutical Manufacturing

1.2 Challenges in Batch Manufacturing

There are a number of challenges that batch manufacturing faces. Batch processes involve scale-up by volume and mass at some point of time in the process development. Usually, batch processes are synthesized in the lab scale and then tested at the pilot plant scale and transferred to the plant scale. The chemical engineering thumb rule of $10\times$ scale-up at each stage holds only to a certain extent in the pharmaceutical industry, where, sometimes, due to issues in scale-up, the pilot-plant scale volumes are maintained in production scale.

Since pharmaceutical products are stringently regulated and mandated to adhere to strict quality levels, the pharmaceutical industry ensures quality by testing the product at various stages of the manufacture. As a result of this *quality-by-inspection* paradigm, a lot of work-in-progress material is held in the manufacturing site, since product cannot proceed without passing the quality inspections conducted by the quality control laboratory.

Such delays in quality assurance increases the cycle times of pharmaceutical products and the cost of manufacturing these products. The inefficiencies in manufacturing are not only limited to the operations, but also to understanding of the phenomena in the manufacturing process. Lack of in-depth understanding of process behavior and lack of in-process controls leads to batch to batch variations that are tightly regulated by the FDA. Also, batch manufacturing poses a considerable risk of material contamination since processes are not closed systems.

1.3 Continuous Manufacturing of Pharmaceuticals

The aforementioned and many more challenges that the pharmaceutical industry was facing at the turn of the millenium prompted the FDA to issue an advisory guideline on changing the course of pharmaceutical manufacturing[33]. In this guideline, the FDA recommended that pharmaceutical industry identify newer technologies and methodologies of manufacture of drugs and specifically refered to continuous manu-

facturing as a process choice for the pharmaceutical industry.

1.3.1 Definition of Continuous Processing

Continuous processing is defined as:

Processing of raw materials without interruption and with continuity of production over a sustained period of time.¹

This translates to balancing the throughput of all the unit operations in a processing line in order to maximize total capacity, capital utilization and the yield and quality of the product while minimizing cycle time and inventory.

1.3.2 Benefits of Continuous Processing

Continuous processing offers many benefits over conventional batch processing. The collective thoughts and opinions from literature and CAMP proceedings² have been listed below. Wherever possible, metrics to assess the level and quality of these benefits have been listed alongwith the corresponding benefits.

1. *Minimization of uncertainty in scale-up*: Scale-up is easily carried out in a continuous processing by one of the two methods.
 - Extension of operation: By extending the duration of operation, the volume of the product can be scaled up without actual scale up of equipment.
 - Parallel units: Parallel continuous processing units can be employed to meet increased demands of the product, again avoiding issues in scale-up.

These two options for scale-up potentially decreases the time for translating the process from phase II clinical trial production to commercial-scale production.

Metric - RSD. The relative standard deviation is a measure of the uniformity of the mixture. If it remains unchanged on scale-up, then it represents reduction in scale-up uncertainty.

¹CAMP workshop on Continuous Manufacturing, April 2004

²ibid.

2. *Reduced space and capital requirements:* Continuous processing units can be used to produce large volumes with small size equipment. Hence, the requirements on space and capital are reduced. Also, this arrangement is suitable to introduce modular manufacturing which offers significant reduction in costs apart from standardising the process resulting in better management of variability.

Metric: Size. The size of the process equipment and auxiliaries are directly proportional to the space and capital requirements.

3. *Support of operation with minimum residence time:* Continuous processing operation works with minimal material hold-up hence reducing the cost of work-in-process.

Metric: Mean residence time. The processing time for unit amount of material in each unit operation can all be added to to measure the reduction in time of operation.

4. *Extension of operation from 8/1 to 24/7:* Continuous processing makes it easy to run the process over longer durations enabling increased throughput while avoiding scale-up problems as discussed above.

5. *Opportunity for improved control:* Unlike a batch process, where process variables are controlled to follow a pre-determined time-evolution profile, a continuous process is fairly simple to control as the process is at steady state most of the time.

Metric: Fraction of Rework or Recalled Product. The fraction of product reworked or recalled can be reduced by effective control system and hence can represent the efficacy of the control systems in use.

6. *Opportunity for improvement through PAT:* PAT offers numerous opportunities for implementation in continuous processes to enable continued process improvement *via* improved process understanding. In addition, continuous processes supplemented with relevant PAT can aim to achieve real-time release of

drug products and decrease the possibility of human error faster than batch processes.

7. *Lean manufacturing*: As discussed before, continuous processes can be used to produce large volume products by increasing the duration of production. This results in a process with reduced capital investment as the process equipment are small in size while improving asset utilization. This increases the capital productivity and process efficiency.

Metric: Capital productivity. Capital productivity defined as value of product processed per \$ of annualized capital cost on the process can be used to indicate an increase in asset utilization.

8. *Reduction in cycle time and work-in-process*: This is closely related to the idea of lean manufacturing. As continuous process works with smaller quantities of materials than a batch process and this reduction in material held in work-in-process coupled with quicker turnover of product reduces cycle times and can potentially increase the profitability of the manufacturing unit.

Metric: Cycle Time. Production cycle time per unit weight of the product can be used as a metric for evaluating the benefit of reduced operating cycle time.

9. *Enhanced materials containment*: Continuous processes have the ability to operate as a closed system with relatively less number of material input and output points. This assists in containing potent active pharmaceuticals and minimizing risks involved in employee exposure. Additionally, in a multi-product facility, the potential for product mixing is minimized.

10. *Synergy with existing unit operations*: Some processes currently employed in the pharmaceutical manufacturing are already continuous or semi-continuous. Introducing continuous processes adjacent to already continuous processes creates a synergetic effect on process efficiency.

11. *Quality benefits from consistent operations*: The variability in the outcome of a process can arise both from raw material and process variations. Controlling a

continuous process in order to reduce temporal variability results in consistent operation of the process at all times. This consistency is in consonance with the FDA's policy of encouraging pharmaceutical manufacturers to build quality into a product by design rather than by testing into it

Metric: Variance Reduction Ratio. As discussed later, the variance reduction ratio is a measure of the performance of mixing operations and can be used to measure the benefits accrued from consistency of operations over time.

12. *Potential for improved yield:* Understanding start-up and shut-down dynamics of a continuous process offers novel avenues for process improvement. This level of process understanding not only improves product yield but also helps minimize loss of valuable process time as downtime.

Metric: Product Yield. This metric defined as the amount of product produced per unit amount of raw material in percentage can be used to assess benefits from reducing downtime.

13. *Small volume of operations:* As the material involved is far less than conventional processes, the risk involved is proportionally less. Also the cost of developing a process with small processing volumes is far less than developing a process with large processing volumes.

Metric: Batch to Continuous Operation Equipment Size. This ratio reflects the reduction in volume by switching to continuous processes and hence can be used in evaluating risk involved in the process.

These benefits coupled with increasing interest in regulatory agencies in process improvement offer a very strong case and provide a sufficiently strong driving force for pharmaceutical companies to transform traditional batch processing units to continuous processing operations.

1.4 Powder Blending

Blending of powders is a crucial unit operation in many industries like the manufacture of chemicals, construction materials, plastics and drugs. Batch blending has been in use in a large number of processes especially when small volumes of materials are processed; as a consequence there is a vast experience in handling powders in batches. However, some high volume materials are often blended continuously. Instead of debating which method of processing is better, one can view these two methods as complementary process design choices that need to be made based on the economics of the process aligned with appropriate quality specifications.

In pharmaceutical secondary manufacturing, schematically depicted in figure 1-3, we see that blending forms a crucial interface between traditionally batch processes like crystallization, drying, milling and granulation and quasi-continuous processes like compaction, coating and packaging. The latter steps are quasi-continuous because they are currently being operated in batch mode, even though they can be operated in continuous mode.



Figure 1-3: Powder Blending at the Interface

If we examine the sources of variance in the product quality during the production in the secondary pharmaceutical manufacturing process, we find that the last step where variance can be introduced, mitigated or managed is the blending step. Beyond this blending step, the product is locked in the final solid dosage form and can seldom be reworked. Therefore, powder blending forms the crucial interface where an exigent need exists for implementing continuous dry powder blending in order to realize an efficient, cost-effective, continuous pharmaceutical manufacturing process that conforms to the *quality-by-design* paradigm.

1.5 Thesis Outline

This thesis begins with an extensive literature review of the published research work on continuous dry powder blending in chapter 2. The literature review focuses on the reported research and results on continuous blending achieved thus far, followed by an analysis of areas where continuous blending phenomena can borrow ideas from work on dry powder batch blending. Before presenting the conclusions on literature review, this chapter also takes a peek at the various non-invasive analytical techniques that were used to examine the quality of a powder mixture.

In chapter 3, The thesis goal is then discussed along with a proposed specific objectives and path of research. In chapter 4, the choices of the powder blending systems, choices of powders, choices of process analytical techniques and the two types of experiments that were performed on all the blenders and powders using the analytical techniques are described in detail. The theories behind evaluating these RTD and blending experiments are also described.

The experimental work on the Patterson-Kelley Zigzag[®] blender and the analysis of the data collected are then described in chapter 5. The results of these experiments are described in chapter 6, where first the results from RTD experiments are described and followed by the results from blending experiments. The effect of operational variables on the blender performance is then described along with the effect of lubricant on blending performance.

The experimental work on double helical ribbon blender and the analysis of the data collected was described in chapter 7. Residence time distribution experiments were performed with different combinations of excipients and APIs. The flow behavior of powder in the ribbon blender is also described with the effect of fill weight on the different operational parameters, fill weight, angle of incline and shaft rotation rate. The effect of variance reduction ratio on the operational parameters and mainly mean residence time is described and time period of disturbance is described in chapter 8.

The connection between microscopic properties and macroscopic phenomena in continuous blending is described in chapter 9. The effect of particle size, cohesion

and shape are discussed. The effect of scale of scrutiny and the predictive capability of blending models from residence time distributions are also discussed.

Finally, the path for future research in this growing area of pharmaceutical continuous processing is described in chapter 10, while chapter 11 focuses on developing and applying a strategic framework for pharmaceutical manufacturing strategies before the concluding the thesis in chapter 12.

Chapter 2

Literature Review

The research on powder blending focused on developing a fundamental perspective and aid predictive modeling of these processes and devices. Within this framework, batch blending of powders received considerable attention compared to continuous blending. This review reflects on the principles and knowledge accumulated over the past half-century in the area of continuous powder blending.

Much of the initial research on continuous blending of powders focused on extending the principles of continuous liquid blending and teasing out the design principles based on response-stimulus experiments. Though powder behavior was poorly understood from a fundamental standpoint, it might be expected that a number of the principles behind powder blending in batch systems would play an important role in continuous systems. For example, the mechanisms of convective mixing, diffusive mixing and shear mixing would be present in continuous blending systems as well. For example, convective mechanism or blending of powders due to bulk movement of powder is a dominant mechanism in V and Y blenders. Diffusive mechanism of mixing refers to the random movement of powders across slip planes or failure zones and on the free exposed surface of the powder is a dominant mechanism in drum and agitated blenders. Shear mechanism, which is predominant in pin mill and other milling devices, results in mixing of powders from the agglomeration and de-agglomeration of powders.

A batch blending system that can be run in continuous mode can be expected

to possess similar mixing mechanisms. This is because in such continuous blending systems, a net axial flow is superimposed on the existing batch system to yield a continuous flow. We can, therefore, extend the studies on powder movement in batch blenders and use this knowledge carefully in designing experimental studies on continuous blending. Therefore, this review also examines the fundamental mixing mechanism studies and their conclusions for batch blending systems with the idea of finding areas of application of these concepts in continuous blending.

2.1 Prior Reviews

A previous review, by Williams [105], on continuous mixing of solids presented the current thinking on the topic. A number of developments have occurred since then and this review examines these developments as well. Also, this review differs from previous reviews in that it emphasizes on applying principles of batch blending to continuous blending. This review is organized into three parts. The first part details the theoretical work that set the stage in understanding and characterizing continuous blending. This theoretical background is of immense use in establishing design and performance limits on continuous blenders as well as to develop process models for continuous blending.

The main focus of the published literature was to study continuous blending in a classical black box type analysis without giving much importance to the interactions of the material in the blender. The second part illustrates the experimental studies that were performed to understand continuous blending systems and to examine the theory proposed. This part tries to extract some conclusions on a number of studies on continuous blending. The third part examines the research on batch blending and mixing mechanisms with the aim of identifying areas of possible complementary exchange and use of ideas between batch and continuous blending. Our goal in this chapter is to bring together the knowledge from over 50 publications and establish a platform on which the attributes of continuous blending can be understood across a wide range of applications.

2.2 Theoretical Developments

The earliest work on continuous blending addressed the assessment of the performance of a continuous blender. Beaudry defined blender efficiency for continuous and semi-continuous blenders based on the variance reduction ratio [5]. The variance reduction ratio (VRR) is the ratio of the variance of the input stream to that of the output stream of the blender and provides a key performance metric in continuous flow systems. The variance of a stream is a measure of the spread of the composition of the component of interest in that stream. Hence, the variance reflects the intensity of segregation of the mixture in that stream and the VRR reflects the performance of the blender in reducing this intensity of segregation. Clearly, we can see that a higher VRR corresponds to better performance of the blender.

In the pharmaceutical industry, the acceptance of a good blend is usually based on the relative standard deviation (RSD) of the concentration of the component of interest in the blend, usually the active pharmaceutical ingredient (or API). A higher variance reduction ratio in a blender gives a powder with lower variance at the output and hence a blend with lower relative standard deviation. This connection between the variance reduction ratio and the size of the blender will be discussed in detail later.

2.2.1 Ideal Continuous Blender

The idea of ideal mixing as developed by Danckwerts [21, 22] was extended to free-flowing non-segregating powders [106, 107]. It was shown that batch to batch variations can be reduced by feeding the batches semi-continuously to the blender [36]. The VRR in continuous blenders as derived by Danckwerts was derived as a limiting case of the semi-continuous blender VRR where an infinitesimal amount of material is simultaneously fed into and removed from the blender.

Based on the idea of the distribution of residence times in a blender, a model was developed assuming that the objective of a blending process was to reduce the output variance of the constituent component in the streams fed into the blender.

This variance reduction ratio defined by equation (2.1), was related to the feed characteristics [22, 105, 106] by assuming an ideal blender with exponential decaying or Poisson distribution of residence times. The feed was assumed to fluctuate with a finite correlation between two different times and the correlation was assumed to decay in a geometric progression as given by equation (2.2) with increasing time of scrutiny.

$$VRR = \frac{\sigma_i^2}{\sigma_o^2} = 1 - \tau \cdot \log a \quad (2.1)$$

$$R(r) = \frac{cov(x_t, x_{t+r})}{var(x_t)} = a^r \quad (2.2)$$

where $\|a\| < 1$ is the serial correlation coefficient, σ_i is the standard deviation of the concentration of a component of interest in the mixture, σ_o is the mean residence time of the blender and subscript i is for input, o for output, t for time, r is the window of observation. In order to describe the non-idealities in the blending process, the residence time distribution (RTD) was modeled using delay and dead volume [107, 109], tanks in series [109] or dispersion models [1, 91, 96].

2.2.2 Non-Ideal Continuous Blender

Segregation of constituents in blending plays a very important role in powder blending. In order to characterize the homogeneity and structure of the blend at the output, it is important to understand and assess the performance of the blender based on the intensity and scale of segregation. While intensity of segregation is a measure of the spread of the concentration of the component of interest in the mixture, the scale of segregation reflects the correlation of the composition of that component in that mixture (as a function of time for continuous systems and as a function of space for batch systems).

Scale and intensity of segregation, therefore, describe the amount of unmixed material within the mixture. A good mixture will have a small scale of segregation and a low intensity of segregation (c.f. figure 2-1). The role of a mixer is to reduce

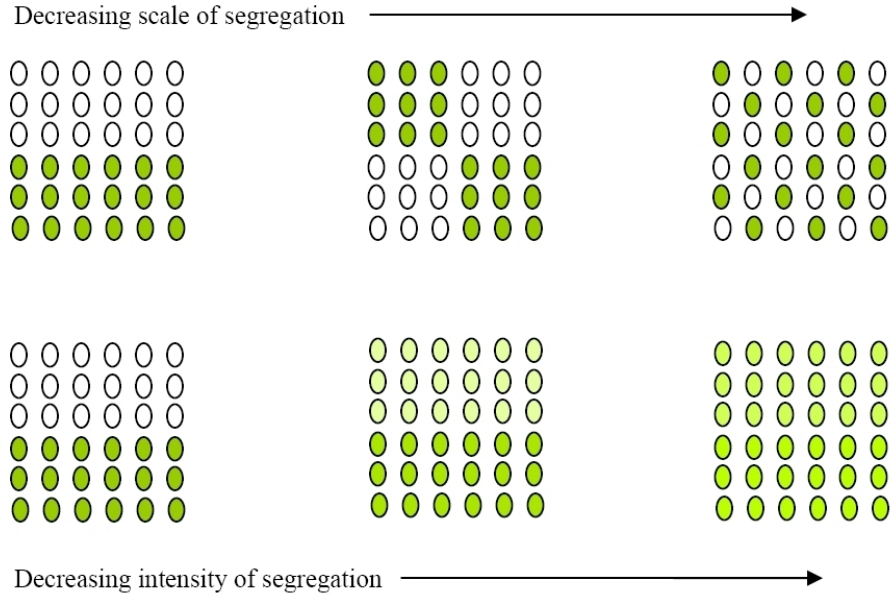


Figure 2-1: Scale and Intensity of Segregation

the scale of segregation and to lower the intensity of segregation. As the scale of examination of the powder depicted in figure 2-1 varies, the observed variance changes accordingly. This scale of examination, called scale of scrutiny [61, 62, 63, 72, 85, 88], is an important experimental variable. Usually, the scale of scrutiny is determined by the aim of the blending process. In pharmaceutical manufacturing, the scale of scrutiny is usually chosen to be $3\times$ the equivalent mass of the tablet or capsule.

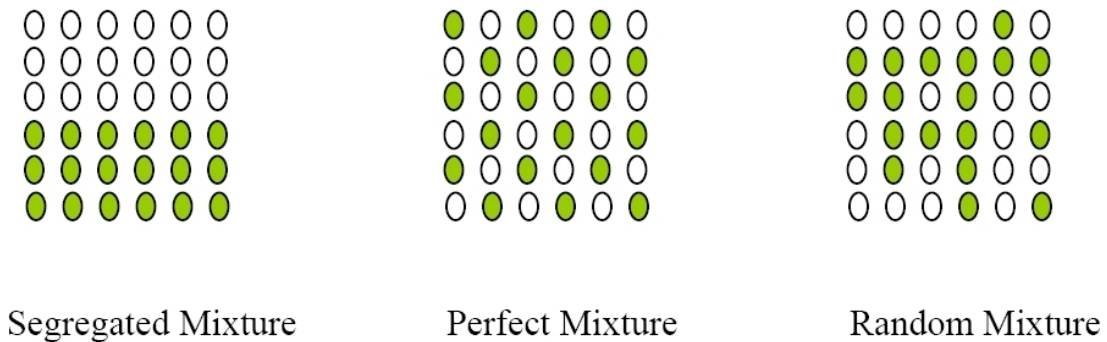


Figure 2-2: Perfect and Random Mixtures

The best mixture that can be achieved by any physically realizable blender is the random mixture shown in figure 2-2. Ghaderi [34] proved that the VRR in a continuous blender was limited by that of a random mixture, first proposed by Weinekötter

and Reh [104], by variographic analysis. Therefore, an ideal blender cannot reduce the variance below this limit. Also, it is clear that the structure of the two blends in figure 2-3 is markedly different though the variances of both are the same. Clearly, the second mixture has a different correlation or scale of segregation. Therefore, time series analysis of the variances or variographic characterization and frequency domain analysis of composition or power density spectrum analysis were used to determine the intensity and scale of segregation during the blending process [34, 104].

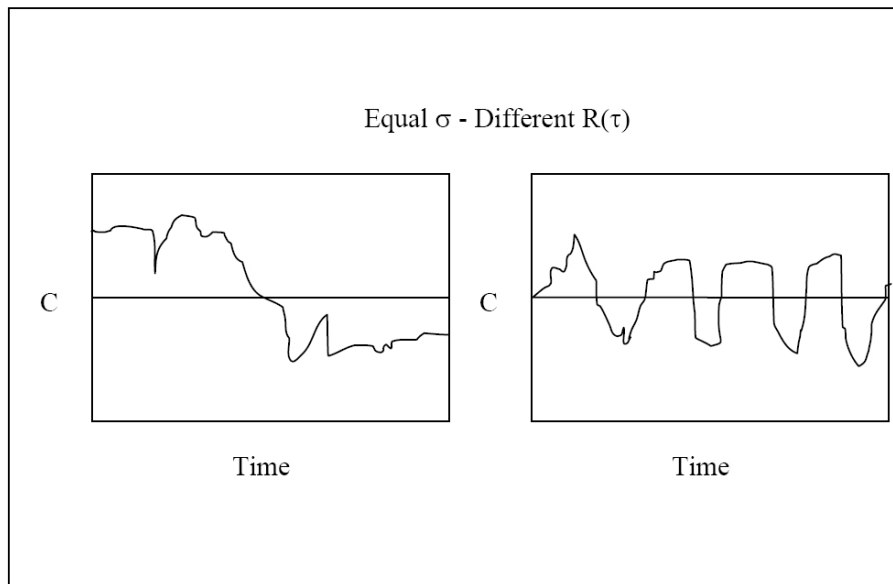


Figure 2-3: Structurally Different Powder Blends

The general relation between the VRR and a general RTD, $E(t)$, is given by equation (2.3)

$$\frac{1}{VRR} = 2 \int_{t=0}^{\infty} \int_{\tau=0}^{\infty} E(t) E(t + \tau) R(\tau) d\tau dt \quad (2.3)$$

Also according to Danckwerts [22], the scale of segregation, I_o is defined by equation (2.4).

$$I_o = \int_{\tau=0}^{\infty} R(\tau) d\tau \quad (2.4)$$

Weinektter and Reh [104] showed that the Fourier transform of the autocorrelation

function as in equation (2.5) could be employed to determine the scale and intensity of segregation.

$$G_f(f) = 4 \int_{\tau=0}^{\infty} R(\tau) \cos(2\pi f\tau) d\tau \quad (2.5)$$

In the frequency domain, the area under the one-sided power density spectrum equation (2.6), gave the intensity of segregation while the value at zero frequency gave the scale of segregation given by equation (2.7).

$$\sigma^2 = \int_0^{\infty} G_f df \quad (2.6)$$

$$I_0 = \frac{G_f(f=0)}{4\sigma^2} \quad (2.7)$$

This analysis was applied to understand the effect of the feeder fluctuations on segregation. Two important conclusions that evolved from these developments are: first, an ideal blender is constrained to reduce the variance to that of a random mixture under ideal feeding conditions. For non-segregating, equal sized particles, a random mixture is the mixture with the smallest attainable variance from any physically realizable blending process [28]. As a result, an ideal powder blender cannot reduce the variance beyond the random mixture limit for free-flowing non-segregating powders. Second, an ideal blender is constrained in its performance to smooth only high frequency fluctuations from the feeder. This means that an ideal powder blender behaves as a low pass filter with the mean residence time as the time constant or the inverse of the mean residence time as the cut-off frequency. Hence, an ideal blender's performance is a function of the feeder consistency.

Fokker-Planck equations (c.f. equation (2.8)) were used to model the dynamics of mixing in a continuous rotary powder blender [48]. FPEs were written for each of the component and were solved using void fraction of each component as the dependent variable varying over time and space. The FPEs for the two components were coupled

at the exit of the blender by adjusting for the opening (or weir height). It was shown that the ratio of the mean residence time to the time period of the fluctuation in the feed is the most important parameter determining the variance reduction ratio.

$$\frac{\partial C}{\partial t} = -\nu \frac{\partial C}{\partial z} + D \frac{\partial^2 C}{\partial z^2} \quad (2.8)$$

where C is the concentration of a component being mixed in the blender, ν is the transport coefficient, D is the dispersion coefficient and z is the axial distance from one end of the blender.

In a recent publication, Markov chains were applied to model continuous blending of fine powders by Berthiaux et al., [6]. The continuous blender was assumed to be made up of a series of well mixed states. The probability of material in a state remaining in the same state in the next time step was ps. The probability of the material in a state moving to the next state in the next time step was pf. The probability of the material in a state moving to the previous state in the next time step was pb. The ratio of pf/pb depends on the angle of the blades installed while ps depends on the fill level of the mixture (or layer height). Obviously, these three probabilities are exhaustive and hence add up to unity. Also, the exit of the material out of the blender depended on the exit probability, w, which in turn depends on the geometry and size of the outlet (weir height and area of opening). Simulations were performed with sinusoidal feeding of one of the components. The general conclusions from the simulations were that the frequency of the disturbance entering the blender along with the mean residence time determines the variance reduction ratio. The effect of the design of the exit of the blender (geometry and size) is significant in continuous powder blender design and operation.

Table 2.1: Theoretical Models from Literature

| Objective | Method | Comments | Refs. |
|--------------------------------------|--|--|--------------|
| Performance of continuous blenders | Mass balance on the continuous blender | An index of performance for semi-continuous and continuous blenders | [5] |
| Characterization of mixing processes | Mass balance on continuous blenders | Defines intensity and scale of segregation and scale of scrutiny discussed | [22] |
| Performance of continuous blenders | Response stimulus method | An expression for performance of a mixer based on fraction of mixer acting ideally was derived and phenomenological explanations were not provided | [106] |

Continued on Next Page...

| Objective | Method | Comments | Refs. |
|--|--|---|-----------|
| Improvement over batch blending | Statistical Analysis | Theoretical performance of semi-continuous blending operation was derived and found to be 2 times that of a batch blender. Moreover, ironing out of the batch to batch variations reduces the volume of failed product units considerably | [36] |
| Characterizing the random variations in a blender output | Power density spectrum and variographic analysis | The assumption of VRR of a continuous blender to be the sum of a random background band limited white noise and a reduction variance of the feed induced fluctuations was theoretically and experimentally justified. | [34, 104] |

Continued on Next Page...

| Objective | Method | Comments | Refs. |
|--|---|--|----------|
| Characterization of blender performance using dispersion model | Stimulus response analysis: RTD analysis | A dispersion model for free flowing powders in continuous blenders was developed based on the continuum approximation. This approximation relies on the diffusion mechanism of the parti- cle on the free surface and the di- lution on the part of the mixture due to agitation | [91, 96] |
| Characterization of blender performance using Fokker Planck Model | Stimulus response analysis: RTD analysis | Fokker-Planck equations were used to determine the output concentration distribution for a impulse input and this was related to the residence time distribution and its statistical moments | [67] |

Continued on Next Page...

| Objective | Method | Comments | Refs. |
|---|--|---|-------|
| Characterization of blender performance using Fokker Planck Model | Stimulus response analysis: RTD analysis | Fokker-Planck equations were used to describe the random mixing of powders. The same theory was used to define segregation kinetics during mixing | [93] |
| Characterization of blender performance using Fokker Planck Model | Stimulus response analysis: RTD analysis | Two Fokker-Planck equations were solved numerically for two components. One component was fed sinusoidally to control the disturbance entering the blender. Ratio of residence time to period of oscillation of the feed disturbance was found to be critical parameter | [48] |

Continued on Next Page...

| Objective | Method | Comments | Refs. |
|--------------------------------------|---------------|---|-------|
| Blender Modeling using Markov Chains | Markov chains | <p>The blender was modeled as a Markov process. The transition probabilities for the blenders used by (Weinekötter and Reh [104]) was used in determining the transition probability matrix. The design of the outlet along with residence time and time period of oscillation of the feed were found to be critical parameters</p> | [6] |

End of Table

A list of the theoretical developments in the published literature is given in Table 2.1. Attempts of using classical RTD models as mentioned before have been made in a number of studies. As in the case of fluids, dispersion superimposed on plug-flow was used to determine the profile of a tracer injected at the input. The profile was solved for by using classic Danckwerts' boundary conditions on the dispersion equation for plug flow. The resulting relation between the coefficient of dispersion and the variance of the tracer as a function of distance from the input was used in determining the VRR [14, 91, 96]. These models work fairly well for non-cohesive powders. However, concerns over their applicability for cohesive powders remain unanswered.

2.3 Studies on Continuous Powder Blending

A number of experimental studies were carried out on continuous blending systems. However, none of these studies examined pharmaceutical powders or pharmaceutical powder mixing closely.

2.3.1 Powders in Continuous Blending Studies

The published experimental studies on continuous powder blending fall into two broad categories. One set was based on testing the applicability and validity of the theoretical developments on continuous blending while the other was aimed at characterizing and understanding the performance of continuous powder blenders for different powders and look for patterns that could be used as generic design rules. Table 2.2 lists the powders described in the literature under continuous blending. Free flowing non-segregating type materials are the most common powders studied. A majority of the powder systems were granular sand or silica with sugar or salt as tracer. Some of the uncommon powders that were reported include chocolate, urania, thoria, zircon and coal. The particle sizes of the powders investigated vary from as small as $0.5\mu\text{m}$ to as large as 2cm. It is interesting to observe that pharmaceutical powders have not been reported in continuous blenders.

2.3.2 Feeding in Continuous Blending Systems

As discussed before, a continuous blender's performance is dependent on the feeding characteristics. The intensity and scale of segregation was shown to be dependent on the scale of scrutiny for powders. Scale of scrutiny also determines the feed accuracy demanded. Therefore, feeding mechanism and monitoring techniques play a substantial role in design and investigation of continuous blending systems. Table 2.3 makes a comparison between the feeding mechanism and the sampling and analytical technique used in monitoring various experiments carried out in continuous powder blending. Different powder feeding systems and their modes of operation were described by Weinekötter and Gericke [103]. A continuous powder feeding system consists of three distinct parts, the feeder unit, the measurement unit and the control unit. The feeder unit produces the requisite volumetric or gravimetric flow of the powder by screw, vibrating, rotary valve, belt, agitator, disc feeders. The measurement unit measures the volume of flow from geometry and operating conditions of the feeder or the weight of flow from direct measurement. The control unit controls the feeder drive to regulate the feeding rate.

Three kinds of feeding systems were described by Weinekötter and Gericke [103]: individual autonomous feeding, recipe feeding and proportional feeding. Individual autonomous feeding systems control the feeding rates of each powder stream independently. Recipe feeding systems maintain constant percentage proportions of the ingredients but the overall volumetric flow rate is adjusted depending on disturbances. Proportional feeding systems control the feeding rates based on one the flow rate of the primary ingredient which acts as a master while the other controllers act as slaves.

The measurement and control system for feeding systems can be performed volumetrically or gravimetrically. Two types of gravimetric feeding systems were reported [103]. Weigh belt feeders operate with the powder flowing from a hopper on to a belt and the weight measurement performed on the hopper or on the belt. Loss-in-weight or differential feeders operate with two hoppers connected with a powder volumetric flow device. The first hopper refilling the second till an upper limit is

reached. The second hopper, whose weight is monitored, then starts feeding continuously via a screw feeder. As the weight of the powder in the second hopper falls below a lower limit, the first hopper restarts its refilling operation.

Volumetric feeding was found to be less reliable than weigh feeding using a vibrated hopper delivering directly onto a moving belt on a weigh machine [41, 103]. Pulsed input was also used as a reliable experimental feeding technique [106]. It was easy to introduce and control the fluctuations thus facilitating the study of blender performance with the feeding mechanism.

Table 2.2: Powders in Continuous Blending

| Blender | Powder | Size | Characteristics | Refs. |
|-------------------------------|--------------------|------------|-----------------|------------|
| Rotating Drum | Sand | 355-420 | Free flowing | [107] |
| | Salt | 355 – 420 | Free flowing | |
| Double Helical Ribbon Blender | Copper | 10 – 85 | Free flowing | [82, 83] |
| | Nickel | 15 – 45 | Free flowing | |
| Double Ribbon & Impact Wheel | Urania | 0.5 – 50 | Cohesive | |
| | Thoria | 2.5 – 15 | Cohesive | |
| Double Auger | Silica Flour | 50 | Cohesive | |
| Centrifugal | Fine Sand | 100 | Cohesive | |
| 'Bow-tie' helical static | Coarse Sand | 700 | Free flowing | [41] |
| Paddle | Fine Sugar | 60 | Cohesive | |
| Zigzag | Granular Sugar | 450 | Free Flowing | |
| Vibrating rotating paddle | Aluminum Hydroxide | 27 – 71 | Cohesive | [104, 103] |
| | Irgalite | 7 – 56 | Free-flowing | |
| Horizontal Double Shaft | Silicon Carbide | 0.05 – 2.3 | Free-flowing | |

Continued on Next Page...

| Blender | Powder | Size μm | Characteristics | Refs. |
|-------------------|--|--------------------------------------|------------------------|---------------------|
| Rotating drum | Red and white Zeolite pellets (40% Silica and 40% Alumina) | L = 3000; D=1500 | Free flowing | [96] |
| Rotating drum | Limestone | | | |
| V blender | Copper | 40 – 200 | Free flowing | [68, 70] |
| Ploughshare mixer | Quartz | | | |
| | Dolomite | 357 | Free flowing | |
| | Dolomite | 359 | Free flowing | |
| | Dry powder | 335 | Free flowing | |
| | Ballitini | 200 | Free flowing | |
| | Rice | L = 5000 D = 2000 | Free flowing | |
| | Lignite | 9600 | Free flowing | As reported in [91] |
| Rotating Drum | Zircon | 1700 | Free flowing | |
| | Coal | 2700 | Free flowing | |
| | Ilmenite | 200 | Free flowing | |
| | Rice | 2000 | Free flowing | |
| | Oats | 2000 | Free flowing | |

Continued on Next Page...

| Blender | Powder | Size μm | Characteristics | Refs. |
|------------------------|-------------------|-----------------------|-----------------|---------------------|
| Rotating Drum | Polystyrene | H=1900 L=3600 | Free flowing | As reported in [91] |
| | Soda | 137 | Free flowing | |
| | Sand | 1500 | Free flowing | |
| | Coal | 500 – 20000 | Free flowing | |
| | Potato starch | 15 – 100 | Free flowing | |
| | Oat groats | 2000 | Free flowing | |
| | Coal with mineral | 6000 – 15000 | Free flowing | |
| Rotating Drum | Glass beads | 3000 | Free flowing | |
| | Maize starch | 15 | Cohesive | [48] |
| | Calcium Carbonate | 2 | Cohesive | |
| Co-rotating twin screw | Chocolate | 10 | Cohesive | [109] |
| Plowshare | Crushed Maize | 370 | Free flowing | [65, 66] |
| Motionless static | Red wheat | $L = 6450$ $D = 2900$ | Free flowing | [14] |
| | Lucite | 3175 – 5770 | Free-flowing | |

End of Table

2.3.3 Process Monitoring of Continuous Blending

Early monitoring techniques for blending with one soluble component were based on weighing the sample from a thief probe before and after dissolution. Some of the recent advances in electronics encouraged more sophistication in monitoring experimental powder blending. Power density spectrum analysis could be easily carried out with electronic monitoring and modern day computing power. Optical imaging, optical reflectance, and positron emission and particle tracking (PEPT) were some of the techniques reported for blend uniformity monitoring in continuous powder blending. For powder systems where the tracer was optically different from the bulk, optical laser and optical image techniques (reflectance based and color analysis based) were used. This technique is amenable and reliable for online monitoring of powder blending if one of the components in the blend differs from the other constituents in color. In the PEPT technique, gamma rays are emitted by a tracer particle followed by capture of these rays in a positron camera. The position and velocity of the tracer particle can then be reconstructed. This technique, however, is not amenable for online monitoring as it involves usage of very special equipment and handling of radioactive tracers. A description of monitoring techniques in literature can be found in tables 2.3 and 2.6.

Table 2.3: Feeding in Continuous Blending Work

| Blender | Feeding Mechanism | Sampling and Monitoring | Control | Refs. |
|--|---|---|---|----------|
| Rotating Drum | Intermittent pulsed manual batch-wise Feeding. Samples withdrawn at the end of the drum. | Weighed before and after dissolution in water (and subsequent drying) | - | [107] |
| Double Helical Ribbon. Double Ribbon with Impact Wheel | <i>Belt feeder</i> : Moving belt suspended from a weigh balance and fed from a vibrated hopper. <i>Mettler feeder</i> : Intermittent feeding at 12s time intervals. | Samples withdrawn at intermediate positions and chemically analyzed using a spectrophotometer | Amplitude of the vibrations of the hopper and the speed of the belt | [82, 83] |

| Blender | Feeding Mechanism | Sampling and Monitoring | Control | Refs. |
|-----------------------------|---|--|--|-------------|
| Double Auger. | <i>Vibrating screw volumetric feeder</i> : vibrating and rotating screw feeder. | Measured the weight of the sample before dissolution with water and after subse- | Amplitude of vibration and rate of rotation of screw feeder. | |
| Centrifugal. Double Ribbon. | <i>Bow-rotating screw feeder</i> . | quent drying (or centrifug- | arbitrarily assigned. [41] | |
| 'Helical Static. Paddle. | <i>Screw volumetric feeder</i> : Screw feeder with a 'pre- | ing in the case of silica | | |
| Vibrating Rotating Paddle. | conditioning' screw encir- | cling feed used for Double Auger type mixer. | | |
| Horizontal Double Shaft. | Electronically weighed feeding from a hopper | Laser light shined through a Fibre-optical inline sensor | - | [104, 103] |
| Concentric Helical Shaft | | | | |
| Flat blade | Hopper | Positron emission particle tracking | - | [55] |
| Rotating drum | Vibrated Hopper. Star Feeder | Rotating Image analysis by photo capture in a digital camera. NIR Sensor. | Flow rate, angle of inclination of the drum and rotation speed | [1, 48, 96] |

Continued on Next Page...

| Blender | Feeding Mechanism | Sampling and Monitoring | Control | Refs. |
|-------------------|---|---|---|--------------|
| Co-rotating screw | twin Accurate feeder | Image analysis with color meter for L value | Flow rate, discharge opening, screw RPM | [109] |
| Plowshare | Vibrating conveyer | Radionuclide tracer | RPM | [66, 65] |
| Motionless | Vertical pre-mixing section with a gate valve | Manual counting of tracer particles | - | [14] |

End of Table

Two kinds of analytical techniques are seen in powder blending research. The first set of monitoring techniques is used for monitoring powder flow behavior in blenders include techniques like positron emission and particle tracking and magnetic resonance imaging. These complicated monitoring techniques usually are unfavorable to be used in control systems for industrial application but are useful research tools for understanding the fundamental behavior of powders in blenders. Another set of analytical techniques are those that can be implemented as a process analytical tool in an industrial manufacturing line process. These include technologies like light induced fluorescence, near infrared spectrometry and optical reflectance. These are simpler than the previous set of techniques and therefore can be applied in an industrial process.

2.3.4 Process Control of Continuous Blending

Control strategies in many of these studies focused mainly on varying the operational parameters such as flow rate, speed of the blender (RPM) and fill percent to control the performance in the blender. None of these studies reported dynamic control of the blend homogeneity. However, these studies did attempt to draw correlations between the performance and these operational parameters. The usefulness of such correlations is limited to the systems under consideration and is discussed later.

2.3.5 Experimental Studies on Continuous Blending

A summary of the conclusions from the investigations on continuous powder blenders is tabulated in table 2.4. The qualitative and quantitative results from these studies show that, for non-cohesive systems, a response stimulus methodology explained the behavior of the blenders fairly and also took into account the variations caused by the feeding system. Some of the parameters reported in literature include fraction of blender behaving ideally, delay, dead volume and dispersion coefficient. The variation of these design parameters with operating parameters was either presented graphically or by response surface methods. The fill percent proportional to the gate opening in the blender of the rotating drum and twin screw blenders showed an op-

imum between 40-60% for many systems reported. For rotating drum blenders, the dependence of the dispersion coefficient on the flow rate and rotational speed was proportionally sub-linear. Correlations between dispersion coefficients, mean residence times and the operational parameters like powder properties, blender geometry and operating variables were proposed and were best fit curves for only the systems under study and for certain regimes of flow in the drums (e.g. slow, avalanche flow). Thus, extending these to other types of powders, blend geometries and regimes of flow without considering the corresponding changes particle-particle interactions is not justified. Further investigations must focus on developing a general correlation between parameters of residence time distributions, operational parameters and particle properties. These correlations must be based on universal aspects of powder behavior like forces between particles, segregation potential based on difference on particle properties and finally the geometry of the blending system.

From the frequency domain analysis, it was shown that an ideal blender acted as a low pass filter allowing the low frequency fluctuations from the feeder to pass through. The structure of the mixture was predicted given the feeder auto-correlogram and the RTD of the blender. The RTD was compared with a dispersion model and this approach worked fairly well in explaining the observations.

In order to capture the dependence of agglomeration of cohesive powders, agglomerate particle size, Poole et al., [82, 83]. used in determining the random mixture limit. De-agglomeration was another viable alternative that they investigated. It was seen that de-agglomeration generally resulted in increased blend uniformity. However, no quantitative relations were reported relating the cohesive powder behavior in this study. In order to deal with the uncertain behavior of cohesive powders some studies have resorted to response-surface experimental methodology attempting to explain the behavior of powders in continuous screw blenders. They performed experiments with different operating points and tried to determine a linear or quadratic dependence of mean residence time and fraction of the blender acting as a plug flow device with operational parameters like gate opening (equivalent to fill percent inside the blender), flow rate and so on. While these methods gave a functional relation

between the operational parameters and the behavior of the blender, these are statistically fitted functions and hence may not be extrapolated to other ranges of the parameters.

The performance of commercial continuous blenders was evaluated for cohesive powders [41]. Based on experiments on seven types of continuous blenders fed with a vibrating hopper volumetric feeder, the blenders were ranked for cohesive powders based on the variance of the exit stream. Harwood et al. concluded that centrifugal blenders worked very well for cohesive powders while screw auger, paddle and ribbon blenders gave above average performance. Use of particle emission and positron tracking in determining the powder flow profiles and residence time were reported [53, 57, 54, 55, 56, 58]. Motionless blenders for free-flowing powders were studied [14, 39]. However, these blenders choke when cohesive powders are used [41].

Merz et al., [65, 66] used radionuclide tracers to investigate the residence time distribution and used the dispersion model for calculating the effect of the shaft rotation rate and influence of internal mixing geometries. It was pointed out that by installing motionless weirs in the blender the dispersion coefficient was increased significantly at high rotation rates. At low rotation rates, the dispersion coefficient was hindered by the placement of weirs. The mean residence time was found to reach a maximum at 1.4 times the critical rotation rate (The critical rotation rate being defined as the rate at which the gravitational force is balanced by the centrifugal force).

Table 2.4: Continuous Blending Work from Literature

| Blender | Mixing Index | Notes on Analysis | Key Conclusions | Refs. |
|----------------|--|--|---|--------------|
| Rotating Drum | Beaudry's index & Fraction of the mixer behaving ideally | The RTD analysis performed involved stimulus experiment with an intermittent pulse input. An ideal mixer with plug flow and dead volume was chosen as the model. The fraction of the mixer behaving as ideal mixer was chosen as a performance index | Introduced the fraction of ideal mixer from RTD analysis as a reliable mixer performance index. Measured output fitted well with the RTD model assumed. Segregation had played a role which could not be judged from the measurements made. | [106, 107] |

Continued on Next Page...

| Blender | Mixing Index | Notes on Analysis | Key Conclusions | Refs. |
|--|--------------------------|--|--|--------------|
| Double Helical Rib- bon & Double Rib- bon with impact wheel | Coefficient of variation | Agglomerate and particle random mixture coefficient of variation was employed. Modification of the Stange formula for random mixture standard deviation was em- ployed. RTD analysis was performed. Microscopic ob- servations of the powders were carried out to get more insight into the process. | Performance comparable to high shear batch blend- ing. Segregation prob- lems are offset by run- ning the ribbons at super- critical speeds. Rate of ap- proach to randomness in- creases with increasing ratio of mixes. Impact wheel de- agglomeration is crucial for cohesive powder mixing | [82, 83] |

Continued on Next Page...

| Blender | Mixing Index | Notes on Analysis | Key Conclusions | Refs. |
|------------------------------|---|---|---|-------|
| 1. Double Auger | 1. Fraction of one of the powder materials | 1. Emergence profiles of the concentrations as fractions were plotted | The double auger, vibrating rotating paddle and double ribbon blenders were in the mid to upper performance range for most powders. | [41] |
| 2. Centrifugal | 2. Standard deviation over a set of samples | 2. Mixers were ranked in the order of increasing standard deviations for cohesive-cohesive, cohesive-free flowing and free-flowing free-flowing powder systems respectively | The double helical static mixer choked for cohesive powders. The centrifugal mixer performed well for cohesive systems. Zig-zag blender is unsuitable for cohesive segregating systems. | |
| 3. Double Ribbon | | | | |
| 4. 'Bow-tie' Helical Static | | | | |
| 5. Paddle | | | | |
| 6. Zig Zag | | | | |
| 7. Vibrating Rotating Paddle | | | | |

Continued on Next Page...

| Blender | Mixing Index | Notes on Analysis | Key Conclusions | Refs. |
|----------------------------|---|---|--|------------|
| 1. Horizontal Double Shaft | 1. Intensity of segregation from variance | From the RTD analysis, the intensity of segregation (or variance) is calculated. The scale of segregation is calculated from the area under the curve of the power density spectrum. The VRR is calculated and plotted as a function of the Bodenstein number (also the Peclet number) and the period of fluctuation in the feed. | A continuous mixer can dampen the disturbances that are only in the high frequency range (hence acting as a low pass filter). The time period of disturbance must be less than the residence time of the mixer. Optimization of feeding system by allowing only high frequency disturbances through the feeder is an essential part of mixer design. | [104, 103] |
| 2. Double Centric Shaft | 2. Scale of segregation from correlation function | | | |
| | 3. Variance reduction ratio VRR | | | |

Continued on Next Page...

| Blender | Mixing Index | Notes on Analysis | Key Conclusions | Refs. |
|----------------|------------------------|--|--|--------------|
| Flat blade | None | Flow paths were generated experimentally and qualitative description of the mixing phenomenon was given. | PEPT can be used to study the flow patterns and residence time distributions of powders in continuous mixers. | [55] |
| Rotating drum | Dispersion coefficient | The response to a tracer introduced in the feed is tracked and the output is subjected to residence time analysis. Dispersion coefficient is calculated by fitting an axial dispersion model to the experimental observations. | RTD curves for various flow rates and at various sampling points along the length of the drum were reported. The shapes of the RTD are self-similar (non-segregating particles). Variation of dispersion coefficient with flow rate, RPM and inclination angle was reported. | [96] |

Continued on Next Page...

| Blender | Mixing Index | Notes on Analysis | Key Conclusions | Refs. |
|----------------|------------------------|---|---|--------------|
| Rotating drum | Dispersion coefficient | PEPT was used to track the particles and dispersion coefficient for batch mixing in a drum was calculated. Dispersion coefficients for rotating drum mixing of other particle systems reported elsewhere were calculated. | Correlations from literature for dispersion coefficient were reported as a function of flow rate, geometry of the drum, particle size, angle of inclination dynamic angle of repose and rotational speed. A new correlation for both batch and continuous dispersion was developed from experimental data of several authors. | [91] |

Continued on Next Page...

| Blender | Mixing Index | Notes on Analysis | Key Conclusions | Refs. |
|----------------|--------------------------------------|---|--|--------------|
| Rotating drum | Transport and Dispersion coefficient | NIR was used to monitor the concentration of the powder at the outlet of the blender. One of the components was sinusoidally fed to control variance entering the system. | Ratio of mean residence time to the time period of oscillation of the component sinusoidally fed was found to be a critical parameter. The height of the weir (and the size of the outlet) was another critical parameter that affected the blend performance. | [48] |

Continued on Next Page...

| Blender | Mixing Index | Notes on Analysis | Key Conclusions | Refs. |
|----------------------|--------------|---|--|-------|
| Co-rotating screw | twin - | Residence time analysis from washout experiment was performed. Delay and dead volume model and tanks in series model were used in explaining the experimental results. Response surface analysis was performed on the effect of feed rates and RPM on residence time and gate opening on fractional tubularity. | The mixer comprised of forward conveying, non-conveying and reverse sections. The tanks in series model was fitted with one parameter (number of tanks fixed). Statistical influences of feed rate and screw RPM on mean residence time and of gate opening on fractional tubularity was observed. A response surface model was used to explain the results. Non-dimensional RTD was identical for high and low feed rate cases. | [109] |

Continued on Next Page...

| Blender | Mixing Index | Notes on Analysis | Key Conclusions | Refs. |
|----------------|------------------------|---|---|--------------|
| Plowshare | Dispersion coefficient | Residence time analysis using radionuclide tracer. Dispersion model for mixing was used. RPM was the only operational variable changed during the experiment. Effect of presence of internal weirs was examined | Different plow configurations gave different mean residence times and standard deviations. The dispersion coefficient in the presence of internal weir was higher than that in its absence only at very high rotation rates. The location of the internal weir was the point where the residence time distribution changed its shape. The mean residence time had a maximum at a particular rotation rate, above the critical rotational rate. In the presence of weirs, the mean residence time had a maximum at much a lower rotation rate. | [66, 65] |

| Blender | Mixing Index | Notes on Analysis | Key Conclusions | Refs. |
|----------------|------------------------|---|---|--------------|
| Motionless | Dispersion coefficient | Residence time analysis from impulse tracer experiment was conducted. Dispersion model was used to explain the results. Hold up times for various weights of particles was reported | Dispersion model explains the mixing of free-flowing particles in motionless mixers. The relation between apparent linear velocity and dispersion was investigated and was found to increase with linear velocity in a non-linear manner. The number of mixing elements (helices) increased the dispersion coefficient. | [14] |

End of Table

2.4 Research on Continuous and Batch Blending

As discussed in the introduction, powder blending has predominantly been a batch process both in practice and research. These research efforts, on batch blenders that can operate in continuous mode also, could prove valuable in understanding the behavior of powders in continuous mode. An attempt to understand how to supplement continuous blending research from batch blending research would be supported by reviewing literature on batch blending. As many reviews tabulated in table 2.5 have appeared before in literature, we chose not to include this in this review.

A number of reviews [28, 29, 61, 62, 63, 72, 85, 88, 102] focus on the various mixing indices in use in industry and research, the mechanisms of mixing, the directions that research had taken at the time of the review and some empirical rules to choose and design blenders. Weidenbaum [102] reviewed about 75 papers before 1960 while Fan et al., [28] reviewed over 200 papers in 1970 in their review. Though the number of published papers in this area has not grown phenomenally, a shift in the areas of emphasis is visible. The earlier reviews [28, 102] detailed the state of the knowledge on blending like empirical kinetic equations, computer simulations of the stochastic blending process, the selection criteria for blenders. The later reviews [29, 61, 62, 63, 72, 85, 88] emphasized fluidized beds, contact number based indices and the concept of ordered mixing for cohesive powders. The series of reviews on solid and liquid blending [61, 62, 63, 72, 88] detailed the blending equipment in the agricultural industry. Williams reviewed the continuous blending literature and presented the theoretical analysis discussed previously [105].

As noted earlier, blenders that can operate in both batch and continuous modes can be expected to have similar powder behavior. Therefore, an understanding of the mixing mechanisms in these batch blenders would, at least qualitatively, give some guiding principles e.g. the effect of blades on powders, the effect of geometry of the blender and the powder-powder and powder-wall interactions for designing continuous blending systems.

Table 2.5: Past reviews on Powder Blending

| Focus | Type | Mixers | Ref. to Continuous Blending | Refs. |
|---|----------------------|---------------------------------------|--|-------|
| Review of literature on solids mixing from 1958 - 1970. Cataloguing mixing indices, mixing parameters, rate laws, mixer selection criteria and simulations in mixing research | Batch and continuous | Ribbon, Flow, Centrifugal, Motionless | Little emphasis on continuous mixing. A listing of general criteria for selecting mixers was compiled. Solids handling problems were highlighted | [28] |

Continued on Next Page...

| Focus | Type | Mixers | Ref. to Continuous Blending | Refs. |
|-----------------------------|----------------------|---------------|--|--------------|
| Continuous mixing of solids | Batch and continuous | Drum, Ribbon | Mathematical analysis of stimulus-response for continuous mixer was given. Qualitative comparison between continuous and batch mixers for powders was made | [105] |

Continued on Next Page...

| Focus | Type | Mixers | Ref. to Continuous Blending | Refs. |
|----------------------|--------------|-------------------------------|--|-------------------------|
| Powder mechanisms | mixing Batch | Bladed, Paddle, Fluidized bed | Dependence of powder tensile strength on the formation of failure zones was described. Convective effects on flow of powder over blades and recirculation of powder over the blades was discussed. Interparticle percolation and diffusive mixing mechanisms were described. An extension of the analysis of mixing mechanism to cohesive and adhesive systems was qualitatively made. | [9, 10, 11, 46, 53, 57] |

Continued on Next Page...

| Focus | Type | Mixers | Ref. to Continuous Blending | Refs. |
|--|----------------------|---|---|-------|
| Literature survey Batch and Continuous powder mixing | Batch and Continuous | | Extensive literature survey and comprehensive classified list of 650 references in Powder mixing before 1975 | [16] |
| Review on the Batch methods of mixer design and geometries | Batch | Gravity force, Pellet, Nautamix, pneumatic, fluidized bed, silo | Characterizes blenders depending on the dominant force of mixing - gravity, push and centrifugal. Knowledge around mixing times and power requirements that go into mixer design are discussed. The role of frictional forces in the work done on mixing is also discussed. | [69] |

Continued on Next Page...

| Focus | Type | Mixers | Ref. to Continuous Blending | Refs. |
|--|-------------|--|---|----------------------|
| Assessments of Batch agitated systems applied in powder mixing | | Drum, cone, twin shell, ribbon, orbiting screw (Nautamix), high speed impeller pan, mill | Comprehensive listing and applications, limitations and orders of magnitude of powder, capacity and mixing times were made. Various scenarios in practical powder mixing design situations were listed. Criteria for selecting blenders were tabulated. | [85] |
| Review of liquid, Batch and slurry and solid tenuous mixing in agricultural industry | | Vertical Orbiting screw, recirculating hopper, fluidized bed | Comparison of mixers under broad categories and corresponding segregation tendencies were listed. Mixers and mixing indices for cohesive powders were also reported. | [61, 62, 63, 72, 88] |

End of Table

2.4.1 Powder Kinematics and Dynamics

Bridgwater [9, 10] discussed the various blending mechanisms in a batch blender and the influence of particle and blender properties on them. It was shown that slip planes or failure zones are formed when a blade moves in the powder. The creation of these zones generates the degrees of freedom for the powder to move in bulk (convection) and for particles to randomly move across these zones (diffusion). Some effort on predicting slip planes will be discussed later. However, it was suggested that in a fundamental mathematical model of a mixer, the mean failure zone height and spacing measured in the same direction would be the characteristic length scales.

The formation of slip planes in convective mixers was shown to be a crucial step in the process of blending. Novosad et al., [73, 74, 75, 76, 77] attempted to theoretically predict the slip planes (and the accompanying failure zones) for non-segregating, free-flowing powders. A blade rotating in a bed of powder was visually examined from outside and the slip planes were predicted using classical powder mechanical constructions. It was reported that theoretical predictions were possible to the zones adjoining and close to the blade (in the fore and the hind). For far away zones, the shape of the slip planes could not be predicted accurately. A state of limiting equilibrium was assumed to exist with an active lateral pressure and inertial forces were neglected. This assumption implied that the static and dynamic slip planes would be of the same shape. With the knowledge of these planes, the shear stress on the blade was also predicted using geometrical methods. The results agreed with analytical Mohr's circle method very closely. The theoretical stresses were then used to develop correlations between the shaft torque on the powder as a function of the geometry of the shaft, the properties of the granular material and wall, and the position of the blade. The correlation developed showed fair agreement with experiments.

Müller et al., studied the effect of internal mixing elements on blending [68, 70]. In the same studies, the effect or rotation rate of blending elements, fill volume, particle size distribution of tracer and bulk powder were also studied. The effect of torque and

work of mixing powders were examined for different internal elements. In a review, the principles of batch mixer design and geometry were studied and correlations for operational parameters and mixer performance indicators were reported for different types of mixer geometries [69],

Cooker and Nedderman [19, 18] reported a theoretical analysis of powder dynamics in a a more complicated geometry of the vertical helical ribbon agitator (HRA). In a more recent study, the torque on high shear impellers was theoretically predicted [49]. They also experimentally verified and found that their model represented the torque behavior fairly well. Extensions of these theoretical methods for cohesive powders were not found. However, a model by Kocova and Pilpel [50] showed that principle of corresponding states could be applied for predicting the tensile stresses in cohesive powders. The tensile stresses in cohesive powders were related to the inter-particle distances and the surface asperities of the powder.

A series of related studies on blending mechanisms using positron emission particle tracking gave an insight into the complex nature of interactions that occur inside the blender. PEPT technique was used to study the powder movement profiles (radial and angular displacement and velocities) in various blenders (ploughs, bars and agitators) [12, 46, 53, 57, 54, 55, 56, 58]. The position of the tracer at different times inside the blender was used in estimating particle movement parameters like the mean radial displacement and axial dispersion coefficient for different blender operational variables. As these parameters were calculated from basic particle movement experiments, these hold great value in characterizing the efficacy of the blender mixing elements in the absence of theoretical models. Also, these experiments predicted the occupancy of the tracer at different points of the blender, thereby giving important information on deposits and dead volumes inside the blender. Using the movement of particles, axial dispersion coefficients and mean radial displacements were determined from first hand experimental information. These investigations therefore are important in independently determining axial dispersion coefficient rather than from parameter fitting in residence time distribution experiments. Even though these studies have been performed on batch blenders, there are some ongoing efforts [53] to

implement this technique in understanding continuous blending systems.

Magnetic resonance imaging (MRI) was used by many authors in characterizing the segregation of granules in rotating drum [42, 43] and tumbling blenders [94]. In order to make the powder amenable to MRI, it was doped with PDMS oil. MRI was used to generate the 3D velocity field of the powder in the blender. The images were used to calculate segregation index (defined as the ratio of the standard deviation of the observed image intensity to its mean). While the results are specific to the batch blenders in consideration, these techniques may be used to test the flow fields of powders in continuous blenders with internal blending elements. Also, MRI gives a 3D image of the content uniformity of the powder inside the blender. The main disadvantage in using this technique is that after doping with an MRI sensitive substance, the powder's flow characteristics might change considerably and therefore must be investigated before applying this technique.

As the VRR depends on the RTD of the powder in the blender, the movement of powder inside the blender, which is reflected by the RTD, determines the blending efficacy. Therefore, quantitative predictions of the movement of powder inside the blender under the influence of the blending elements would prove invaluable as these can then be used to predict the RTD of the powder inside the blender. No studies were found that related and predicted the VRR of the continuous blender to the powder movement inside the blender. Predictions of powder movement based on tracking the individual particle motion (discrete element methods) have been reported and used [15]. But these methods have been successful for small numbers of particles and for simple geometries. As the number of particles that can be used in DEM simulations is limited and maintaining geometric similarity would require a large number of particles in simulation, the DEM simulation results can only be qualitatively used in understanding the powder movement in industrial blenders. Even to pursue DEM simulation of a smaller number of particles in a small blender, the computational effort required is considerable and may be challenging to realize this in the near future.

2.4.2 General Monitoring Techniques

It is clear that an understanding of the complicated relations between the performance of blender and the powder movement in the blender is sine qua non for predictive modeling and design of a continuous blender. Also, it is clear that the powder movement inside the blender is related to various particle parameters like particle size, shape, topology, geometry, cohesiveness and operational parameters like flow rate, fill percent and blender speed. As developing mathematical models for such complicated systems is difficult, qualitative understanding by monitoring the powder behavior and blender performance forms a crucial step in the research phase. Non-invasive techniques that do not disturb the powder during monitoring are very valuable and present two main advantages; they reflect the powder behavior without affecting it; and have an immense potential for being incorporated into a control system loop of continuous blending systems in a manufacturing set up. Various monitoring techniques used by authors in the past have been listed in table 2.6. These monitoring techniques fall into two categories - powder behavior sensing techniques and blender performance monitoring techniques.

Powder flow behavior sensors like positron emission particle tracking and magnetic resonance imaging, as discussed earlier, depict the movement of powder in the blenders. Other powder behavior sensors have also been reported. A thermistor and tribo-electric probe was used to detect the dead volume or deposits in a blender [90]. This sensor was used to determine an agitation coefficient that reflected the extent of agitation as a function of the distance from the agitation blade. Some other techniques like capacitive probing and radio pill tracking were reported to assess blender voidage and powder movement [86]. Very few techniques were applied for cohesive powders.

Techniques like near infra red spectroscopy (NIR) and light induced fluorescence (LIF) have been used to predict the blend homogeneity in tumbling blenders [40, 52]. These techniques were reported to be fast and accurate. However, these techniques were not used for monitoring blend homogeneity in a continuous blender. These

sensors can be easily connected to a control system loop and hence are very amenable for automation.

Table 2.6: Monitoring Techniques in Literature

| Objective | Monitoring Techniques | Notes | Refs |
|--|-----------------------|---|------|
| Particle tracking in batch and continuous mixers. Assessment of mixing effectiveness and agitation | PEPT | <ol style="list-style-type: none"> 1. Radionuclide decay by positron emission is followed by gamma ray emission when the positron is neutralized by the electrons in the powder. 2. Accurate and fast technique. 3. The radionuclide must possess similar properties as the powder being studied 4. Radionuclide can be used as a tracer for residence time distribution determination. | |

Continued on Next Page...

| Objective | Monitoring Techniques | Notes | Refs |
|--|-----------------------|--|------|
| Particle tracking in batch and continuous mixers. Assessment of mixing effectiveness and agitation | MRI | <ol style="list-style-type: none"> 1. Hydrogen nuclei resonate with external magnetic field giving the position of the hydrogen atoms 2. Powder was doped with an organic oil that is MRI sensitive and the powder movement was followed in the mixer 3. Is comparable to the “freezing” and imaging technique and is also faster | [94] |
| Particle tracking in batch and continuous mixers. Assessment of mixing effectiveness and agitation | Radio pill | <ol style="list-style-type: none"> 1. A radio frequency transmitter is inserted into the powder mass and an aerial network is used to detect the position and velocity of the pill 2. Useful to give bulk powder movement characteristics like circulation velocities, angular velocities and average velocities 3. Safer as the method does not involve radioactive substances | [17] |

| Objective | Monitoring Techniques | Notes | Refs |
|--|-----------------------|--|------|
| Particle tracking in batch and continuous mixers. Assessment of mixing effectiveness and agitation | Thermistor | <ol style="list-style-type: none"> 1. A Thermistor with epoxy coating protecting the core was used 2. The Tribo-electric sensor was a stainless steel probe that was sensitive in the nA current levels 3. The current and the resistance from Thermistor was used to calculate the heat transfer coefficient between the Thermistor and the powder was experimentally 4. An agitation index was defined based on difference in the heat transfer coefficient in static powder and the agitated powder | [90] |

Continued on Next Page...

| Objective | Monitoring Techniques | Notes | Refs |
|--|-----------------------|--|----------|
| Particle tracking in batch and continuous mixers. Assessment of mixing effectiveness and agitation | Capacitor sensor | <ol style="list-style-type: none"> 1. A charge transfer type sensor was use 2. Voidage was measured at different positions of the blade angle as mixing proceeded | [86] |
| Sampling and Characterization of mixing process | NIR | <ol style="list-style-type: none"> 1. A NIR spectrophotometer is used with a fiber optic probe with which the concentrations of the samples are calibrated 2. The scan time is of the order of 15 seconds to obtain statistically good results. 3. Accurate measurements of sample concentrations were possible | [40, 48] |

Continued on Next Page...

| Objective | Monitoring Techniques | Notes | Refs |
|---|-----------------------|--|------|
| Sampling and Characterization of mixing process | LIF | <ol style="list-style-type: none"> UV light is shined on the sample which reflects light at lower frequencies which is measured and calibrated. The method is fast compared to NIR measurement techniques Not all powders fluoresce | [52] |
| Sampling and Characterization of mixing process | FTIR | <ol style="list-style-type: none"> Consists of a Fourier Transform Raman Spectrophotometer with a Fibre optic probe Signal was weaker than that in NIR spectroscopy but was less complicated and was easily used in analysis | [98] |

Continued on Next Page...

| Objective | Monitoring Techniques | Notes | Refs |
|---|-----------------------|---|---------------------|
| Sampling and Characterization of mixing process | Optical sensor | <ol style="list-style-type: none"> 1. Color difference between the components used to find the homogeneity of blend 2. Fiber optic probes can transmit the light without any noise corruption | [47, 104, 103, 109] |

End of Table

2.5 Conclusion

Continuous dry powder blending offers many benefits. Employing parallel units avoids scale up issues. Capital and space requirements are considerably reduced. As the process is under steady state, process control using process analytical techniques is easily implemented. Material containment is achieved reducing cross-contamination of products and employee exposure. Also material in work-in-process being small in quantity, there is considerable increase in flexibility and decrease in risk.

Industrially, batch blending systems were used to handle small volumes. Continuous blending is a very good option for materials processed in large volumes. Continuous powder blending needs accurate feeding systems. It also increases the complexity in analysis by introducing flow in spatial dimension. Little emphasis was laid on research in continuous powder blending compared to batch blending. But now, with the advancement in electronics, online monitoring and control has become quick and reliable. Feeding systems using electronic weigh feeders have also been shown to be reliable. Therefore, continuous powder blending is an attractive alternative for large volume processing in the pharmaceutical industry where traditionally batch blending is in place. However, investigations on the behavior of cohesive pharmaceutical powders in these systems need to be pursued.

This paper reviews the developments in continuous blending since the last review of Williams. The following conclusions can be made on state of the current research on continuous blending:

1. A continuous blender can only reduce the short-term (high frequency) fluctuations introduced by the feeding mechanism. Hence the design of the feeding system takes a critical role in design of continuous blenders. The demand posed on the blender performance can be greatly reduced by designing a feeding system that is consistent and accurate.
2. The formation of slip planes (powder failure zone) in the powders due to the movement of the blender mixing elements combined with the powder properties like the size, shape and topology determines the powder movement inside

the blender. This in turn determines the RTD of the powder in the blender. Therefore, the mean failure zone height and spacing are important characteristic length scales in blender design

3. Techniques like PEPT and MRI offer the advantage of visualizing the dynamics in 3D while blending is in progress. The effect of powder properties and blender operational parameters on powder movement and blending performance can be studied in real time using these techniques giving useful insights on the efficacy of the blender. These techniques offer the additional advantage of determining parameters like dispersion coefficient from average particle movement inside the blender. These parameters can then be used in predicting the RTD and hence the size of the blender for a given load and VRR requirement
4. Cohesive powders are very common in many industries like pharmaceuticals. These powders, which fall in the size range 0.5 - 200 μm , need to be investigated in continuous blenders. Consistent feeding of powders that do not flow freely is a considerable challenge in feeding system design. Studies on cohesive powders should concentrate on designing an efficient feeding system that delivers the consistency demanded by the continuous blender. Also, the mechanisms of mixing for cohesive powders in such continuous blenders are not clear. Efforts must be directed towards investigating the movement of these powders in continuous blenders

In a review on continuous mixing of solids, Williams [105] commented that prediction of blender performance from a fundamental particle movement study in continuous blenders were valuable but not practical. As process understanding is important to minimize the risk of operations in the pharmaceutical industry, understanding particle interactions and translating these microscopic interactions into macroscopic powder behavior is necessary.

Though mathematical modeling and prediction of the blender performance may be very difficult, the current available technology can be used effectively in performing a multi-scale analysis of the behavior of powders in continuous blenders. Further

research is needed in establishing a connection between the particle characteristics, blender operational parameters and the particle movement under the influence of the blender mixing elements with the performance of the continuous blender.

Chapter 3

Thesis Objectives

The main goal of this thesis was to test and understand a continuous blending system for mixing dry pharmaceutical powders. A satisfactory understanding of the continuous blending process should uncover the underlying relationships between the properties of raw materials, the quality attributes of the product of the process and the operating conditions.

Ngai [71] used a multi-scale analysis framework to establish the relationships between fundamental particle parameters like size, cohesion/adhesion surface energies and friction with macroscopically observed phenomena occurring during batch mixing. In this work, we utilised a similar framework to understand the dependence of the performance of continuous dry powder blending system with blender design parameters, operating variables and material properties. However, as noted later the main approach in this work is experimental in nature whereby various particle and operational parameters are varied experimentally and the experimental blending performance determined. The work was pursued in two parts catering to two different objectives as outlined below. A third objective based on the management education of the program focused on creating and applying a framework for internationalization of pharmaceutical and biologics manufacturing.

3.1 Specific Objectives

In order to achieve the aforementioned goal of developing a phenomenological understanding of dry powder continuous blending and its impact in pharmaceutical

manufacturing, the following objectives are proposed.

3.1.1 Investigation of powder flow behavior

The flow behavior of powders in different blender geometries was to be studied using stimulus-response techniques. These studies were to focus on understanding the effect of particle-particle interactions alongwith the influence of material properties on the performance of dry powder blending. Residence time distributions of the continuous blenders was to be modeled using simple models like Dispersion model.

It was expected that the parameters in such models (for e.g., axial dispersion coefficient) could be a function of the macroscopic and microscopic properties of the powders and the conditions under which the experiments were conducted. It was proposed to study this underlying dependence of dispersion coefficient on fundamental particle properties like cohesion and adhesion surface energies, particle sizes and operational variables like rotation rates and flow rates of the material in the blender.

3.1.2 Understanding macroscopic blending behavior

The macroscopic behavior of continuous dry powder blending system will be studied. The influence of design parameters and operating variables on process performance will be assessed. The phenomenological, microscopic understanding from the last phase will be integrated with the operational, macroscopic understanding of the current phase to tease out key design principles in continuous dry powder blending.

A relationship for theoretically estimating the VRR was described in equation (2.3). This was to be utilised in predicting the performance of the continuous blending system and compared with the experimental VRR. A valid prediction of the continuous blenders performance was expected to be a critical tool in both design and control of the continuous blending process.

3.1.3 Analyzing economics of continuous blending

The economic analysis of implementing dry powder continuous blending in the pharmaceutical industry will need focus on integrating and translating the potential de-

crease in capital investment and production cycle times into financial benefits. This analysis should serve to justify the value addition in implementing continuous powder blending.

The current manufacturing paradigm in the pharmaceutical industry is one of *quality-by-inspection*. Under this paradigm, the product is rigorously tested for quality at several stages of the manufacturing process. This adds considerable delay in the production cycle causing increased work-in-progress inventories. The FDA recently recommended moving to a new paradigm, one of *quality-by-design*. Under this new paradigm, quality of the product would have to be built in the design phase and the product would need very minimal quality assurance steps in the manufacturing process. Continuous manufacturing in general and continuous blending in particular are processes that are amenable to the *quality-by-design* paradigm. The economic argument for implementing continuous blending will not be investigated in this thesis.

3.1.4 Framework for Globalization of Manufacturing

While technology and processed based competitive advantage of pharmaceutical companies was the primary focus of this thesis, the capstone project aimed to identify a framework for globalization of pharmaceutical and biologics manufacturing that could be useful for operations managers in making the right location choices.

Chapter 4

Method of Approach

Domike [25] and Ngai [71] have shown the importance of particle adhesion and cohesion on the macroscopic behavior of powders in processes like blending and phenomena like flow of powders in piles and heaps. This multiscale analysis framework can be utilised in understanding the behavior and pharmaceutical powders in continuous blending systems. In order to experimentally understand the effect of operational variables and particle parameters, two different blenders and six different powders (API and Excipients) were investigated over a range of operational variables.

4.1 Choice of Continuous Blender

Literature on continuous mixing argued that mixers imparting high shear and fluidization energy while mixing the powders caused problems with segregation. On the other hand mixers imparting low shear by convection avoid segregation problems but mix the powders only to a certain degree of performance. In this work a high shear fluidizing mixer and moderate shear mixer were examined. A Patterson Kelley & Co. Zigzag[®] blender and a ribbon blender designed in-house were chosen as the choices for the blending system.

4.1.1 Patterson Kelley ZigZag Blender

A plant scale Zigzag[®] blender (at Patterson-Kelley & Co., East Stroudsburg, PA.), shown in figure 4-1, consists of a drum section that houses an *intensifier bar* and a *V section* which drives the powder from the inlet to the outlet. The design of the

Zigzag[®] blender has been optimized for best performance in the nutraceutical and food industries. However, its application in mixing pharmaceutical powders will be studied in this research. The intensifier bar is made up of a flat stainless steel disc with four very small mixing paddles at the circumference of the disc as shown in figure 4-1. This disc rotates about its surface normal at very high rates ($1500 \leq N_{Int} \leq 3000$ RPM).

The external *shell* of the blender, made of perspex plastic and comprising of the drum section and the V section, can rotate about its own axis. The V section is eccentric to the center-line of the blender and, therefore, traces a slightly eccentric rotation about the center line. The powder is fed into the drum section, as shown in figure 4-1 and leaves the blender at the V section's exit. The angle of incline of the blender can be altered to change the fill volume and mean residence time of the powder in the blender.

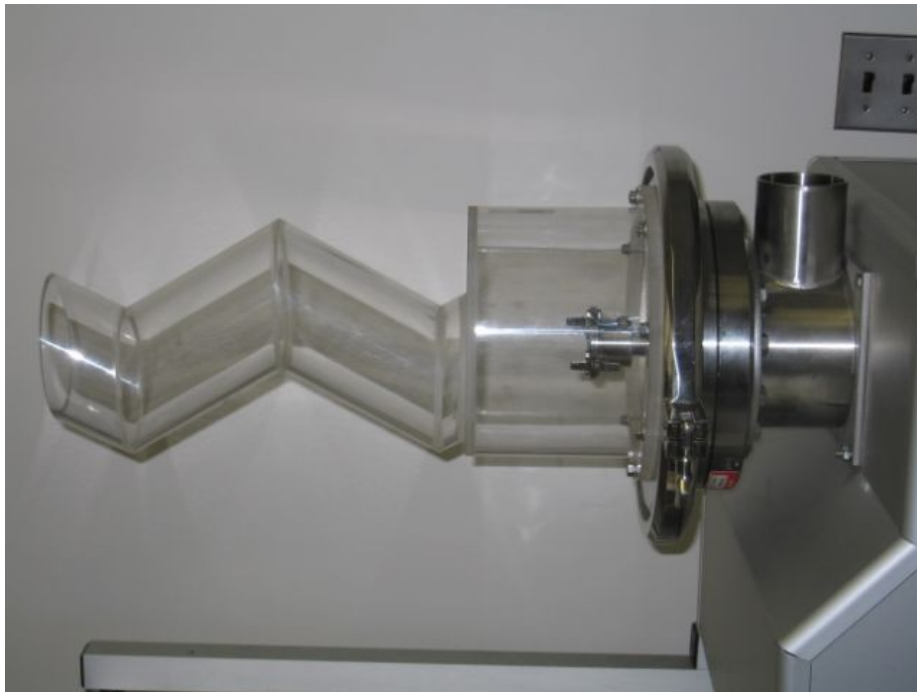


Figure 4-1: Picture of Zigzag Blender

4.1.2 Double Helical Ribbon Blender

A laboratory-scale double helical ribbon blender was designed and fabricated at the MIT Central Machine Shop. The blender, shown in figure 4-2 consists of two concentric helical elements, with the outer helix having twice the pitch of the inner helix. The outer helix was in the direction from inlet to outlet while the inner helix was in the opposite direction. Both these helices sat on a stainless steel shaft mounted inside a perspex cylinder 6" in length and 2" in diameter. As shown in figure 4-2, The cylinder was held fixed at one end by four holding rods connected to a vertical plate that houses a 12 V DC motor driving the shaft of the blender on the other side of the plate. The entire blender unit was placed on top of a Mettler-Toledo weigh-balance to measure the fill weight of the powder in the ribbon blender. A hopper was placed above the inlet of the blender shown in figure 4-2 to minimize the distance between the exit of the feeder and the inlet of the blender.

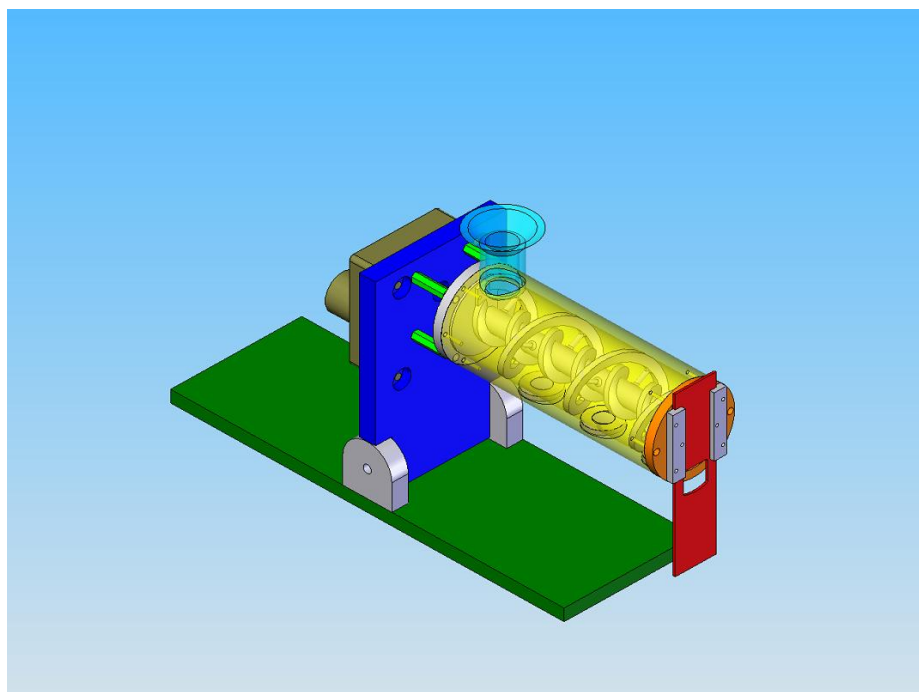


Figure 4-2: Double Helical Ribbon Blender

The double helix was made from a polymeric stereolithographic resin and is placed over the shaft using epoxy polymer and steel pins that hold the helix onto the surface

of the shaft. The length of the blender was chosen to be 6" and the diameter to be 2" by computing the hold-up volume required for an average mean residence time of 30s at 50% fill volume of lactose with a bulk density of 610 kg/m³ at a nominal flow rate of 5 kg/hr. The pitch of the inner helix was set to twice that of the outer helix with the expectation that, for every single rotation of the shaft, the powder in the inner zone would "mix" with 2× the powder in the outer zone giving rise to increased back-mixing. The process of fabricating the helical ribbon constrained increasing the inner pitch any more than twice that of the outer pitch. A clearance of 0.5 mm was kept between the wall of the blender and the outer helical ribbon. A radial clearance of 5 mm was maintained between the two concentric inner and the outer helix in order to have a buffer zone of powder mass where free surface is created due to the opposing movements of the two helices.

The angle of incline of the blender could be set anywhere between -45° to $+45^\circ$ about the plate that holds the blender and the motor in place. Three quartz glass windows are provided at the bottom side of the cylindrical perpeX shell, in order to measure the concentration of components using various analytical techniques. The blender's exit end cap has two open slots through which powder would flow out when the blender is in action. A gate to close either of the exits was present, although, it was never used and the blender was always run with the exit under fully open conditions.

4.2 Powder Feeders

Feeding (dispensing) system plays a very critical role in determining the performance of the overall blending system. An imprecise feeder can cause a blender to underperform, simply because the blender is unable to reduce the variance introduced by the feeder in the inlet stream. Literature suggested that loss-in-weight (LIW) feeders deliver material at very high precision and accuracy at all flow rates. Hence, LIW feeders from Schenck Accurate Inc., Whitewater, WI, were used to feed the excipients and APIs in this work. Schenck Accurate Mechatron[®] feeders were used to feed powders to the Patterson Kelley Zigzag[®] blenders and Tuf-flex[®] feeder was used to feed

the double helical ribbon blender. These feeders consist of counterbalanced hoppers from which helix draws the powder out. An internal control system (Intecont Plus[®]) controls the feeding rate with a PID control algorithm, utilising the weight of the counterbalanced hopper as the response from the system.

The Mechatron[®] feeders delivered three different flow rates ranges: 40 to 60 kg/hr, 0.5 to 5 kg/hr and 0.05 to 1 kg/hr. Different materials were fed at different rates, depending on the concentrations of the ingredients, to the Zigzag[®] blender. The Tuf-flex[®] feeder was rated between 1 and 10 kg/hr and was used to feed only the excipient.

4.3 Sampling and Analytical Techniques

Two non-destructive analytical techniques were used in this work. *Light Induced Fluorescence* works on the principle of excitation and relaxation of electrons from and to ground state molecular orbitals. *Near Infra-red Spectroscopy* works on the principle of vibrational excitation and relaxation of molecules.

4.3.1 Light Induced Fluorescence, LIF

When high energy radiation (like the photons in UV wavelength range of the electromagnetic spectrum) impinge on molecules with high resonance energies (like aromatic-ring containing caffeine and acetaminophen) electrons are excited to higher energy levels [52]. Relaxation of these electrons to lower energy levels occurs by emission of a low wavelength radiation, a process called called *fluorescence*. At low enough concentrations of the fluorescing molecule, the intensity of the emitted radiation is proportional to the concentration of the fluorescing ingredient. Thus, this signal can be used as a proxy for concentration of that ingredient in a mixture, especially a powder mixture. However, this linearity in fluorescent signal to the the concentration is lost at higher concentrations.

An LIF sensor, developed by Lai et al. [52] and manufactured by Honeywell Automation, (Honeywell, Morristown, NJ), was used to measure the concentration of the active ingredient and has been described in detail elsewhere [52]. Caffeine was

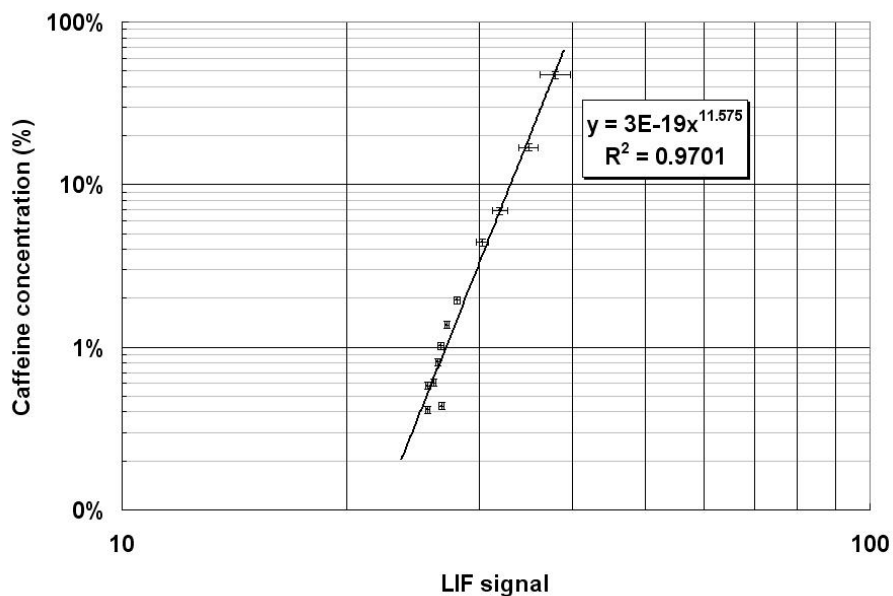


Figure 4-3: Logarithmic LIF Calibration Curve

measured using XF-01 filter sets procured from Omega Filters (Omega Filters, Brattleboro, VT). A fiber optic probe extension was used to reach the quartz glass near the exit under the blender. The LIF signal was calibrated to the concentration of caffeine by shining LIF through a quartz glass window on premixed caffeine and lactose of different concentrations.

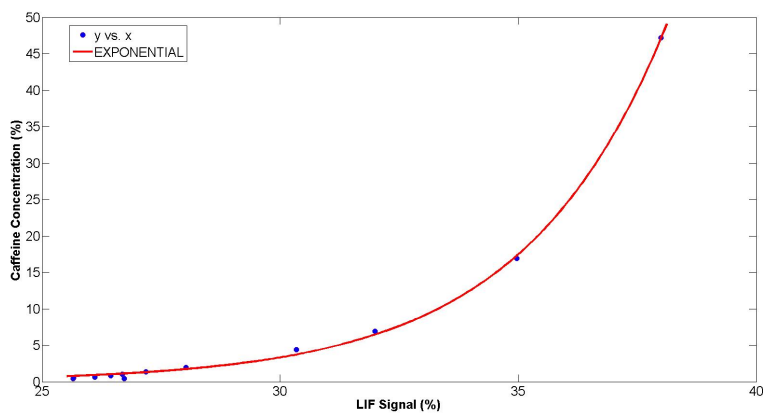


Figure 4-4: Exponential LIF Calibration Curve

The calibration curve was found to be very non-linear and is shown in figures 4-3, 4-4 and 4-5. Two kinds of calibrations were pursued. In the first type, the signal was

directly calibrated to the concentration of caffeine, while in the second type the signal was ratioed with background signal at 100% lactose concentration and this ratio was calibrated with the concentration of caffeine. Figures 4-3, 4-4 and 4-5 show these calibration curves. The calibration equations, parameters and R^2 values are given in table 4.1.

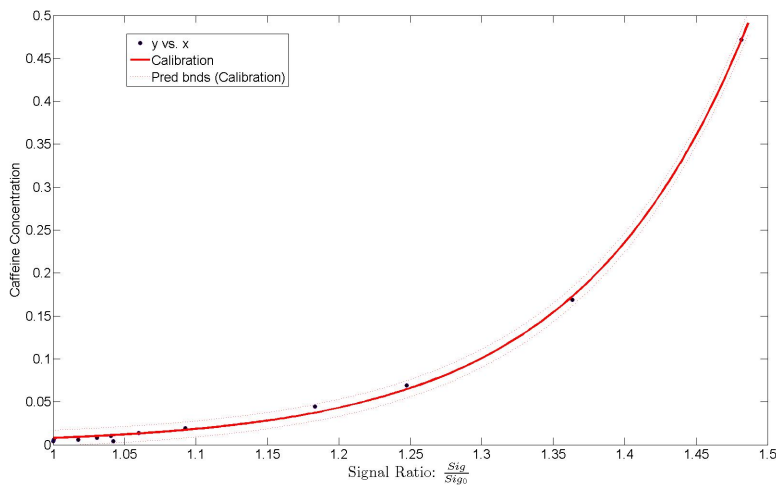


Figure 4-5: LIF Signal Ratio Calibration Curve

Table 4.1: LIF Calibration Parameters

| # | Equation | Parameters | R^2 |
|---|---|--|--------|
| 1 | $C = \alpha Sig^\beta$ | $\alpha = 3 \times 10^{-19}$ $\beta = 11.58$ | 0.9701 |
| 2 | $C = \alpha \exp(\beta \cdot Sig)$ | $\alpha = 1.6 \times 10^{-4}$ $\beta = 0.33$ | 0.9992 |
| 3 | $C = \alpha \exp\left(\beta \frac{Sig}{Sig_0}\right)$ | $\alpha = 1.6 \times 10^{-6}$ $\beta = 8.49$ | 0.9992 |

4.3.2 Near Infra-red (NIR) Spectroscopy

The *Equipartition Theorem* states that the thermal energy of a substance is partitioned equally into translational, vibrational and rotational energy states. Collisions between molecules lead to exchanges in translational energies. When light falls on a substance, some of it is absorbed by the molecules in the substance thereby exciting some of the molecules into higher vibrational energy states. These molecules then

relax from the higher vibrational states by emitting electromagnetic radiation in the Near Infrared (NIR) range. At low concentrations it has been shown by Kubelka and Munk that the absorbance, $\log \frac{1}{R}$, is proportional to the concentration as described by Olinger et al. [78]. R is the reflectance of the light falling on the sample and absorbance is related to the concentration of a component in the mixture. Since every compound has distinct vibrational energy states determined by the chemical structure of the molecule, the NIR spectrum of a mixture carries information on all the components in the mixture.

However, the observed spectra consist of a number of overlapping bands arising from overtones and anharmonicities of the vibrational states. Therefore, the absorbance over the entire near-infrared range $1100 - 2500 \text{ cm}^{-1}$ is measured to capture the spectra of all the components. A calibration curve can be generated relating the NIR spectra to the concentrations. However, as mentioned, the overtones and anharmonicities of the spectra cause considerable analytical errors when multiple linear regression (MLR) is used [108]. Therefore, a partial least squares regression of projections to latent structures (PLS) model is used to calibrate the NIR spectra to concentrations [7, 8, 64].

An Axsun NIR Spectrometer (from Axsun Technologies, Billerica, MA) was employed in the experimental work. The spectrometer consists of a laser light source inside a main block connected to an IntegraSpec[®] integrating sphere via a fiber optic cable. This integrating sphere collects the reflected light and transmits the light through fiber optic cables to the photomultipliers in the main block. The collected intensity is converted to absorbance after ratioing with the background taken using a Spectralon sample (which has a reflectivity of 1.) The collected spectra are processed using multivariate statistics software called SIMCA-P+ (Umetrics Inc., Kinnelon, NJ). Data processing and subsequent analysis is described below.

Partial Least Squares by Projection to Latent Structures (PLS) is used to calibrate the NIR sensor. The experimental technique involved pre-blending mixtures of different APIs and different excipients in a V-blender for half an hour and then taking 25 NIR spectra by dividing the powder from the V-blender into two samples of

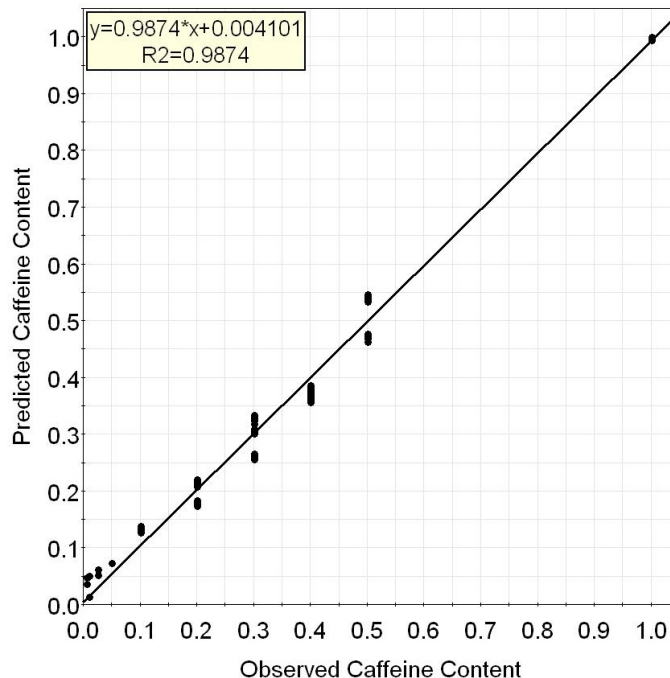


Figure 4-6: PLS Calibration Plot for Caffeine and Lactose DCL14 Mixture

approximately equal weight at the same location as the collection during the blending process. Each of these spectra are first converted scaled to a unit variance, then a first derivative 11 point Savitzky-Golay transform is applied. Following this, a standard normal variate transform is applied. These transformed spectra are devoid of errors arising from changes in density, particle size and external light.

PLS regression on this data model that had R^2 values between 0.95 and 0.98. Figure 4-6 shows an example PLS calibration plots where the predicted and actual concentrations of the mixture are plotted on X and Y axis. The number of terms, R^2 values and Q^2 which is a measure statistically accuracy of the predictions is given in table 4.2

Table 4.2: PLS Calibration of NIR Spectra

| # | API | Excipient | N_{comp} | R^2 | Q^2 |
|---|----------|-----------|------------|-------|-------|
| 1 | Caffeine | DCL 11 | 3 | 0.991 | 0.991 |
| 2 | Caffeine | DCL 14 | 4 | 0.987 | 0.987 |
| 3 | Caffeine | MCC | 2 | 0.973 | 0.973 |

| # | API | Excipient | N_{comp} | R^2 | Q^2 |
|---|---------------|-----------|------------|-------|-------|
| 4 | Acetaminophen | DCL 11 | 1 | 0.99 | 0.99 |
| 5 | Acetaminophen | DCL 14 | 3 | 0.987 | 0.987 |
| 6 | Acetaminophen | MCC | 2 | 0.983 | 0.983 |

Three component calibration was performed by blending varying concentrations of Magnesium Stearate, Caffeine and Lactose DCL-11 in a V-blender for half hour. The mixture was divided into two samples by collecting the powder in the two different legs of the V blender into two different weighing dishes. The powder samples from the blender were placed on the quartz glass window of the ribbon blender and 25 NIR spectra were taken for each sample. The concentration of MgSt was varied between 0.01, 0.02, 0.03, 0.25, 0.5 and 0.75 and caffeine was varied between 0.05, 0.1, 0.2, 0.3 and 0.25, 0.5 and 0.75. The PLS calibration of the multicomponent NIR spectra after pre-processing gave a PLS model with an R^2 value of 0.90 for Caffeine and 0.93 for MgSt as shown in figures 4-7 and 4-8

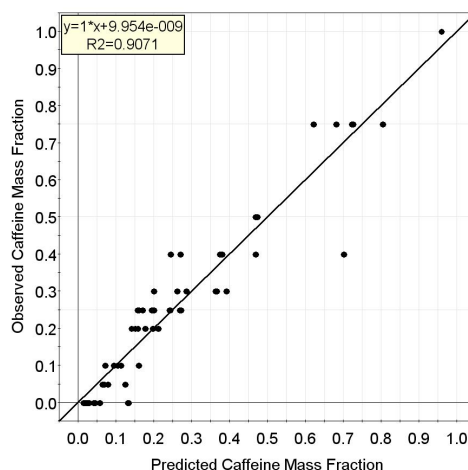


Figure 4-7: PLS Calibration for Caffeine in (Caffeine+Lactose+MgSt) Three Component System

It was hypothesized that the pre-blended powder mixture had not achieved steady state in the batch V-blender due to the presence of MgSt due to inadequate blending time. This was expected to have caused the calibration model to yield an unsatis-

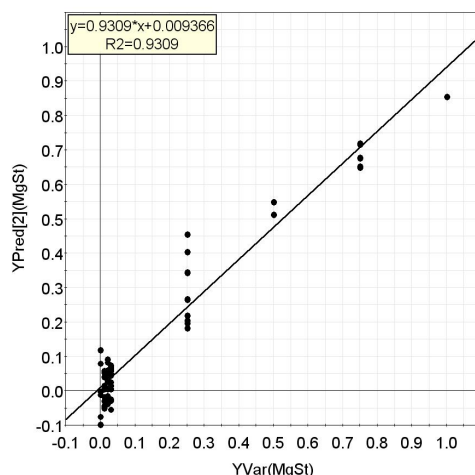


Figure 4-8: PLS Calibration for MgSt in (Caffeine+Lactose+MgSt) Three Component System

factory calibration model. Therefore, it was decided to pursue a different method of data analysis for three-component systems and this method has been described in detail in §5.2.3 and §7.2.3.

4.3.3 Ultra-Violet Absorption Spectroscopy

In solution, UV light is absorbed by chemical substances that contain highly conjugated π -electrons. The absorbed UV light promotes the electron in Highest Occupied Molecular Orbital (HOMO) to the Lowest Unoccupied Molecular Orbital (LUMO). Each chemical substance that is characterized by this absorption, called a *chromophore*, has a maximum absorbance at a certain wavelength. At low concentrations, the absorbance is proportional to the concentration of the chromophore in the solution. This linearity is also known as Beer's law is shown in figure 4-9 for caffeine solution in water at 272 nm. Powder mixtures are dissolved in de-ionized water and diluted sufficiently to reach the linear range of UV absorption spectrometry in order to measure the concentration of the chromophore in the mixture.

A HP8452 UV-Visible Spectrophotometer (Hewlett Packard, Palo Alto, CA) was used in this work. The cuvettes transparent in the UV range (CD-UV1S square cuvettes from Ocean Optics Inc., Dunedin, FL) were used for holding the liquid samples

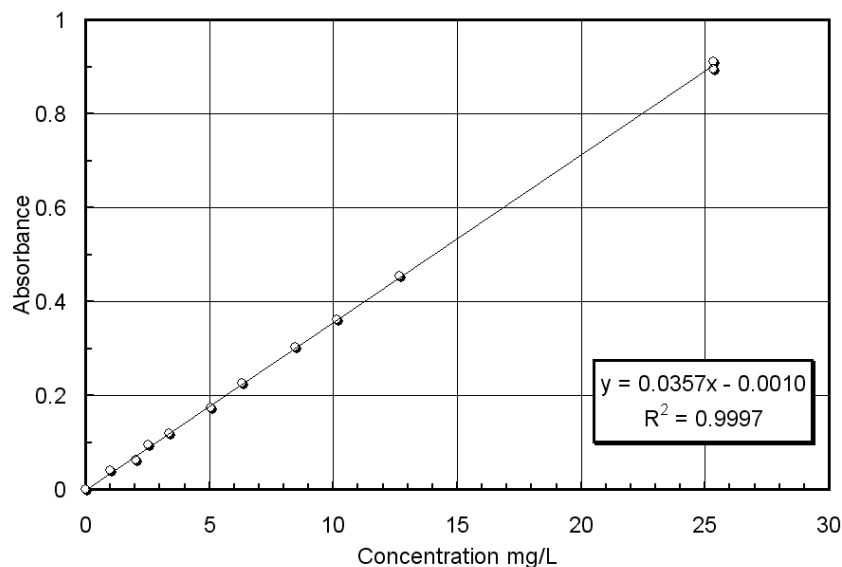


Figure 4-9: UV Calibration of Caffeine in Water (272 nm)

in the spectrometer. Dissolution was performed in a *Distek Dissolution System 2100B* (Distek Inc., North Brunswick, NJ).

4.4 API and Excipients

All pharmaceutical products contain one or more active pharmaceutical ingredients (API) that delivers the desired pharmaceutical action on the body. In addition inactive ingredients, called excipients are added for a variety of reasons. There are many different types of excipients used in the industry and are listed below along with the reasons for using them.

1. *Fillers* make up the bulk of the tablet or capsule. Cellulosic derivatives and plant cellulose are generally used as fillers.
2. *Binders* keep the tablet together intact in the form it is made and holds the different components together. starches, sugars, lactose and alcohol derivatives of sugar like mannitol are some popular excipients.
3. *Lubricants* or Glidants are fine particles that coat the powder to aid flow of powders as well as ejection of tablets from compression dies. Fatty acids and

their salts like magnesium stearate and silica are a few popular lubricants.

4. *Coatings* prevent attack of tablets by moisture and aid in consumption of tablets by changing their taste. Coatings are usually cellulose derivatives and sometimes made up of proteins from corn
5. *Flavors, Colors and Sweeteners* are added in small quantities to enhance the look, feel and taste of the tablet or capsule and usually do not serve any other purpose.

Domike [25] and Ngai [71] have studied the interparticle forces of adhesion for caffeine and popularly used excipients in the pharmaceutical industry, micro-crystalline cellulose and lactose. As one of the goals of the project is to understand the effect of microscopic properties of powders on the macroscopic phenomena in continuous blending, the choice of API and excipients was made based on the availability of experimentally determined microscopic properties like cohesion, adhesion surface energies and friction coefficients of powders. Table 4.3 shows the various properties of relevance of individual powders used in this work. The mean and standard deviations of the cohesion energies per unit area are shown under μ and σ respectively.

4.4.1 Caffeine

Anhydrous Caffeine (1,3,7-trimethyl Xanthine) is a xanthine alkaloid and a central nervous system stimulant. USP grade caffeine powder was obtained from Sigma Aldrich (Sigma Inc., St. Louis, MO.) Caffeine is a white powder that has a melting point of 238°C. ESEM pictures of caffeine particles are shown in [71]. Caffeine is an irregularly shaped particle that has particle size of 196 μm with a very large standard deviation of about 100 μm . Caffeine is not a free flowing powder and usually agglomerates in the presence of atmospheric moisture. Therefore, caffeine was manually de-agglomerated before all experiments. The density of caffeine varied between 0.41 g/cc and 0.53 g/cc depending on whether the caffeine powder was outside exposed to the atmosphere for a long time (overnight) or was freshly removed from an air-tight container. The mass-volume curve is shown in figure 4-10.

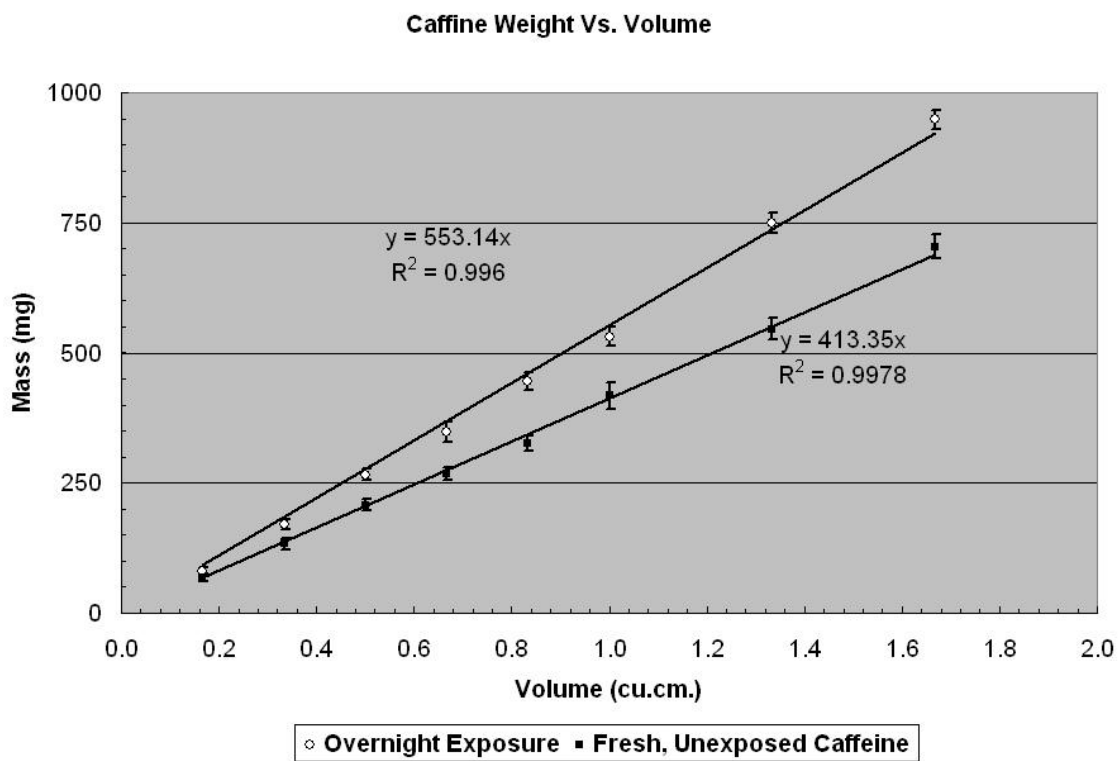


Figure 4-10: Mass Volume Curve for Caffeine Stored Outside and Inside an Airtight Container

4.4.2 Acetaminophen

Acetaminophen (N-(4-hydroxyphenyl)-Acetamide) is widely used as an analgesic and anti-pyretic and is the active ingredient in the popular OTC drug Tylenol[®]. Acetaminophen was obtained from Sigma Aldrich (Sigma Inc, St. Louis, MO) and is a white powder with a melting point of 169°C. Acetaminophen has a bulk density of 1.293g/cc. Acetaminophen agglomerates in the presence of moisture and anhydrous acetaminophen was used in all the experiments. Acetaminophen, too, was de-clumped as and when required.

4.4.3 Lactose

Lactose (a disaccharide that consists of β -D-galactose and β -D-glucose molecules bonded through a β 1-4 glycosidic linkage, 4- α - β -D-pyranosyl D-Glucose) is a white powder that is found in both amorphous and crystalline forms depending on the process of synthesis. Spray dried lactose usually gives spherical particles, that has superior flow characteristics and at the same time is cohesive enough to act as a binder in the tablet. Two grades of direct compressible lactose (DCL) have been used in this work. Both these grades were procured from DMV-International (DMV-Fonterra Excipients, Delhi, NY). The bulk density of both the grades of lactose was 0.61g/cc. Lactose is less cohesive than microcrystalline cellulose with a mean cohesion surface energy of 0.52 and a standard deviation of 0.41 mJ/m².

1. *Direct Compressible Lactose (DCL) - 11* has a mean particle size of 100 μ m with a standard deviation of 50 μ m with a log-normal distribution. DCL-11 is spray dried lactose and contains a mixture of α -lactose monohydrate crystals with some amorphous lactose. DCL-11 consists of spherical particles that has very good flow characteristics. However, DCL-11 possesses the tendency of caking in the presence of moisture and gravity. This mild caking tendency was not a problem in delivering the material through the Schenck Accurate[®] feeder since the design of the feeder takes this caking into account and the hopper walls in the feeder massaged the powder thereby breaking the agglomerates. An SEM

image of DCL-11 is shown in [24].

2. *Direct Compressible Lactose (DCL) - 14* has a mean particle size of $110\ \mu\text{m}$ with a standard deviation of $70\ \mu\text{m}$ with a log-normal distribution. DCL-14 is also a spray-dried grade of lactose consisting of a mixture of α -lactose monohydrate crystals mixed with greater proportions of amorphous lactose. While the characteristics of this grade of lactose is similar to that of DCL-11, the particle sizes distribution is considerable wider. DCL-14 posed a reduced risk of caking in the feeder due to the presence of a wider distribution of particles reducing the possibility of increased stresses in the material. For some of the experiments, DCL 14 was sieved into powders of two different particle size ranges $40 \leq D_{50} \leq 150\ \mu\text{m}$ and $150 \leq D_{50} \leq 250\ \mu\text{m}$. Both these powders were evaluated for the effect of particle size on blending. An SEM image of DCL-11 is shown in [24].
3. *HMS Impalpable Lactose* has a mean particle size of $90\ \mu\text{m}$. HMS Impalpable lactose is α -lactose monohydrate in amorphous form. It is non-spherical and has a higher surface area compared to other grades of lactose. HMS lactose flows very irregularly and agglomerates very easily. These powders were tested in both types of blenders in this work. The powder due to its inability to flow easily clogged the ribbon blender, but performed very well in the Zigzag[®] blender. The powder required considerable amount of shear forces to mobilize and the the Zigzag[®] blender supplied the required energy to move and blend this excipient.

4.4.4 Microcrystalline cellulose

Cellulose is a biopolymer present widely present in plants and plant extracts. Cellulose is a long chain polymeric polysaccharide carbohydrate of β -D-Glucose, is generally used as a filler in tablets. Microcrystalline Cellulose facilitates quicker disintegration of tablets exposing the API to the liquids in the body in addition to acting as a undigested dietary fiber. Two grades of cellulose were used in this work. MCC

comparatively more cohesive than lactose. The cohesive surface energy of MCC has a mean of 1.58 and standard deviation of 0.96 mJ/m².

1. Avicel[®] microcrystalline cellulose PH-102 has a mean particle size of 100 μm is an irregular sized particle with a flat flaky microscopic structure as shown in the ESEM picture figure 4-11. Avicel[®] was procured from FMC Biopolymer(FMC Biopolymer, Philadelphia, PA) and has bulk density of 0.3 g/cc. Avicel[®] flow behavior is very erratic and is highly influenced by moisture. In the absence of moisture, electrostatic forces on Avicel[®] particles cause it to flow erratically. Avicel[®] usually has a moisture content of 3 – 5% by weight.

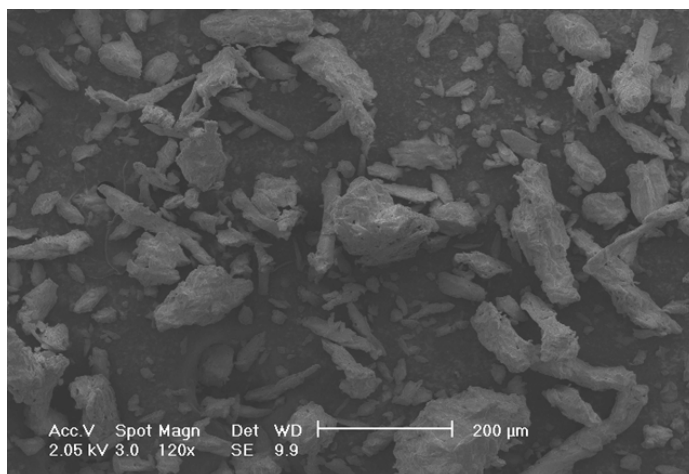


Figure 4-11: ESEM of Avicel MCC PH102

2. Celphere[®] microcrystalline cellulose CP-102 has a mean particle size of 150 μm is a spherical particle as described in [31]. Celphere[®] was procured from Asahi Kasei (Asahi Corp., Tokyo, Japan) and has bulk density of 0.83 g/cc. Celphere[®] flow behavior is less erratic than Avicel. However, Celphere[®] is less frequently used in the pharmaceutical formulations than Avicel[®]/

4.4.5 Magnesium Stearate, MgSt

Magnesium Stearate (MgSt) is a white amorphous powder comprising of fine particles in the size range 20 to 70 μm . It is a generally recognized as safe (GRAS) substance and is sourced from vegetable oil or animal fat. The MgSt used in all our experiments

were vegetable sourced and were procured from Sigma Aldrich (Sigma, St. Louis, MO). MgSt is used as a lubricant in the pharmaceutical industry and aids in the flowability of powders. It also aids in the ejection of the table from the tablet die and acts by coating the surface of the die with fine particles of MgSt which reduce the cohesive forces between the tablet and the die wall [101].

Table 4.3: Properties of APIs and Excipients Used

| Material | Particle Size | | Bulk Density g/cm^3 | Cohesion Energy $\mu mJ/m^2$ | Melting Point $^{\circ}C$ | Refs. |
|--------------------|---------------|-------------------|--------------------------|---------------------------------|------------------------------|--------------|
| | $\mu_V \mu m$ | $\sigma_V \mu mm$ | | | | |
| Caffeine | 196 | 100 | 0.413 | 0.43 | 238 | [71, 37] |
| Acetaminophen | 110 | n.a. ¹ | 1.293 | 0.65 | 169 | [71, 37] |
| Lactose DCL-11 | 100 | 50 | 0.61 | 0.21 | - ² | [71, 60, 24] |
| Lactose DCL-14 | 110 | 70 | 0.61 | 0.21 | - | [71, 60, 24] |
| MCC Avicel® | 100 | - | 0.3 | 1.58 | - | [71, 31] |
| MCC Celphere® | 150 | - | 0.83 | 1.58 | - | [71, 20] |
| Magnesium Stearate | 50 | 30 | n.a | 0.22 | - | [101] |

End of Table

¹Not Available

²Not measured

4.5 Flow Behavior Experiments

Simple impulse response experiments with an impulse input of the active ingredient in a continuous blender where the excipient is constantly flowing through the system can be used to compute the residence time distribution of the active in the blender. This residence time distribution can then be abstracted to a fewer set of parameters like the Axial Dispersion Coefficient (or simply Dispersion Coefficient, \mathcal{D}) and the velocity (or space time if length of the blender is fixed, also called the Transport Coefficient, \mathcal{T}) which is useful in comparing and understanding the mobility of the active ingredient in the blender.

4.5.1 Axial Dispersion Model

In axially mixed systems, such as a double helical ribbon blender and rotating drum blender, the residence time distribution can be modeled using an axial dispersion model [81, 104, 103, 48]. In moderate to high shear mixing systems like the Nautamix[®] and the Zigzag[®] blenders, the residence time distribution normally follows a ideal blender followed by plug flow blender model [47].

Axial dispersion model given by equation 2.8 describe the movement of powders in axially mixed systems. Following Fogler [32] non-dimensionalized this Fokker Planck Equation using, $\theta = \frac{tV}{L}$, $\zeta = \frac{x}{L}$, $\Psi = \frac{C}{M/V}$ and $Bo = \frac{VL}{\mathcal{D}}$, where Bo is the Bodenstein number (Peclet number for liquids), L is the length of the mixer and V is the average (mean) velocity of the powder in the mixer, we get equation (4.1).

$$\frac{\partial \Psi}{\partial \theta} = -\frac{\partial \Psi}{\partial \zeta} + \frac{1}{Bo} \frac{\partial^2 \Psi}{\partial \zeta^2} \quad (4.1)$$

The initial condition for solving this equation is given by.

$$\Psi(0^+, 0) = 0 \quad (4.2)$$

We can solve this PDE given the boundary conditions for an impulse input. There are three different kinds of boundary conditions called the Danckwerts' Boundary

Conditions.

4.5.1.1 Closed-Closed Boundary Condition

When dispersion does not occur both upstream and downstream of the mixing section in a blender (i.e. points upstream to tracer addition and downstream to tracer measurement), the boundary conditions are called closed-closed boundary conditions. Mathematically this is represented by,

$$\left[-\frac{1}{Bo} \frac{\partial \Psi}{\partial \zeta} \right]_0 + [\Psi]_0 = 1 \quad (4.3)$$

$$\left[\frac{\partial \Psi}{\partial \zeta} \right]_1 = 0 \quad (4.4)$$

Using the closed-closed boundary conditions in equations (4.3) and (4.4), and the initial condition from equation (4.2), the dispersion equation (4.1) can only be solved numerically.

4.5.1.2 Open-Open Boundary Condition

Dispersion occurs both upstream and downstream of the mixing section in a blender (i.e. points upstream to tracer addition and downstream to tracer measurement), the boundary conditions are called open-open boundary conditions. Mathematically this is represented by,

$$\left[\frac{\partial \Psi}{\partial \zeta} \right]_{0+} = \left[\frac{\partial \Psi}{\partial \zeta} \right]_{0-} \quad (4.5)$$

$$[\Psi]_{0+} = [\Psi]_{0-} \quad (4.6)$$

$$\left[\frac{\partial \Psi}{\partial \zeta} \right]_{1+} = \left[\frac{\partial \Psi}{\partial \zeta} \right]_{1-} \quad (4.7)$$

$$[\Psi]_{1+} = [\Psi]_{1-} \quad (4.8)$$

Using the open-open boundary conditions in equations (4.5) to (4.8), and the initial condition from equation (4.2), the dispersion equation (4.1) be solved under certain conditions to give the concentration at the exit of the blender $E(t) =$

$\Psi (\zeta = 1, \theta = \frac{t}{\tau})$.

$$E(t) = \frac{1}{2\tau \sqrt{\left(\frac{\pi}{Bo}\right) \left(\frac{t}{\tau}\right)^3}} \exp\left(-\frac{\left(1 - \left(\frac{t}{\tau}\right)\right)^2}{\left(\frac{4t}{\tau Bo}\right)}\right) \quad (4.9)$$

This model is true only if the length of the blender is considerably larger than the characteristic length of dispersion. In many of the real blending cases, this condition is satisfied. The most important parameter in this model is the Bodenstein number and can be estimated by performing non-linear regression of the observed response to a unit impulse in the continuous blender.

4.5.2 Determination of Residence Time Distribution

The response from Impulse response experiments are usually concentration curves as a function of time, beginning with time $t = 0$ when the tracer (API in the case of determining RTD of blending of powders) is introduced. The concentration curves can be converted to residence time distribution and the mean residence time by two different methods. In the first method, both the RTD and mean residence time can be computed using the equations (4.10) and (4.11).

$$E(t_i) = \frac{C(t_i)}{\sum_i C(t_i)(t_i - t_{i-1})} \quad (4.10)$$

$$\langle t \rangle = \sum_i t_i E(t_i)(t_i - t_{i-1}) \quad (4.11)$$

Alternatively, we can estimate the space time τ of the tracer (API) and the Bodenstein number Bo in the blender by using equation (4.9), but by taking into account a multiplying factor A that converts concentration curves into residence time distribution. We note that parameter A is a measure of the area under the concentration curve given by the denominator in the equation (4.10). Therefore, we can use the concentration curves to estimate A , τ and Bodenstein number (or \mathcal{D}) at the same time as shown in equation (4.12)

$$C(t) = \frac{A}{2\tau \sqrt{\left(\frac{\pi}{Bo}\right) \left(\frac{t}{\tau}\right)^3}} \exp\left(-\frac{\left(1 - \left(\frac{t}{\tau}\right)\right)^2}{\left(\frac{4t}{\tau Bo}\right)}\right) \quad (4.12)$$

4.5.3 Summary

The approach, therefore, consisted of measuring the impulse response of the continuous blending system, modeling the residence time distribution with simple RTD models, like Axial Dispersion models, and subsequently predicting the variance reduction ratios for sinusoidal and other kinds of inputs to the blender. Experiments will be performed with different combinations of excipients and APIs in order to understand the effect the cohesive and adhesive forces on the behavior of powders in continuous blenders.

4.6 Blending Experiments

Two component and three component blending experiments can be carried out to assess the performance of a continuous blending system. Literature suggested that a continuous blender mixing non-segregating, non-cohesive powders can reduce variance introduced by disturbances of time periods less than the mean residence time of the continuous blender. A model for the blender would relate the performance of the blender to the flow behavior in the blender and the input characteristics at the feeder.

4.6.1 Theoretical Variance Reduction Ratio

The variance reduction ratio of a continuous dry powder blender with a residence time distribution $E(t)$ and a feeding input with autocorrelation $R(t')$ is given by equation (2.3). The output of a continuous blending system depends on the forcing function (feeding input) and the system response of the blender to that forcing function. In other words, one other way to arrive at equation (2.3), is by taking the convolution integral of the input forcing function, $C_{in}(t)$ and RTD, $E(t)$ and subsequently taking the variance ratio at steady state of the output.

$$C_{out}(t) = E(t) \otimes C_{in}(t) \quad (4.13)$$

$$\Rightarrow C_{out}(t) = \int_0^t E(t') C_{in}(t-t') dt' \quad (4.14)$$

$$= \int_0^t E(t-t') C_{in}(t') dt' \quad (4.15)$$

$$VRR = \frac{var(C_{out,ss}(t))}{var(C_{in}(t))} \quad (4.16)$$

When the blender is an ideal blender, the residence time distribution follows an exponential decay as discussed by Danckwerts [21] and given by equation (4.17). For a sinusoidal forcing function, given by equation (4.18), we can compute the autocorrelation from equation (2.2) to give:

$$E_{ideal}(t) = \frac{1}{\tau} \exp\left(-\frac{t}{\tau}\right) \quad (4.17)$$

$$C_{in}(t) = b \sin\left(2\pi \frac{t}{t_d}\right) \quad (4.18)$$

$$R_{in}(t') = \frac{\lim_{T \rightarrow \infty} \frac{1}{T} \int_0^T C_{in}(t) C_{in}(t+t') dt}{\sigma^2} \quad (4.19)$$

$$\Rightarrow R_{in}(t') = \cos\left(2\pi \frac{t'}{t_d}\right) \quad (4.20)$$

Then, we can use either equation (4.15) with (4.16) or equation (4.20) with (2.3) and compute the VRR to be:

$$VRR_{sin} = 1 + \left(\frac{\tau}{t_d}\right)^2 \quad (4.21)$$

where $\tau = \frac{W}{F}$ is the space time of the blender, W is the fill weight of the blender, F is the flow rate of the powder in the blender, t_d is the time period of the forcing function (disturbance) entering the blender. As we see from equation (4.21), the Variance reduction ratio is proportional to the residence time and inversely proportional to the time period disturbance. Equation (4.21) suggests that an ideal blender behaves as a first order low pass filter, allowing disturbances with time periods greater than

space time (τ , which in this case is the mean residence time too) to pass through the blender. All disturbances whose time-periods are lesser than τ , the blender reduces the fluctuations at those frequencies as shown in figure 4-12.

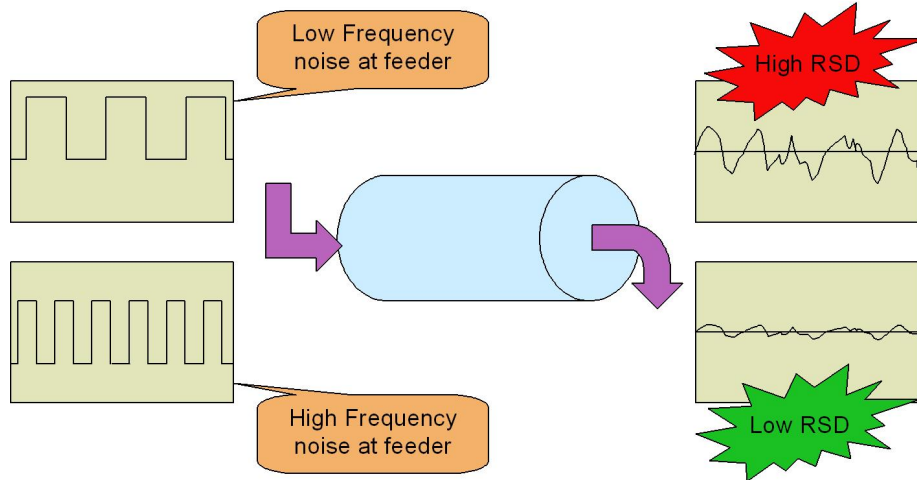


Figure 4-12: Effect of Input Fluctuation

4.6.2 The Random Mixture Limit

However, powders are made up of discrete particles and arranging them in a uniform mixture with a variance of zero takes an inordinate amount of energy. Also, once this uniform state is achieved any force acting on the powder mixture will tend to destabilise the mixture and cause the mixture's variance to increase. Lacey [51], proved the existence of a limit to which powders can be mixed and called this limit an “ideal” random mixture shown in figure 2-2. In an ideal random mixture, the distribution of the components is determined by simple random chance and hence is the best mixture one can achieve by imparting energy to a completely segregated mixture. Lacey showed that the variance of the random mixture and a completed segregated mixture is given by equations (4.22) and (4.23) respectively,

$$\sigma_{rand}^2 = \frac{pq}{n} \quad (4.22)$$

$$\sigma_{seg}^2 = pq \quad (4.23)$$

where p and $q = 1 - p$ are the number fractions of the particles of components 1 and 2 and n is the number of particles in a single sample from the mixture whose variance is being determined. Equation (4.22) considers the particles in a powder mixture to be monodisperse of a single particle size. Stange [95] modified this equation (4.22) for powders with a particle size distribution and showed that the random mixture variance for components 1 and 2 with coefficient of variance in particle sizes $c_p = \frac{\sigma_p}{m_p}$ and $c_q = \frac{\sigma_q}{m_q}$ are given by equation (4.24)

$$\sigma_{rand}^2 = \frac{pq}{M} [p m_q (1 + c_q^2) + q m_p (1 + c_p^2)] \quad (4.24)$$

where M is the mass of the particles in a single sample, σ_p & σ_q and m_p & m_q are the standard deviation and mean value estimates of the particle size distributions of components 1 and 2 respectively.

Therefore, we see that the variance reduction ratio in equation (2.3) has a limit determined by the random mixture and hence the variance reduction ratio with this random mixture limit becomes,

$$\frac{1}{VRR} = 2 \int_{t=0}^{\infty} \int_{\tau=0}^{\infty} E(t) E(t + \tau) R(\tau) d\tau dt + \frac{\sigma_{rand}^2}{\sigma_{in}^2} \quad (4.25)$$

4.6.3 Summary

Therefore, two component blending experiments were carried out in continuous blenders and where possible, theoretical modeling of the VRRs from RTD models was carried out using the equations described above. The excipients and active ingredients described in §4.4 were used in the blending experiments. The effects of operational variables and particle (raw material) properties were delineated by experimental observations on continuous blending. The predictions of performance from equation (4.25) were compared with the experimental blending performance thereby validating the modeling of the continuous blending process.

Chapter 5

Patterson Kelley Zigzag Blender

As mentioned in the §4.5 and §4.6 two types of experiments were performed on the Patterson Kelley Zigzag[®] blender. Flow behavior experiments were used to determine the RTD of the API in the blender. Blending experiments were performed to examine the effect of operational variables on the performance of the blending process.

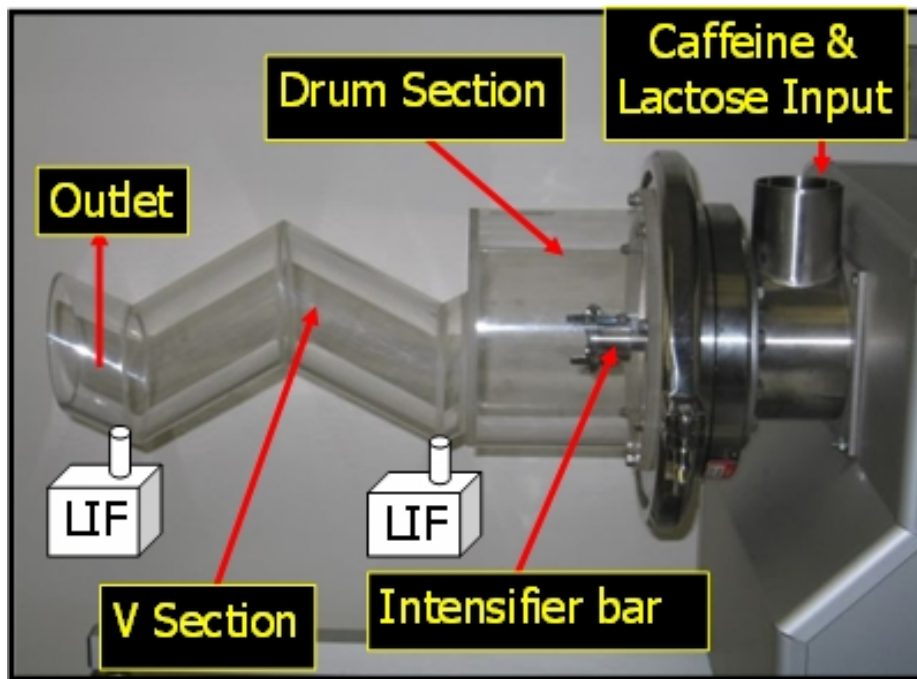


Figure 5-1: Zigzag Blender with LIF Sensors

The experimental set up is shown in figure 5-1 with the lactose and caffeine inputs and LIF sensor locations. Two quartz glass windows were mounted on the wall of the Zigzag[®] blender right in front of the locations of the LIF in figure 4-1. The LIF

sensor was triggered by a metallic detector that triggered the proximity sensor of the LIF unit. The data was collected on two computers that communicated with the RF devices of the two LIF units separately.

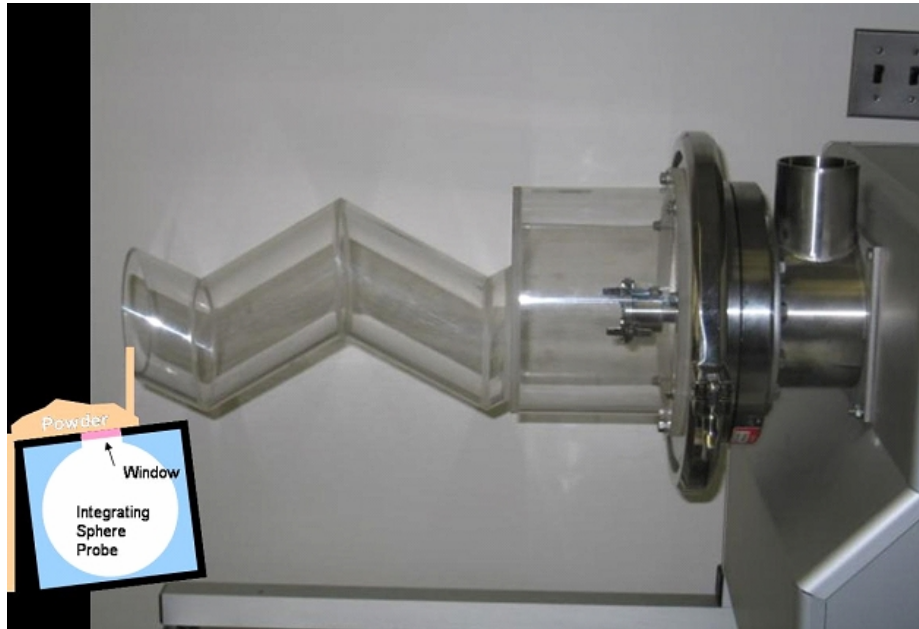


Figure 5-2: Schematic of the Placement of NIR sensor on the Zigzag Blender, courtesy: Bart Johnson, Axsun Tech. Inc.

The experimental set up was slightly modified when LIF and NIR sensors were incorporated at the end of the blender. As shown in figure 5-2 and 5-3, the NIR sensor was placed beneath a quartz glass plate adjacent to the LIF sensor. An air nozzle operated by a solenoid valve and controlled by a computer communicating with the NIR sensor was placed above the quartz glass window as shown in figure 5-3. The solenoid valve purged the quartz glass with a compressed air burst to remove the powder from the surface of the quartz glass. This air purge was triggered after at 3 second delay of the NIR sensor scan. The total scan time (inclusive of the collection of three spectra) of the NIR sensor was 5 seconds and hence the collection frequency was 0.2 Hz.

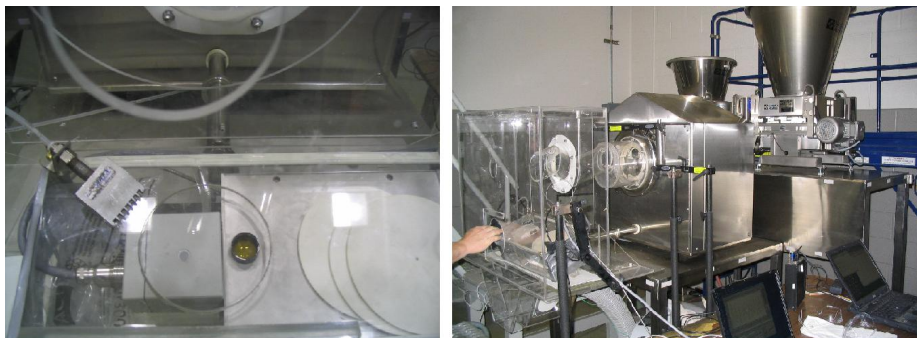


Figure 5-3: NIR Setup on the Zigzag Blender

5.1 Flow Behavior Experiments

Investigation of flow behavior was done in two parts. In the first part, steady state in the blender was confirmed. In the second part the flow behavior was determined by RTD experiments.

5.1.1 Confirmation of Steady State

In all the residence time distribution experiments performed, the output from the blender was collected for a period of 10 minutes and the mass of the powder collected was measured. This was compared with the total flow rate fed into the blender. The equivalence of the input and output flow rates was assumed to indicate achievement of steady state.

5.1.2 RTD Experiments

Determination of flow behavior through residence time experiments were performed with caffeine as the API and HMS Impalpable Lactose as the excipient. The total throughput was fixed at 50 kg/hr and a shot of caffeine corresponding to 3% of the lactose present in the blender over a period of $3 \times$ the mean residence time (estimated from flow rate and theoretical fill volume from the vendor) was administered. The concentration of the API at the end of the drum section and at the exit of the Zigzag[®] was monitored using an LIF sensor. The LIF sensor was configured in such a way that it would be triggered when the quartz glass window described in §4.1 passes directly in front of the LIF sensor collection window.

The intensifier bar rotation rate was varied between 1500 and 3000 RPM and the external shell rotation rate was varied between 25 and 50 RPM. The concentration of the API (caffeine) was changed from 1% to 3%. These three factors were changed in a full factorial design, with one repeat and one center point. The LIF responses, however, could not be converted to concentrations since a priori calibration of the LIF signal with concentration was not carried out with the Zigzag[®] blender.

5.1.3 Analysis of Data

In confirming achievement of steady state, the mass of the powder collected 15 minutes after feeding the impulse shot of caffeine was collected for ten minutes. The flow rate was computed and compared with the total mass flow rate through the blender.

Since, LIF calibration was not carried out on the impulse response data, raw LIF data from those experiments were statistically regressed with an empirical residence time distribution and these results were graphically presented to understand the spread and dead volume in the blender. However, LIF data from blending was used to determine the residence time distribution, by converting the blending data from LIF to concentrations by using an exponential fit of the ratio of the LIF signal to the LIF signal for the pure excipient (0% API). The exponential calibration parameters for each run were determined separately and the data was converted to concentrations.

In order to model the residence time distribution at the exit of the Zigzag[®] blender two models were employed. The first model was a log-normal distribution that was used for RTD obtained from impulse response experiments, shown in equation (5.1). This empirical distribution was regressed statistically based on the observations on the data.

$$E(\theta) = \frac{1}{\theta \sigma \sqrt{2\pi}} \exp\left(-\frac{(\log(\theta) - \mu)^2}{2\sigma^2}\right) \quad (5.1)$$

Another RTD model was used for determining the residence time distribution from blending data (from varying throughput experiments). This model consisted of a plug flow (delay) and mixed flow (ideal) blender in series was used. It was expected

Mean Residence Time

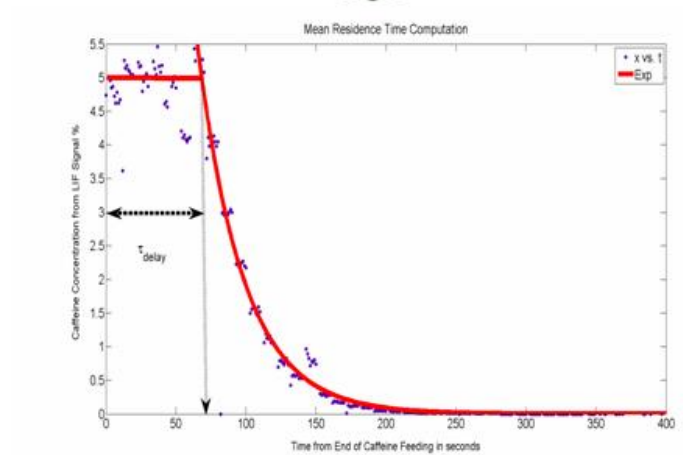


Figure 5-4: RTD of Plug Flow and Ideal Mixer in Series

that the drum section and the V-section would act as an ideal and plug flow blender respectively. This is graphically depicted in 5-4 and the equation for this residence time distribution is given in equation (5.2).

$$E(t) = \frac{1}{\tau_d} \exp\left(-\frac{t - \tau_v}{\tau_d}\right) \quad (5.2)$$

where τ_d is the residence time in the drum section (corresponding to the residence time in the ideal blender and τ_v is the residence time in the V-section of the blender.

5.2 Blending Experiments

Three sets of blending experiments were performed in the Zigzag[®] blender. In the first set, caffeine and HMS impalpable lactose were mixed while the operational variables like shell and intensifier bar rotation rates and caffeine content in the blend were varied in the experimental design. In the second set of experiments, caffeine and HMS lactose were blended with variations in the overall throughput rate and external shell rotation rate. In the final set of experiments, caffeine, lactose and magnesium stearate were blended in the Zigzag[®] blender.

5.2.1 Two Component Blending

Caffeine and HMS impalpable lactose were mixed in the Zigzag[®] blender. Similar to the residence time distribution experiments on the Zigzag[®] blender, the total throughput (flow) rate was maintained constant at 50 kg/hr. The angle of incline of the blender was fixed at 0°. In all two component blending experiments, 15 – 20 gm samples at 3 minute intervals were collected at the exit of the blender. LIF sensor was used to monitor the progress of the blending system.

5.2.1.1 Varying Rotation Rates

In this set of experiments, a 2-level, 3-factor full factorial experimental design was created by changing the external shell rotation rate from 25 to 50 RPM, the internal intensifier bar rotation rate 1500 to 3000 RPM and the caffeine content from 1% to 3% by weight. Two LIF sensors were placed as shown in figure 5-3, one at the end of the drum section and one at the end of the V section. Quartz glasses were mounted to let the UV light through the walls for exciting the powder. A metallic plate on the blender triggered the LIF sensor to radiate the sample with UV light and collect the ensuing fluorescent response. This ensured that the LIF collected one data point per rotation of the blender.

15 to 20 g powder samples were collected at the exit of the blender. These were weighed and dissolved in 500 mL of de-ionized water in the Distek[®] dissolution system. Lactose and caffeine are both soluble in water and the solution diluted 20 \times , 30 \times and 40 \times depending on the expected concentration of caffeine in the powder mixture. The expected concentrations of caffeine in the powder mixture were estimated from the mean concentration of caffeine at steady state for samples collected at steady state, $\frac{1}{2}\times$ this mean concentration for samples collected during the transient period, and 0% caffeine concentration for the samples collected before caffeine flow rate was started and after the caffeine flow rate was cut off. The concentration of caffeine in solution was determined by UV absorption spectroscopy using the calibration curve described in §4.3.

5.2.1.2 Varying Throughput

In this set of experiments, a 3-level, 2-factor full factorial experimental design was created by changing the external shell rotation rate between 37.5, 50 and 75 RPM and the total throughput (flow rate) between 40, 50 and 60 kg/hr. The intensifier bar rotation rate was fixed at 3000 RPM, so was the angle of incline at 0° and the caffeine content at 3%. For this set of experiments, the powder was allowed to fall on a quartz glass plate below which a LIF sensor was placed to collect the fluorescent response as shown in figure 5-1. The calibration curve #3 in §4.3 and in table 4.1 was used to convert LIF signal to caffeine content. The LIF sensor collection frequency was set at 1 Hz.

15 – 20 g powder samples were collected at 3 minute intervals at the exit of the blender. These samples were then weighed and dissolved in 500 mL of de-ionized water in the Distek[®] dissolution system. Similar to the experiments on varying rotation rates, the solutions were diluted to 20 \times , 30 \times and 40 \times depending on the expected concentration of caffeine in the powder mixture. The expected concentrations of caffeine in the powder mixture were estimated from the mean concentration of caffeine at steady state for samples collected at steady state, $\frac{1}{2}\times$ this mean concentration for samples collected during the transient period, and 0% caffeine concentration for the samples collected before caffeine flow rate was started and after the caffeine flow rate was cut off. For some solutions, the linear range was achieved only at 80 \times the dilution in de-ionized water at dissolution. The concentrations of caffeine in the diluted solutions were determined by UV absorption spectroscopy using the calibration curve described in §4.3.

5.2.2 Three Component Experiments

Pharmaceutical dry powder blending involves mixing multiple components with different physical and chemical properties for various reasons. A continuous blender should be able to blend multiple components simultaneously or sequentially as the process demands. In order to investigate the effect of three-component mixing on the performance of continuous blender, three components were blended in the Zigzag[®]

blender.

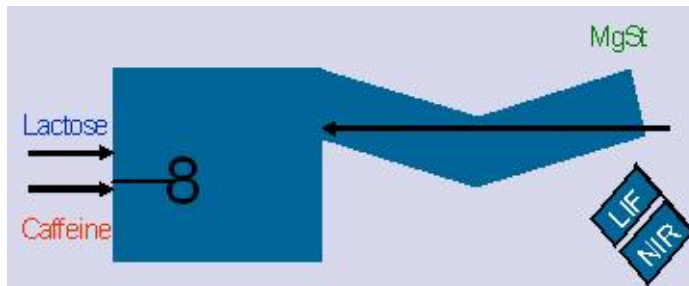


Figure 5-5: Schematic of Three Component Mixing in Zigzag Blender

Caffeine and HMS Impalpable Lactose were used as the API and excipient and magnesium stearate (MgSt) was used as the lubricant. The introduction of the lubricant was decided to be carried out at the end of the drum section, i.e. at the interface (connection joint) of the drum and the V-section. This decision was taken with the prior knowledge that the lubricant would overcoat the caffeine and lactose particles causing a very strong potential for segregation. Therefore, the lubricant was made not to see the drum section where the powder was fluidized and dispersed using the intensifier bar. This arrangement is schematically shown in figure 5-5.

The concentrations of MgSt was varied between 0.5 and 1.5%. In this set of experiments, a 3 level, 2 factor full factorial experimental design was created by changing the concentration of MgSt between 0.5%, 1% and 1.5% by weight and the external shell rotation rate between 37.5, 50 and 75 RPM. The intensifier bar rotation rate was fixed at 3000 RPM, the angle of incline at 0°, the caffeine content at 3% by weight and the total flow rate at 50 kg/hr.

NIR and LIF sensors were placed beneath a quartz glass plate near the exit of the blender on which powder fell after exiting from the blender as shown in figure 5-3. An air purge (blowing a gust of compressed air) was connected via a solenoid valve which was triggered by the NIR sensor after a delay of 5 seconds from the time instant of scanning the powder for NIR spectrum. Therefore, the frequency of sampling for the NIR sensor was 0.2 Hz. The LIF sensor collection frequency was set to 1 Hz.

5.2.3 Analysis of Data

Different data analysis methodologies were carried out depending on the type of experiments and the kind of data collected. LIF data were converted using a linear calibration plot for the blending experiments where the caffeine content was varied between 1% and 3% for different external shell rotation rates and internal intensifier bar rotation rates.

5.2.3.1 Two Component Blending - Varying Rotation Rates

The experiments where external and internal rotation rates were varied, LIF data was collected for caffeine contents of 1%, 1.5% and 3%. The steady state LIF signal values for each of these concentrations were linearly regressed after subtracting the baseline LIF signal at 0% caffeine that was obtained before caffeine flow rate was started into the blender. This is done because of the fact that LIF signal at very small changes in concentration is linear in nature. The linear calibration curve is specific to the Zigzag[®] blender experiments and was not used elsewhere.

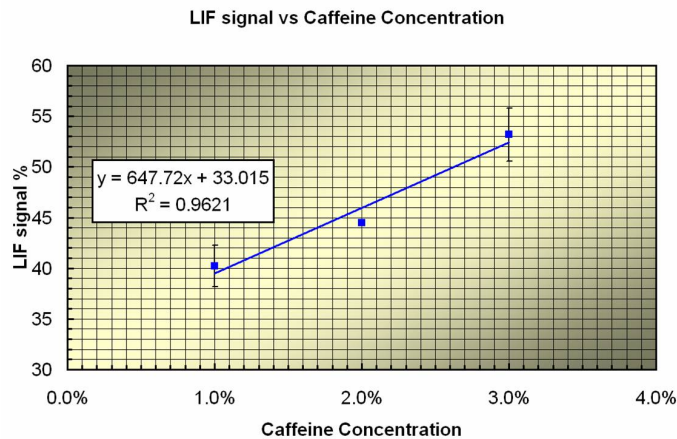


Figure 5-6: Linear Calibration of Baseline Adjusted LIF signal on Zigzag Blender

The LIF sensors measures the fluorescence from caffeine and collects the signal as a fraction of total collection capacity. This fraction can be calibrated to the caffeine concentration. Generally, the LIF signal is non-linear over the entire range of 0 to 3%. However, within 1 to 3% the LIF signal can be approximated to linear if the

baseline is adjusted. Figure 5-6 shows this calibration line. Using this calibration plot the LIF data can then be converted to caffeine concentrations at the position of the LIF sensor.

The variance at the output was computed from the concentration data at steady state obtained from LIF described above. The variance introduced at the input was computed from the flow rate data obtained from the Schenck Accurate Mechatron[®] feeders. The time stamped flow rate data were converted to mass fractions of caffeine every second. This inlet data was used in computing the variance in the input caffeine concentrations. The computed VRR ($= \sigma_{in}^2 / \sigma_{out}^2$) was compared to a target variance reduction where the outlet variance was set to an $RSD = \frac{\sigma_{tar}}{\mu} = 3\%$. Also, the RSD was computed from the variance in the outlet caffeine concentration. The caffeine concentrations obtained by dissolving the powder samples in water and running UV spectroscopy were used in determining the VRR in the same manner.

A response surface model was used to determine the effect of independent operational variables (external shell rotation rate and internal intensifier bar rotation rates). On performing a response surface analysis on the dissolution assay data, a four term second order model fitted the data within 5% level of significance. Tip speed was found to interact with shell speed and shell speed was found to have a non-linear (quadratic) influence. This response surface is shown in figure 5. The model equation that was used to fit the data is given in equation (5.3).

$$VRR = A + B \cdot RPM_{shell} + C \cdot Conc_{caf}^2 + D \cdot RPM_{shell}^2 + E \cdot RPM_{shell} \cdot RPM_{int} \quad (5.3)$$

where A , B , C , D and E are constants whose sign determines the direction of correlation (positive or negative) to the respective operational variables (or their quadratic terms). The response surface was plotted as a function of the independent variables, $Conc$ and RPM_{shell} for three different values of RPM_{int} .

5.2.3.2 Two Component Blending - Varying Throughput

The experiments where the throughput rates were varied with fixed caffeine content in all the runs, were analyzed by taking ratios of the observed LIF signal with the LIF signal at 0% caffeine content. This ratio was exponentially calibrated with the highest and lowest caffeine contents and the calibration curve so created for each individual run was used in determining the caffeine concentrations. The time data of caffeine concentrations was then used to determine RSD of the powder at the exit. Caffeine concentrations from dissolution analysis of the powder samples collected in the blending experiments were also used to determine RSD.

Since, response surface analysis with two factors (operational variables) changed would have not have a serious statistical validity, a Principal Component Analysis of the data matrix comprising of the operational variables (total throughput, external shell rotation rate, total mean residence time, mean residence time in the drum and v sections and the RSDs computed from LIF and dissolution assays) was carried out.

SIMCA-P+ (Umetrics Inc., Kinnelon, NJ) was used to perform the PCA analysis and using this software, the first two principal component loadings were plotted in a loadings bi-plot to assess the correlations between operational variables (independent variables like total throughput and shell rotation rate and dependent variables like residence times) and the observed RSD of caffeine at the exit of the blender. In order to achieve statistical accuracy, all the principal components till the number of independent variables in each dataset were calculated and only the first two principal components were utilized.

5.2.3.3 Three-component Blending

NIR and LIF data were collected from the three component blending experiments. The data from LIF were converted to concentrations of caffeine by first taking the ratio of the observed signal during blending to the LIF signal at 0% caffeine content. This ratio was calibrated using an exponential calibration function between the highest concentration (5%) and lowest (0%) concentration of caffeine and corresponding signal ratios at these two concentrations. The calibration function was then used to convert

the LIF signals to concentrations and RSD at steady state for LIF was determined. This RSD was used in the principal component analysis described in this section later on.

The collected NIR data were processed using SIMCA-P+ (from Umetrics Inc., Kinnelon, NJ). The spectra were first converted to have unit variance over all the wavelengths for each spectrum. These univariate spectra were then transformed by taking a 11 point Savitzky-Golay first derivative and were normalized using the Standard Normal Variate (SNV) spectral transform. These transforms are regularly used in the literature and have been discussed in detail elsewhere [64, 7].

The transformations used here remove two important sources of noise in the spectral data. The first source arises from the variations in the density and particle size of the powder in the NIR scan area. It was studied that changes in particle size and density shifted baselines and offsets in NIR spectra. First derivative transformations removed these baseline shifts. SNV transformation normalized all the spectra to a unit variance within each wavelength.

Pure component spectra of MgSt, caffeine and lactose were taken at the end of all the three component blending experiments on the Zigzag[®] blender on the quartz glass plate. The aforementioned transformations on the spectra were carried out on the entire set of blending spectra and pure component spectra.

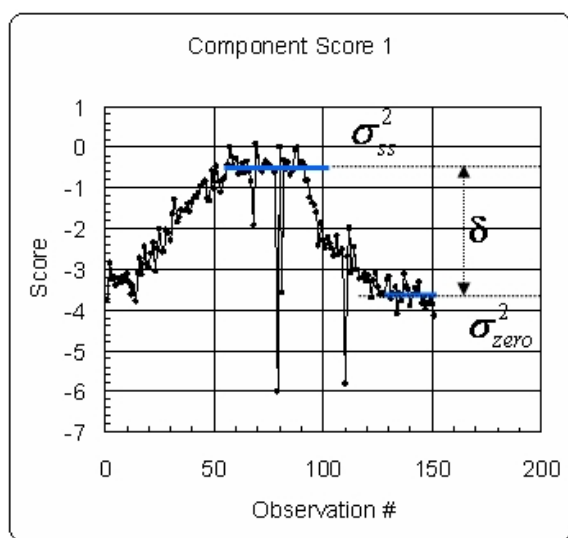


Figure 5-7: Computation of Spectral RSD from Principal Component Analysis

On computing first three principal components of the spectral data over all the experimental runs, it was observed that in general three components explained the variance in the spectra to about 95 – 99%. The loadings curve of the first two principal components indicated maxima over the peaks corresponding to caffeine and magnesium stearate spectral loading curve respectively. This indicated that the first two principal components represented chemometric contributions from caffeine and MgSt and hence were used in determining the spectral RSD.

The spectral RSD was computed by calculating the variance in the principal component score corresponding to caffeine (first component) and subtracting the variance observed at the 0% caffeine. The square root of this variance was divided by the absolute value of the difference between the mean principal component score observed at 0% caffeine and mean principal component score observed at steady state. The spectral RSD computed this way shown in figure 5-7, was expected to reflect the real chemometric RSD of caffeine in the mixture, since the errors arising from density and particle size fluctuations were removed by the spectral transformations. The exact same procedure was followed for determining the RSD of MgSt and the second principal component score was used to determine the spectral RSD of MgSt.

Chapter 6

Zigzag Blender Performance

Data from the flow behavior and blending experiments on the Zigzag[®] blender were analyzed as discussed in the last chapter. The residence time distributions at the drum and the exit were plotted with shell rotation rate, intensifier bar rotation rate and caffeine content as parameters. The effects of each of these variables was studied.

6.1 Results of Flow Behavior Experiments

Flow behavior experiments consisted mainly of residence time distribution experiments. Residence time distributions were computed from both impulse response experiments and blending experiments for varying throughput rate experiments as described in the previous chapter. The effect of external shell rotation rate, internal intensifier bar and caffeine content is described in the sections below.

6.1.1 Confirmation of Steady State

Steady state in flow rate was achieved within the first ten minutes of the blending run. The flow rates of material at the exit of the blender 15 minutes into the experimental run was observed to vary within 3 – 5% of the nominal total throughput. This balance of flow rates indicated that steady state was indeed achieved in the blender. Fill weights could not be measured in the blender due to engineering problems in weighing the blender in real time.

6.1.2 RTD of API in Zigzag Blender

RTD from impulse response experiments were fitted with a log-normal distribution given by equation (5.1). The R^2 values for this statistical fit were around 0.95 with the lowest R^2 value at 0.61. Although, this distribution had no theoretical foundation, similarities with the axial dispersion model, c.f. equation (4.9), were easily seen. A Pareto histogram of the mean residence time observed all the runs was created and as shown in figure 6-1. In the subsequent presentation of results, a combination of the results obtained from RTD experiments would be used.

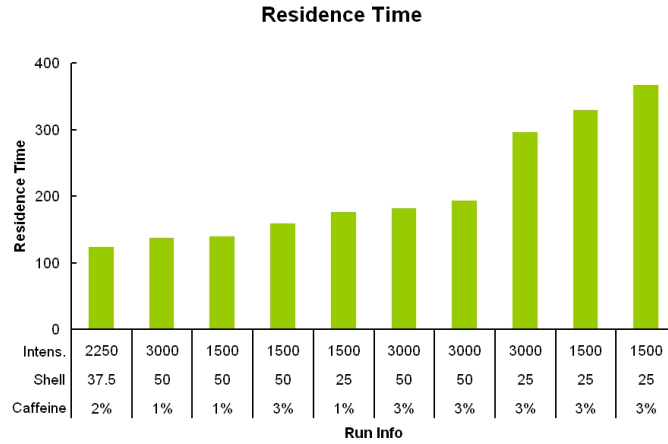


Figure 6-1: Mean Residence Times in the Zigzag Blender

6.1.2.1 Effect of Intensifier Bar Rotation Rate

The exit residence time distribution for the same external shell rotation rate of 50 RPM and caffeine impulse corresponding to 1% (25 gm) was plotted and is shown in figure 6-2. We see that as the rotation rate of the intensifier bar is increased, the from 1500 to 3000 RPM, the residence time distribution has the same peak and spread.

The results from comparing the effect of intensifier rotation rate on dispersion seemed to indicate that the effect of the intensifier bar had a negligible effect at a given external shell rotation rate. However, as the mean residence time determined the exposure time of the powder to the intensifier bar, a non-linear interaction affect of tip rotation rate with external shell rotation rate was expected.

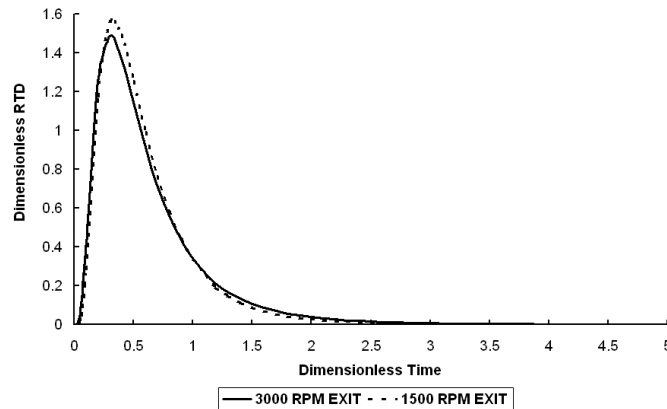


Figure 6-2: Effect of Intensifier Bar Rotation Rate on RTD

It was observed from figure 6-1 that intensifier bar has little effect on the mean residence time. This was expected since the movement of the powder was determined by the rotation rate of the external shell and the opening at the end of the drum that moved the powder from the drum section to the V-section.

6.1.2.2 Effect of External Shell Rotation Rate

The exit residence time distributions for a given intensifier bar rotation rate (3000 RPM), a given caffeine impulse input (3% or 75 gm caffeine impulse input) but varying external shell rotation rates are shown in figure 6-3. The RTD at the lower external RPM had a higher dispersive component as seen by the broad spread of the distribution.

The results from comparing the effect of the shell rotation rate on dispersion yielded an inconclusive evidence of the effect of shell rotation rate on the measure of dispersion. The plot of the measure of dispersion indicated that at 25 RPM a small difference in mixing dispersion was observed. However, at 50 RPM, this difference did not exist.

However, shell rotation rate affected the mean residence time as seen in figure 6-1. Therefore, it could be expected that the shell rotation rate would have an affect on the performance of the blender by influencing the residence time and therefore the time exposure of the powder to the intensifier bar.

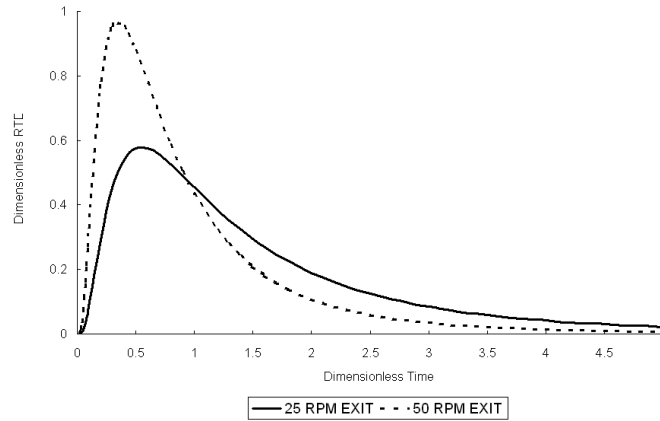


Figure 6-3: Effect of Shell Rotation Rate on RTD

6.1.2.3 Effect of Caffeine Content

The exit residence time distributions for a given intensifier bar rotation rate (3000 RPM) and a given external shell rotation rate of 50 RPM but two different caffeine impulse inputs (3% or 75 gm and 1% or 25 gm caffeine impulse inputs) are shown in figure 6-4. The RTD at both the levels of caffeine showed no significant difference as evinced by the spreads of the two RTDs. When the measure of dispersion, given by (σ^2/t_m^2) , was plotted *vis-a-vis* the caffeine impulse input loading for differing shell rotation rates (25 and 50 RPM) and intensifier bar rotation rates (1500 and 3000 RPM), the difference observed was not significant.

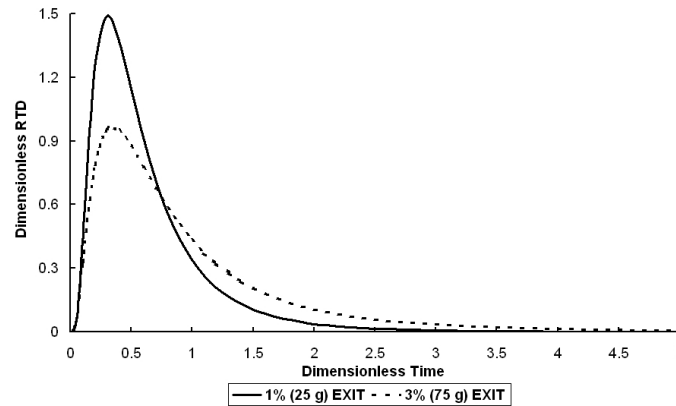


Figure 6-4: Effect of Caffeine Content on RTD

The results from comparing the effect of caffeine content on the measure of dispersion seemed to indicate either negligible effect or lack thereof within the experimental variance. However, higher caffeine contents required longer clearance times as seen in figure 6-1. Therefore, it could be expected that the caffeine content would have an affect on the performance of the blender by influencing the residence time and therefore the time exposure of the powder to the intensifier bar. Also, API content is inversely proportional to the RSD of the powder mixture and hence a higher variance in mixtures with higher caffeine content would still give acceptable mixtures. In other words, it would be easier to mix caffeine at 3% than caffeine at a concentration of 1% since the equal RSD for both mixtures allows higher variance in 3% mixture than the 1% mixture.

6.1.2.4 Artefacts of the LIF Data Collection Method

The technique employed to measure LIF signal introduced errors in the data collected. Due to the geometry of the blender, the LIF sensor was placed close to the quartz glass windows in the Zigzag[®] blender shown in the figure 5-1, on one side of the blender. This arrangement caused two important errors.

1. It was observed that in consequent rotations of the external shell, the powder layer varied in depth and thickness on the quartz glass. This error was suspected when the observation that some rotations went past the LIF sensor without complete powder coverage was made. The reason for this variation in the depth of the quartz glass arises from the fact that powder moves in cascades or avalanches in the V-section of the Zigzag[®] blender causing powder to fall erratically on the quartz window.
2. It was observed that the powder layer in contact with the quartz glass window was not being replenished during subsequent rotations of the Zigzag[®] blender. This observation was made, only after the LIF data were collected. The LIF data collected and a statistical log-normal curve-fit is shown in figure 6-5. This example showed that a number of LIF scans passed before powder replenished on

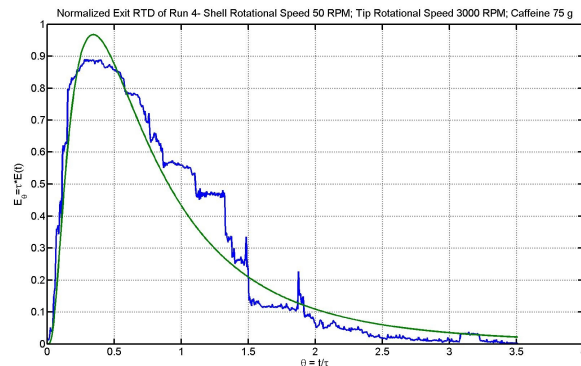


Figure 6-5: Experimental RTD and Log-Normal Statistical Regression in Zigzag Blender

the quartz glass window as evinced by the static signal for about 3-5 rotations. This static nature of the signal gave rise to additional errors in computing the measure of dispersion in the blender using the log-normal RTD curve.

As a result of these issues, the RTD analyses from impulse-response experiments were not expected to match the experimentally determined performance characteristics of blending performance in the Zigzag[®] blender.

6.2 Results of Blending Experiments

LIF data and dissolution assay of powder samples were analyzed for determination of the variance reduction in the Zigzag[®] blender. The variance reduction ratios from LIF and dissolution assays for two component blending and from NIR for three-component systems were analyzed. Response surface analysis and Principal component analysis was carried out on the VRR data for two component blender as described in §5.2.3.

6.2.1 Varying Rotation Rates in Two Component Blending

The VRRs from LIF data for two component (Caffeine + Lactose) blending were plotted as a histogram as shown in figure 6-6 for all the experimental runs. The VRRs from dissolution assay for two component blending Caffeine+Lactose were plotted as a histogram as shown in figure 6-7.

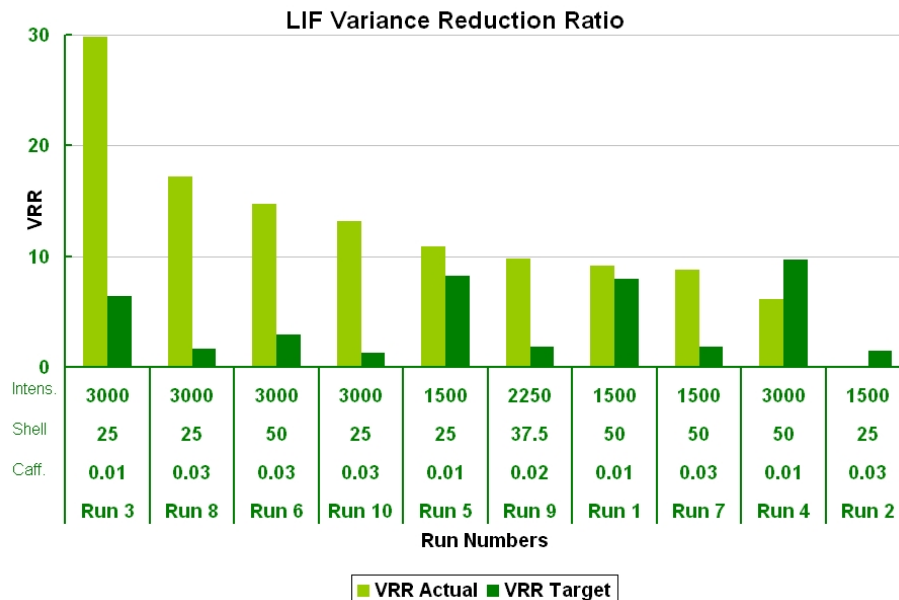


Figure 6-6: VRR in Zigzag Blender from LIF data

These histograms were arranged in a Pareto format with the highest From both figures, it was found that the observed VRR was higher than the target VRR computed as described in §5.2.3 for most of runs. It was also found that the higher intensifier bar speed exceeded the target VRR compared to the lower intensifier speeds and that the target was easily achieved at higher caffeine contents than at lower caffeine contents. Response surface analysis provided a mathematical process of analyzing these effects.

6.2.1.1 Response Surface Analysis of VRR

Equation (5.3) was statistically regressed with the VRR data obtained from dissolution. It was decided to use the dissolution data than the LIF data as the expected error from the LIF data was higher than that in the dissolution assay data as discussed in the previous section. SAS (SAS Institute, Cary, NC) was used to perform the statistical regression of the VRR from dissolution. ANOVA was performed and the results were tabulated in 6.1. It was found that the model has a very high significance $Pr > F = 0.0005 \ll 0.05$ at 95% level of confidence.

Table 6.1: ANOVA of Response Model

| Source | Sum of Squares | F | $Pr > F$ |
|-----------------|----------------|------|----------|
| Model | 537.1 | 42.9 | 0.0005 |
| Error | 15.6 | | |
| Corrected Total | 552.7 | | |

Since the model was found to be highly significant, the significance for individual effects were calculated. The magnitude and direction of various effects, rotation rate of the external shell RPM_{shell} , rotation rate of the intensifier bar RPM_{int} , caffeine content $Conc$ and their quadratic combinations of these effects as shown in equation (5.3), were tabulated in table 6.2.

Table 6.2: Statistics of Individual Effects on VRR

| Variable | Parameter | Estimate | t | $Pr > t $ |
|-------------------------------|-----------|----------|-------|------------|
| Intercept | A | 67.88 | 4.41 | 0.007 |
| RPM_{shell} | B | -4.17 | -4.63 | 0.006 |
| $Conc^2$ | C | -3625.65 | -2.43 | 0.060 |
| RPM_{shell}^2 | D | 0.052 | 4.32 | 0.008 |
| $RPM_{shell} \cdot RPM_{int}$ | E | 0.00023 | 11.34 | < .0001 |

End of Table

All parameters were significant except the coefficient C, corresponding to the effect of caffeine content. This effect failed the 95% test by a very small margin and potentially could still be an important significant effect. Intensifier rotation rate showed a positive effect and the external shell rotation rate showed a quadratic effect on the variance reduction ratio.

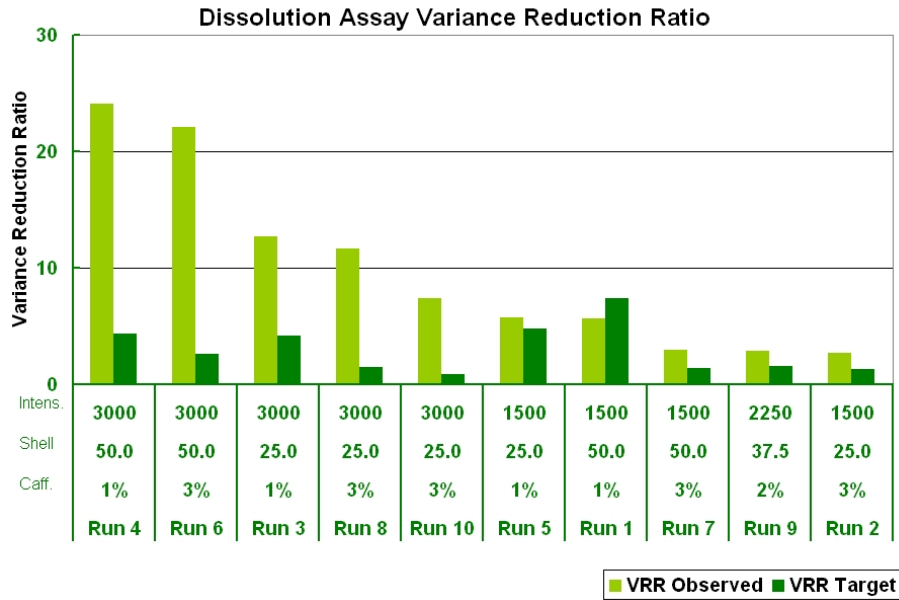


Figure 6-7: VRR in Zigzag Blender from Solution UV Analysis

6.2.1.2 Effect of Intensifier Bar Rotation Rate

The effect of the intensifier bar rotation rate was found to be significant only as an interaction effect with the external shell rotation rate as seen in table 6.2. When the intensifier bar rotation rate was increased at the same external shell rotation rate, the powder in the drum section undergoes increased agitation and dispersion and hence the blender VRR was expected to increase with increasing intensifier rotation rates.

As the external shell rotation rate was increased at the same intensifier rotation rate, the time of exposure of the powder to the intensifier bar would be changed and this would be expected to exert influence on the performance of the blender. An investigation on the influence of the shell rotation rate on drum section residence times revealed that an increase in shell rotation rate increased the residence time of the powder in the blender and would be discussed in §6.2.2.

6.2.1.3 Effect of External Shell Rotation Rate

The effect of the external shell rotation rate was found to be of a non-linear (quadratic) form as seen in table 6.2. An increase in the external shell rotation rate caused an initial decrease in VRR changing from 25 to 37.5 RPM and subsequent increase in

changing from 37.5 to 50 RPM.

The non-linear effect of the external shell rotation rate was attributed to two factors. First, as discussed above, a change in the external shell rotation rate changed the residence time (increasing Shell RPM increased residence times) and second, a change external shell rotation rates changed the dynamic angle of repose and thereby changed the fill weight of the powder in the blender. It was found that these effects worked to counterbalance each other and cause the non-linearity observed in the effect of the external shell rotation rate.

6.2.1.4 Effect of Caffeine Content

The effect of caffeine content on VRR failed to be statistically significant at the 95% level of statistical significance. However, an increase in the caffeine content was found to decrease the variance reduction ratio. At the outset, this effect seemed to indicate that increased caffeine content lead to decreased VRR. But theory indicated that increase in concentration of the API should increase the VRR if the input variance were identical.

Now, the feeder was known to perform better and introduce less variance at higher concentrations. As a result of this effect from the feeder, VRR at higher concentrations might have been lower. This was confirmed when we examined the difference of Target and Observed VRRs shown in figures 6-6 and 6-7. This difference was higher for 3% indicating that the performance was better at 3% since a higher difference indicates a better reduction compared to the target variance.

6.2.2 Varying Throughput in Two Component Blending

Relative standard deviations (RSDs) of caffeine content for these blending experiments were computed by converting LIF data to concentrations as described in §5.2.3. These RSDs of caffeine content were plotted on a histogram as shown in 6-8. Caffeine content were also determined from dissolving powder samples and subsequent UV spectrometry on the samples. These concentrations were also used in determining the RSD and were displayed graphically in a histogram format as shown in 6-9.

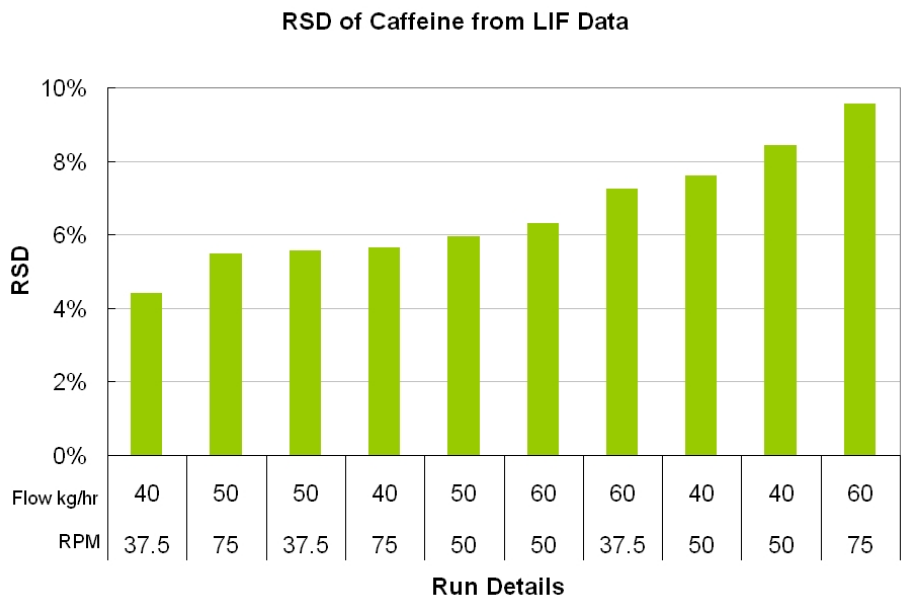


Figure 6-8: RSD of Caffeine from LIF - Throughput Experiments

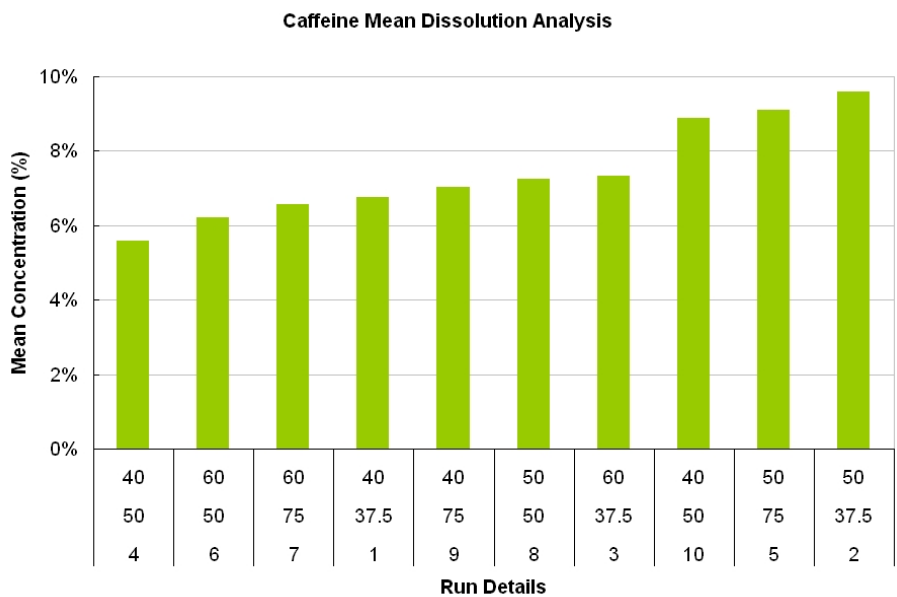


Figure 6-9: RSD of Caffeine from Solution Analysis for Throughput Experiments

The correlation between the mean values and RSDs of caffeine content determined from both these techniques were plotted as shown in figures 6-10 and 6-11. It was found that RSDs computed from LIF and UV spectrometric analysis were very different. The mean values, however, had a very good correlation. Only three powder samples at steady state were collected and this sample set did not give enough statistical significance to the results from Dissolution analysis. As a result it was found that the variance observed in the dissolution data were much larger than that observed in the LIF data as shown in figure 6-11. Therefore, in the subsequent analyses, only the RSD computed from LIF data were used.

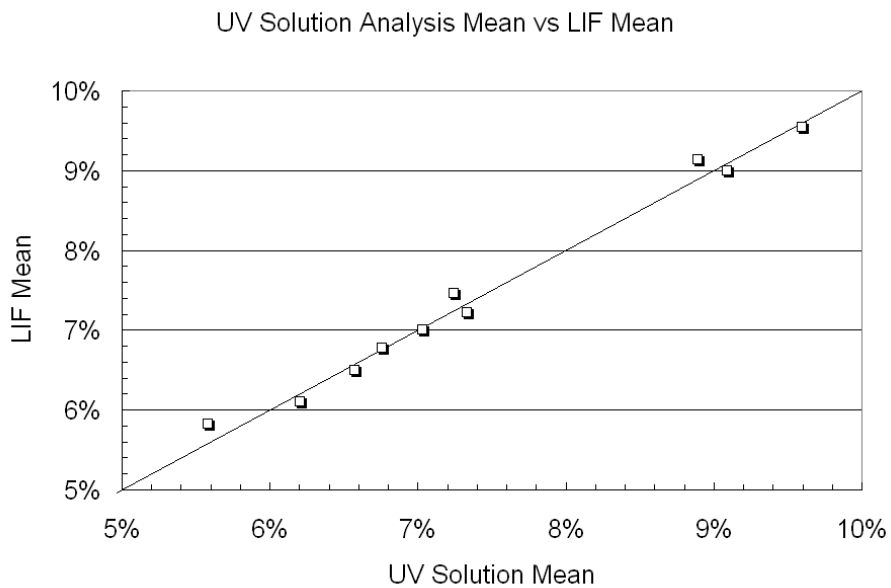


Figure 6-10: Mean Caffeine Content: from LIF vs from Solution Analysis

6.2.2.1 PCA of RSD and Operational Variables

In order to understand the effect of operational variables on the RSD of the powder mixture computed by converting LIF data to caffeine concentrations, principal component analysis was performed as described in §5.2.3. Figure 6-12 the loadings plot of various variables that affect the blending process. These are rotation rate of the external shell, the total throughput rate, the mean residence time in the drum section and the mean residence time in the V Section.

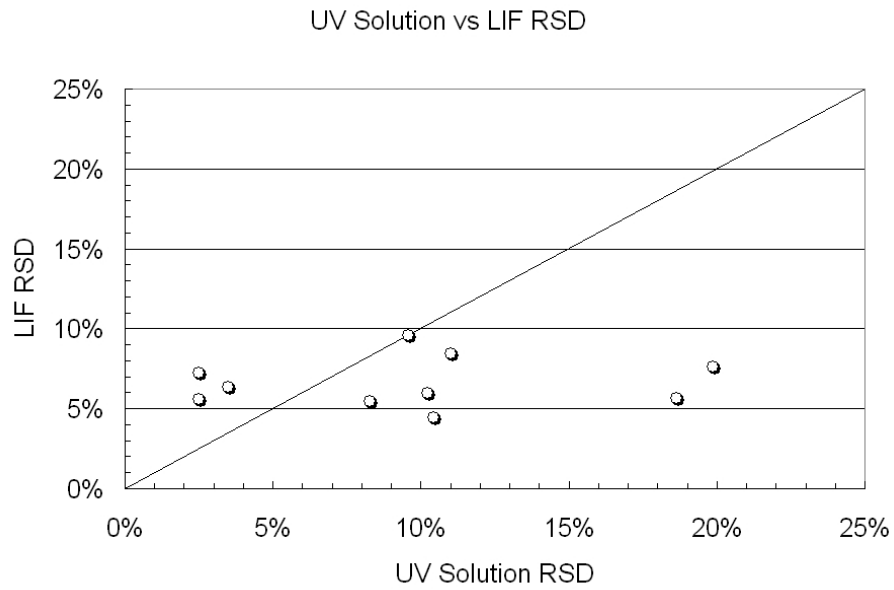


Figure 6-11: RSD of Caffeine: from LIF vs from Solution Analysis

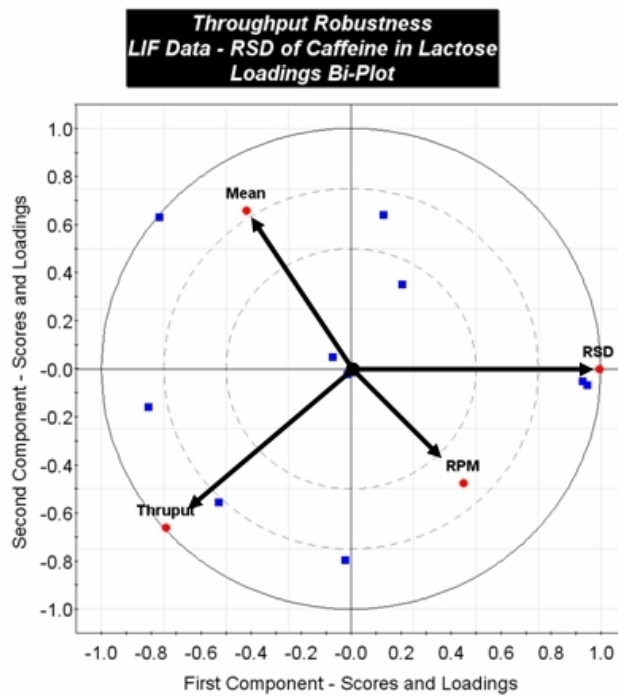


Figure 6-12: Loadings Plot of Caffeine RSD - Rotation Rate and Total Flow Rate

6.2.2.2 Effect of External Shell Rotation Rate

The scalar product of the position vectors (from the origin in the loadings score plot) of different variables on a loadings score plot determined the sign and extent of the correlation between two variables. As the direction and magnitude of the position vectors of The external shell rotation rate and RSD from LIF had positive scalar product c.f. figure 6-12, the effect of Shell RPM on RSD of LIF within this experimental design was positive. This meant that as rotation rate of the shell increased, the RSD of caffeine increased or the quality of the mixture deteriorated.

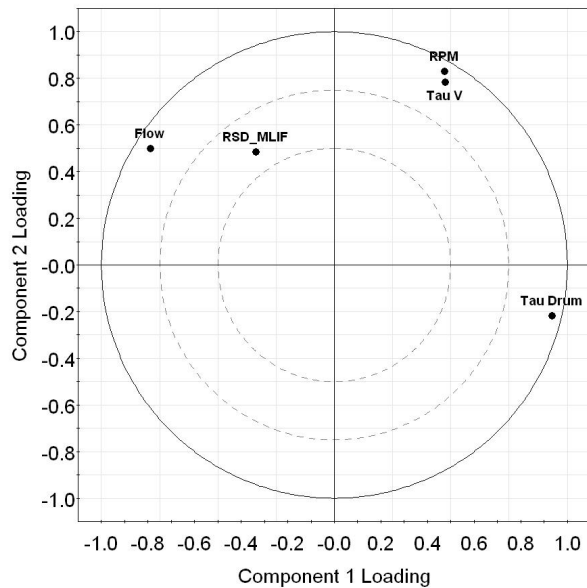


Figure 6-13: Loadings Plot with RSD, Total Flow Rate, Mean Residence Times and Shell Rotation Rate

In order to understand this effect, correlation between V-section residence time and RPM was examined. From the figure, it was seen that these variables were highly correlated, since the vectors have the same magnitude and direction. The drum section, v section and total mean residence times were plotted as a function of external shell rotation rates as shown in figure 6-13. Clearly this indicated that an increase in the external shell rotation rate, increased the mean residence time in the V-section causing an increase in the RSD of the powder mixture observed. Our expectation was that as the residence time in the V-section increased, powder that

was mixed in the drum section began to segregate due to convective and gravity forces and hence an increase in RSD was observed.

6.2.2.3 Effect of Total Throughput

The direction and magnitude of the position vectors of total flow rate and RSD indicated that these variables were positively correlated. This meant that as the total flow rate increased, the observed RSD from LIF data also increased.

To understand this, the effect of flow rate on drum section residence time was observed. It was found that the drum section mean residence time and the flow rate were negatively correlated. This meant that an decrease in the total flow rate caused an increase in the drum section mean residence time which caused a decrease in the RSD of the mixture due to reduced mixing time in the drum section.

6.2.3 Three Component Blending

Spectral RSDs that act as proxies for the actual RSDs of Magnesium Stearate and Caffeine were computed as described in section §5.2.3. Since these RSDs were computed on the principal components of transformed spectra, these did not represent the real RSDs of the individual components, caffeine and MgSt. However, since spectral data carried chemometric information, RSDs of the spectral principal components were expected to reflect the trends in the RSDs of the individual component concentrations in the powder mixture.

PCA was performed on different set of variables in order to understand the influence of different variables on the blending performance. PCA was performed on the following sets of combinations of variables:

- Shell rotation rate, MgSt content and Caffeine spectral RSD.
- Shell rotation rate, MgSt content and MgSt Spectral RSD.
- Shell rotation rate, MgSt Content, MgSt Spectral RSD and Caffeine Spectral RSD.

The effect of operational variables on these proxy spectral RSDs were investigated by PCA analysis again described in §5.2.3. It is important to note that the spectral RSDs in the results described below were all proxy RSDs computed from principal components and are only a measure of the actual concentration RSD.

6.2.3.1 PCA of Spectral RSD with Shell Rotation Rate

As seen before, shell rotation rate had a positive effect of caffeine spectral RSD which meant that as the rotation rate increased, the spectral RSD of Caffeine increased or the blend quality deteriorated. In the two component blending scenario, increase in shell rotation rate lead to an increase in V-section residence time and it was suspected that the same effect was causing this correlation in these three component blending experiments.

The effect of V-section mean residence time on the RSD computed from LIF measurements made on the three component blending experiments shown in Figure 6-14 reinforce the results from the two component experiments c.f. figure 6-12. As the V-section residence time increased, the spectral RSD of caffeine increased. Since MgSt was introduced at the end of the drum section (i.e. after caffeine was mixed with lactose in the drum section), and since MgSt lubricated particles by coating caffeine and lactose with MgSt particles thereby decreasing cohesion and friction, the mixture segregated in the V-section since the time of exposure to the tumbling section under an increased segregation potential was more during its sojourn in the V-section.

6.2.3.2 Effect of MgSt on Caffeine RSD

The results from PC analysis of MgSt content on caffeine spectral RSD was plotted on a loadings plot as shown in figure 6-14. It was found that the scalar product of the position vectors of caffeine spectral RSD and MgSt content was positive which indicated a positive correlation. In fact it was found that the position vectors were approximately of same magnitude and in the same direction, which indicated that these were very strongly correlated.

This effect of MgSt content on caffeine spectral RSD could be explained by the

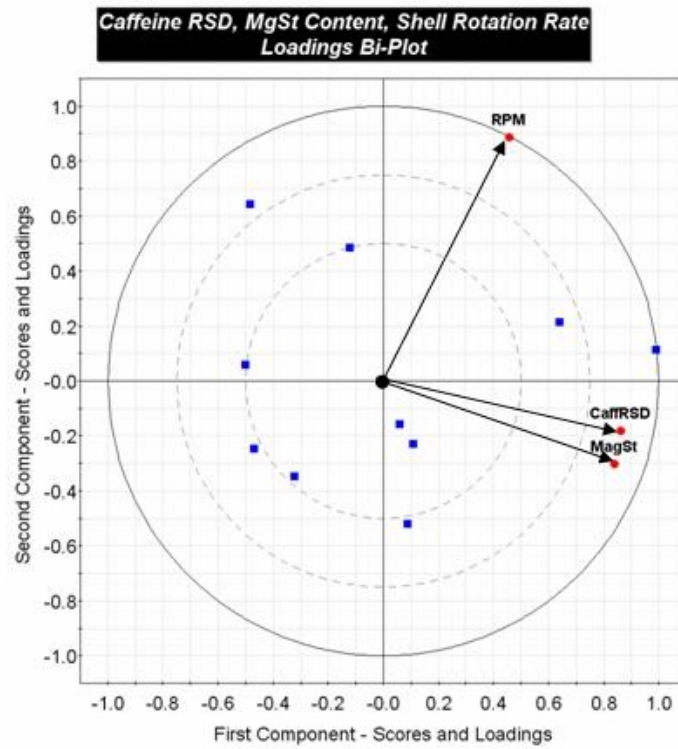


Figure 6-14: Loading plot for Caffeine RSD, MgSt Content and Shell Rotation Rate

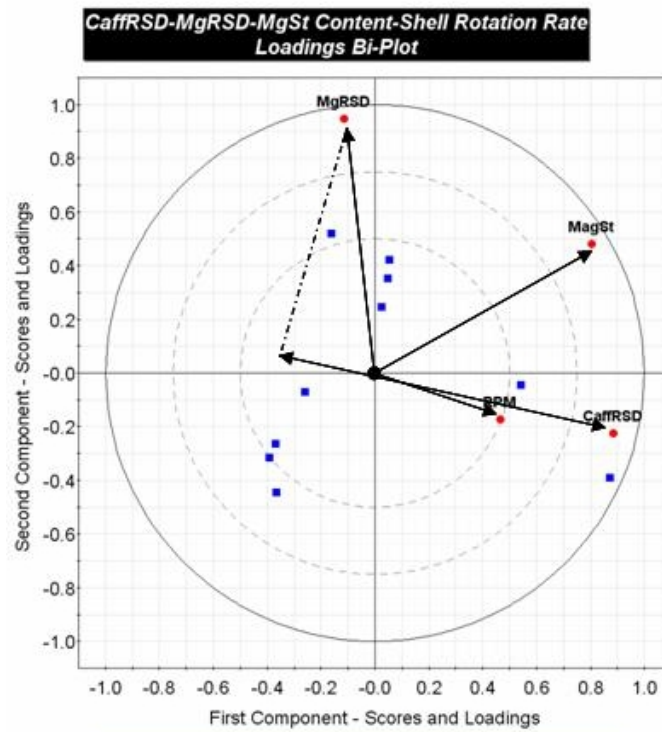


Figure 6-15: Loadings plot for MgSt RSD, MgSt Content, Caffeine RSD and Shell Rotation Rate

microscopic behavior of how MgSt particles interact with caffeine and lactose particles. Caffeine and lactose particles were coated by fine MgSt particles during the blending process in the V-section. MgSt coated caffeine and lactose particles lost their cohesive and adhesive strength due to the reduced cohesion between MgSt - Caffeine and MgSt - Lactose. This reduction in cohesion increased the potential for lactose and caffeine particles to segregate in the V-section, where the only forces of mixing were gravity forces, which increased segregation in the V-section. Increased segregation resulted in a deteriorated mixture quality at the end of V-section (i.e. higher caffeine spectral RSD).

6.2.3.3 Effect of MgSt on MgSt RSD

The results from PC analysis of MgSt content on MgST spectral RSD was plotted on a similar loadings plot as before as shown in figure 6-15. It was found that the scalar product of the position vectors of MgSt content and MgSt spectral RSD was positive which indicated a positive correlation. The scalar product of the position vectors of MgSt spectral RSD and shell rotation rate was found to be negative which indicated a negative correlation.

It was expected that as MgSt content increased, the spectral RSD of MgSt would decrease since RSD has a direct inverse proportionality with mean MgSt content. However, the variance in MgSt content was found to exceed this inverse proportionality leading to a positive correlation between MgSt content and MgSt RSD. It was not clear if this was a result of preferential coating of MgSt on caffeine or lactose over the other causing an increased spectral RSD.

The effect of RPM (which was positively correlated with the V-section residence time) on the MgSt spectral RSD was positive, indicating that an increased residence time in the V-section decreased the spectral RSD of MgSt, i.e, gave rise to a better blend homogeneity with respect to MgSt RSD. However, at this point it was foreseen that an increase in shell RPM would decrease the spectral RSD of MgSt, but might cause problems with caffeine spectral RSD and this is discussed below.

6.2.3.4 Effect of MgSt RSD on Caffeine RSD

The results from PC analysis of MgSt content, MgSt spectral RSD and shell rotation rate on caffeine spectral RSD was shown in a loadings plot in figure 6-15. It was found that the scalar product of the position vectors of MgSt spectral RSD and caffeine spectral RSD was negative which indicated a negative correlation between the lubricant and API RSD.

As MgSt spectral RSD increased, the spread of MgSt in the powder mixture decreased. This meant that fewer caffeine and lactose particles were coated with MgSt thereby maintaining the cohesive and adhesive forces between caffeine and lactose at their original levels leading to retained blend homogeneity in caffeine at the end of the blender or in other words a decreased spectral RSD of caffeine.

We also observed that an increase in RPM (which lead to an increase in the residence time in the V-section) decreased the spectral RSD of MgSt but increased the spectral RSD of caffeine. In other words, increased time spent in the V-section deteriorated the mixture quality in terms of caffeine spectral RSD, but increased the spread of MgSt as evinced by decreased spectral RSD of MgSt with increased RPM of the shell.

6.3 Summary of Results

The Zigzag[®] blender was shown to exceed the performance achievable in batch blending. It was shown that the blending system could be monitored in real time using a non-invasive technique like LIF. Effect of external shell rotation rate and internal intensifier bar rotation rate, and total throughput of material through the blender were also delineated. It was shown that residence time in the drum and V-sections were affected by the shell rotation rates and flow rate of the material in the blender.

The effect of three component blending was also examined and it was shown that lubricant like MgSt could be monitored in real time. It was shown that the definition of blend homogeneity with respect to one component in a multi-component blending system does not necessarily mean homogeneity in another. In fact, it was shown that

an increase in RSD of the lubricant leads to a decrease in the RSD of the active. This meant that there were trade-offs involved in the optimization of blending processes. What could be good for one component need not necessarily be good for the rest of the mixture.

Finally, a pilot scale Zigzag[®] blender was tested and operated for blending two and three component mixtures. It was shown that online monitoring of this system is possible and that the blender and feeder system should be considered a single entity while designing the blending process.

Chapter 7

Double Helical Ribbon Blender

As mentioned in §4.5 and §4.6, two types of experiments were performed on the double helical ribbon blender. Flow behavior experiments were used to determine the RTD of the API in the blender. Blending experiments were performed to examine the effect of operational variables on the performance of the blending process. In addition, various excipients and APIs that are listed in §4.4 were used in the flow behavior and blending experiments. The effect of change of various parameters like particle size, cohesion and adhesion energies and shape were examined.

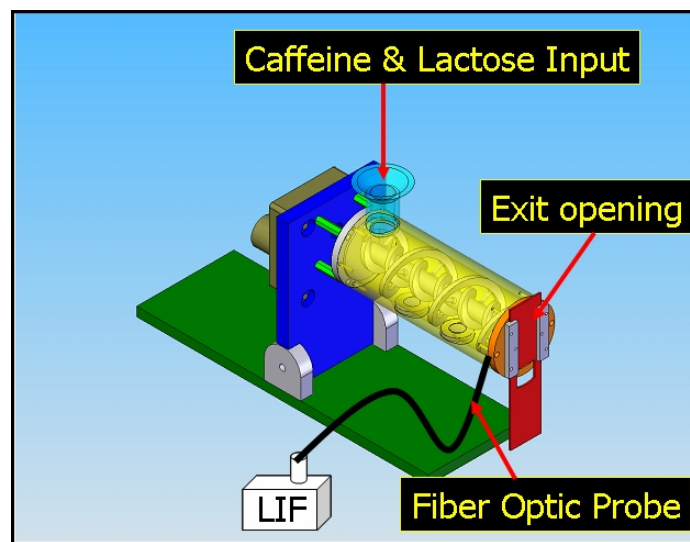


Figure 7-1: Schematic of Ribbon Blender Experimental Set-up

The experimental setup of the double helical ribbon blender was as shown in Figure 7-1. An automatic feeder fed excipient at the inlet. An LIF sensor (with a fiber optic probe) was placed at the exit quartz glass window. When used, the NIR

was placed so that the integrating sphere probe was directly beneath the quartz glass window close to the exit of the blender. The exit opening was kept fully open in all our experiments. The scan frequency with LIF was 1 Hz and with NIR was 0.5 Hz. The NIR sensor averaged eight NIR scans in within 2 seconds and the average scan was saved.

The input of API was carried out by weighing the API out in weigh dishes and emptying the dishes into the blender at preset intervals of time. This is described in detail in the subsequent sections. The powder falling out of the blender was made to fall on a sloping groove through which it was collected in a bin. Powder sample collection was performed at the exit of the blender before the powder contacted the sloping groove.

7.1 Flow Behavior Experiments

Investigation of flow behavior in the lab scale double helical ribbon blender was done in two parts. In the first part, the fill weights in the blender for Lactose DCL 11 was measured as a function of the rotation rate, flow rate and angle of incline. In the second part, the RTDs for the API with the excipients in the blender was determined.

7.1.1 Fill Weight Experiments

The empty blender was tared on the weighing machine. Excipients were manually fed into the blender by weighing out masses of excipient equivalent to flow rates of 0.72 to 7.2 kg/hr as shown in table 7.1. When the blender reached steady state, the maximum and minimum weight of the blender was noted down as blending proceeded. The average of the maximum and minimum was noted down as the fill weight of the blender at that rotation rate and flow rate. In order to study the effects of presence of powder before the start of the flow behavior experiments, two different initial fill weights, 40 and 100 gm were used. The fill weight for flow rates (2.16 and 4.32 kg/hr) were noted for these initial fill weights at 10 RPM shaft rotation rate.

Flow rates ranging from 0.72 to 7.2 kg/hr were used in the fill weight determination. The angle of incline was changed between -5° , 0° & $+5^\circ$. The shaft rotation

rates were varied between 10, 20 & 30 RPM. Fill weights were determined over all flow rates, rotation rates and angles of incline. However, certain flow rates were inaccessible in the blender due to overflow (high flow rates, slower shaft rotation rates and higher inclines) and due to complete clearance (at low flow rates, faster shaft rotation rates and lower inclines) of powder in the blender.

Table 7.1: Excipient Massing for Manual Feeding

| Excipient Flow | | Mass of Excipient | Time Interval |
|----------------|---------|-------------------|---------------|
| (g/sec) | (kg/hr) | (g) | (sec) |
| 0.2 | 0.72 | 1 | 5 |
| 0.4 | 1.44 | 2 | 5 |
| 0.6 | 2.16 | 3 | 5 |
| 0.8 | 2.88 | 4 | 5 |
| 1.0 | 3.60 | 5 | 5 |
| 1.2 | 4.32 | 6 | 5 |
| 1.6 | 5.76 | 8 | 5 |
| 1.8 | 6.48 | 9 | 5 |
| 2.0 | 7.20 | 10 | 5 |

End of Table

Fill weight experiments were also performed with the Tuf-flex[®] automatic feeder. Flow rate at each rotation rate was increased from 1 kg/hr to 3.5 kg/hr in steps of 0.5 kg/hr and the fill weight at each flow rate was measured. In one round of experiments, the blender was not emptied at the end of each fill weight measurement and the flow rate was increased from 1 to 0.5 and then back to 1 kg/hr. This was performed to examine whether the same steady state fill weight would be achieved starting from any fill weight in the blender.

7.1.2 RTD Experiments

Determination of residence time distribution was carried out by performing impulse response experiments. Before the installation of the feeder, manual feeding of both the excipient and API was carried out by weighing out masses of excipient equivalent to flow rates of 1.08, 2.16, 4.32 and 7.2 kg/hr. In each experiment, LIF monitoring started at time $t = 0$. The excipients were weighed out in weigh boats and emptied into the blender at regular, pre-determined intervals of time. Before the feeder was installed, Lactose DCL 14 was used after sieving the powder so that two cuts were obtained. The first cut had particle sizes between 45 and 150 μm and the second cut had particle sizes between 150 and 250 μm .

The fill weight of the blender was noted at steady state, as the average between the higher and lower values in the blender. The fill weight fluctuates in the blender due to the discrete nature of powder flow at the exit and inlet of the blender. The space time for the blender was estimated by dividing the fill weight at steady state with flow rate at the inlet.

A shot of API (Caffeine in this case) corresponding to 3% by mass of the powder in the blender over $3\times$ the mean residence time (using τ , the space time, as an estimate of mean residence time) was fed at the inlet of the blender and the time of the impulse shot was noted. LIF signal was collected at a frequency of 1 Hz and was converted to concentrations using the calibration curve #2 from table 4.1. The concentrations were converted to residence time distributions using two different methods discussed in §7.1.3.

An automatic feeder was installed to feed the excipient at the inlet of the blender. The feeder delivered flowrates between 1 to 10 kg/hr. Lactose DCL-11, Lactose DCL-14, MCC Avicel PH-102, and MCC Celphere CP-102 were used as excipients in this set of experiments. Caffeine and Acetaminophen were used as two different APIs. NIR monitoring in each experiment started at $t = 0$. The fill weight of the blender was noted at steady state, as the average between the higher and lower values in the blender. The fill weight fluctuates in the blender due to the discrete nature of powder

flow at the exit and inlet of the blender. The space time for the blender was estimated by dividing the fill weight at steady state with flow rate at the inlet.

A shot of API (Caffeine or Acetaminophen) corresponding to 3% by mass of the powder in the blender over $3\times$ the mean residence time, (using τ , the space time, as an estimate of mean residence time) was fed at the inlet of the blender and the time of the impuse shot was noted. NIR spectra were collected at a frequency of 0.5 Hz and these spectra were converted to concentration using the PLS models described in §4.3. The angle of incline in the presence of the automatic feeder was fixed at 0° . All the types of excipients described in this chapter were used. The concentration were subsequently converted to residence time distributions using the methods discussed in §4.5.

7.1.3 Analysis of Data

The fill weight data was used to compute the space times in the blender. The impulse response data were used to compute the Bodenstein number and mean residence time. These methods of analysis of data are described below.

7.1.3.1 Fill Weight Experiments

The average fill weights in the blender at a particular flow rate, rotation rate and angle of incline, were used in computing the space time. Space time was computed by dividing the fill weight at steady state in the blender by the flow rate at the inlet. These space times were used to determine the API shot corresponding to 3% by mass of the powder in the blender over $3\times$ the space time in the blender.

The fill weights were plotted as a function of the shaft rotation rates, the flow rates and angles of incline to examine the effect of each of these variables. The effect of initial fill weight was also examined. The steady state fill weights for the same flow rates were plotted for different initial weights. Also, a closed loop of changing initial fill weights based on the steady state fill weight achieved by an earlier flow rate was plotted.

7.1.3.2 Residence Time Distribution

The LIF data from impulse response experiments were converted to concentration using calibration #1 in table 4.1. The converted concentrations were then converted to residence time distribution using equation (4.10) and (4.11). The residence time distribution was normalized using the space time and the subsequent dimensionless residence time was statistically regressed with equation (4.9). In this regression, the Bodenstein numbers for each of the experiments were determined. The dispersion coefficients were determined using the length of the blender $L = 6''$ and mean velocity of the powder in the blender $V = \frac{L}{\tau}$, where τ s is the space time in the blender.

The NIR data were first pre-processed by taking 11-point Savitzky-Golay first derivative followed by a standard normal variate transform described in §4.3. The pre-processed data were converted to concentration of the API using the PLS calibration models from SIMCA-P+ given summarized in table 4.2. The converted concentrations were directly regressed with equation (4.12) to obtain the parameters A , τ , Bo .

A principal component analysis using SIMCA-P+ was carried out on the Bodenstein number along with the mean residence time and rotation rate, fill weight and the types of excipients and API. It was expected that this analysis would yield the effect of particle and operational parameters on the bodenstein number and mean residence time.

7.2 Blending Experiments

Powder blending experiments were performed in two sets. In the first set, two component blending experiments were carried out in the ribbon blender. Both Caffeine and Acetaminophen were used in combination with Lactose DCL-11 and DCL-14 and MCC Avicel PH-102 excipients. In the second set, three component experiments with magnesium stearate were examined. Acetaminophen and caffeine were mixed separately with Lactose DCL-11 and Magnesium Stearate (MgSt).

7.2.1 Two Component Experiments

Powder blending experiments were performed with both caffeine and acetaminophen in combinations with the excipients: two grades of lactose (DCL 11 and DCL 14) and MCC Avicel PH102. The excipients were fed using the Schenck Accurate Tuf-flex[®] automatic feeder. The feed rates and the masses of API fed into the blender are given in table 7.2. Experiments were carried out at three rotation rates, 10 , 20 & 30 RPM. The angle of incline of the blender was maintained at 0°. An NIR spectrometer was placed at the third quartz glass window of the blender just before the exit of the blender as shown in figure 7-1.

Table 7.2: API and Lubricant Feeding Profile Masses

| Excipient Flow Rate, kg/hr | Mass of API (g) | | | | Mass of Lubricant (mg) | | | |
|---------------------------------------|------------------------|-----|-----|-----|-------------------------------|-----|-----|-----|
| | 0% | 25% | 40% | 50% | 0% | 25% | 40% | 50% |
| 2.16 | 0 | 0.2 | 0.4 | 0.6 | - | - | - | - |
| 4.32 | 0 | 0.4 | 0.8 | 1.2 | 0 | 20 | 40 | - |
| 6.48 | 0 | 0.6 | 1.2 | 1.8 | 0 | 30 | 60 | - |
| 8.64 | 0 | 0.8 | 1.6 | 2.4 | 0 | 40 | 80 | - |
| 10.8 | 0 | 1.0 | 2.0 | 3.0 | - | - | - | - |

Two kinds of feeding profiles were used in introducing the feeder fluctuations. The only fluctuations that entered the blender were the pulsed feeding of API that was generated to approximate a sinusoid. This approximated sinusoid feeding of the API generated a feeding variance at the input that the blender was expected to reduce. In order to administer the feeding profile, API was weighed out in the dishes as shown in the tale 7.2 for various flow rates of the excipient. These weighed out dishes were emptied out into the blender at time intervals as shown in the table 7.3 and is depicted in 7-2. NIR spectra were taken at a frequency of 0.5 Hz. Noise in the NIR spectra were minimized by covering the back-end of the blender with aluminum foil.

Powder flowing out of the blender was collected in continuous back-to-back in-

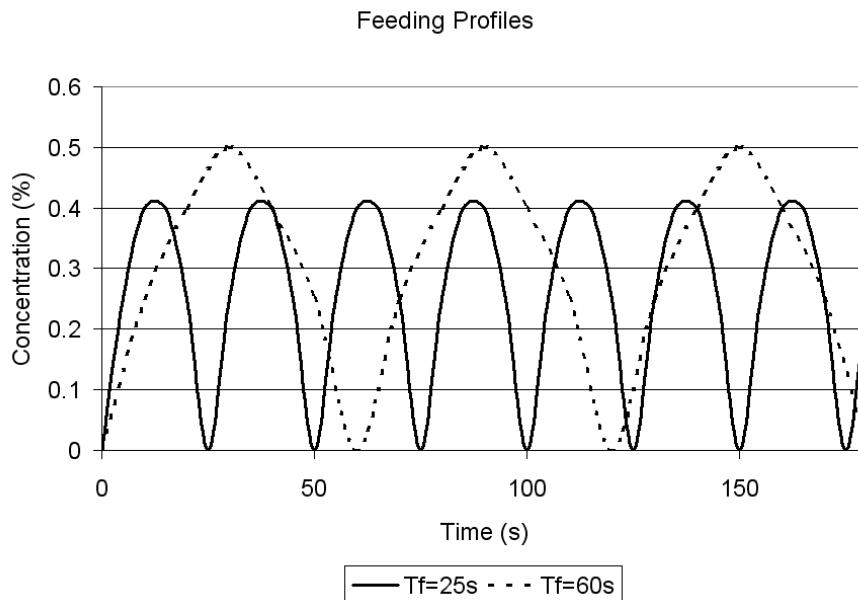


Figure 7-2: Input Fluctuations of API Content to the Ribbon Blender

tervals of 10 s each for one run at each rotation rate. This process yielded about 5 to 10 gm of powder in the sample vials. The spectra of these powder samples were taken offline by placing the sample vial on the NIR sensor window and scanning the NIR spectrum (after taking a background with the Spectralon tablet inside the vial). This process gave an averaged concentration of the API in a powder sample corresponding to $3\times$ the dose size that the FDA requires for validation of the blending process. Hence offline spectra of these powder samples were expected to reflect the blend quality as required by the FDA.

Table 7.3: API Feeding Time Profiles

| Profile | Time Period | Time Instant | Concentration |
|-------------|-------------|--------------|---------------|
| Normal Peak | 25s | 0s | 0% |
| | | 5s | 25% |
| | | 10s | 40% |
| | | 15s | 40% |
| | | 20s | 25% |

Continued on next page...

| Profile | Time Period | Time Instant | Concentration |
|---------------|-------------|--------------|---------------|
| | | 25s | 0% |
| | | 0s | 0% |
| | | 10s | 25% |
| | | 20s | 40% |
| Extended Peak | 60s | 30s | 50% |
| | | 40s | 40% |
| | | 50s | 25% |
| | | 60s | 0% |

End of Table

7.2.2 Three Component Experiments

Magnesium stearate (MgSt) was blended in the continuous blender with both active ingredients caffeine and acetaminophen with the excipient DCL-11 in three component blending experiments. The active ingredients were weighed out according to the Mass of API column in table 7.2 and corresponding lubricant masses was added on top of the active ingredient according to the Mass of lubricant column in the same table. The lubricant masses corresponded to a concentration of 1.5% of magnesium stearate by mass.

The Normal peak time profile feeding from table 7.3 was followed in feeding the API and lubricant that had been weighed out together in the same weigh boats. Only one rotation rate of the shaft - 10 RPM - was used for both caffeine and acetaminophen. Excipient Lactose DCL-11 was fed in accordance to the feed rates mentioned in table 7.3. Magnesium stearate was weighed out in dishes along with caffeine or acetaminophen, whichever was the API, in accordance to the masses given in the table 7.3. These dishes were emptied out to the blender at a frequency corresponding to the normal peak wave ($T_f = 25s$) in intervals of 5 seconds.

NIR spectra of the powder at the quartz glass window closest to the exit was collected. Powder samples were also collected in a fashion similar to the two component

experiments. One set of powder samples corresponding to each rotation rate were collected for both the APIs. These powder samples were equivalent to $3\times$ the dose size of the tablet as mandated by the FDA. Hence offline spectra of these powder samples were expected to reflect the blend quality as required by the FDA.

7.2.3 Analysis of Data

The PLS calibration method was used to convert the NIR data to concentrations. Variance reduction ratios were computed based on these concentrations. In order to address the effect of scale of scrutiny a 15 point moving average model was used to smooth the data. These methods and reasoning behind utilising these methods of analysis of data is described below.

7.2.3.1 Two Component Blending

Just like the NIR data from impulse response experiments, the NIR data were first pre-processed by taking 11-point Savitzky-Golay first derivative followed by a standard normal variate transform described in §4.3. The pre-processed data were converted to concentration of the API using the PLS calibration models from SIMCA-P+ given summarized in table 4.2.

Variance reduction ratio was computed by dividing the input variance by the the variance of 100 sample points at steady state computed by converting the NIR spectra to concentrations. Theoretical variance reduction ratio was computed using equation (4.25). The random mixture variance was computed by calculating the number of particles that the NIR spectrometer scans in each scan. The diameter of the NIR spectrometer scan window was 1mm. The penetration depth was known to be close to 2mm. With this estimate, the number of particles was computed using the particle size distribution of the excipients and API was found to be 12,000. Using this as the number of particles in equation (4.22), the random mixture variance was determined and used in computing the theoretical variance reduction ratio.

The number of points in the moving average model was determined as follows. The mass of powder examined at each NIR scan was determined. The size of the scan

window was 1mm in diameter. The penetration depth was 2mm. The scan volume therefore was 156mm^3 . The mass of powder scanned using the nominal density of lactose as 0.61 mg/mm^3 was 95gm. Since the scale of scrutiny mandated by FDA for a dose size of 500mg is $3 \times 500 = 1500\text{mg}$, the number of samples to be averaged for a 500gm tablet is $1500/95 \approx 15$. Therefore, a 15 point moving average model was used in determining the RSD of the powder mixture.

7.2.3.2 Three Component Blending

The NIR data from three component blending experiments were first pre-processed by taking a 11-point Savitzky-Golay first derivative followed by a standard normal variate transformation described in §4.3. The calibration model for the three component system had a low R^2 value (of 0.83) and high RMSE value. Hence, the method used to analyze the data was similar to that described in §5.2.3 for three component blending is used.

Principal component analysis was carried out on the pre-processed spectral data with the spectra of pure components appended to the time profile of the blending spectra. On computing first three principal components of the spectral data over all the experimental runs, it was observed that in general three components explained the variance in the spectra to about 90 – 95%. The loadings curve of the first two principal components indicated maxima over the peaks corresponding to magnesium stearate and caffeine spectral loading curve respectively. This indicated that the first two principal components represented chemometric contributions from MgSt and API and hence were used in determining the spectral RSD.

The spectral RSD was computed by calculating the variance in the principal component score corresponding to caffeine (first component) and subtracting the variance observed at the 0% caffeine. The square root of this variance was divided by the absolute value of the difference between the mean principal component score observed at 0% caffeine and mean principal component score observed at steady state. The spectral RSD computed this way shown in figure 5-7, was expected to reflect the real chemometric RSD of caffeine in the mixture, since the errors arising from density

and particle size fluctuations were removed by the spectral transformations. The exact same procedure was followed for determining the RSD of MgSt and the second principal component score was used to determine the spectral RSD of MgSt.

Chapter 8

Ribbon Blender Performance

The experiments described in chapter 7 and the analysis described in §7.1.3 and §7.2.3 were carried out. The effect of operational variables like shaft rotation rate, flow rate of excipient, angle of incline on the flow behavior and blending performance were studied.

8.1 Results on Flow Behavior Experiments

The steady state fill weight suggested a dependence on the initial fill weight in the blender. In order to establish qualify this dependence, the steady state fill weights were determined by running the blender in a cycle from 1 kg/hr to 3.5 kg/hr and then back to 1 kg/hr in a loop. From the RTD data, strong effects on mean residence time were detected from shaft rotation rate and flow rate, but insignificant dependence of Bodenstein number on operational variables was detected.

8.1.1 Fill Weight Experiments

Fill weight experiments were performed in the presence and absence of the automatic excipient feeder. In the absence of the automatic feeder, the effect of initial fill weight was examined by setting different initial fill weights. When the automatic feeder was used, a cycle experiment where the flow rate was increased from 1 to 3.5 kg/hr and then back to 1 kg/hr was performed as described in the chapter 7.

When the blender was manually fed, the fill weight fluctuated between a maximum and a minimum. This fluctuation was also seen in the evolution of flow rate with

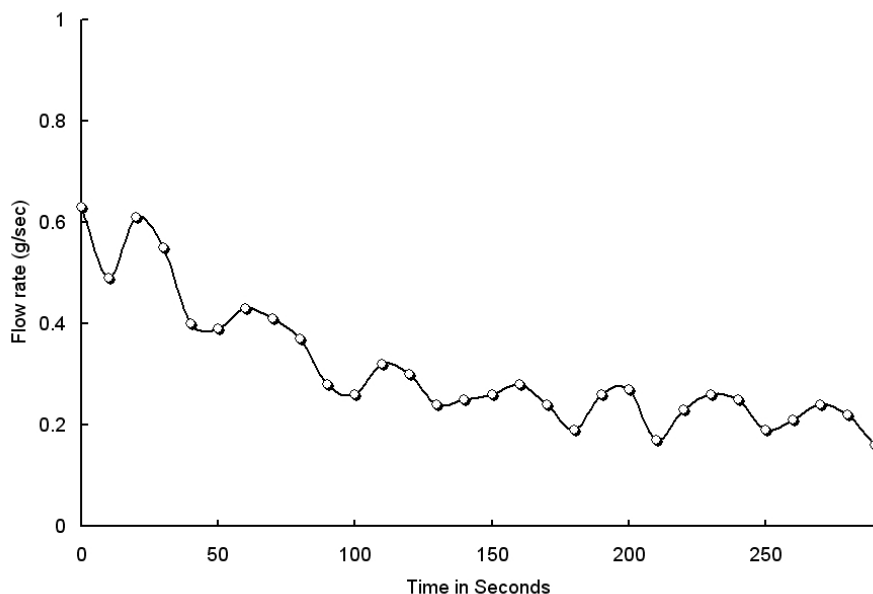


Figure 8-1: Time Profile of Flow Rate Evolution in the Ribbon Blender (Manual Feeding)

time as shown in figure 8-1. The maximum and minimum flow rates obtained at different flow rates were consistently parallel to each other as shown in figure 8-2. The reason behind this fluctuation is the fundamental concept that powders are inherently discrete (particulate) and hence do not flow continuously, as liquids and gases do, but at some level have a discretized nature embedded in their flow behavior.

As a result, it was decided to average the maximum and minimum fill weights at steady state and use that averaged value as the steady state fill weight for a given experimental run.

8.1.1.1 Effect of Initial Fill Weight

Since the flow behavior of powders are dependent on chaotic fluctuations and interactions, it was speculated that the fill weight could be dependent on the initial conditions. Hence experiments in the absence of and presence of the automatic feeder were carried out to examine this.

During manual feeding of excipient, When the initial fill weight was changed

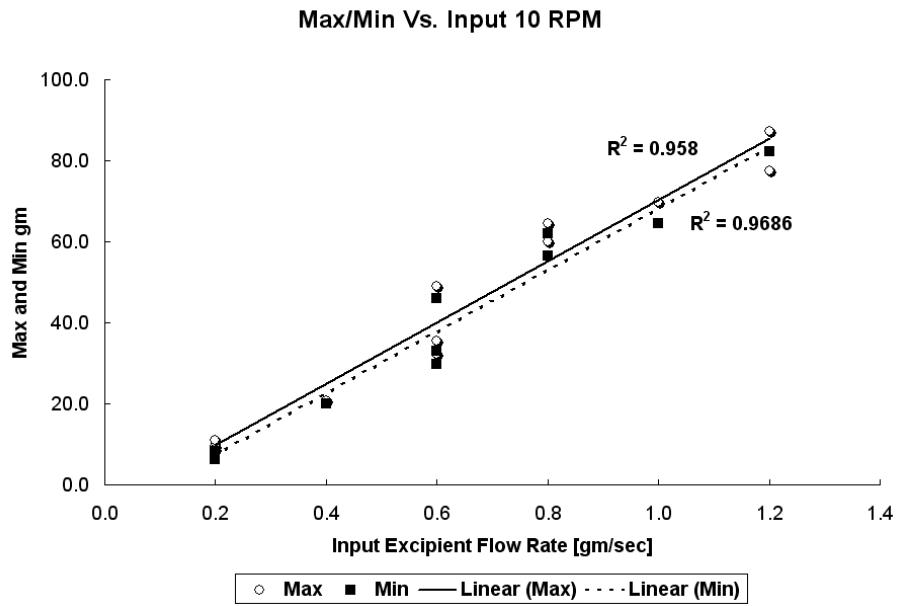


Figure 8-2: Maximum and Minimum Fill Weight at 10 RPM (Manual Feeding)

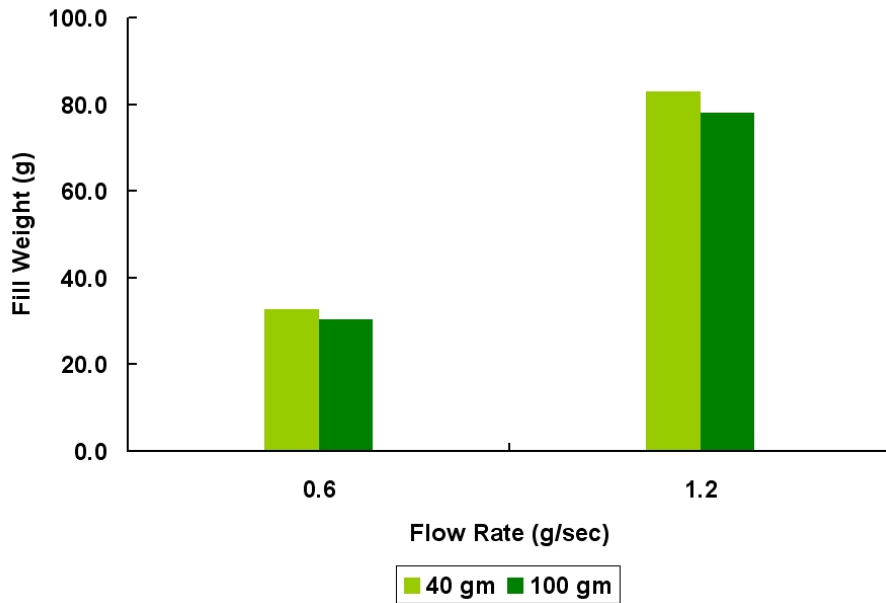


Figure 8-3: Dependence of Fill Weight on Initial Conditions

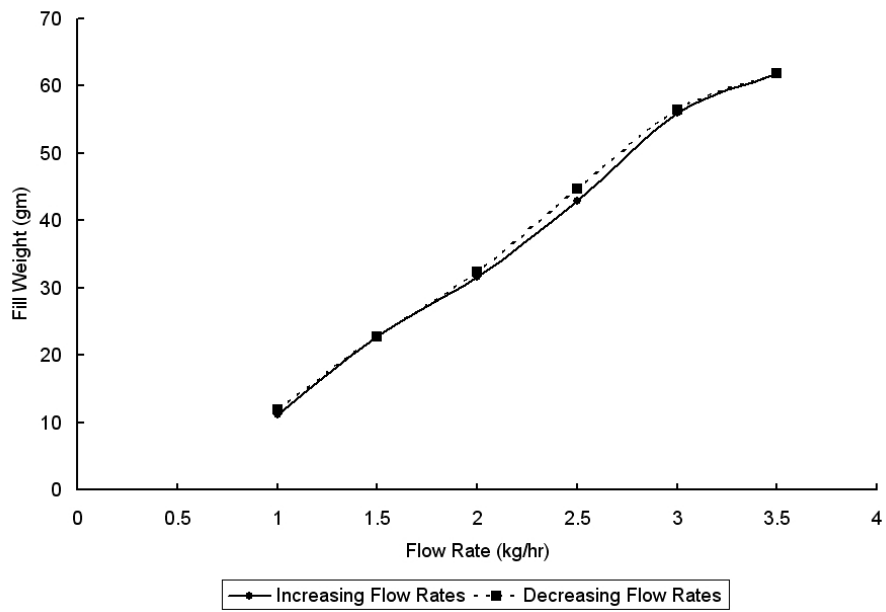


Figure 8-4: Steady State Fill Weights: Changing Initial Conditions with Automatic Feeder

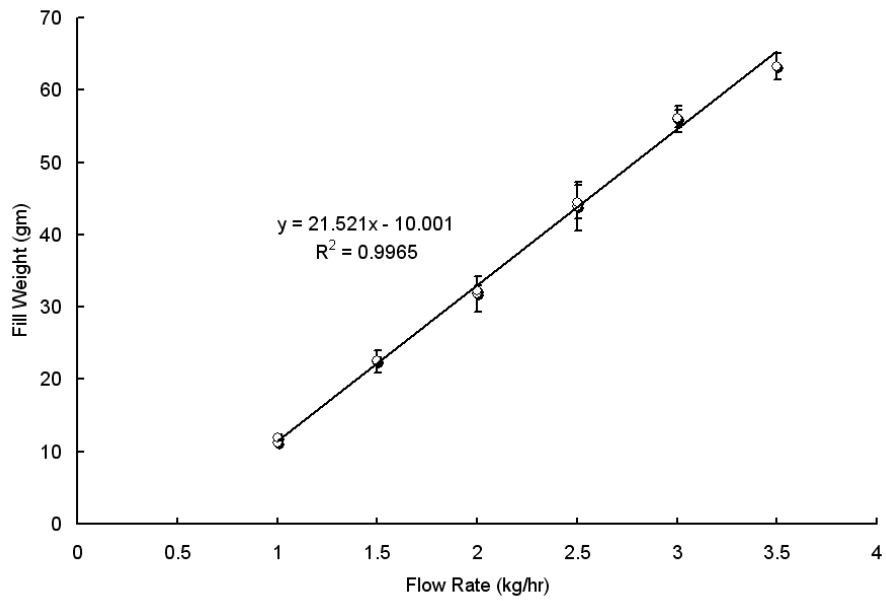


Figure 8-5: Repeatability of Fill Weights

from 40 gm to 100 gm the fill weight changed nominally as shown in figure 8-3. The difference between the observed steady state fill weights at these two initial conditions seemed quite small (only 6%.) The automatic feeder was used to feed lactose DCL 14 to the blender and a cycle experiment of increased and decreasing the flow rates was performed. No considerable effect of changing initial fill weights in the blender as shown in figure 8-4. Therefore, it was concluded that the scale of operation of the blender did not give rise to fluctuations in the fill weights to a large extent. A repeat experiment on determining fill weights showed that the linearity of fill weight was very repeatable as shown in figure 8-5.

8.1.1.2 Effect of Flow Rate on Fill Weight

As flow rate was increased, the fill weight in the blender increased linearly as shown in figures 8-5, 8-6, 8-7, and 8-8. This was in agreement with the fact that ribbon blender was a moderate shear equipment and no deformation or particle size reduction causing changes in density occurred. Therefore, a linear change in the fill volume with flow rate was expected. However, at $+5^\circ$ a change in the slope of the linear curve of fill weight vs flow rate was observed at all rotation rates and this effect would be discussed later.

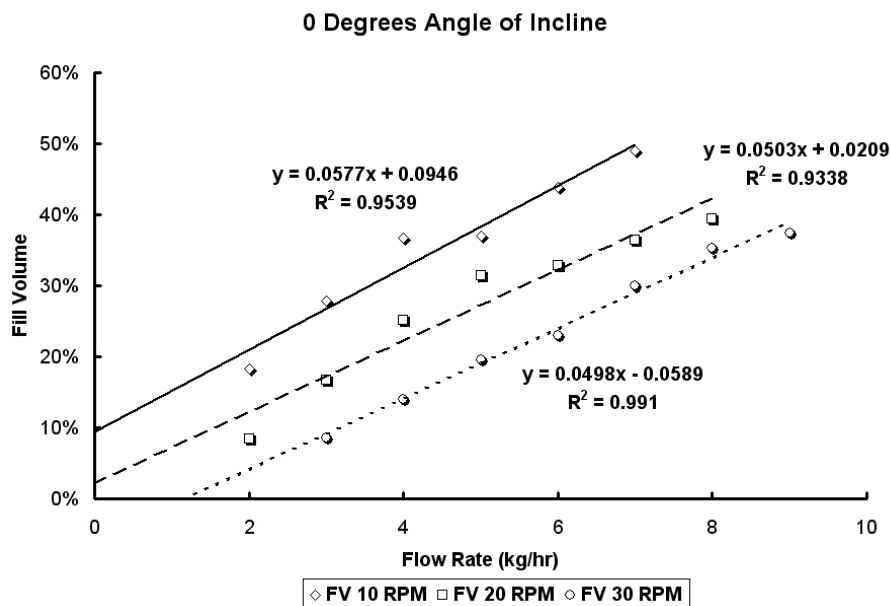


Figure 8-6: Steady State Fill Weights at Zero Degree Incline

8.1.1.3 Effect of Shaft Rotation Rate on Fill Weight

As the rotation rate increased, the fill weight in the blender decreased. This could be explained due to the fact that as rotation rate increased, the rate of removal from the blender increased causing a fall in the fill weight of the powder in the blender. However, it was observed that all the three angles of incline did not show the same effect with rotation rate and would be discussed below.

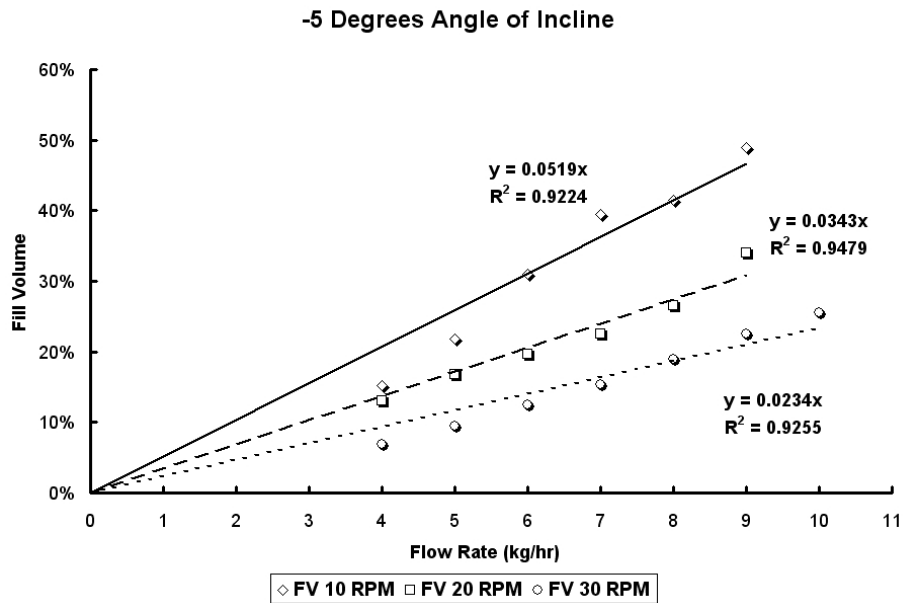


Figure 8-7: Steady State Fill Weights at -5 Degree Incline

8.1.1.4 Effect of Angle of Incline on Fill Weight

At 0° the fill weight linearity with flow rate had different X-intercepts at different rotation rates as shown in figure 8-6. This was due to the fact at very low flow rates the blender was cleared of all powder at 20 and 30 RPM causing X intercept to be 0 or positive. At 10 RPM the blender the fill weight of the blender was non-zero at very low flow rates and this limit was shown to be 10% of the maximum fill weight in the blender.

At -5° the fill weight linearity with flow rate had the same X-intercepts at different rotation rates and was at 0% as shown in figure 8-7. This was due to the fact at very

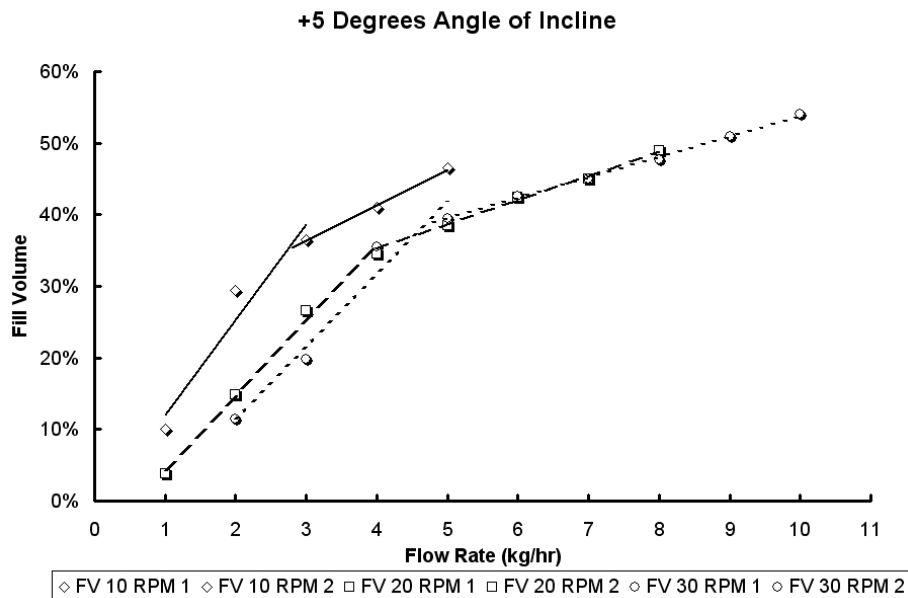


Figure 8-8: Steady State Fill Weights at +5 Degree Incline

low flow rates the blender was cleared of all powder at all rotation rates causing X intercept to be 0.

At +5° the fill weight linearity with flow rate changed slopes as flow rates increased as shown in figure 8-8. The effect of 20 and 30 RPM were not very different above this critical flow rate. It was observed that the second window of the blender (c.f. figures 4-2 and 7-1 became active and powder began flowing out of the second window. This caused a reduction in the slope of the fill weight vs flow rate line as more flow rate was required to achieve a certain fill weight after the critical flow rate.

8.1.2 RTD of API in Ribon Blender

The impulse response experimental data from LIF and NIR experiments were converted to concentrations and the axial dispersion model was used to fit the data as shown in figure 8-9. It was observed that this axial dispersion model could statistically explain over 85% of the variance in all the observed data. Many of the experimental RTDs had an R^2 value of 0.9 or higher using the open-open axial dispersion model (c.f. equation (4.9)). The fitted values of Bo and τ were analyzed in terms of their dependence on different operational parameters.

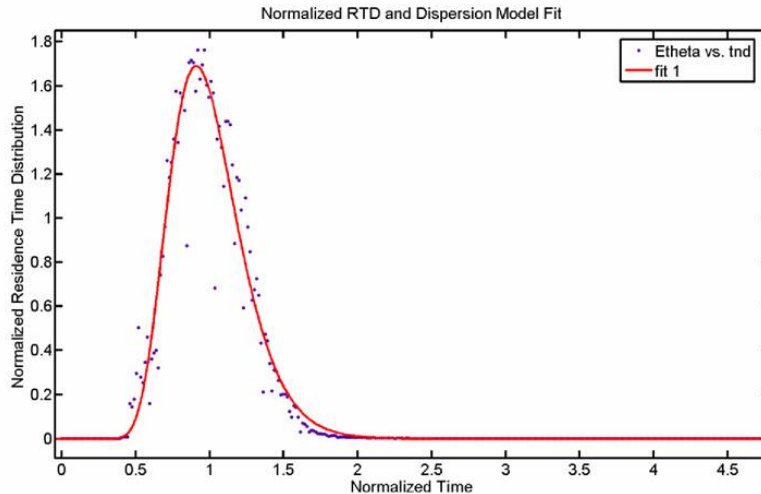


Figure 8-9: Non-linear Regression of Experimental Data with the Open-open Axial Dispersion Model

8.1.2.1 Effect Shaft Rotation Rate on Mean Residence Time

The mean residence time of caffeine in sieved lactose powder decreased with increasing shaft rotation rates at all angles of incline as shown in figures 8-11, 8-13 and 8-12. This decrease was observed when the NIR spectrometer was employed instead of the LIF sensor as well as shown in figure 8-10.

Increasing the shaft rotation rate increased the mean velocity of the powder in the blender and therefore caused a decrease in the mean residence time of the caffeine in the blender. The repeatability in mean residence time was very poor and a number of sources of variance were found to exist that would be discussed in §9.3.

8.1.2.2 Effect of Angle of Incline on Mean Residence Time

RTD results from LIF data shown in figures 8-11, 8-13 and 8-12 showed that excipient flow rate had a different effect at different angles of incline. At 0° , shown in figure 8-11, as flow rate increased, the residence time decreased due to increased mean velocity of the material in the blender.

At -5° , shown in figure 8-12, as flow rate increased, the mean residence time showed a mild increase. This was a result of decreased fill weights in the blender due to the reduced angle of incline. At low flow rates, due to reduced fill weights, powder

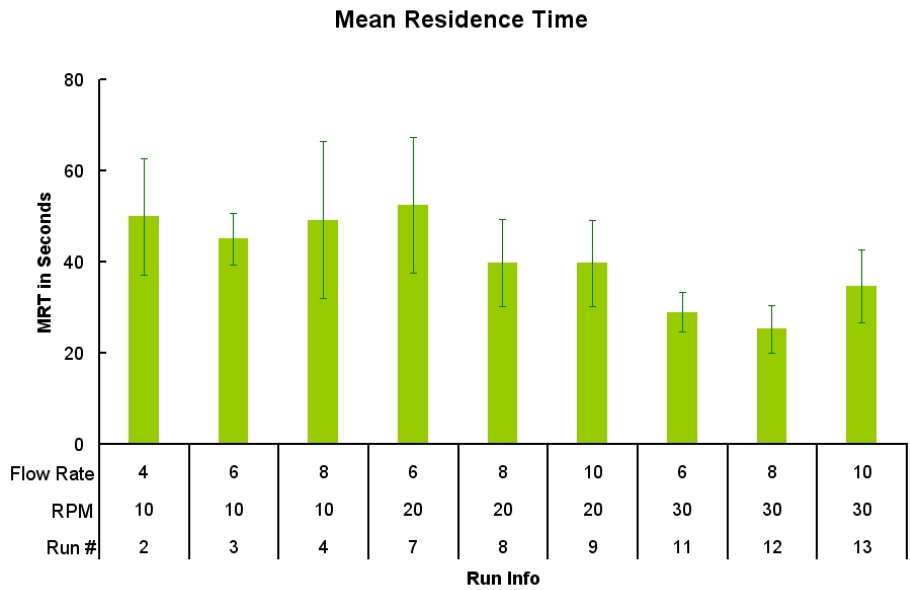


Figure 8-10: Mean Residence Times from NIR Data

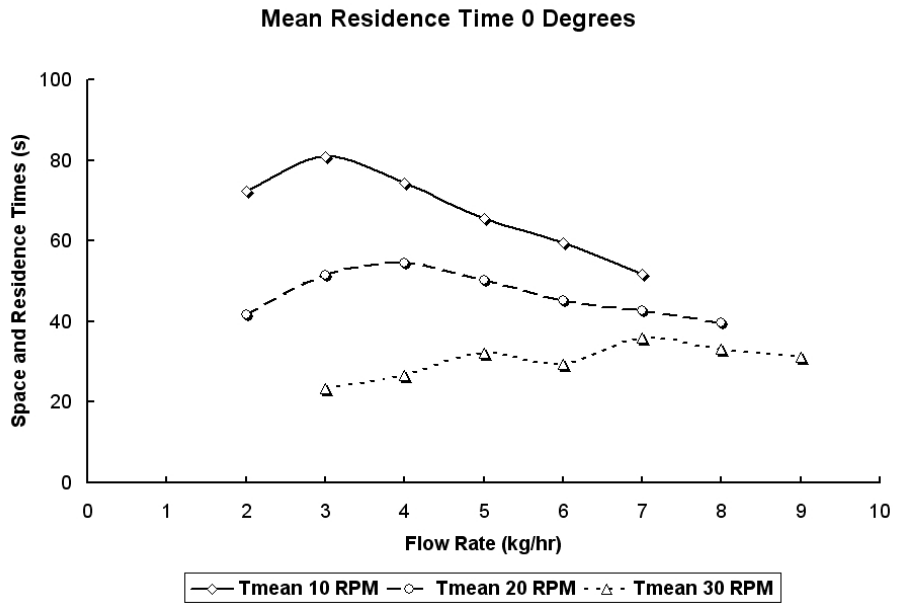


Figure 8-11: Mean Residence Times (0°)

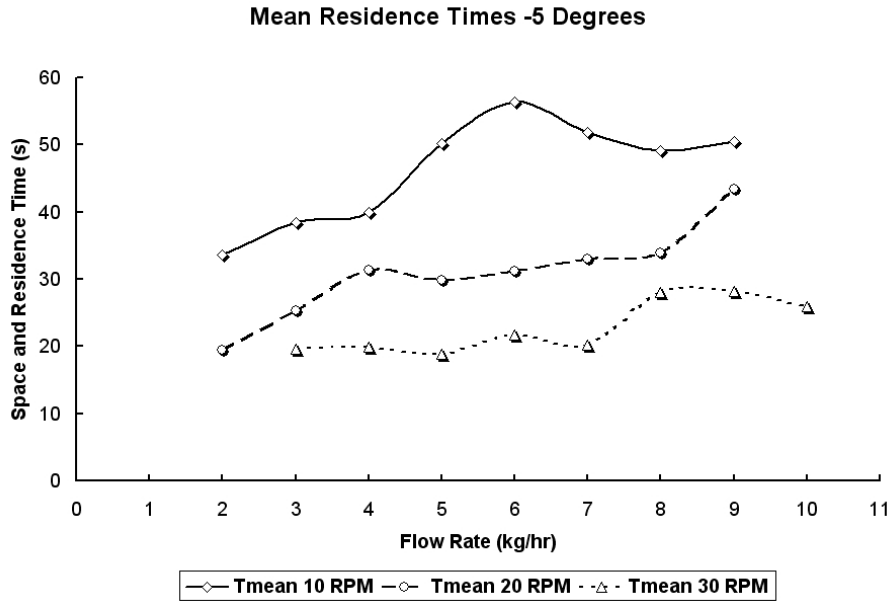


Figure 8-12: Mean Residence Time (-5°)

did not come in contact with the inner ribbon of the blender and hence the residence time was lower than what was observed at 0° and 5° . But as the flow rate increased fill weights increased, which lead the powder to come in contact with the inner ribbon thereby increasing the mean residence time of powder in the blender.

At $+5^\circ$, shown in figure 8-13, a similar phenomenon, as was observed in the fill weights, was seen. The mean residence times increased from low flow rates to a critical flow rate after which the the mean residence times began to decrease with increasing flow rate. It was observed that this maximum occurred at the point where the second exit in the ribbon blender as shown in figures 4-2 and 7-1 was activated and powder began flowing out of the second exit as well. After the second window was active, the mean residence times began decreasing with increasing flow rate due to increased mean velocities of the particles in the blender. As with the observations on fill weights, 20 and 30 RPM were found to give similar mean residence times at higher flow rates.

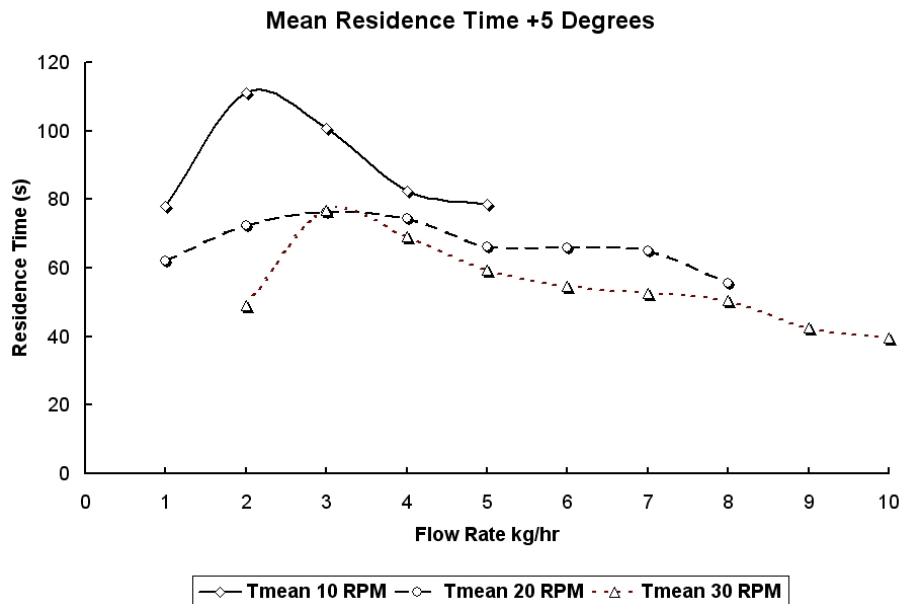


Figure 8-13: Mean Residence Times (+5°)

8.1.2.3 Effect of Flow Rate on Mean Residence Time

Increasing Flow rate was expected to decrease the mean residence time of caffeine in the blender. However, this effect was found to interact with the shaft rotation rate and the angle of incline. When angle of incline was increased, a maximum in mean residence time was observed near the critical flow rate where the second window was activated. When the angle of incline was decreased, the inner ribbon was not activated due to low fill weights and hence caused an increase in mean residence times as flow rates increased. It was found that within a given regime of operation, increasing flow rates decreased mean residence times due to increased mean velocities of particles in the blender.

8.1.2.4 Effect Shaft Rotation Rate on Dispersion Coefficient

Dispersion coefficients were computed using experimentally determined mean residence times and Bodenstein numbers as described in §7.1.3. As rotation rates were increased, the dispersion coefficient at +5° and -5° (c.f. figures 8-15 and 8-16) angles of incline showed an increase at higher flow rates. This was attributed to the increase in fill weight of the powder in the blender which resulted in increased mixing

by both the inner and outer helices. The overall effect of rotation rates on dispersion coefficient at different angles of incline, however, was found to be inconclusive.

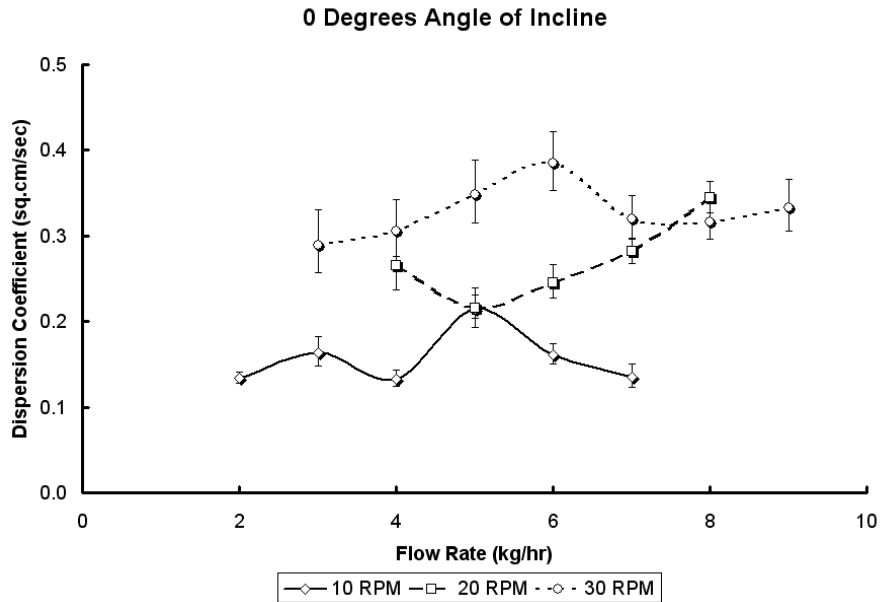


Figure 8-14: Dispersion Coefficient of Caffeine in Sieved Lactose (0° Incline)

8.1.2.5 Effect of Flow Rate on Dispersion Coefficient

The effect of flow rate, as seen in the graphs plotting dispersion coefficients with flow rate and rotation rates for different angles of incline in figures 8-14, 8-15 and 8-16, on dispersion coefficient was very negligible. The dispersion coefficient remained independent of the flow rate over all the experiments.

8.1.2.6 Effect of Angle of Incline on Dispersion Coefficient

Decreasing the angle of incline from 0° to -5° was found to have a large effect of dispersion coefficients. The dispersion coefficients at -5° and 30 RPM averaged at 1 cm²/s while at 0° and +5° the dispersion coefficients were considerably less (≈ 0.5 cm²/s) as seen by comparing figures 8-14, 8-15 and 8-16. However, the errors in the estimating dispersion coefficients from the RTD are considerably higher, casting doubts on the validity of this effect.

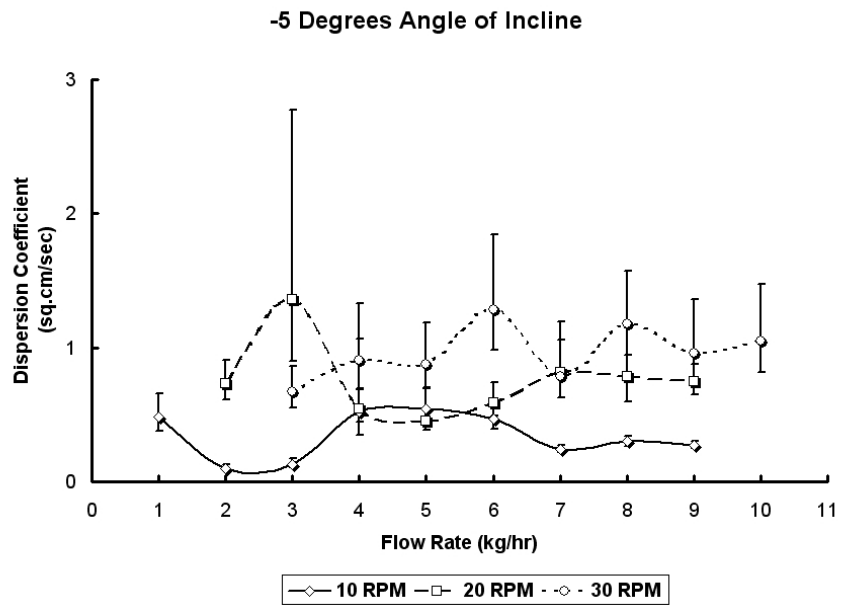


Figure 8-15: Dispersion Coefficient of Caffeine in Sieved Lactose (-5° Incline)

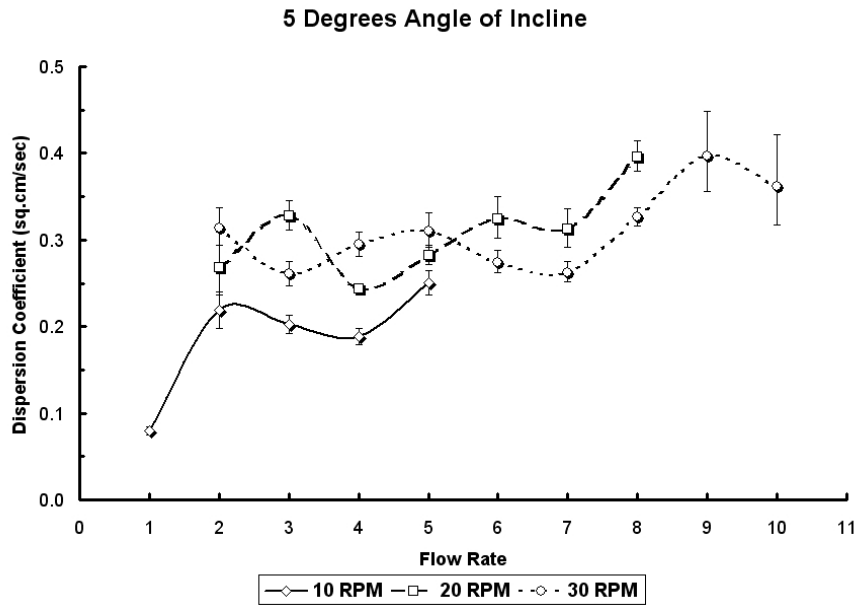


Figure 8-16: Dispersion Coefficient of Caffeine in Sieved Lactose ($+5^\circ$ Incline)

8.2 Results of Blending Experiments

Blending experiments were performed as described in chapter 7 and the data was analyzed as described in §7.2.3. The angle of incline was fixed at 0° and the two exits of the blender were completely opened for all the blending experiments. For the two component experiments, the effect of rotation rate, time period of fluctuation and mean residence time and dispersion coefficient on variance reduction ratio was examined. For the three component experiments, the comparison between the spectral RSDs in the presence and absence of the third component was examined.

8.2.1 Two Component Experiments

Blending experiments were performed with three excipients, two APIs and at two different feeding fluctuation frequencies. From the RTD experiments, it was gleaned that the mean residence time was the factor that varied the most while dispersion coefficient was predominantly invariant within many of the experiments. It was therefore expected that dispersion coefficient would have little effect on variance reduction ratio within the range of experiments performed.

8.2.1.1 PCA of VRR

Principal component analysis of variance reduction ratio data, axial dispersion coefficients and mean residence times was performed on all the experiments. It was found that the mean residence time had the strongest correlation with VRR as shown by figure 8-17 where the position vector of the variable, VRR has a positive scalar product with the position vector of mean residence time, indicating that a higher mean residence time increases the variance reduction ratio. The scalar product of the position vector of dispersion coefficient is almost orthogonal to the position vector of variance reduction ratio.

8.2.1.2 Effect of Dispersion Coefficient

The effect of dispersion coefficient was shown to be negligible on variance reduction ratio in the experimental design space of the set of experiments performed in this

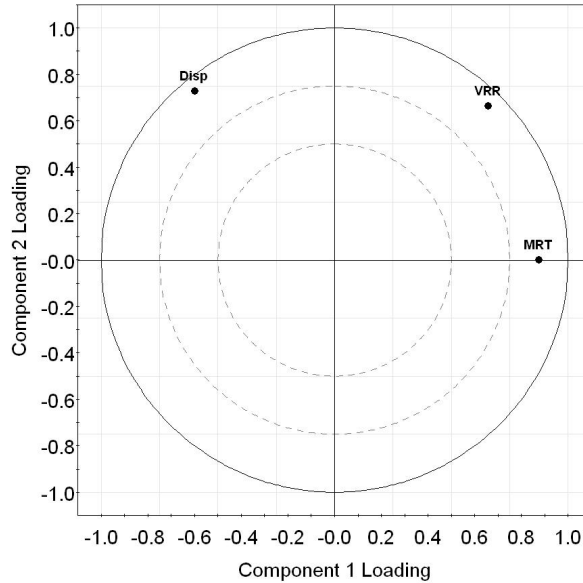


Figure 8-17: Loadings Plot of VRR, Mean Residence Time and Dispersion Coefficient

work. The reason behind this negligible effect can be reasoned out by taking recourse to the fact that the dispersion coefficients in our work did not vary greatly, but were bounded between 0.1 and 2 cm²/sec. Also, considering equations (4.9) and (4.25), it was seen that such a small variation in dispersion coefficient would have very small effect on the variance reduction ratio since variance reduction ratio was proportional to $\sqrt{Bo} \exp -Bo$ which did not exhibit strong changes in VRR even though Bo varied 10× within the experimental space. However, as we shall see later, mean residence time had a strong effect on VRR and also varied from 25 secs to 90 sec in our experiments.

8.2.1.3 Effect of Shaft Rotation Rate

Principal component analysis of variance reduction ratio, shaft rotation rates, flow rate, and fill weight and mean residence time was carried out. The resulting loading plot showed that the variance reduction ratio has a negative correlation with the shaft rotation rate and fill weight. This was evident from the negative scalar product of the position vectors of VRR with shaft rotation rate and fill weight as shown in figure 8-18. As an aside, it was found that the shaft rotation rate correlated negatively with

the mean residence time and this was in agreement with the results from the RTD analysis where an increase in shaft rotation rate resulted in decreased mean residence times and fill weights.

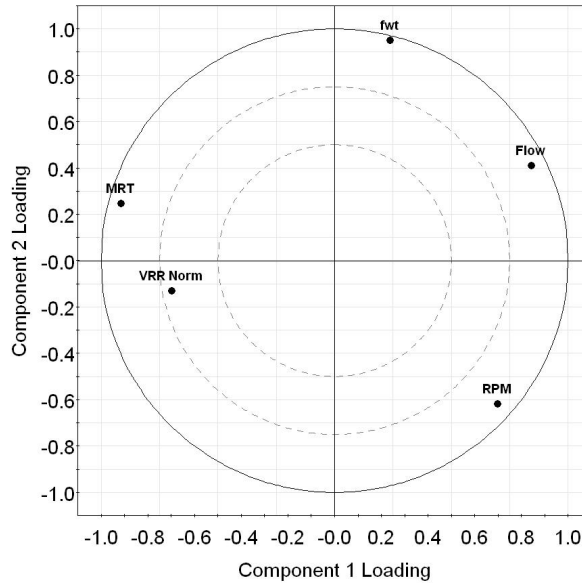


Figure 8-18: Loadings plot of VRR, Mean Residence Time, Flow Rate and Fill Weight

8.2.1.4 Effect of Flow Rate

Principal component analysis of variance reduction ratio, shaft rotation rates, flow rate, and fill weight and mean residence time was carried out. The resulting loading plot showed that the variance reduction ratio has a negative correlation with the flow rate and fill weight. This was evident from figure 8-18 where the position vectors of the points flow rate and fill weight have a negative scalar product with the position vector of VRR. As an aside, it was found that the shaft rotation rate correlated negatively with the mean residence time and this was in agreement with the results from the RTD analysis where an increase in flow rate resulted in decreased mean residence times and fill weights at 0° incline.

8.2.1.5 Effect of Mean Residence Time

Mean residence time was shown to have the strongest effect on variance reduction ratio. It was clearly seen that mean residence time was affected by fill weight, flow rate and rotation rate and hence the indirect effect of these operational variables on variance reduction ratio. VRR was found to be strongly affected by mean residence time as shown in figure 8-19.

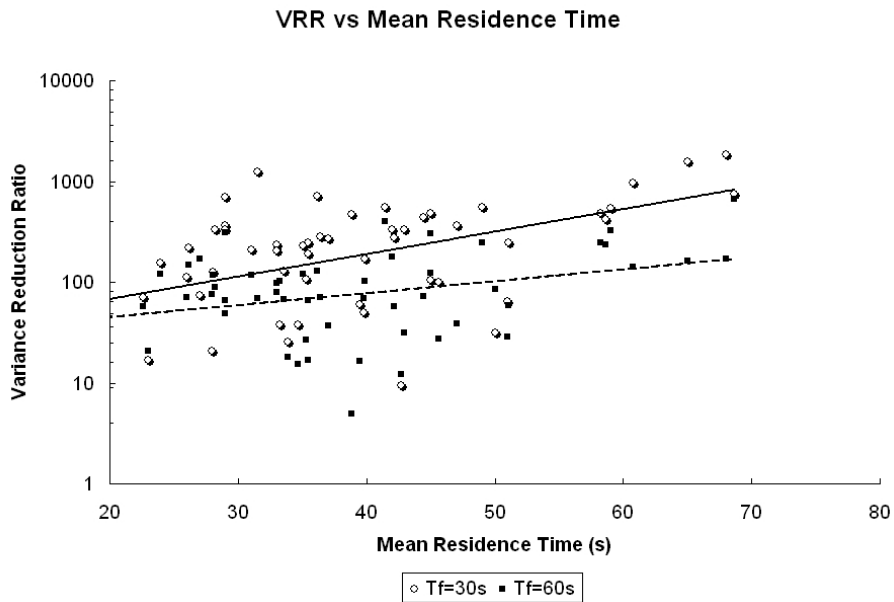


Figure 8-19: Variance Reduction Ratio vs Mean Residence Time

It was seen that as mean residence time increased the variance reduction ratio increased indicating a better performance of the blender. Clearly, as the mean residence time increased, the amount of time the powder spent in the blender, the amount of energy spent on the powder by the blender and the amount of backmixing provided by the mixer were all higher. Therefore, the effect of mean residence time was seen to be the strongest on variance reduction ratio. As demonstrated in §9.3 that the variance reduction ratio can be predicted from the residence time distribution c.f. equation (4.25), and within experimental errors in determining the mean residence time, the predictions were very satisfactory.

8.2.1.6 Effect of Disturbance Time Period

The effect of time period of the fluctuations introduced into the blender on variance reduction ratio was expected to be in agreement with equation (4.21) where the variance reduction ratio was proportional to the ratio of mean residence time to time period of fluctuation entering the blender. It was found that the variance reduction decreased with increasing fluctuation time period in line with the effect that as the time period of fluctuation entering the blender increased, the blender was unable to reduce and modulate the disturbances leading to increased VRRs. It was also found that the VRR decreased with increasing ratios of mean residence time to time period of fluctuations entering the blender as shown in figure 8-20. The theoretical predictions of VRR and dependence on $\frac{T_m}{T_f}$ will be discussed in §9.3.

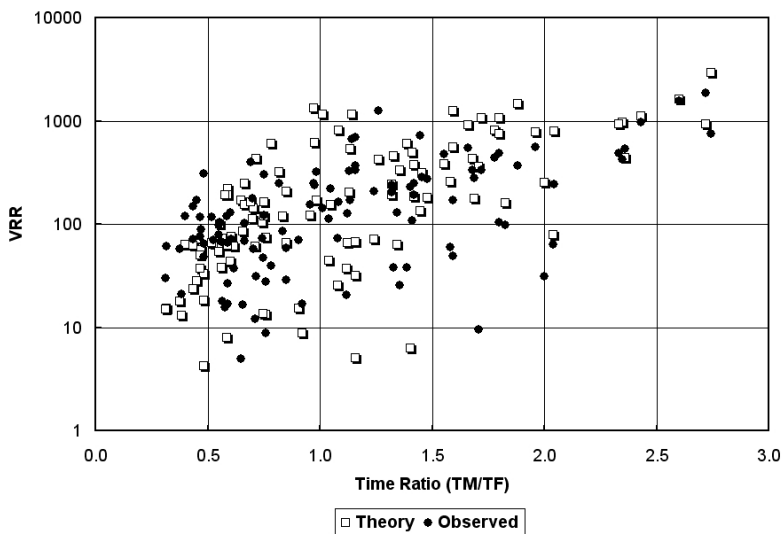


Figure 8-20: VRR vs $\frac{T_m}{T_f}$

8.2.2 Three Component Blending

Three component experimental data and offline samples were collected and analyzed as described in §7.2 and §7.2.3. The spectral RSD computed from principal components of the blending spectra were used to understand the effect of three component blending as described in §7.2.3. In order to understand the difference between two

and three component blending, spectral RSD from the two component blending spectra of experimental runs corresponding to the three component blending experiments were also computed.

8.2.2.1 Effect of MgSt on API RSD

MgSt was found to have deteriorating effect on the spectral RSDs of caffeine and acetaminophen. The spectral RSD of caffeine was found to increase when caffeine was blended with MgSt and lactose DCL-11 as shown in figure 8-21. However, it was noted that the increase in the spectral RSDs of caffeine upon addition of MgSt was not very significant at both 4.32 and 8.64 kg/hr.

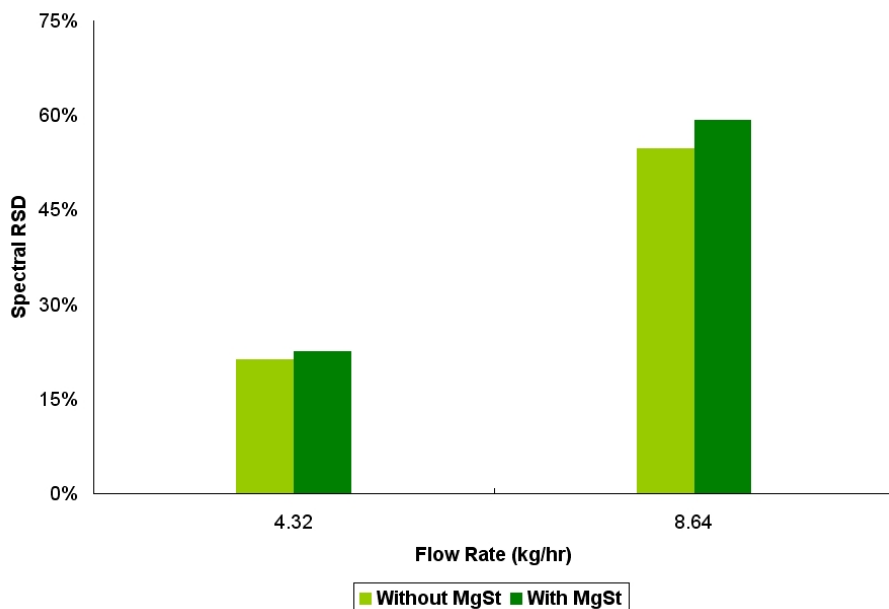


Figure 8-21: Effect of MgSt on Caffeine RSD in Ribbon Blender

The spectral RSD of acetaminophen was also found to increase when acetaminophen was blended with lactose DCL-11 and MgSt, as shown in figure 8-22. The increase in RSD of acetaminophen when MgSt was added was very significant at both 4.32 and 8.64 kg/hr. MgSt decreases the cohesion between particles by means of forming a thin layer (coat) of MgSt particles around the API and excipient particles. MgSt was found to have the strongest effect on Acetaminophen because cohesion between acetaminophen particles were brought down from a value of 0.65 to a low of 0.22 mJ/m^2

compared to a drop from 0.43 to 0.22 mJ/m^2 for caffeine. This decrease caused considerable demixing along the length of the blender and therefore resulted in increased spectral RSDs for acetaminophen.

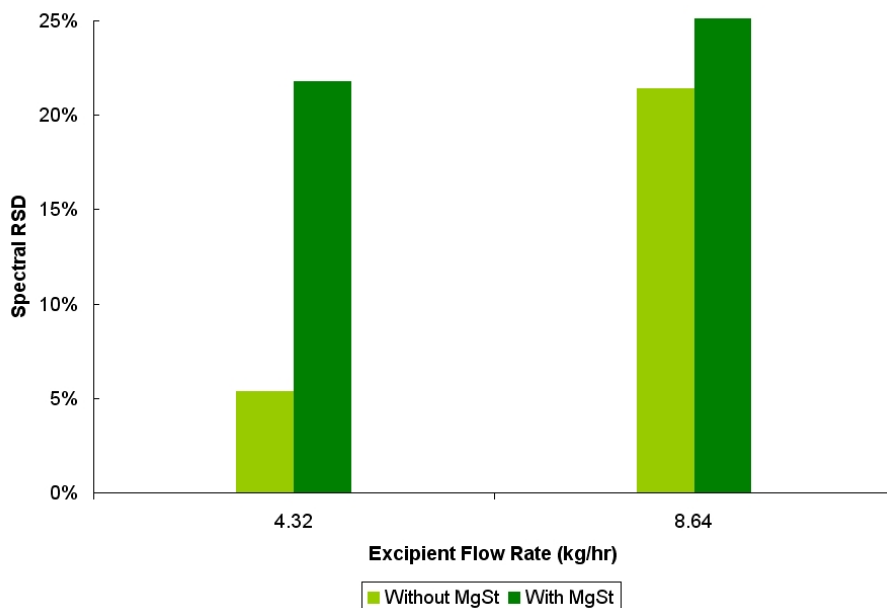


Figure 8-22: Effect of MgSt on Acetaminophen RSD in Ribbon Blender

8.2.2.2 Effect of Residence Time on API RSD and MgSt RSD

As flow rate increased, the residence time at a given rotation rate of the shaft decreased. Hence, from figures 8-21 and 8-22 we found that an decrease in the residence time increased the spectral RSD of caffeine and acetaminophen. The presence of MgSt exacerbated the increase in acetaminophen RSD because of reasons already discussed.

The spectral RSD of magnesium stearate decreased, as shown in figure 8-23, when blended with acetaminophen, with a decrease in mean residence time (i.e., increase in flow rate). This decrease in spectral RSD of MgSt implied a well-distributed MgSt coating on acetaminophen than that of caffeine. Therefore, the RSDs of acetaminophen increased more than that of caffeine due to the addition of MgSt.

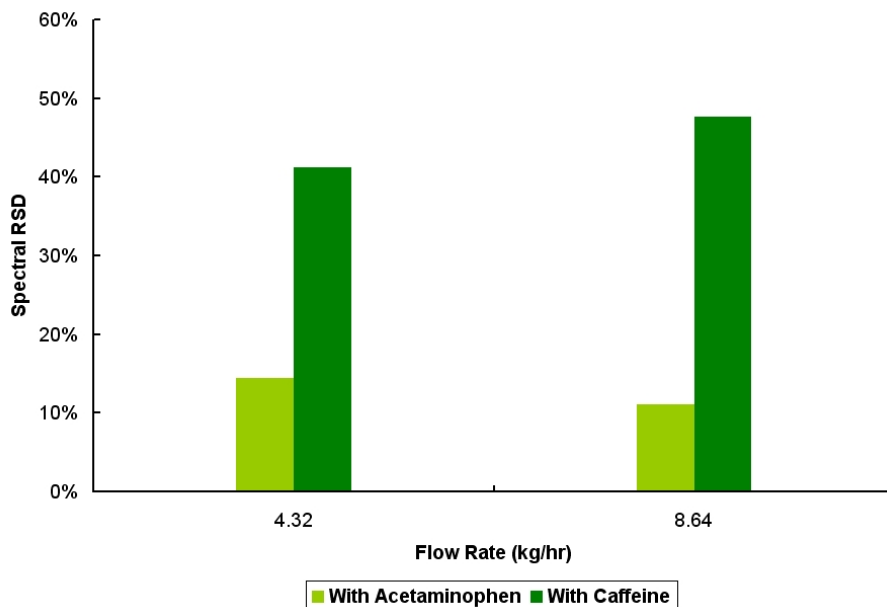


Figure 8-23: Effect of MgSt on MgSt RSD in Ribbon Blender

8.3 Summary of Results

It was shown that since powders were comprised of discrete particles, the achievement of steady state and the measurement of fill weights needed averaging over a maximum and minimum observed fill weights at steady state. Nevertheless, the averaged fill weights were linearly proportional to flow rate and inversely proportional to rotation rate. The mean residence times decreased with increasing the shaft rotation rates. The dependence of dispersion coefficients on operational variables was found to be inconclusive. There was no apparent trend that was consistent with the physics of the process and it was expected that it could be a parameter dependent on the fundamental particle properties than the macroscopic operational variables.

It was shown that the variance reduction ratio was a strong function of mean residence time and fluctuation time period and was found to be proportional to the ratio of T_m to T_f . Within the experimental design space, the axial dispersion coefficient was found not to have a significant effect on variance reduction ratio. The operational variables like flow rate, shaft rotation rate and fill weight were affecting the variance reduction ratio only through mean residence time. The effect of three

component blending showed that the spread of the third component, lubricant in this case, dictated the homogeneity of the API. An increase in lubricant deteriorated the mixture quality.

Chapter 9

The Effect of Microscale Properties on Macroscopic Phenomena

Much like the phenomenological behavior of fluids that depends on the molecular properties of materials, the phenomenological behavior of powders depends on the microscopic properties of particles composing the bulk powder. The determination of this relationship is of critical importance in assuring that powder processing phenomena are well understood, well characterized and well controlled. Domike [25] and Ngain [71] related the microscopic properties of particles like particle size, cohesive and adhesive surface energies to macroscopically observed phenomena. The effect of particle size, cohesion and adhesion surface energies and particle shape were examined in this work and the results are described in subsequent sections.

9.1 Effect of Particle Size

In order to understand the effect of microscopic properties on continuous blender performance, two sets of experiments were performed. First, the particle size of the excipient was within the same type of the excipient. Lactose DCL 14 was sieved and was divided into excipients of two different particle size cuts $45 \leq D \leq 150 \mu\text{m}$ and $150 \leq D \leq 250 \mu\text{m}$. Impulse response experiments (described in §7.1) were carried out with these excipients and caffeine of a fixed particle size distribution, $D_{mean} = 200 \mu\text{m}$ and $\sigma = 100 \mu\text{m}$. The impulse response experimental data were converted to concentrations and subsequently regressed with the dispersion model c.f.

equation (4.9) as described in §7.1.3.

9.1.1 Effect of Size on Bodenstein Number

An increase in size of the excipient particles that forms the bulk of the powder mixture resulted in a decrease in the Bodenstein number as shown in figure 9-1 at 0° incline. This meant that as particle size of the excipient increased or the size ratio of excipient to active ingredient increased, the dispersive mixing component in the Bodenstein number increased in relation to the convective mixing component.

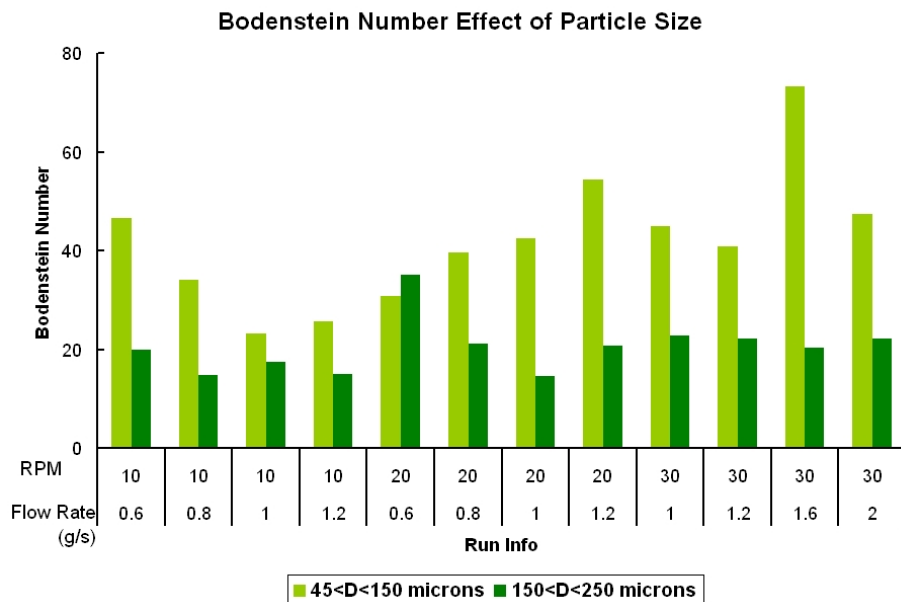


Figure 9-1: Effect of Particle Size on Bodenstein Number

It was expected that as particle size increased, the dispersive component of mixing would be increased as larger particles were expected to overcome the forces of cohesion and adhesion due to gravity and were expected to disperse more freely in the mixture. However, A separate evaluation of the dispersive mixing component was also performed as described below.

9.1.2 Effect of Size on Dispersion Coefficient

As the size of the excipient increased (or the ratio of the excipient to API particle size increased), the dispersion coefficient increased as shown in figure 9-2. Clearly,

particle size played a critical role in determining the extent of dispersive mixing in the blender. As particle size increased, Ngai [71] showed that the particle balanced the forces of gravity with cohesive and adhesive forces. If the size was increased even further, the cohesive effect of the particles no longer played a role in holding the particles together and hence random movement of particles on the free surface generated by the movement of the ribbons in the blender increased. This increased random movement resulted in increased dispersion coefficients as shown in figure 9-2.

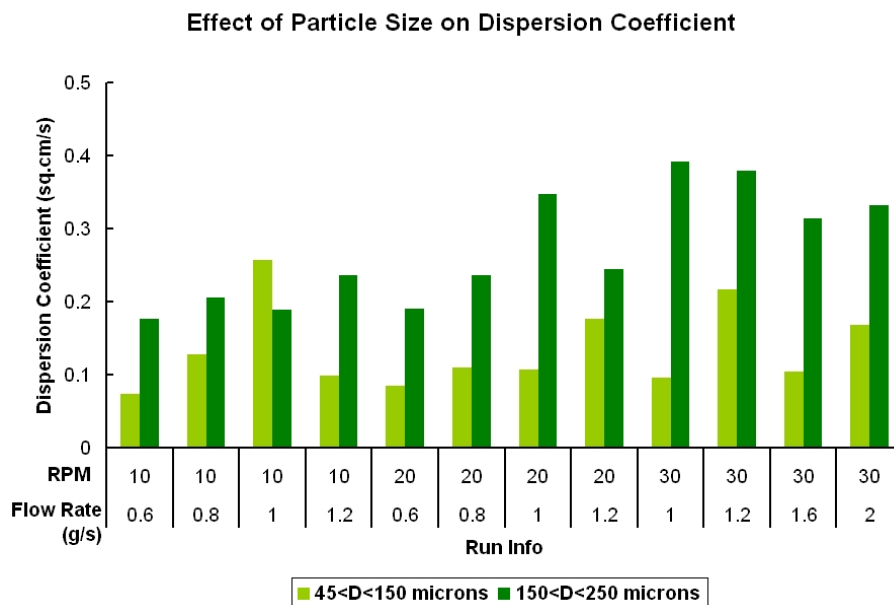


Figure 9-2: Effect of Particle Size on Dispersion Coefficient

9.1.3 Effect of Size on Variance Reduction Ratio

The effect of increasing the particle size of excipient at constant API particle size on blender performance was theoretically estimated. The theoretical estimation procedure was carried out on the basis of equation (4.16). The variance reduction ratio was determined by using the experimentally determined RTD and the sinusoidal forcing input function of equation (4.18). Two disturbance time periods, 30 and 50 seconds, were used in determining the theoretical variance reduction ratios for the RTDs from the two different particle size distributions (whose dispersion coefficients were shown

in figure 9-2).

As the particle size increased, the variance reduction ratio plotted as a function of the mean residence time was higher for the particles of larger excipient size. This was observed at both the disturbance time periods as shown in figures 9-3 and 9-4. The effect of time period of fluctuation was also seen to be in consonance with observations made before on the effect blender performance due to the time period of fluctuation.

As seen in figures 9-5 and 9-6, the variance reduction ratio decreased with increasing time period of the input fluctuations, indicating that as the time period of fluctuations increased, the blender was unable to modulate or reduce the variance at the inlet. This was in consonance with the observation made from literature, as shown in equation (4.21) and from the results of blending experiments at two distinct input fluctuation time periods as described in §7 and figure 8-20.

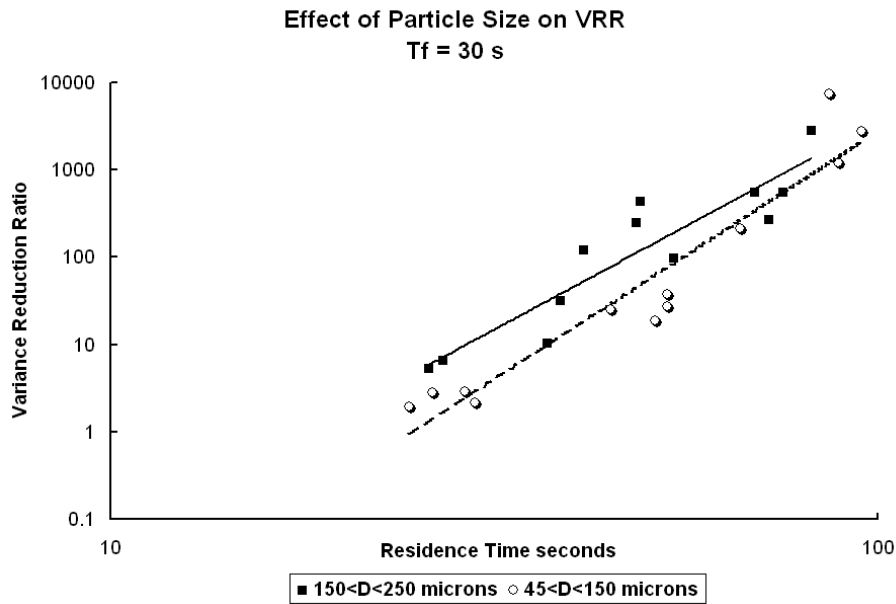


Figure 9-3: Effect of Particle Size on VRR $T_f = 30s$

9.2 Effect of Microscale Properties

The effect of microscale properties like cohesive and adhesive surface energy, effect of shape of particle and the effect of lubricant were studied by varying the types

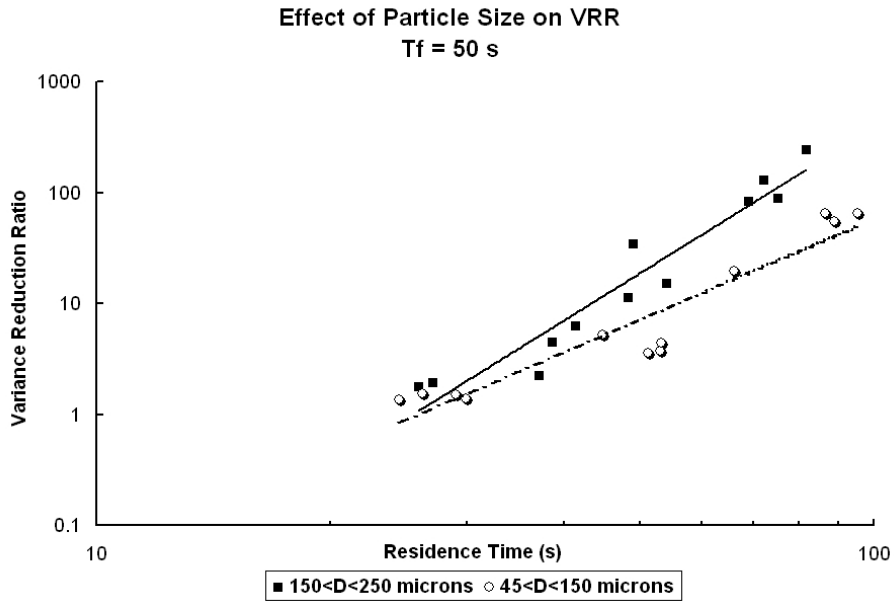


Figure 9-4: Effect of Particle Size on VRR $T_f = 50$ s

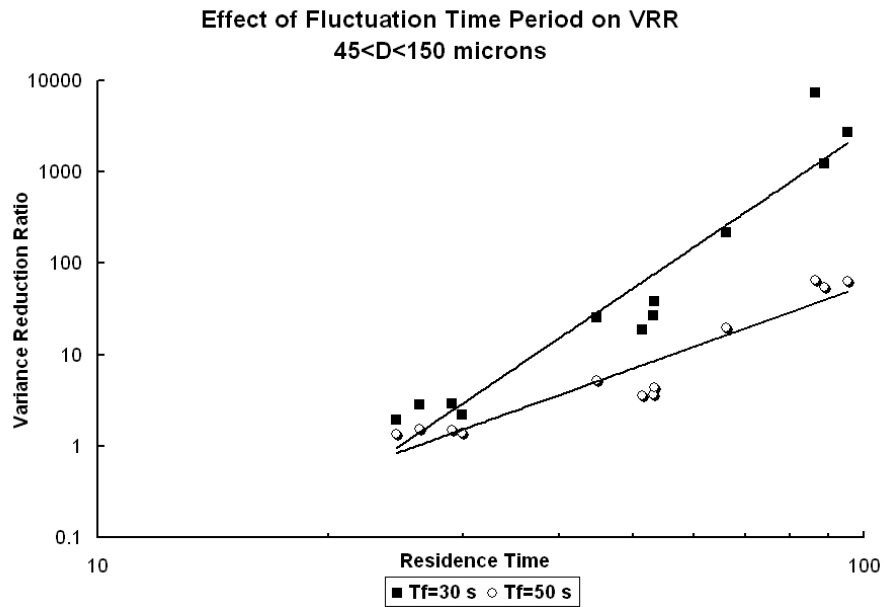


Figure 9-5: Effect of Time Period of Fluctuation on Theoretical VRR, $45 \leq D \leq 150 \mu\text{m}$

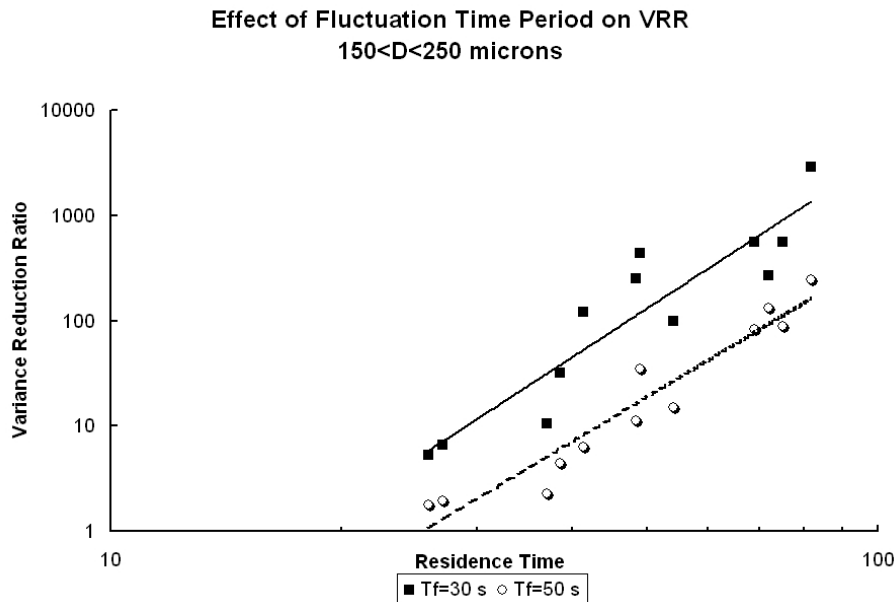


Figure 9-6: Effect of Time Period of Fluctuation on Theoretical VRR, $150 \leq D \leq 250 \mu\text{m}$

of powders (excipients and APIs) on which flow behavior and blending experiments were performed at the same operating conditions. Since microscale properties cannot be increased or decreased on same particles (unless environmental conditions are changed), the current work focused on changing the material while maintaining the other parameters like shape and particle size constant. For e.g., in order to examine the effect of cohesion, acetaminophen and caffeine were chosen as APIs which have similar particle sizes but differing cohesion values. Similarly, in order to examine the effect of cohesion of excipient, lactose and MCC of similar particle size but strongly different cohesion values were used. In order to examine the effect of shape, MCC of different shape but similar particle size were used in the RTD experiments.

9.2.1 Effect of Cohesion and Adhesion Surface Energy

Principal component analysis of the dispersion coefficients, operational variables, types of excipients and APIs was carried out in SIMCA-P+. The results were plotted as a loadings plot between the first two components as shown in figure 9-7. Here excipient 1 was DCL-11, Excipient 2 was DCL-14, Excipient 3 was MCC Avicel PH102

and Excipient 4 was MCC Celphere CP-102. Active ingredient 1 was caffeine and 2 was acetaminophen.

All correlations were found by taking the scalar product of the position vectors of the observed response in the loadings plot with the parameter of interest. For example, acetaminophen (Act(2)) was found to negatively correlate with dispersion coefficient while caffeine (Act(1)) was found to positively correlate with dispersion coefficient in figure 9-7. Caffeine's cohesion energy was lesser than the cohesion energy of acetaminophen from table 4.3. As cohesion energy increases, the dispersion coefficient decreases. Thus, this explained the reason why going from acetaminophen to caffeine the dispersion coefficients increased.

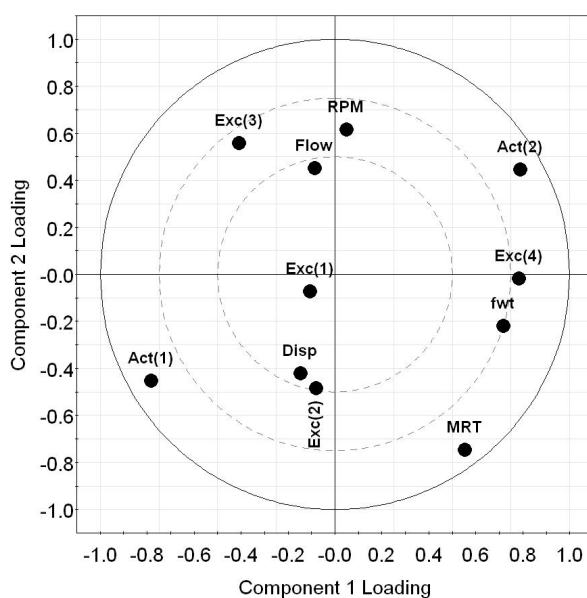


Figure 9-7: Loadings Plot of Effect of Excipients and APIs

Similarly, excipient 2, DCL-14 was found to have a strong correlation with dispersion coefficient when compared with excipient 1, DCL-11. This was attributed to the excipient to active ingredient particle size ratio. DCL-14 comprised of larger particles that gave rise to increased dispersion coefficients. Excipients 3 and 4 were both MCC particles which had high cohesion values. As a result of high cohesion, these excipients correlated negatively with dispersion coefficients and had approximately

equal scalar products. Clearly, increasing cohesion energy and dispersion coefficients showed a negative correlation over all the materials observed. The dispersive nature of particles therefore was strongly dependent on the microscopic surface energies of the particle.

Changing the active ingredients, caffeine to acetaminophen, did not affect the mean residence time since the line from API 1 to API 2 is orthogonal to mean residence time, indicating a zero scalar product. Since the bulk of the powder flowing in the blender was the excipient, it was expected that the excipient properties would dominate the dependence of mean residence time. In going from lactose to cellulose, where the cohesion energies were higher for cellulose, it was found to reduce the mean residence time. However, it was noted that the bulk density of the cellulose Avicel PH102 (excipient 3) was much lower than that of lactose which caused the powder to exit out of the system in a shorter time.

9.2.2 Effect of Particle Shape

As the particle shape was changed by changing the excipient from needle and flat plate MCC Avicel PH-102 particle to spherical Celphere CP-102 particles, the dispersion coefficient remained the same as shown in figure 9-7. However, it was found that the mean residence time was positively correlated with spherical Celphere MCC particles. It was found that the fill weight of the blender positively correlated with MCC Celphere CP-102 as the density of CP-102 was much higher than density of MCC Avicel PH-102. It was expected that a change in shape caused changes in density and increased the fill volume in the blender for the same fill weight and caused the activated the second window at the exit. As a result, the residence times of the particles were observed to be less for MCC Avicel PH-102 when compared with MCC Celphere CP-102.

9.2.3 Effect of Lubricant

Magnesium stearate was shown to influence the blending process by coating the excipient and API particles with a fine layer of lubricant particles. The interaction of

lubricant with API, excipient and wall materials had smaller surface energies causing reduction in cohesion. These lubricant particles considerably reduced the cohesion and adhesion forces of interaction between API and excipients. Depending on where in the mixer the lubricant was added, the effect of lubricant could be detrimental to the mixture quality. This was observed in the Zigzag blender where the lubricant, MgSt was added after much of the blending of API and excipient was complete. In this case, increasing MgSt content lead to a layer of MgSt particles on API and excipients and reduced cohesion and adhesion surface energies causing the mixture to lose the quality obtained before adding MgSt. The loadings plot showing the effect of MgSt RSD on Caffeine RSD in figure 6-15 supported this observation.

The deteriorating effect of MgSt in terms of increasing spectral RSD was seen in the ribbon blender as well. Blending of MgSt reduced the quality of the mixture when compared to the two component blending of API and excipient. A decrease in the RSD of MgSt lead to a drastic increase in the RSD of acetaminophen when compared to caffeine as evinced in figures 8-22, 8-21 and 8-23. MgSt had, therefore, consistently shown a trend of deteriorating the mixture quality due to reduced cohesion forces at the end of the blending process causing increased potential for segregation.

9.3 Theoretical and Experimental Performance

Predicting the behavior of the continuous blending process formed the critical linkage between what was experimentally observed in the experimental systems in this thesis and with how the industry would like to implement the process in the pharmaceutical manufacturing line. In order to implement the *quality-by-design* paradigm, it would be necessary to design the process with proper process control loops in place. Therefore, it was necessary to develop process models for continuous blending processes and to evaluate the predictive capability of such process models.

A process model for continuous blending system has already been described in §4.6. The residence time distribution of the API in the blender can be measured *a priori* and modeled using one parameter models like axial dispersion models. This residence time distribution can then be utilized in predicting the blending performance

as described in §4.6 using equations (4.16) for determining the theoretical VRR and (4.25) for determining the prediction intervals arising due to errors in mean residence time.

9.3.1 Prediction of VRR from Axial Dispersion RTD Model

Online process control of a continuous manufacturing process was mentioned as one of the main advantages of shifting from batch to continuous mode of processing. In order to implement process control, process models must be developed for designing controllers. In chapter 8, the axial dispersion model was shown to depict the flow behavior of the blender well. It was also discussed in §4.6, that the RTD model can be used to predict VRR using equation (4.25). In this section, experimentally measured RTD data were used in predicting the variance reduction ratio and effect of errors in mean residence time were discussed.

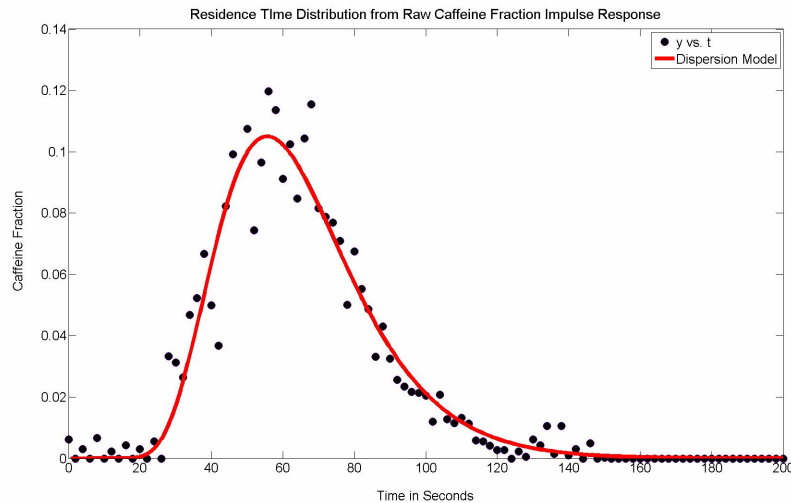


Figure 9-8: Non-linear Regression of Axial Dispersion Model with NIR Data

When model parameters obtained from non-linear regression of experimental RTD data with the axial dispersion model were used, the predicted VRR's were 3 – 4 orders of magnitude higher than the experimentally observed values as depicted in figure 9-9. This meant that the axial dispersion model overpredicted the blender performance to a very large extent. From the statistical regression of the experimental data to axial dispersion model shown in figure 9-8, it was suspected that the deviation from the

axial dispersion model was causing this over-prediction. In other words, statistical regression of RTD data was suspected to smoothen the natural variance in the RTD data.

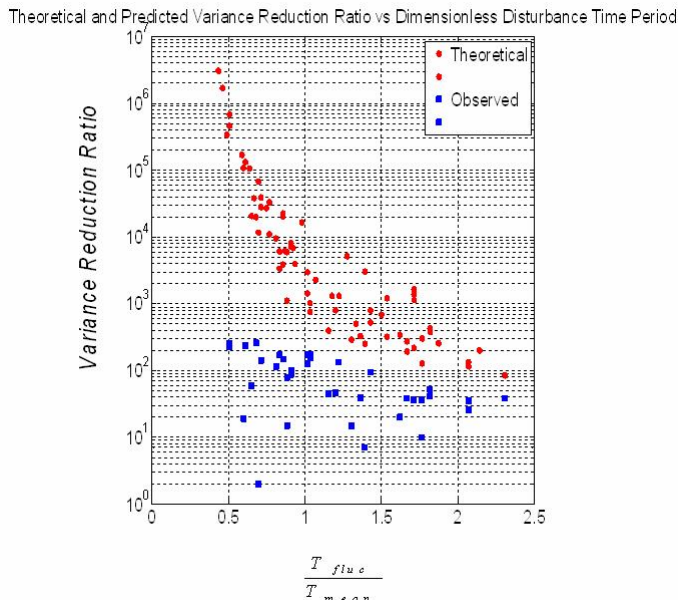


Figure 9-9: Over-prediction of Variance Reduction Ratio

This hypothesis was tested, by predicting the blending profiles by first using the axial dispersion model and then using an axial dispersion model with an addition of magnitude dependent gaussian noise. The smoothened and noise-added RTD's are shown in figure 9-10. A magnitude dependent gaussian noise that was 20% of the magnitude of the dispersion model was added as shown in the figure 9-10.

The predicted blending profiles before and after the axial dispersion model was mixed with the aforementioned noise was shown in figures 9-11 and 9-12 respectively. By mixing the axial dispersion model with the magnitude dependent Gaussian noise, it was observed that the variance reduction ratios fell by $10^3 - 10^4$, increasing the possibility of matching with the experimentally observed VRRs.

This analysis showed the importance of two attributes of powder mixtures that demand further investigation. The first attribute was the fact that use of the axial dispersion model was smoothing and eliminating inherent variance existing in the powder mixture. This noise arose from the chaotic behavior of powder in the blender

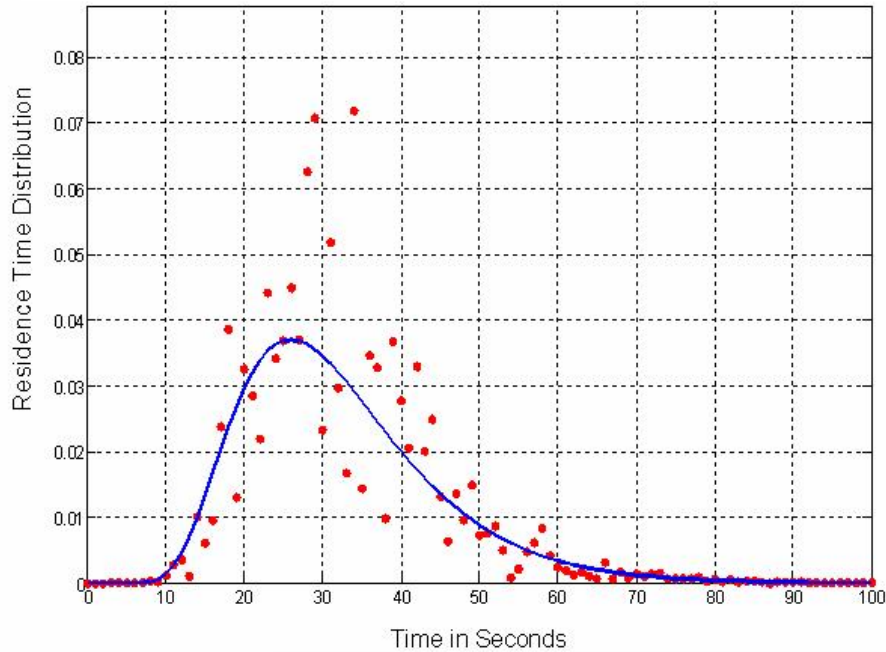


Figure 9-10: Axial Dispersion RTD with Magnitude Dependent Gaussian Noise

and due to distributions in micro-scale properties like size, shape, cohesion, adhesion and friction. Thus, in order to improve the predictions of variance reduction ratio, it was necessary to use data that reflected the noise and variance present in the blender. As a result, experimentally measured residence time distributions were used as the RTD models instead of the axial dispersion model.

The second attribute was that the scale of scrutiny of the powder mixture, as discussed in chapter 2, should depend on the scale of segregation. Powders being inherently discrete materials, require to be sampled at a certain scale of scrutiny to determine the quality of the mixture. But the online non-invasive measurements on the ribbon blender were performed at very high frequencies over very small scales of scrutiny of the powder mixture. This was remedied by a moving average model described after the theoretical predictions of VRR.

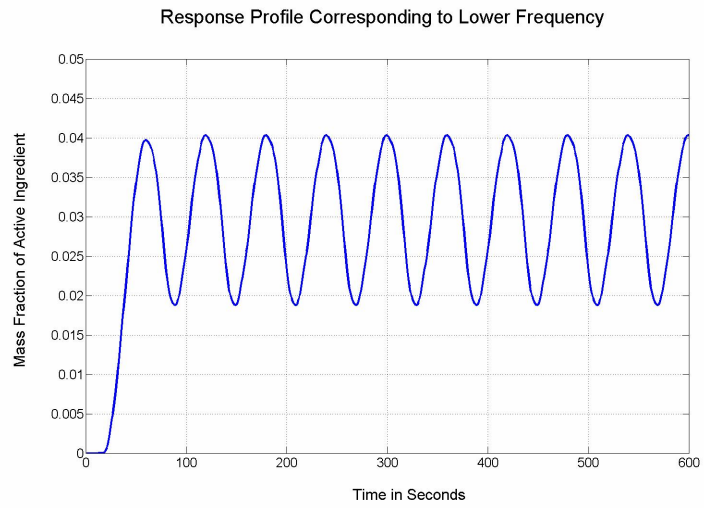


Figure 9-11: Predicted Blender Response Without Noise Addition in the RTD Model

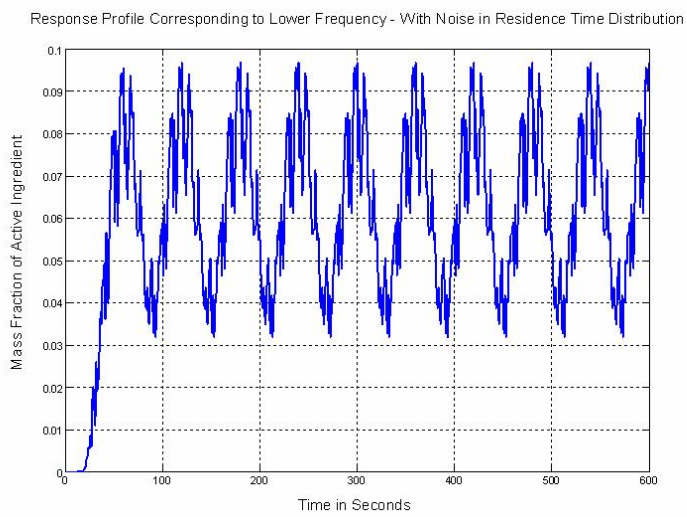


Figure 9-12: Predicted Blender Response With Noise Added to the Dispersion Model

9.3.2 Theoretical prediction of VRR from Experimental RTD

Theoretical prediction of variance reduction ratio was carried out using equation (4.25). The random mixture limit was computed by averaging the number of particles on the NIR scan area using the frequency distribution of the particle sizes of the excipient and a penetration depth of 2 mm. The number of particles in the scan area averaged to about 12000 and this was used in determining the random mixture limit for the powder mixture. The experimentally determined residence time distribution was used in equation (4.25) along with the input fluctuations shown in figure 7-2 and in table 7.2.

9.3.3 Comparing of Theoretical Predictions with Experimental VRR

The experimentally determined residence time distributions were mathematically convolved with the input fluctuations shown in table 7.2 using equation (4.16). The theoretical predictions for $T_f = 25\text{s}$ and $T_f = 60\text{s}$ shown in figure 9-13 and figure 9-14 respectively were found to be spread out when compared with the experimentally determined variance reduction ratios.

In order to understand why the theoretical predictions were found to over-predict in some cases and under-predict in some others, theoretical error limits (confidence intervals) based on an average standard deviation of the experimentally determined mean residence times shown in figure 8-10. The mean residence times were found to vary between $\pm 10\text{s}$ and hence theoretical predictions with experimental mean residence times $\pm 5\text{s}$ and $\pm 10\text{s}$ were carried out and graphed in figures 9-13 and figure 9-14.

9.3.4 Sources of Error in Theoretical Prediction

In order to estimate the error in theoretical predictions of the variance reduction ratio, a 45° line along with two sets of dashed and dotted lines were shown in the figures. The dashed lines in both figures were drawn by computing the theoretical variance reduction ratio predicted using the axial dispersion model given by equation

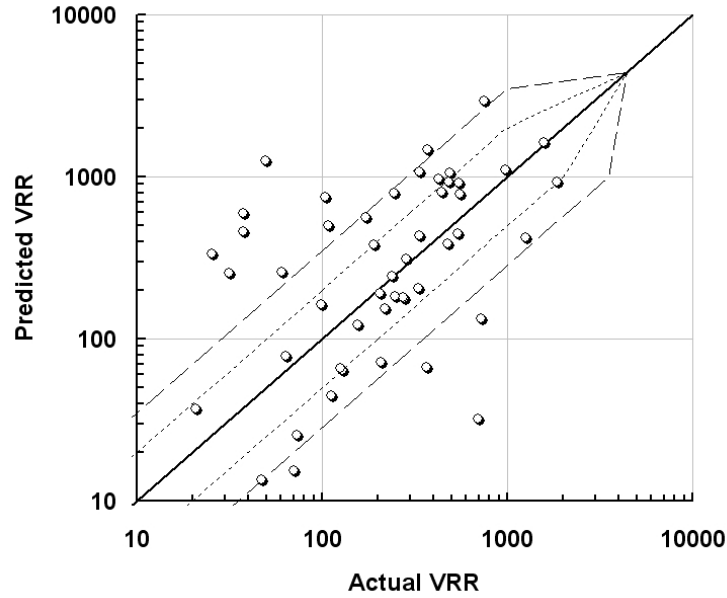


Figure 9-13: Theoretical and Experimental Variance Reduction Ratio $T_f = 25s$

(4.9) as the RTD but with the mean residence times of $\pm 10s$ of the experimentally determined mean residence times. The dotted line in both these figures were drawn by computing the theoretical variance reduction ratio predicted using the axial dispersion model given by equation (4.9) as the RTD but with the mean residence times of $\pm 5s$ of the experimentally determined mean residence times.

It was observed that within the experimental errors in measuring the mean residence time of the residence time distribution, the RTD theory predicted the variance reduction ratio satisfactorily. Also, it was observed that the standard deviation of 10s in the mean residence times made the predictions over-predict or underpredict the theoretical VRRs by $10\times$. A discussion on explanation for such errors in variance reduction and whether such errors were acceptable in the blending process would be carried out later.

In figures 9-13 and figure 9-14, it was observed that the confidence limits based on the errors in mean residence times, converged at VRRs of 4200 and 4700 respectively. These VRRs were the random mixture limits for $T_f = 25s$ and $T_f = 60s$. Clearly, any blender performance must be less than the variance reduction to the random mixture limit.

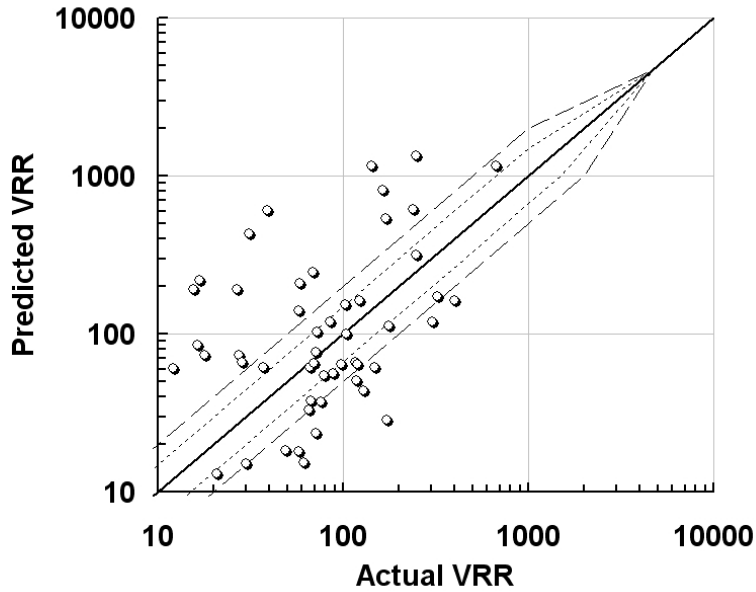


Figure 9-14: Theoretical and Experimental Variance Reduction Ratio $T_f = 60s$

9.4 Effect of Scale of Scrutiny

Just as the smallest element that influences properties of and phenomena in a fluid is a *molecule*, the smallest element that has significance in properties and phenomena in powders is a *particle*. At the particle level, the powder mixture is completely segregated, since each particle is comprised of a chemically unique species. As discussed in the chapter 2, the scale of segregation depends on the scale of scrutiny at which we are investigating the properties of the powder mixture.

As the scale of scrutiny decreases, the scale of segregation decreases. In other words, if we examine the entire powder mixture, the mixture would seem to be completely mixed. However, as we divide the mixture into parts, we find that the individual parts would be different in composition and that there would be a variance between each of these parts. If we make these divisions all the way to the particle level, we find that the variance between the parts (in this case individual particles) to be the highest. Therefore, it is important to understand and decide a relevant scale of scrutiny for examination of the powder mixture.

In the case of pharmaceutical powder mixtures, the FDA had mandated that the

scale scrutiny would be a powder sample that would be $3\times$ the dose size (or tablet weight) in the final product. This definition of scale of scrutiny ensures that the powder mixture's quality is within the safety limits of consumption when the powder is processed (compressed) to a tablet.

All the experimental data in this work were gathered at a sampling frequency of 1 Hz in the case of LIF unit and 0.5 Hz in the case of the NIR spectrometer. Sampling at this frequency, as described below, examined powder at scales of scrutiny lesser than what was mandated by the FDA. It was therefore necessary to compute the scale of scrutiny at this sampling frequency and subsequently convert the data to compute the mixture RSD based on the scale of scrutiny mandated by the FDA.

9.4.1 Theoretical Calculation of Scale of Scrutiny

The scale of scrutiny was computed by making the following assumptions. The spot size of the NIR spectrometer was 1 cm in diameter and hence the NIR scan area was 78 mm^2 . A conservative estimate of the average penetration depth of the NIR spectrometer was reported to be about 2 mm [45]. Therefore, the volume of powder mass sampled was 156 mm^3 . The mass of powder sampled at a density of 0.61 mg/mm^3 was therefore, 95 mg.

Assuming a 500mg dose size for a sample tablet product, the scale of scrutiny mandated by the FDA was $3 \times 500 = 1500\text{mg}$. Therefore, the number of consecutive scans that need to be averaged to yield the sample concentration that reflected the concentration in 1500mg of powder mass was $1500/95 \approx 15$. Therefore, 15 points were averaged to yield an averaged concentration of the API in the mixture.

9.4.2 RSD from Moving Averages

The RSD's computed by taking a 15 point moving average for blending profiles of Caffeine and Acetaminophen with DCL-11 and DCL-14 were compared in figure9-15. The RSD of acetaminophen was found to be higher than that of caffeine. This was in consonance with the observation made on the effect of cohesion surface energy on the dispersion coefficient and subsequently the blending performance of acetaminophen

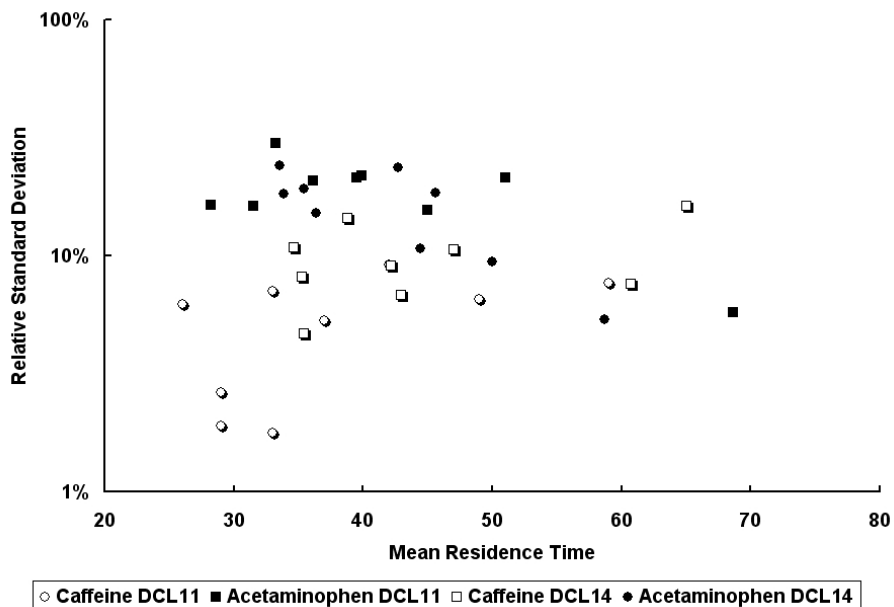


Figure 9-15: RSD from Moving Average Model

compared with caffeine. Caffeine was less cohesive compared with acetaminophen and the RSDs achieved when caffeine was used as the API were higher than the RSDs achieved when acetaminophen was used as the API.

As mentioned in the section §7.2, powder samples were collected in glass vials at the end of ribbon blender during some of the experiments. The collected samples were placed on the NIR spectrometer and offline spectra were collected. These offline spectra were converted to concentrations using the PLS calibration models shown in table 4.2. The results from the offline sample collection and spectral analysis were compared with the results from the 15 point moving average profiles.

The variance reduction ratios computed using these two methods shown in figure 9-16 was found to be in fair agreement with each other (considering the fact that the variance in VRR within blending experiments was very large as evinced by figures 8-20, 9-13 and 9-14. Therefore, It was found that performing a moving average computation of the blending profiles smoothed the data and matched the online observed API concentrations with the concentrations of the offline samples.

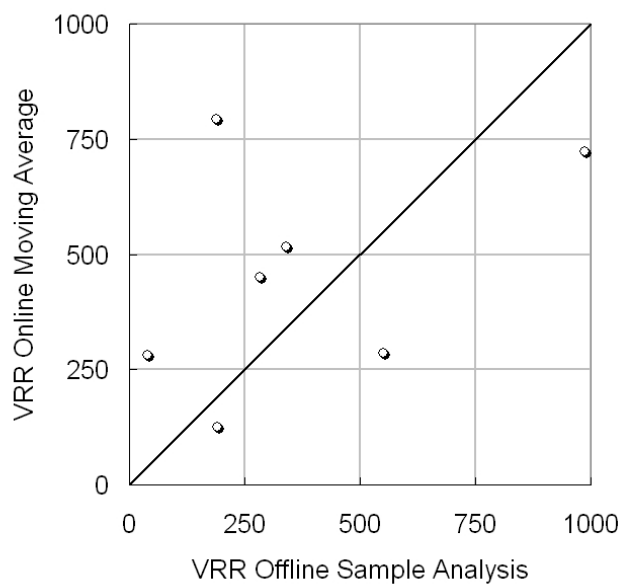


Figure 9-16: Compariosn of VRR from Offline Sample Spectra and Moving Average of Online Data for MCC Avicel

Chapter 10

Path for Future Research

Continuous dry powder blending is the starting point in a larger roadmap for transforming the current manufacturing paradigm in pharmaceuticals to one that involves continuous assessment and improvement. While the current thesis work focused on dissecting the phenomenological behavior of pharmaceutical powder blending into powder flow behavior and blender performance modeling and assessment, the lessons learnt from this work will be widely applicable to other unit operations that are potential candidates for moving from a batch mode to continuous mode of operation.

The suggested path for future research will be divided into three sections. First, the path for future research in continuous blending of pharmaceutical powders will be discussed. Following this, an assessment of the potential for the other unit operations in secondary pharmaceutical manufacturing to move to a continuous mode of operation will be discussed. And, finally, a systems analysis of continuous secondary manufacturing in pharmaceuticals will be needed to be carried out.

10.1 Path for Continuous Blending Research

The current thesis focused on one blender type in high-shear and one blender type in moderate shear blenders. The material choices were driven by needs felt by the industrial sponsors of the research work, in addition to prior experience in classifying and characterizing the microscopic properties of these powders. The variables chosen in this work were a result of both what the literature suggested to be worthwhile in examining as well as a physical understanding of the phenomenological behavior of

particles in powder mixtures. However, there are many promising avenues pursuing which might prove to be very rewarding both academically and in practice in the industry. These avenues are discussed below.

10.1.1 Blender Design

As mentioned earlier, the choice and design of the experimental blending shrank the experimental design space by the largest fraction. Therefore, examining different blender types and mechanisms for mixing powders in them will be useful not only in characterizing and benchmarking that blender type but also in understanding the limits of the design space defined by the types, characteristics and specifications of materials and changeable operational and environmental parameters to be used in process.

One of the early design decisions made in this work was to work with small quantities of powder in the order of 1 – 10 kg/hr. The laboratory scale helical ribbon blender was designed to mix powder at the current industrial production rate of 100,000 tph (tablets per hour). The decision to keep the blender size small was speculated to be one of the causes behind the wide variation in results, most importantly, the theoretical and experimental predictions using the theories described in this work.

Thus, one of the future research goals in using double helical ribbon blender would be to increase the volume and residence times of the powder in the blender which are expected to reduce the variations observed in the blending process. It is envisioned that the ribbon blender designed in this work would be appended with an extension piece that would increase the length, volume and residence times of the the powder in the mixture.

In addition to increasing residence times and fill weights of the powder in the blender, recycle of powder from the exit to the entrance will also cause additional mixing (increased back-mixing) and would approach the desired ideal blending behavior. Also, this recycle arrangement would extend the lower limit of API content as two staged mixing can be carried out in such a recycle based ribbon blender. Thus, one of the future research goals should be experimentally design and test such a

recycle system for powder mixing.

Literature review revealed that high shear powder blenders, like zigzag blenders, delivered better blend performance due to the combined effects of shear, convective and dispersive mixing and by imparting higher energies into powders. Moderate shear mixers, like the ribbon blender, impart less energy than high shear mixers, but work considerably well for most cohesive powders. Therefore, a change in the internal shaft design to simple systems to incorporate newer designs like paddled, paddled with ribbons etc., will increase the dispersion coefficient and back mixing of the material in the blender. These changes in design of the internal blending elements are seen as one of the future potential research directions for the work on continuous dry powder blending.

10.1.2 Material Properties

A number of raw material properties were examined in this work. Particle size, cohesion and adhesion and shape of particles were examined in great detail. Much of this work was done by changing the excipients and APIs while trying to maintain the other properties constant within reasonable experimental errors. This method of experimentally examining the effects of microscopic properties has both merits and demerits.

The materials used in the experiments in this work reflected the choice of excipients and APIs with properties that mirror those available for the pharmaceutical industry. In this sense, the work reflected the material choices faced by formulation scientists in pharmaceutical industry and hence examined the effect of varying microscopic properties within these constraints of commercially available materials. However, there is a critical need to examine the effect of varying the microscopic properties of materials independently. This can be achieved both by experiment and simulation.

In experiment, the material properties can be modified by pre-treatment. There are many choices for pre-treatment: solvent treatment, milling, granulation are a few examples. However, the effect of pre-treatment will have to be characterized before blending experiments on pre-treated materials is accomplished. Alternatively,

a simulation based approach would be very effective in determining the effect of varying microscopic properties independently.

Discrete Element Method simulations, discussed in the literature review, mathematically solve the kinematics and dynamics equations of particle movement in the powder bed. These simulation techniques were used by Domike [25] and Ngai[71] in understanding the effect of microscopic properties on macroscopic phenomena. These multiscale analytical techniques can be employed in understanding the effect of altering the microscopic properties like particle size, cohesion/adhesion, shape and friction on blending by use of DEM simulations. However, DEM simulations need long computational times for statistically valid results to be generated. Therefore, an intermediate mesoscale modeling of the blending operation, like residence time distribution models or markov chain models could be employed to predict the blending performance.

10.1.3 Environmental Variables

Environmental variables like humidity and temperature play a very critical role in pharmaceutical processes. Humidity changes the moisture content of powders and increases the cohesive forces by forming liquid bridges between particles. Temperature, can affect these liquid bridges via it's effect on surface tension and can increase or decrease the cohesive effect.

It was decided in the beginning not to examine the effect of controlling these environmental variables in this work. However, the final implementation of continuous pharmaceutical processes will have to consider the effect of environmental variables. Therefore, examining the effect of humidity on the blending process will be a necessary step before implementation of continuous blending operation in pharmaceutical secondary manufacturing.

10.1.4 Analytical Techniques

In this work, non-invasive analytical techniques like LIF and NIR spectroscopy were employed to assess the quality of the powder mixture and the state of the blending

process. The measurement was carried out at the wall of the blending process and was found to correlate fairly accurately with the bulk of the powder based on our observations on offline and online sample analysis. However, the need for advances in analytical techniques that can probe the bulk of the powder mixture for structure and segregation.

Capacitive probes [86] have the potential to examine the powder bulk, but lacked the capability to differentiate between the chemical identities and chemometric properties of APIs and excipients. It would be worthwhile to develop new analytical techniques based on the capacitive probe principle but using spectroscopy as the basis for differentiating the chemometric properties.

Another alternative would be to develop at-line analytical techniques like drawing off a portion of the material from the exit for automated LIF/NIR spectral analysis and subsequently returning the sample stream to the bulk would reflect the powder mixtures structure better than surface measurements.

10.2 Transforming Batch to Continuous

In the introduction, it was discussed that blending was the last unit operation where variance was introduced before the powder was finalized into the final product form, the tablet or capsule. It was also discussed that the unit operations preceding blending were all currently batch processes and succeeding blending were quasi-continuous operations (operations that are inherently continuous, but being run in a batch mode as the whole process is operated in batches).

The next step in implementing continuous manufacturing in secondary pharmaceutical manufacturing would be to examine the transformation of these operations preceding blending operations. As the current manufacturing processes in the pharmaceutical industry are all batch processes, transformation to continuous operation must need to progress in steps. The process of implementing continuous operations will involve a considerable amount of research effort in not only developing process understanding of each individual operation, but also a systems view of what is the best path to implementation, in what order should the unit operations be transformed to

continuous mode and whether a complete rethinking and redesign of pharmaceutical operations would be justified for improving the efficiency in manufacturing.

10.2.1 Crystallization

Continuous crystallization is a new area of research in pharmaceutical manufacturing and is being currently investigated. Control of kinetic rates of formation of crystals, the size distribution and crystal faces determine the properties of the API that will be used in the subsequent operations. The effect of thermodynamic and kinetic properties of mother liquors and crystals will be required for understanding and implementing continuous crystallization process.

10.2.2 Granulation

Continuous granulation devices are being employed in food and construction industries. The challenges in continuous granulation are around prediction of particle size growth, mechanical and surface properties of particles formed and understanding the evolution of cohesion, adhesion and surface frictional energies on particles during granulation. It is worthwhile to note that granulation is generally employed as a corrective operation of changing particle size, shape and morphology and hence if the crystallization step and choice of excipients are carried out optimally, milling step could be avoided.

10.2.3 Drying

Continuous dryers are employed in many process industries where the volumes of the product are very large. Developing process models to control the quality of the product coming out of a continuous dryer will require development of reliable process sensors for measuring the moisture content inside the powder bed. NIR sensors have been used to determine moisture content, but are not reliable predictors of powder bed moisture. The theory and design of continuous dryers and effect of particle properties like particle size have been investigated in other process industries, notably manufacture of chemical solids like common salt.

10.2.4 Milling

Continuous milling operation has been employed in a number of industries. The challenges in continuous milling are around controlling the particle size distribution of the product and imparting uniform energy density to particles of different sizes. Like granulation, milling is generally employed as a corrective operation of changing particle size, shape and morphology and hence if the crystallization step and choice of excipients are carried out optimally, milling step could be avoided.

10.3 Economic Analysis of Continuous Blending

The economic argument for implementing continuous processes in general and continuous blending in particular in a pharmaceutical setting needs to be examined. Further work on this area should focus on analyzing the economics of continuous processing and need provide a framework to assess the business impact of implementing continuous manufacturing.

Chapter 11

A Framework for Global Pharmaceutical Manufacturing Strategy

Worldwide pharmaceutical sales for the top 11 'big pharma' were over \$270 billion in 2006. The year on year earnings growth was over 6.5% indicating a strong sector with considerable potential for value creation in the developed world [89]. Developing nations like India, China, Russia and Brazil have seen significant increases in healthcare spending in the past five years. Countries like India and China have also become favorite destinations for some pharmaceutical companies to establish satellite distribution locations. Since 1998, pharmaceutical industry has been experiencing increased pressure to improve bottom-line performance in the face of drug patent expirations. Drugs like Losec and Prilosec lost patent protection in 1999 and blockbusters like Zocor and Zolofit lost patent protection between 2005 and 2007.

This increased pressure has forced pharmaceutical companies to examine sources of value along its entire value chain. Research and product development were always seen as activities that added shareholder value. Pharmaceutical manufacturing was perceived as a cost center rather than value adding activity along the pharmaceutical value chain. Reports of manufacturing issues and increasing pressure from generics on off patent drugs have forced pharmaceutical companies to re-examine their strategies in manufacturing.

In addition to investing in bringing science into pharmaceutical manufacturing,

pharmaceutical companies have focused on an integrated strategy of building value by expanding manufacturing to countries outside of US, EU and Japan. This capstone project focuses on the development of the pharmaceutical manufacturing outside of US, EU and Japan. For the purposes of this discussion, we will consider both pharmaceutical (small molecule) and biologics (large molecule proteins) manufacturing together unless otherwise a distinction is made.

11.1 Overview of Manufacturing

Pharmaceutical manufacturing described earlier in this thesis contains two distinct sequence of steps called primary synthesis (of the API) and secondary manufacturing (of the drug product) and is shown in figure 11-1. The formulated drug product is then taken to a fill finish facility where the final product is packaged and labeled according to the market and regulatory specifications. In biologic manufacturing, the steps begin with either a fermentation process where genetically modified microorganisms synthesize API or mammalian synthesis where genetically modified mammalian cells are carefully grown in bioreactors and the complex protein products are synthesized. This is then purified in the downstream processing stages and sent to secondary manufacturing where the drug product is finally formulated as seen in figure 11-2. Just like in pharmaceutical manufacturing, the last stage involves a fill-finish process after which the product is packaged according to market needs and regulatory specifications.

11.1.1 Differences between Pharmaceuticals and Biologics

There are a number of important distinctions between pharmaceutical (small molecule API) and biologics (large molecule proteins) therapeutics. Small molecule manufacturing process is based on chemical synthesis while large molecule proteins are grown inside genetically modified microorganisms that synthesize the therapeutic. Chemical syntheses are much easier to replicate and transfer than microbial fermentation based synthesis.



Figure 11-1: Schematic of Pharmaceutical Manufacturing



Figure 11-2: Schematic of Biologics Manufacturing

The technological complexity of biologics manufacturing and significant intellectual property infringement risks and technology transfer risks are some of the challenges that biologics companies have to overcome in globalization of manufacturing. A higher average capital outlay in biologics (\$400 million compared to \$100 million for pharmaceuticals) also plays a role in determining the level and spread of globalization of manufacturing.

11.1.2 Pharmaceutical Manufacturing Output

Data from UNIDO industrial statistics database [79] showed that the real pharmaceutical manufacturing output has been steadily flattening from 1997 to 2002. While the real GDP growth has been between 0.8% and 1.5%, the Purchasing Power Parity (PPP)-adjusted pharmaceutical manufacturing output has risen steadily as seen in figures 11-3 and 11-4. In order to derive the PPP conversion factor for a particular country, the ratio of Purchasing Power Parity based GDP to Real GDP was used [2] and is shown in table 11.1.

Table 11.1: Average PPP Conversion Factors, 1997-2002 [2]

| Country | PPP Conversion Factor |
|----------------|------------------------------|
| US | 1.00 |
| UK | 0.99 |
| India | 3.28 |
| Singapore | 1.40 |
| Poland | 2.15 |
| Austria | 1.10 |
| Hungary | 2.34 |
| Italy | 1.16 |
| Japan | 0.76 |
| France | 1.04 |
| Germany | 1.03 |

End of Table

While the real value added in pharmaceutical manufacturing was also flattening from 1997 to 2002 indicating that the real cost of manufacturing was rising in these countries as a fraction of the pharmaceutical output. The PPP-adjusted value added in pharmaceutical manufacturing in US, EU and Japan was increasing, indicating that the PPP-adjusted cost of manufacturing was declining from 1997 to 2002. The reason behind such a difference in the real value added and PPP-adjusted value added is attributed to the rising costs of manufacturing in EU and Japan where it was more expensive than in the US.

Disaggregation of the manufacturing output for US, EU and Japan showed that the real manufacturing output in Japan in figures 11-5 and 11-6 was declining while the PPP-adjusted output was rising. Notwithstanding the changes in PPP of Japan, this change seems to point that the manufacturing output in US and Japan were flattening or growing modestly. In comparison, the growth in real manufacturing

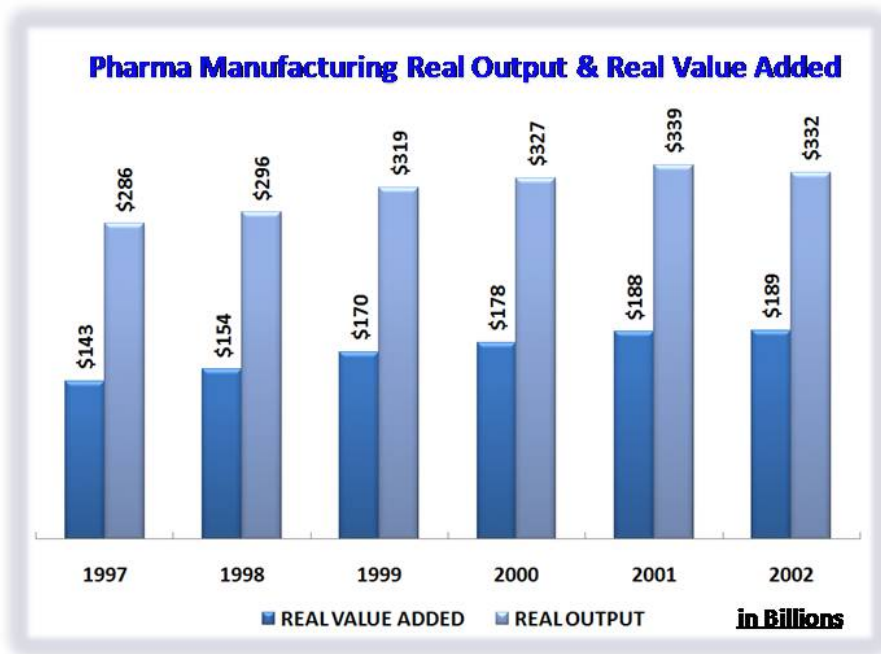


Figure 11-3: Pharmaceutical Output and Value Added for OECD Countries

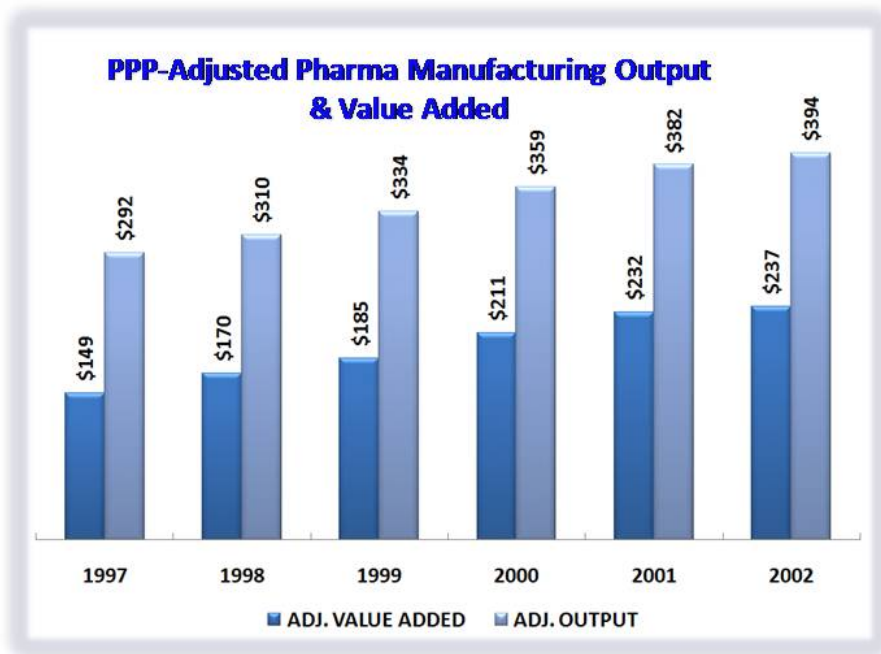


Figure 11-4: PPP-Adjusted Output and Value Added for OECD Countries

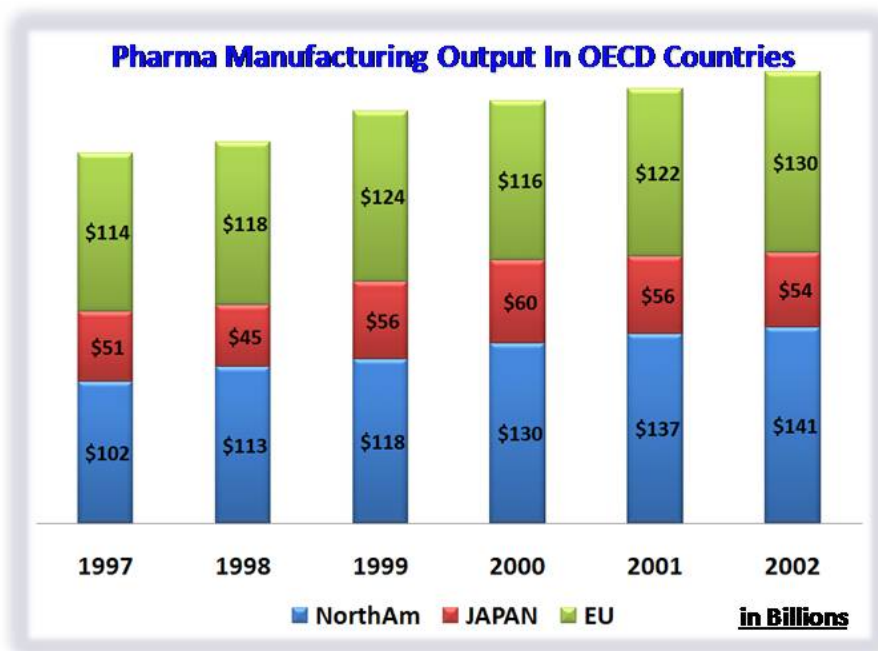


Figure 11-5: Pharmaceutical Output for US, EU and Japan

output from EU was significant, but on a PPP-adjusted basis EU showed similar flattening or modest growth just like US and Japan.

11.1.3 Asia and Eastern Europe Manufacturing Output

It is important to observe that while PPP-adjustment brings out the equivalent value of the pharmaceutical output in a given country on a uniform basis, this conversion would mean that the pharmaceutical output from that country or region was sold in the global market without any market frictions. Therefore, PPP-adjustment is a semi-empirical, uniform valuation of the output and value added of the pharmaceutical output of a particular country.

A steady growth in Asian manufacturing output was observed from 1997 to 2002 according to the UNIDO INDSTAT data shown in figures. The first observation to make is that the real manufacturing output seemed to be flattening in India, when compared to that in Singapore or South Korea as seen in figure 11-7. Even on a PPP-adjusted basis, the value of the India's pharmaceutical output, seen in figure 11-8, was growing very modestly when compared to Singapore. Clearly, Singapore

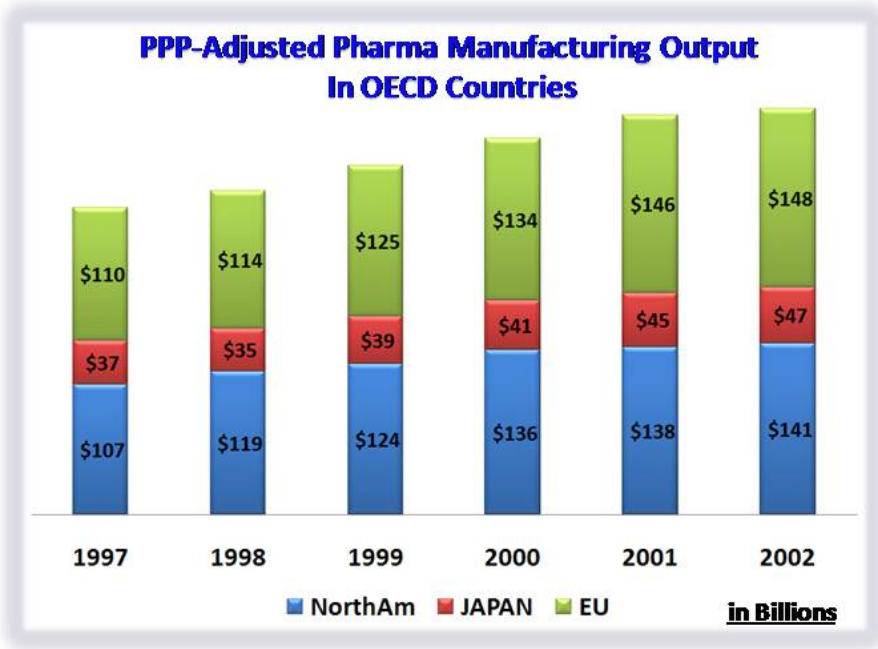


Figure 11-6: PPP-Adjusted Output for US, EU and Japan

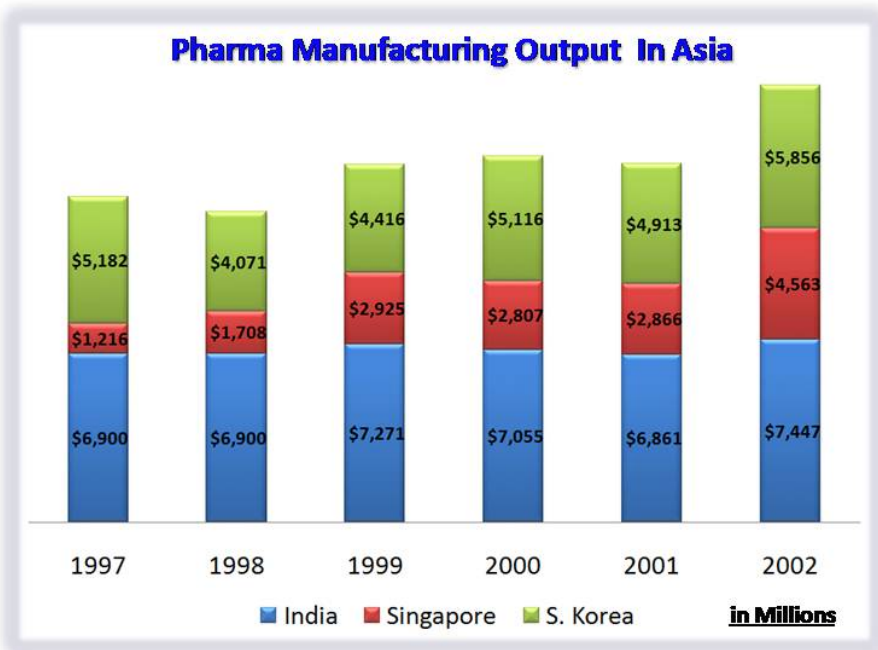


Figure 11-7: Pharmaceutical Output for Asia

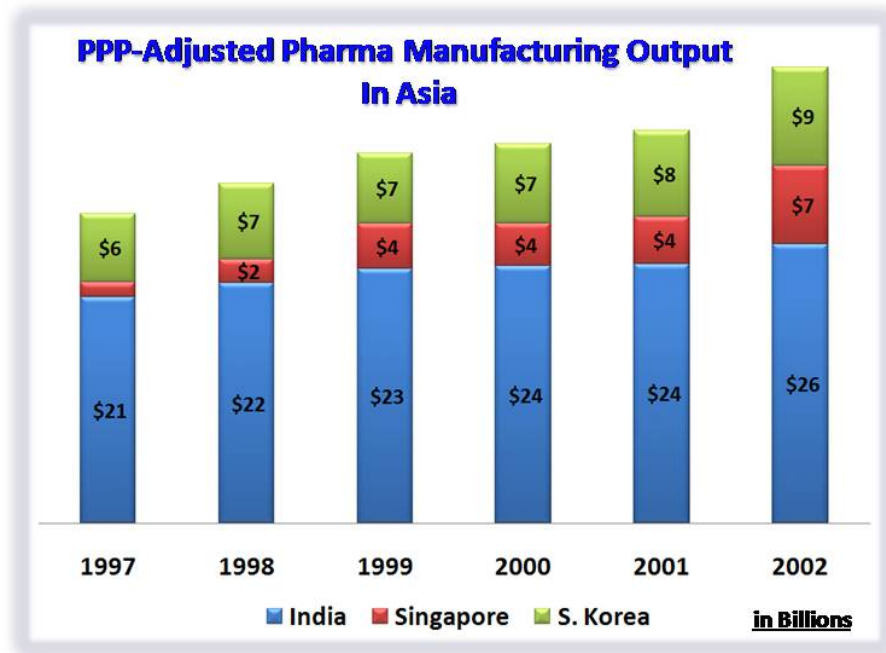


Figure 11-8: PPP-Adjusted Output for Asia

has emerged as a hub for pharmaceutical manufacturing outside of US, EU and Japan between 1997 and 2002 and is expected to grow in significance. On an as-exported (PPP-adjusted) basis, shown in figure 11-8, the value of India, Singapore and Korea’s manufacturing output is extraordinarily large than the real output.

Former Communist Bloc countries in Eastern Europe have begun significant investments in pharmaceutical manufacturing and a clear, steady growth in manufacturing output is seen in figures 11-9 and 11-10. Both the real output and PPP-adjusted output has been steadily growing in Eastern European countries. Gross manufacturing output from Asia and Eastern Europe seems to show signs of growth and expansion, both due to pharmaceutical companies in US and EU beginning to expand manufacturing into those countries as well as due to the explosion of contract manufacturing organizations that serve the big pharmaceutical companies.

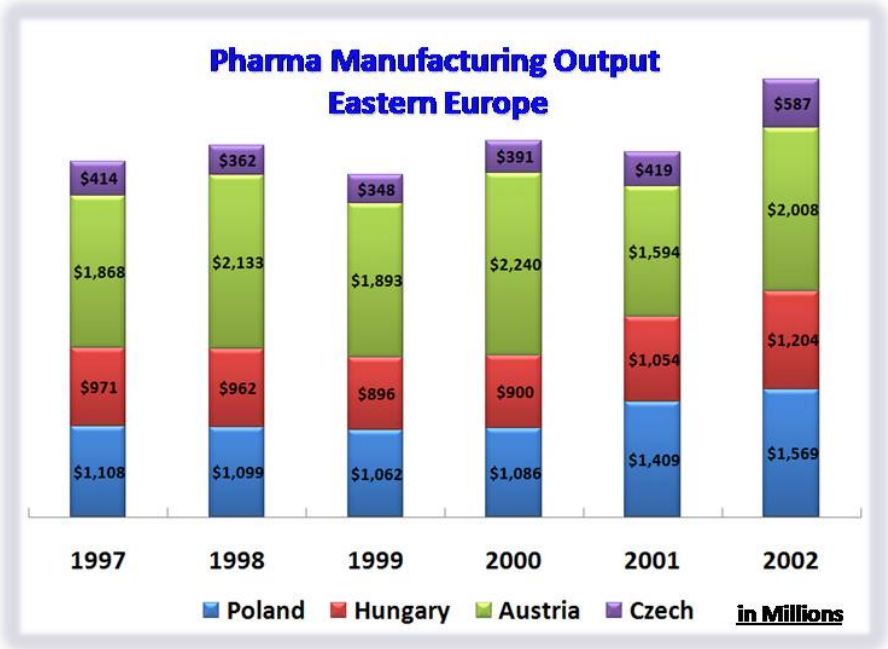


Figure 11-9: Pharmaceutical Output for Eastern Europe

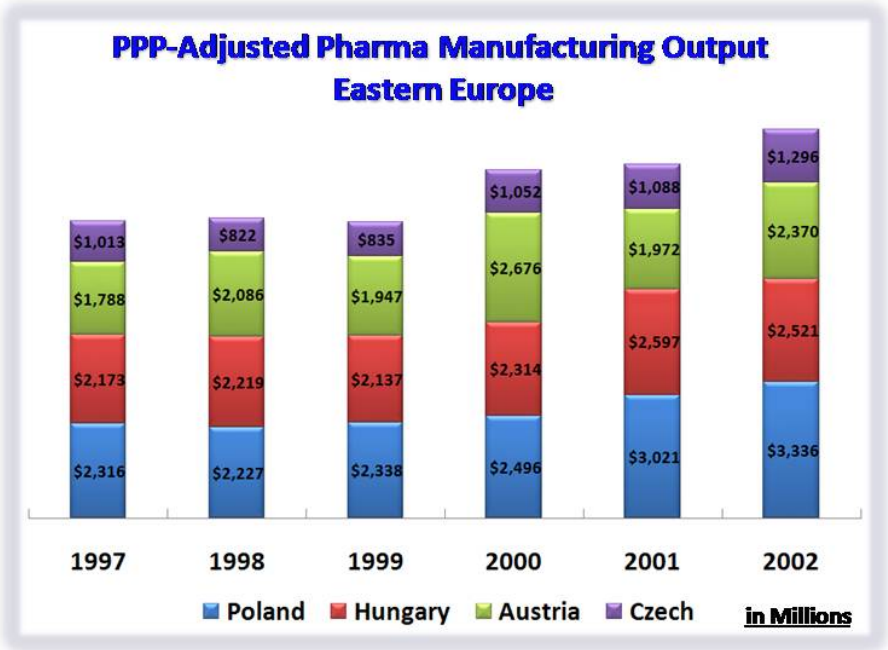


Figure 11-10: PPP-Adjusted Output for Eastern Europe

11.2 Prior Literature

Literature on manufacturing location decisions and strategic frameworks for organizing global organizations were carefully reviewed to identify any applicable frameworks for pharmaceutical manufacturing

11.2.1 Determinants of Manufacturing Location

Manufacturing location theories were directed towards understanding location decisions made by firms seeking to minimize the cost of factor inputs (which included the delivery cost of the manufactured goods) from the chosen location. Subsequent theories of foreign investments and manufacturing expansions focused on identifying the contributing factors for firm's choice of out-of-country (particularly out-of-US) manufacturing locations.

By dividing product life-cycle into new, maturing and standardized products, Vernon [99, 100] identified that the product lifecycle plays a significant role in location decisions. The unstandardized nature of a new product like its factor inputs, manufacturing process, product specifications are highly variable. The need to maintain adequate freedom to change these characteristics defining the product (inputs, process and specifications), relatively higher price elasticity of demand for the product given its novelty in the market and the need to swiftly communicate and be informed by the market precludes firms from moving manufacturing locations far off from the location where the product was first developed. As a product matures, Vernon speculates that the need for flexibility declines due to commitments from firms towards establishing standards in product specifications and the manufacturing processes. Firms become increasingly interested to invest in fixed set of manufacturing assets whence factor costs begin to play larger role in manufacturing decisions. During this changing and decreasingly uncertain period, manufacturing location decisions tend to move away from the primary location where the product was developed depending on the speed of the transition in this phase of the product cycle. Finally, as a product becomes standardized, Vernon's model postulates that less-developed countries might be offer-

ing cost competitive advantages for becoming preferred locations of manufacturing. The standardized product and the manufacturing process give the firm the ability to replicate the production in any location, within a certain measure of variability. The familiarity with the market and the price competition also dictates the need for firms to push their factor costs to more cost-efficient locations.

Subsequent studies focused on identifying the determinants of which firms pursue foreign investments within an industry and the determinants of foreign investments in manufacturing across industries. Horst's [44] empirical study of the determinants showed the impact of factors like economies of scale by virtue of firm size (*viz.*, defined by the firms assets), the target foreign market where the foreign investment is headed and the profitability and experience of the firm in the production and manufacturing of the product to be the determinants of which firms pursue foreign investments. In a four industry study comprising of hand tools, apparel, personal computers and electronic components, Dubois et al. [27], tested the influence of maturing product life-cycle and process technology, market and geographic proximity, logistical complexity and responsiveness on the decision to re-locate the manufacturing assets of a firm in a given industry. In addition, experience and competitive priority of firms also influenced the decision to move manufacturing assets while environment variables like government policies, taxes, tariffs and regulations at the target locations played a parametric role in determining location strategies in these industries.

Experience heavily affects the location decisions of manufacturing firms. In a study analyzing 130 firms making 70,000 investments globally, Davidson [23] concluded that while firms with limited experience in making global investments tend to limit their subsequent investments in familiar locations they are actively operating in. On the other hand, firms with extensive experience tend to explore and invest in more uncertain locations and respond more efficiently to global economic opportunities.

11.2.2 Frameworks for Global Strategy

Frameworks for organizing companies globally were proposed through several works by Porter [84], Doz et al., [26], Bartlett [3], Bartlett and Ghoshal [4], Ghoshal [35]

and Prahalad and Doz [87]. A sequential view of the industry, the region and the firm were considered and the factors influencing global expansion and organization were proposed. International managers could organize, depending on the nature of their industry and the region specific factors, either to manage global integration or local responsiveness. Functions that needed a local market input were high on local responsiveness, while functions like research and development that were fairly scale independent and needed global coordination were organized to meet global integration as a primary goal.

Lessard [59], in extending industry level framework by Doz et al., [26], geographic region competitiveness framework by Porter [84] and firm level organization framework by Bartlett [3] and Bartlett and Ghoshal [4], proposed local to global variation in organizing an international firm across its market spread and configuration of core activities with the depth of the localization of its activities and the strength of the connections of its operations. While, the aforementioned global organizing framework considered all functions of firm, factors specific to globalization of manufacturing were not investigated. The frameworks discussed in this work are an extension and Lessard's firm level internationalization, but with focus entirely on manufacturing in pharmaceuticals and biologics.

Ferdows [30], in his factory organization model of proposed that every factory in an organization has a purpose that the organization assigns and that every factory has to traverse a path to become the lead factory of that company to add value to the company's bottom-line. In his framework, Ferdows identifies factories to be one of six types - outpost, offshore, server, source, contributor and lead factory and these have been shown in increasing value to the firm from bottom to top in figure 11-11.

A factory established as a minimum basic investment in a particular region to gather market information and for keeping the organization plugged into the network of a particular geography was termed an outpost. An outpost, according to Ferdows, is almost always either a server or an offshore facility. An offshore location is established with the goal of catering to the local market and present cost advantages of selling into the local market. A server on the other hand has comparatively more

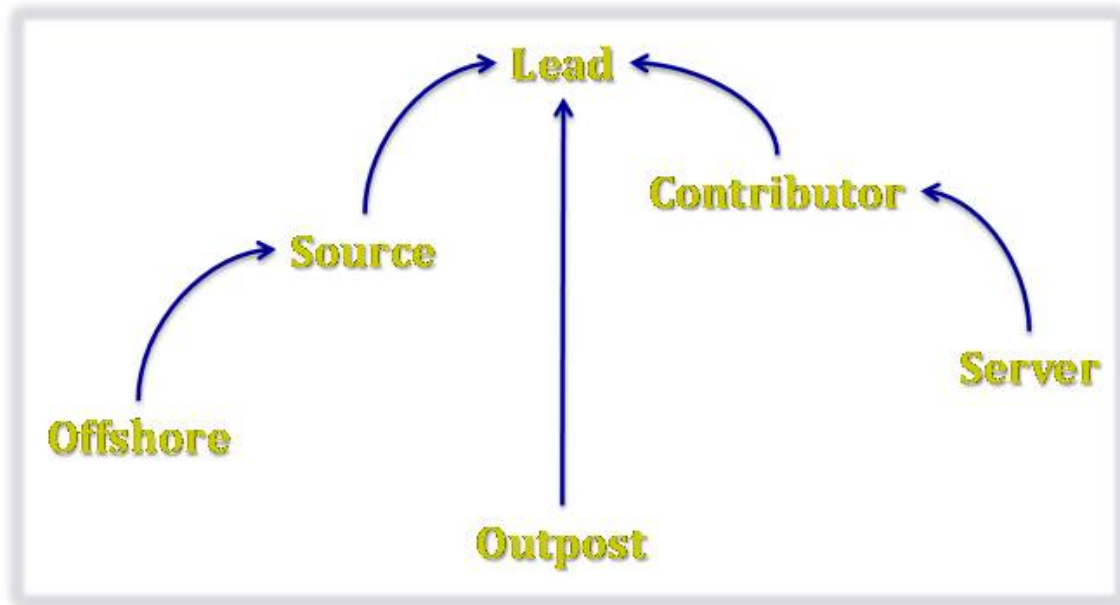


Figure 11-11: Ferdows [30] Model for Organizing Manufacturing Plants

freedom to improve processes and products and significantly more freedom to establish, validate and develop suppliers. A source factory, in addition to having unlimited flexibility in defining process and product improvements, usually has limited flexibility in the development process. A contributor factory contributes significantly to the company bottom-line by providing services similar to that of lead factory in terms of product and process development, but is also in-line to becoming a lead factory for the company with subsequent investments. A comparison of the various factory types is shown in table 11.2.

In another model of coordinated manufacturing plants within a firm, Shi and Gregory [92], proposed that different firms could be identified into four different types; home exporters (for example, Boeing) where the manufacturing is in a single region or location, regional exporters (for example, pharmaceutical companies) where manufacturing is carried out in more than one region with each region supplying locally, globally integrated manufacturers (for example, Coca-Cola concentrate producers and bottling companies) where manufacturing is distributed globally and the global demand is met with an integrated manufacturing network and globally coordinated manufacturers (for example, Mc Donald's) where manufacturing is heavily

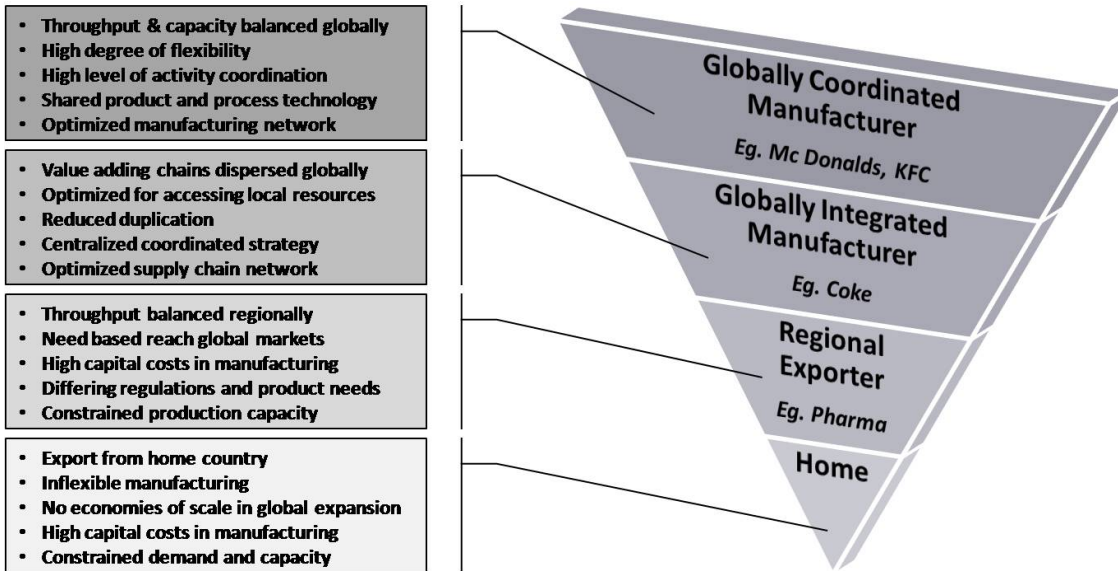


Figure 11-12: Shi and Gregory [92] Model for Organizing Manufacturing Plants

coordinated between different plant locations and the demand is met by varying production between the integrated facilities as shown in figure 11-12. One of the chief critiques of such a model is its inability to prescriptively determine which organizing framework would best suited for a business keeping both the risks and benefits of such an organizing framework while creating such an organization strategy.

Table 11.2: Characteristics of Ferdows Factory Model [30]

| Factory Type | Market Presence | Supplier Development | Process Improvement | Product Improvement | Process Development | Product Development | Hub |
|---------------------|------------------------|-----------------------------|----------------------------|----------------------------|----------------------------|----------------------------|-------------------|
| Outpost | No | No | No | No | No | No | Sensing |
| Offshore | No | Limited | No | No | No | No | Specific Part |
| Server | Yes | Unlimited | Limited | No | Limited | No | National |
| Source | Yes | Unlimited | Unlimited | Limited | Unlimited | Limited | National-Regional |
| Contributor | Yes | Unlimited | Unlimited | Unlimited | Unlimited | Unlimited | Regional-Global |
| Lead | Yes | Unlimited | Unlimited | Unlimited | Unlimited | Unlimited | Global |

End of Table

11.3 Objectives and Scope

There are two main objectives of this framework. First, the work proposes a global pharmaceutical manufacturing model that has been observed so far in the market. And second, the work proposes a new strategic lens, based on Bartlett and Ghoshal's framework, that a pharmaceutical or biologics company could employ to craft an global manufacturing strategy. While the first objective identifies the path that pharmaceutical and biologics companies have taken to reach to the current situation in global manufacturing, the latter objective builds a strategic framework that is useful in addressing the challenges faced by companies planning on globalizing their manufacturing plants.

The scope of this work pertains to the pharmaceuticals and biologics manufacturers with a strategy to sell products in the OECD countries (especially North America, Japan and the European Union). The manufacturing output data from UNIDO industrial statistics database [79] was limited to the available range from 1997 to 2002. However, whenever possible, current thinking on the topic was identified by informal interviews with professionals, managers and consultants to the pharmaceuticals and biologics industries. Finally, this work is intended to give a prescriptive framework for the different issues that a firm needs to think about and is in no way intended to be predictive of what the industry is set to look like 5 or 10 years from now.

11.4 The Growing Influence of Emerging Economies

Manufacturing output growth in the emerging economies of Asia and Eastern Europe was clearly seen in figures 11-7, 11-8, 11-9 and 11-10. However, to draw a holistic picture we need to examine and overlay the in-country pharmaceutical demand and demand growth with pharmaceutical manufacturing real output (unadjusted for PPP) and output growth.

Figure 11-13 overlays the market output and market demand for the year 2002 in India, Singapore, Poland and Hungary. The market demand data were obtained from Datamonitor industry profile reports published by Datamonitor USA [97]. We

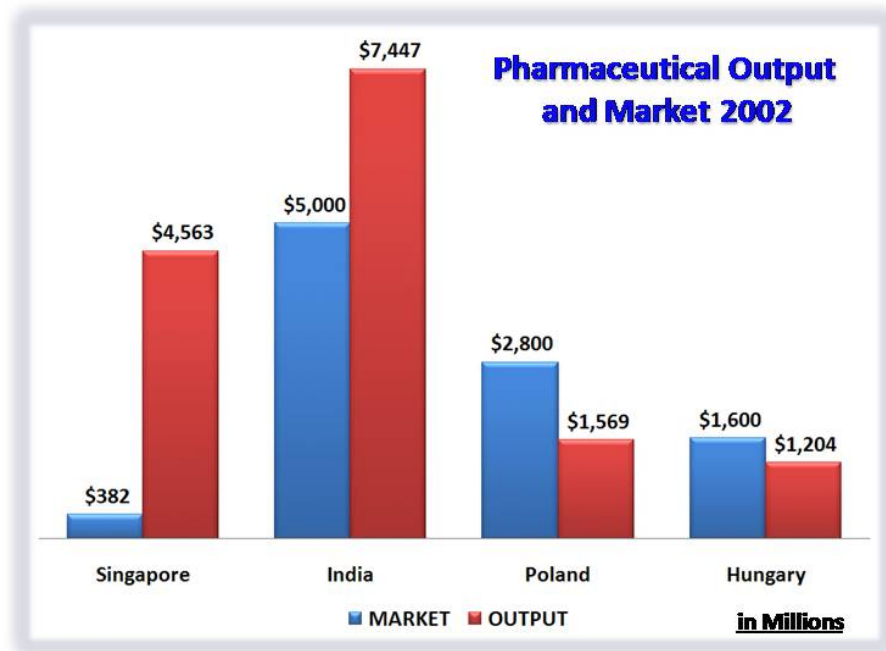


Figure 11-13: Output and In-Country Market Demand for 2002

observe that in both India and Singapore, the in-country pharmaceutical market demand is significantly lower than the manufacturing output. India and Singapore are seen to be net exporters of pharmaceutical products and this can be seen as evidence of expansion of manufacturing and not necessarily expansion of US/EU based pharmaceutical companies into these countries. Manufacturing output in Poland and Hungary were found to be lower than the in-country market demand as showing in figure 11-13. Since these are aggregate demand and manufacturing output data, it is important to note that these countries might be net-exporters in specific manufactured pharmaceutical products or intermediates.

Figure 11-14 overlays the pharmaceutical market demand and manufacturing output growth for the year 2002. Singapore has shown extraordinary growth in manufacturing output in 2002 due to the specific actions of the Singapore government towards encouraging growth of pharmaceutical manufacturing in Singapore through various incentives that shall be discussed later on in this chapter. India exhibited higher market demand which is believed to be related to population in India as well as the economic growth leading to increased healthcare expenditure. Hungary and

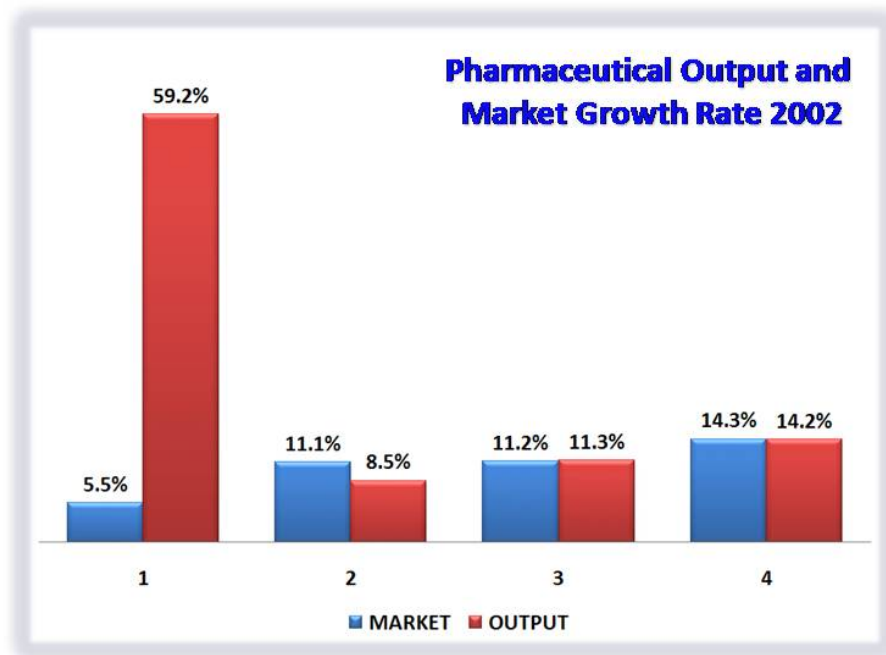


Figure 11-14: Output and In-Country Market Demand Growth for 2002

Poland exhibited very close growth rates in both output and market demand meaning that these countries might very well maintain their positions as net pharmaceutical importers.

UNIDO INDSTAT data on pharmaceutical manufacturing establishments show that (c.f. figure 11-15) while the number of establishments (defined as a single ownership entity performing an activity in a single location) in Japan and Eastern Europe have remained same between 1998 and 2002, the number in EU and US have been falling considerably since 2002. At the same time, the establishments in Asia are on the rise. It was found that this increase in Asia and other countries were not equal to the decrease in the number of establishments in US and EU, indicating that the cost cutting measures might be a strong impetus behind such closures since new matching facilities were not being opened in other countries.

The number of employees in pharmaceutical manufacturing establishments provided a telling tale of how employment has been affected by the growth of manufacturing in Asia and other locations. Clearly, figure 11-16 shows a considerable decline in the number of people employed in pharmaceutical manufacturing in the US, but

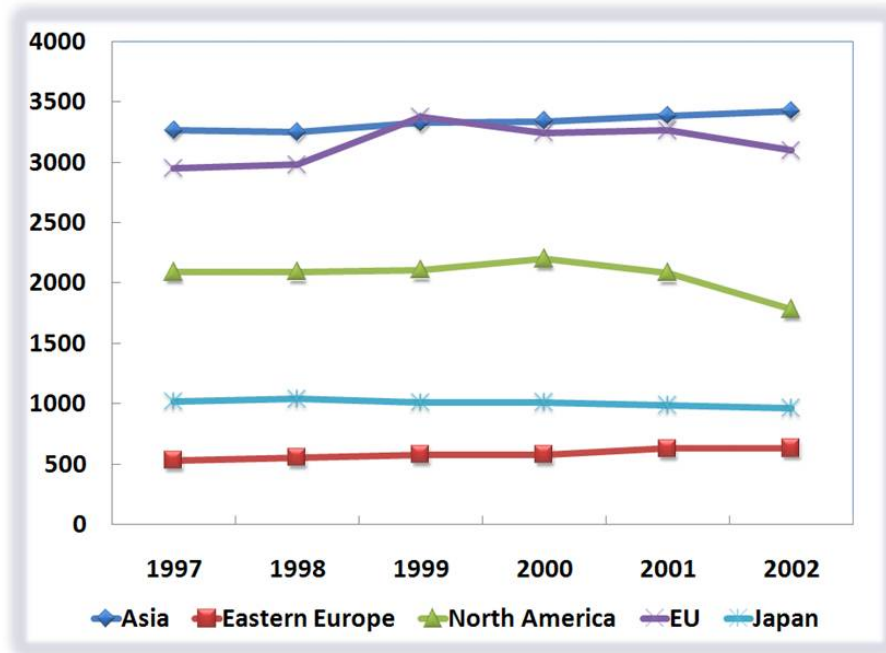


Figure 11-15: Pharmaceutical Manufacturing Establishments

the rise in employment, surprisingly is highest in Europe and not Asia or Eastern Europe during the period 1997 to 2002. European Union employment considerably increased during this period and is possibly due to the unionized nature of the work force in Europe and due to the growth of Italy, Spain and Portugal as locations within the EU where manufacturing began to pick up speed towards the end of the 1990s.

The evidence overwhelmingly points to the fact that manufacturing output is growing without question in the emerging markets of Asia and Eastern Europe. While it is unrealistic to expect this growth to have come solely from manufacturers in US, EU and Japan shifting their manufacturing bases, it is very apt to expect considerable growth in the number and exports of contract and generics manufacturers in emerging economies.

11.4.1 Factor Cost Advantages

Countries in Asia and Europe enjoy clear factor cost advantages. In figure 11-17, the real factor costs are shown as a fraction of the PPP-adjusted pharmaceutical output. This analysis assumes that a company located in US or EU would be able

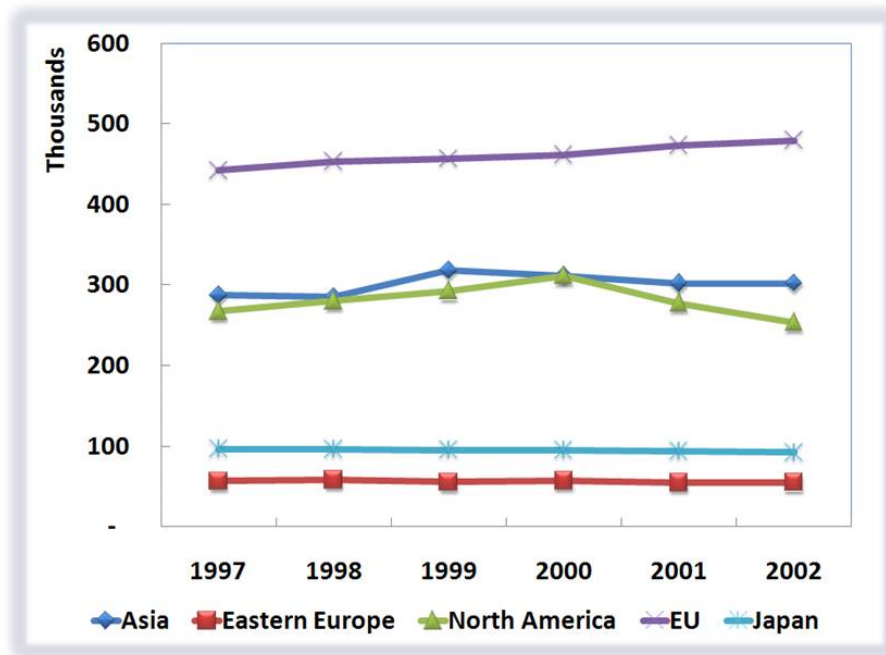


Figure 11-16: Employees in Pharmaceutical Manufacturing

to gain factor cost advantages by manufacturing at the real costs of a country in Eastern Europe but by selling the product in the developed world. By adjusting the pharmaceutical output with the Country PPP conversion factor, the actual value of the pharmaceutical product could be found in order to fairly compare the factor costs in the developed world.

The figure 11-17 shows that countries in Eastern Europe enjoy cost advantages that are very much in line with what was found in the Asian countries like India. A value of 10% in factor costs could be saved by manufacturing products in the developing world and subsequently selling the products in the developed world. While this by itself may not be a winning argument for off-shoring manufacturing or the emergence of low-cost contract manufacturers in these developing countries, it is nevertheless a compelling factor that contributes to the bottom-line if companies are careful in the execution of utilizing the low cost advantage.

Another notable observation to be made from figure 11-17 is that the cost of manufacturing is falling in countries like US, possibly as a combination of learning curve effects as well as increased value capture due to growing prices of pharmaceuticals.

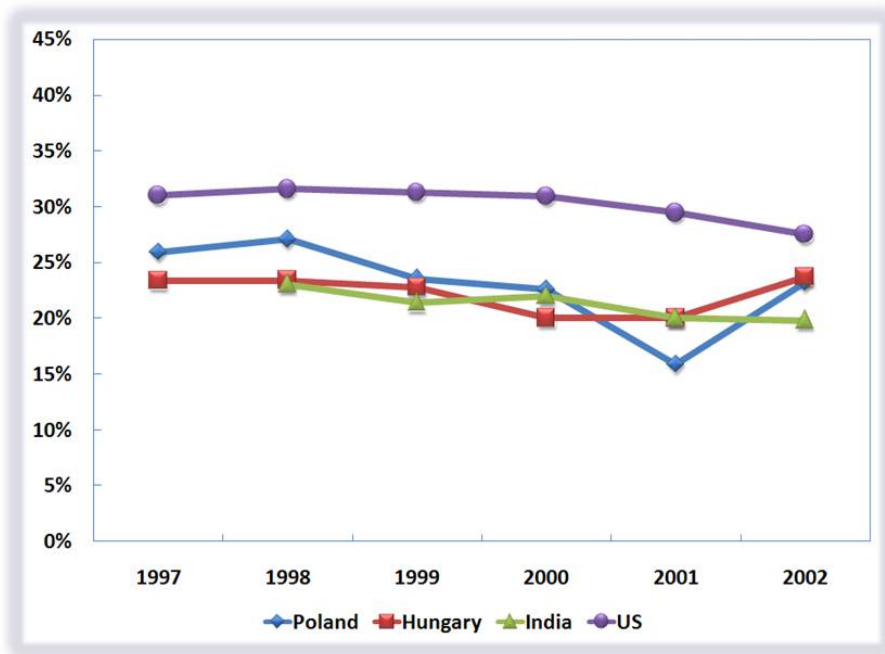


Figure 11-17: Factor Cost Percentages on a PPP basis for Eastern Europe

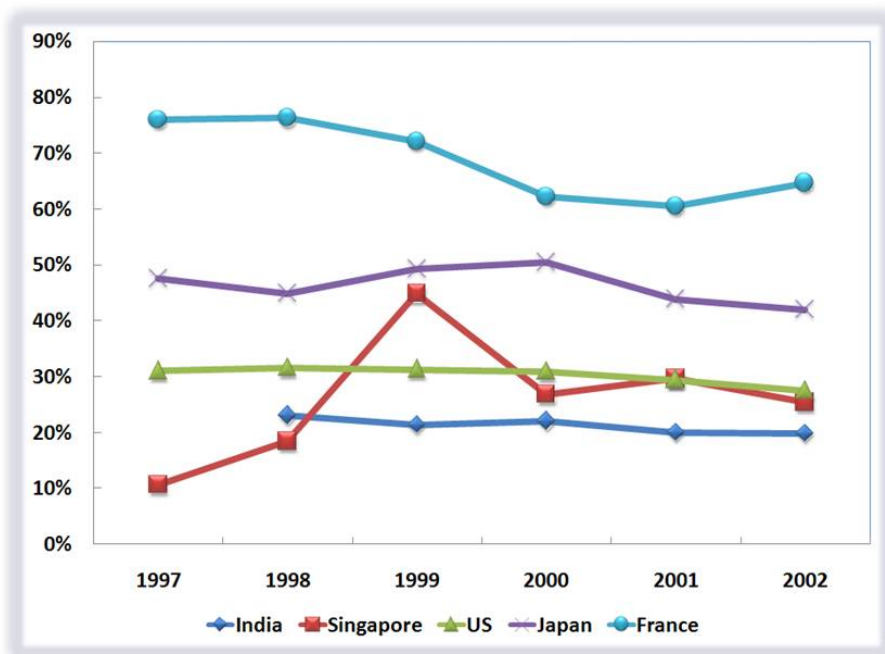


Figure 11-18: Factor Cost Percentages on a PPP basis for Asia

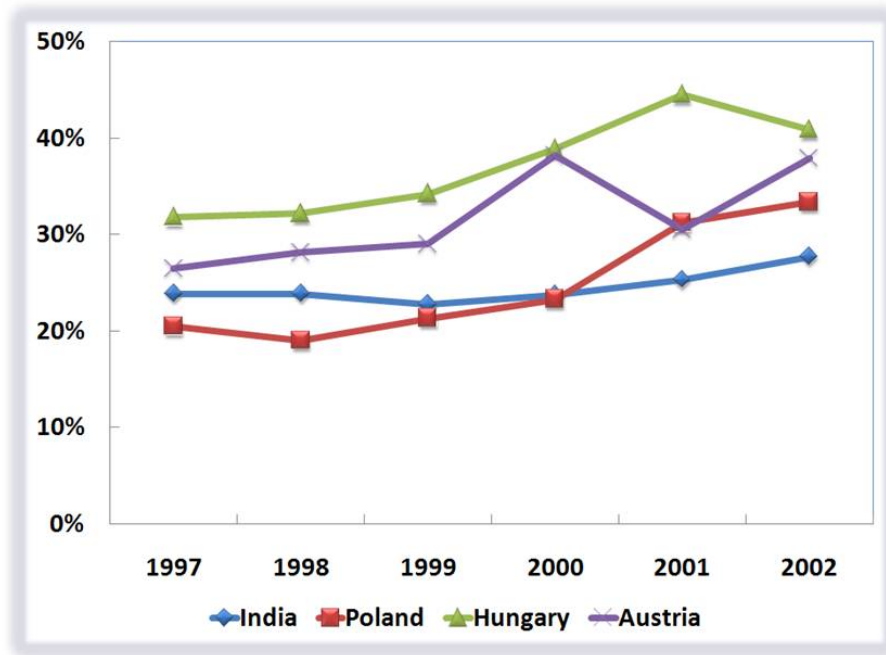


Figure 11-19: PPP-Adjusted Value Added Per Employee as a Percentage of that in the US

However, if factor costs in EU countries, shown in figure 11-18, are compared with those of US, the distinct labor cost advantage that US establishments enjoy is obvious. EU having a very high fraction of unionized work force has considerably higher factor costs than that in the US.

11.4.2 Labor Productivity

Doubts would have to be expressed in the face of data on labor productivity about the real value in moving manufacturing to low cost countries outside of EU and US. While the advantages of cheaper man power cannot be easily overlooked, the fact that the labor productivity (adjusted value added per employee as a fraction of that contributed by an employee in the US) is abysmally low is very disconcerting if we were to accept the assumption that eventually the cost advantages in different parts would iron out over time.

While it is worthy to note that the extraordinary healthcare and drug costs in the US may skew the actual value added in countries like US and EU, it is very telling to

observe that some of the countries only a 30% to 40% labor productivity as the US. This brings to fore the question of low-cost advantage as a sustainable competitive advantage for pharmaceutical companies deciding to move manufacturing to low cost locations. As a result, it can be expected that there must be reasons other than simply cost advantages behind why firms decide to move manufacturing to locations outside the US and EU.

11.5 A Life-cycle Model for Globalization of Manufacturing

The dependence of manufacturing location decisions taken by firms on product lifecycle proposed by Vernon [99, 100] points out that lifecycle stages of the product alters the ability of firms to take on risks of investing in new locations. A holistic perspective of manufacturing location decisions needs to take into account the industry level constraints, firm level objectives, country level factors and product level issues.

A pharmaceutical or biologics manufacturer (referred to as the firm) disaggregates its goal of maximizing shareholder value into market seeking and/or resource seeking and/or efficiency seeking objectives whereby the firm maximizes expected returns for a given level of underlying, undiversifiable risk. The magnitude of the importance that the firm places on the three independent objectives, the ability and the appetite of the firm to undertake risk, and the lifestage of the firm, its products and its markets significantly set the direction and strategy of the firm.

Conceivably, at an early stage of product development, the firm, following Vernon's [99, 100] model, look for talent (resource) and customers (market). At this stage, the undiversifiable risk of product failure looms large on the firm and the firm is heavily invested in bringing the first product to market. As the product begins to diffuse into the market reaching peak sales, the firm begins to shift emphasis, much like in Vernon's model, to better resources while learning to manage said resources efficiently. Finally, a mature, generic product would have its premium price position considerably eroded and the onset of price competition forces firms to seek for higher

efficiencies. In addition to the aforementioned objectives and risk appetite of the firm, exogenous factors like government regulations and policy both places constraints and presents opportunities for firms. For example, while stringency of safety regulations presents unavoidable constraints on the firm, government tax policy, incentives for relocation and investment and so on present opportunities for value creation by the firm. The rest of the section will focus on the implications of this lifecycle based location model for pharmaceuticals and biologics.

11.5.1 Model for Pharmaceuticals

After a target has been identified as a cause of a particular medical condition or disease pharmaceutical companies screen their in-house chemical compound libraries to attack the target in order to cure the condition. These optimized leads, called *New Chemical Entities* or *NCEs*, that attack the target is then optimized by synthetic chemistry and are tested for efficacy in animals. When the safety profile of the NCE is satisfactory based on animal trials, the companies begin human clinical trials in three phases. At the end of each phase, the product is approved by the FDA depending on the data from that stage and the company can begin selling the product after passing scrutiny in all stages. The main challenge here is that the timeline when the patents on the NCE expire and the timeline for drug product approval leave very little wiggle room for pharmaceutical companies to extract value from successful, blockbuster drug products. As soon as patents expire, a number of generics manufacturers enter the market and the gross margins and market share of the original innovator of the product are driven down.

As the lifecycle of the NCE progresses from being patented to subsequent loss of patent protection, the manufacturing technologies and locations change. To begin with, when the NCE enters the market as a drug product, its manufacturing predominantly occurs in US, EU or Japan. Although, in the recent past, some intermediates are being outsourced from contract manufacturers, this has been a relatively new development. As the product nears patent expiration, generic companies begin to prepare for entry and most usually have locations outside of the first location. As

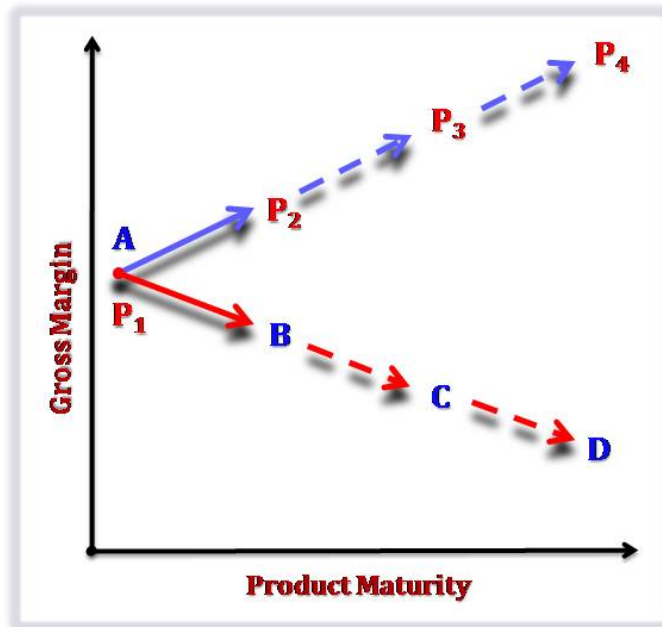


Figure 11-20: Global Expansion Model for Pharmaceutical Manufacturing

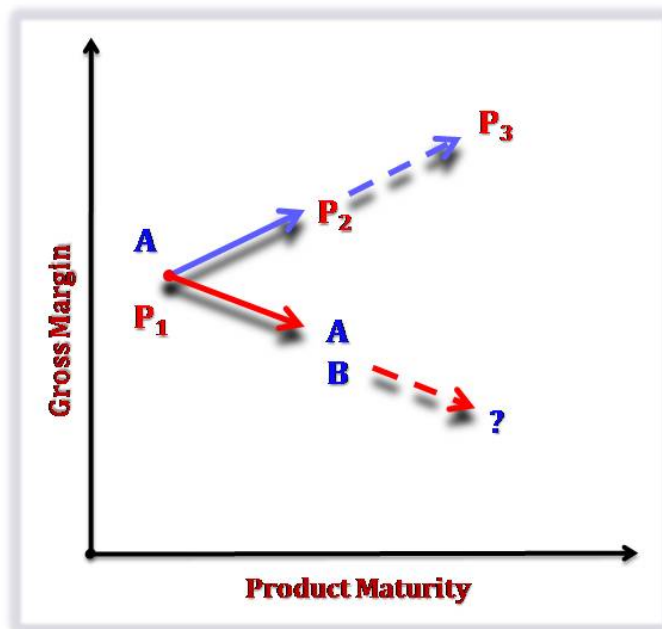


Figure 11-21: Global Expansion Model for Biologics Manufacturing

the patent expires, prices and market share take a hit and the gross margins on the product begin to fall, as shown in figure 11-20. This movement in gross margins might also force the original innovator of the NCE to move manufacturing to newer locations to save on the cost of goods sold on this pharmaceutical product. During this period of transition of manufacturing from high cost to a low cost location, as shown in figure 11-20, another NCE with higher gross margins might be introduced in the original location (for example in the US) causing another cycle to begin for that product.

11.5.2 Model for Biologics

A different model for biologics needs to be proposed. The biggest challenge in proposing such a model for biologics manufacturing is with the fact that while pharmaceuticals have seen more than 50 years of innovation based business models, biologics have been around for less than 30 years now. In addition, pharmaceutical generic product approvals have been ironed out a long time ago, compared to the follow-on biologics approval regime in the US (which is still in the making as of May 2008). Therefore, since cost-based manufacturing pressures have not yet hit biologics, manufacturing had been limited to US, EU and Japan thus far. However, tax holidays and growing expertise in India, Ireland and Singapore have been encouraging biologics manufacturers to look outside the US and EU for their manufacturing needs. Nevertheless, current thought indicated that given the extraordinary fixed costs of biologics manufacturing, the manufacturing capacity in US and EU would always be put to use in order to decrease the average cost of manufacturing biologics. As a result, the proposed model, in figure 11-21, shows that as gross margins tend to decrease, manufacturing of biologics would still be carried on in the location where the product innovation was first carried out (US in a large number of cases). It is as yet unclear what the future state of biologics manufacturing would be, if the US were to begin approving follow-on biologics.

11.6 A Framework for Global Manufacturing Strategy

Following Lessard's [59] extension of the strategic global organizing framework proposed by Porter [84], Doz et al., [26], Bartlett [3], Bartlett and Ghoshal [4], Ghoshal [35] and Prahalad and Doz [87] organizing framework for global strategy, the firm's industry is analyzed for identifying its globalization potential with a focus on manufacturing. Following this, geographic region level framework for making strategic location decisions is presented.

11.6.1 Industry Level Framework

Four key factors need to be considered before deciding whether a particular industry is set to extract value from globalization than another. This industry-framework captures economies of scale and scope and the level of risk (related to both technology transfer and intellectual property infringement) and stringency of regulations on that industry. Four industries - beverages, pharmaceuticals, biologics and airplanes - have been compared on a spider web diagram in figure 11-22.

11.6.1.1 Scale

Economies of scale refer to the decrease in average cost as the scale of production increases. While this is almost always true, demand constraints limit the economies of scale that can be achieved by global expansion of manufacturing. For example, the beverage industry can highly utilize the economies of scale by expanding its manufacturing (bottling) to far away regions across the globe in order to be very close to markets and receive instant demand profiles of the local market. However, for an industry like airplanes it would be unwise to build manufacturing sites at more than one location, given that the overall demand in the world is constrained and that a new facility entails huge capital investment making it difficult to recover the fixed costs effectively.

Construed another way, a beverage manufacturer can decrease the average delivered cost of a finished product when manufacturing is spread out across the markets

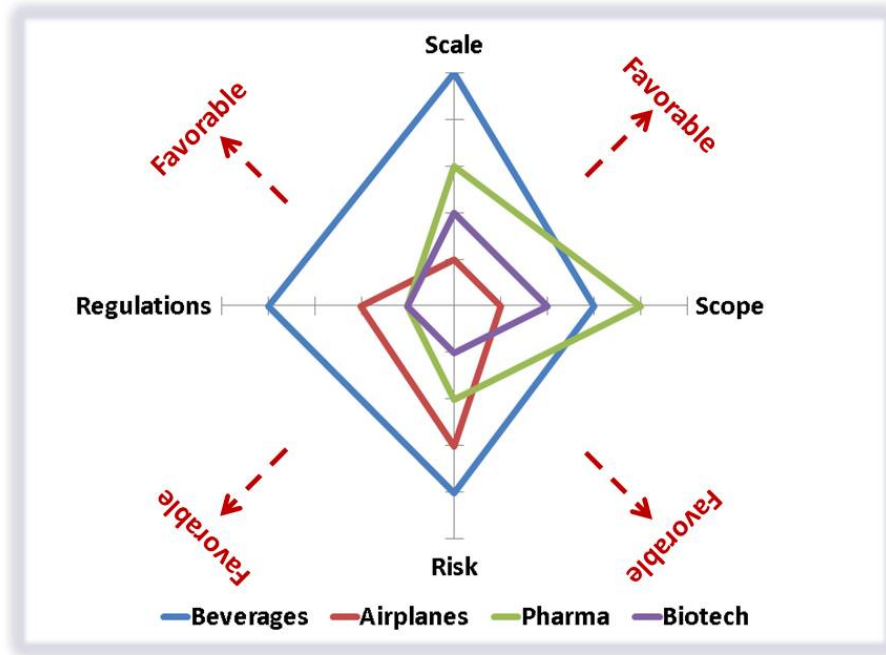


Figure 11-22: An Industry-Level Framework for Global Manufacturing Strategy, Extension from [59]

being served. Clearly, for this to be true the fixed costs of manufacturing at multiple locations across the globe should be less than the lost market demand due to the firm's inability to supply efficiently. In the case of pharmaceuticals and biologics, the initial capital expenditure is significantly higher than that in beverages. This makes it unattractive for firms to pursue building multiple locations for the same pharmaceutical or biologics product. However, as seen in the figure 11-22, biologics manufacturing facilities are significantly more capital investment intensive than pharmaceutical facilities and hence have much less attractive economies of scale [13].

11.6.1.2 Scope

Economies of scope refer to the decrease in average cost as the scope (number or variety) of products manufactured at a given manufacturing facility or location increases. Clearly, global expansion plays well with industries where the number of products tends to be higher than usual. The beverage industry sells 7 to 8 flavors of beverages that can be manufactured at a single location. Therefore, this product scope

in manufacturing spreads the fixed cost of manufacturing across different products and is allows for beverage manufacturers to explore new locations that serve multiple products to the local market.

Pharmaceutical and biologics manufacturing facilities, on the other hand, have single product manufacturing facilities. Between these two sub-industries, the relatively easier to replicate chemical synthesis based pharmaceutical manufacturing facilities are usually more broader in product scope than the dedicated manufacturing facilities used by biologics manufacturers as seen by the increased favorability in the industry level framework in figure 11-22. Clearly, the minimal scope of airplanes severely limit the manufacturing location product scope in the case of the airplane manufacturers.

11.6.1.3 Risk

Presence of substantial risk in the business environment, in the process of bringing products successfully to market, in ensuring product success in the market, in technology transfer, and in intellectual property infringement pose significant hindrances discouraging globalization of manufacturing. The beverage industry, perhaps, has the most amenable risk profile given the least uncertainty in technology transfer of manufacturing, least risk in market share losses because of strong brand differentiation and conspicuous lack of intellectual property risks (notwithstanding trade secrets). In the case of airplane manufacturers, while technology transfer risks are very large, the intellectual property associated with the airplanes is well protected by means of the capital intensive nature of the business.

Pharmaceuticals and biologics manufacturers exhibit riskier profiles towards globalization of manufacturing. In the case of pharmaceuticals, while the capital investments are significant, competitors can raise sufficient capital easily to invest in pharmaceutical manufacturing facilities. However, intellectual property infringement risks are very prevalent in this sector, especially in emerging economies that are entering the WTO patent protection regime. Given the nature of the manufacturing process, as discussed before, pharmaceutical manufacturing poses very low risk of technology transfer.

The risk profile of biologics manufacturers is starkly different from pharmaceuticals. There are substantial technology transfer risks in moving manufacturing locations. Many manufacturing processes that are apparently well characterized are hardly replicatable even by the firm that had developed it in the first place. Complications in technology transfer and process qualification, validation and process control probably are the single biggest risk that biologics manufacturers have to mitigate in their decision to globalize manufacturing. While intellectual property infringement risks are lower compared to pharmaceuticals, growing educated demographic in Asian countries and a new-found love in the life sciences in these countries might change how firms perceive intellectual property risks in the process of globalization of manufacturing.

11.6.1.4 Regulations

Industries that are mandated to adhere to stringent regulations, standards and practices usually are not incentivized to expand their manufacturing globally, unless such standards and regulations are globally harmonized and reconciled or the firm has more and better experience in managing multiple country and regional regulations and standards. In general, firms are better of adhering to the common minimum standards across the entire manufacturing assets in order to be able to hold the option of moving manufactured goods from any location to any location. Even within this perspective, a firm with headquarters in the US *versus* a firm operating with the US as primary location might

A heavily regulated industry like pharmaceuticals or biologics is much less amenable to globalization than beverage manufacturing. The general rule that many pharmaceutical companies in the US follow is to meet more than the common minimum regulatory standards across the different markets and locations these firms operate in so that the chance of failing to meet regulations is minimized. Such policies would not only increase the fixed costs in building such safeguards, but also increases the monitoring costs on the firm deciding to globalize manufacturing. Notably, pharmaceuticals and biologics manufacturers have been very expansive in spite of differing

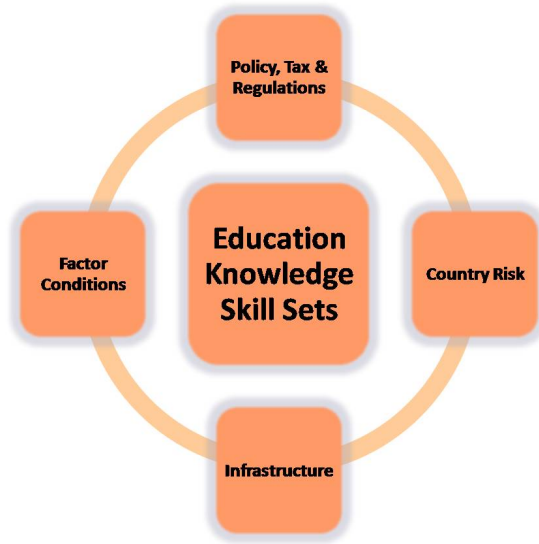


Figure 11-23: A Geographic Region Level Framework for Global Manufacturing Strategy

regulations between countries, in part because of their comfort in meeting US, EU and Japanese standards and regulations and also because of the increasing harmonization of the standards and regulations at other locations.

11.6.2 Geographic Region Level Framework

On geographic level, firms need to think of five different sets of criteria in order to devise a strategy for global manufacturing shown in figure 11-23. These factors can be grouped as - Factor cost advantages, regional/country policies, taxes and regulations, regional/country risk, infrastructure and availability of skilled human resources and expertise in the region or country.

11.6.2.1 Factor Cost Advantages

On-going operating cost advantages will play a significant role in determining whether a firm would build manufacturing at a particular location or not. From the UNIDO INDSTAT data [79], factor costs of Asia/Eastern Europe were found to be at least 10% lower than those in the US (c.f. figure 11-17) and up to 50% lower than those in EU countries (c.f. figure 11-18). While these factor cost differences are attractive for firms looking to explore new regions, it must be cautiously mentioned that factor

cost advantages do not mean that moving manufacturing will be value additive to the firm's bottom-line. At the same time, firms would never move manufacturing to high cost countries or countries with high growth rates in factor costs.

For biologics, it is worth mentioning the consumables for downstream processing plays a larger role in determining factor costs and since consumables almost exclusively are imported from US and EU, the advantages in materials cost is substantially lesser. In addition, employees in biologics manufacturing are considerable more educated, decreasing the cost differential further, than in pharmaceutical manufacturing. Finally, storage and transportation costs are substantially lesser for pharmaceuticals; the requirements on cold chain capabilities would mean that biologics manufacturers might have to consider building those capabilities in countries where such capabilities are underdeveloped.

11.6.2.2 Tax Policy and Regulations

Tax holidays and reduced tax rates allow big pharmaceutical and biologics companies to add substantial value to their bottom-line. Tax holidays are provided by national governments to help jumpstart the local economy in a particular industry or sector depending on the local needs and aspirations. The successful examples of tax holiday countries include Puerto Rico (where the tax holiday status expired in 2006 for pharmaceutical companies), Ireland (where the tax rate is currently at 10% and is set to increase to 12.5% in 2010) and Singapore where the tax rate for manufacturers has been 0%.

The following example shows how tax advantages arise in moving to low tax location. Consider a blockbuster drug with \$1 billion in non-US revenues. With 25% cost of goods sold (COGS), the pre-tax income for the product would be \$750 million shown in table 11.3. If this were to be taxed at US tax rates (35% corporate tax rate), this tax would be amount to \$262.5 million. If the tax rate were to be 10% as in Puerto Rico, the tax on this would amount to only \$75 million, a tax savings of \$187.5 million on a yearly basis. Assuming 0% growth in revenues and COGS, and a 15% weighted average cost of capital for a company like Pfizer or Merck, this

would translate to more than \$940 million over a 10 year period. In comparison, a new biologics manufacturing plant would cost about \$400 million [13].

Table 11.3: Tax Savings Calculations

| US Tax | | Ireland Tax | |
|------------------|----------------------------|-----------------------|----------------------------|
| Line Item | Value (in Millions) | Line Item | Value (in Millions) |
| Revenues | \$1,000.0 | Revenues | \$1,000.0 |
| COGS | \$250.0 | COGS | \$250.0 |
| Gross Income | \$750.0 | Gross Income | \$750.0 |
| Tax (35%) | \$262.5 | Tax (10%) | \$75.0 |
| Income after tax | \$487.5 | Income after tax | \$675.0 |
| | | Yearly Savings | \$187.5 |

End of Table

There are a couple of caveats to the tax holiday regime. First, US tax code allows using the lower tax rate if substantial IP in manufacturing is transferred to locations outside the US. Second, the products imported into US are taxed at US rates, though income generated at manufacturing locations outside the US can be deferred to realize lower tax rates on income statements. In 2005, the US government allowed a one-time transfer of cash when pharmaceutical companies could bring income outside of US into the US without affecting the tax rates on that income.

In order to claim tax credits from a tax-free or low-tax location, US Tax Code requires a majority part of the intellectual property reside in the tax-free or low-tax location. With this regulation, pharmaceutical and biologics manufacturers face a trade-off in deciding the stage of development at which the technology transfer and movement and development of IP is carried out. Process and intellectual property development is advantageous if it is carried out in a high tax location because of the tax write off that it enables the firm to claim on the research expenditure. On the other hand, manufacturing of products for commercial sale is best carried out in a low tax location because of the tax credits that US tax code allows the firms to assume.

In the case of pharmaceuticals, given the nature of intellectual property and the technological complexity of the process, a pharmaceutical manufacturer would incur very minimal technology transfer cost when this technology transfer is carried out at later stages of product development (during Phase III clinical trials, for example). This implies that the trade-off that manufacturing strategy managers face is more inclined towards investing in process development in a high tax location, claiming tax credits on the research and development expenditure, then incurring some technology transfer costs in moving the manufacturing process to a low tax location.

In the case biologics, given the nature of technological complexity of the process and difficulties in replicability, late stage process technology transfers are significantly risky, time consuming and expensive. On the other hand, by choosing to develop the manufacturing process and carrying the process development in a low-tax location, the firms leave valuable research and development tax credits on the table. In addition, given that biologics process development is more complex and needs a stronger connectedness (as defined by Lessard [59]) with the product and clinical research groups, transferring process development to a low-tax location early on in the product life cycle might prove to be a very risky proposition.

In-country manufacturing and environmental regulations play a critical role in determining the attractiveness of a particular location. First, the stringency of such regulations and sophistication of the regulatory bodies determines the difficulty level in receiving timely approval from national regulatory bodies. In recent times, many attractive manufacturing destination countries have begun to emulate or harmonize their regulatory regimes in alignment with the US FDA or the European EMEA. Secondly and more importantly, the closer the regulatory standards to the US standards, the better the local expertise in understanding and following US regulations in the manufacturing sites of those countries. Governmental incentives in the form of land grants, sponsored training programs, matching capital investments, utility supply guarantees etc. are some other incentives that attract pharmaceutical and biologics manufacturers to relocate their facilities to these countries.

11.6.2.3 Country risk profile

Idiosyncratic country risks that cannot be diversified away play a significant role in determining which locations pharmaceutical firms choose not to explore for manufacturing. Examples of non-diversifiable idiosyncratic risks include Puerto Rico for hurricanes, Singapore for earthquakes and tropical storms, China for political risk, India for IP risk and so on. There are some other idiosyncratic risks (like exchange rate risk and inflation risk) that can be diversified away by proper hedging mechanisms.

In addition to the country specific risks, pharmaceutical companies also need to look at addressing supply risk by choosing one location as a sole supplier of a particular API. Most pharmaceutical companies source intermediates and APIs from more than one location in order to hedge the bets on supply risk.

11.6.2.4 Infrastructure

The presence of developed infrastructure to ensure continuous supply is an important criterion firms could use to identify the locations for manufacturing. Infrastructure includes the hard, physical infrastructure like roads, uninterrupted utilities and services, living conditions and finally the legal infrastructure. Access to uninterrupted utilities and services are very critical for pharmaceutical and biologics manufacturing. For example, the fact that Singapore receives its water supply from Malaysia is a critical criterion that firms need to think about when deciding locating plants in Singapore. Access to transport infrastructure is important, not only to transport materials but also allow people to commute or reach their workplaces uninterrupted.

A large number of biologics manufacturing companies would need to send employees from US and EU as expatriates to the manufacturing locations for training, installation, validation and commissioning and operation of the plant. In such cases, the living conditions and the ability of the local population to communicate in English plays an important role for unhindered operation of the plant. Finally, legal infrastructure including an efficient police and security force and a stable legal system would be considered in determining the location of a manufacturing plant. The ability to gather land grants from landowners will also play a role in determining the

viability of a particular location.

11.6.2.5 Knowledge and Skills of Local Population

Pharmaceutical and biologics companies have differing requirements in terms of employee education levels. An average pharmaceutical manufacturing employee might simply have to be able to read standard operating procedures and write batch records while an employee in biologics manufacturing might need to know the science and reasoning behind the process. For this reason, an average employee in biologics manufacturing is expected to be a college graduate (80% college graduates in biologics manufacturing). Therefore, access to and availability of educated human resources would have to be considered especially in the case of biologics manufacturing.

The growing population of graduates and post graduates in India and China is a testament to the growing supply of qualified labor that is increasingly demanding challenging opportunities. The growth of contract manufacturing organizations in India has been banking on the rise of these graduates from numerous science and engineering colleges in India. India, Singapore and Ireland are at an advantageous position as English is the preferred language of communication and is widely spoken in these countries. The interest of employees in US and EU to go to manufacturing locations as expatriates is also dependent on the infrastructure, cultural and physical proximity to the Western world, the school system and the facilities near the manufacturing location and is a factor to be considered if there is no substantial at-the-location expertise.

11.6.3 Deriving Implications of the Framework on Biologics Companies

In an attempt to test the framework's validity, the strategic directions and implications of the manufacturing locations and positions of top 5 biologics companies by revenue were studied. These biologics companies have had rich, distinct histories since Genentech was founded in 1976 kickstarting the biotechnology industry. Amgen, Inc., Genentech, Inc., Novo Nordisk A/S, Genzyme Corporation and Biogen Idec, Inc were

the top product revenue companies in the biologics sector shown in table 11.4. The revenue, %US Sales, Cost of Sales, Tax rate and the manufacturing facilities were all gathered from the Form 10-K EDGAR filings of these companies from the US Securities Exchange Commission website.

Amgen and Genentech had revenues that were predominantly based on US sales, while Genzyme, Novo Nordisk and Biogen had more than 40% non-US sales. The skewed share of US based sales at Amgen and Genentech are a direct result of some of the marketing arrangements these pioneering companies had to enter into with *big pharma* companies like Johnson & Johnson, Roche and Wyeth. Non-US Revenues from Amgen's top two drugs are shared with Johnson & Johnson and Wyeth Biopharma. Genentech's products are marketed outside of the US by Roche's pharmaceutical subsidiary based in Basel, Switzerland.

Cost of sales (a measure of the labor and materials cost of manufacturing) are in the lower range for Amgen, Genentech and Biogen Idec. These values are at the lower end of the expected 15%-25% of product revenues. Such lower end cost of sales might arise from premium pricing of their products, efficiency in manufacturing or better factor cost optimization. It is difficult to identify the real cost advantage that these companies realize in their operations.

Tax rates as measured from the income statements of these companies make a telling argument on the companies strategies to manufacture in low-tax locations. The observations made by Grubert and Mutti [38] on the movement of firm incomes to low tax or tax holiday locations seem to be effectively explaining the lower taxes at Amgen and Novo Nordisk. The locations of manufacturing for Amgen's primary blockbuster products are based in Puerto Rico and until recently being developed in Ireland. The tax rates of other biologics companies were significantly higher than that of Amgen signaling that closely managed tax savings strategy is being employed at Amgen.

It is interesting to note that if we trace the taxes on the products sold by Genentech outside of the US and hypothetically compute the tax rate of Genentech's product line as if Genentech owned all the rights to market the product, we might specu-

| | Amgen | Genentech | Biogen Idec | Novo Nordisk | Genzyme |
|---------------------------------------|--|--|---------------|---|----------------------------------|
| Factor Cost Implications | 1. High margin products 2. Lesser emphasis on mfg. cost savings | | | 1. Market Proximity 2. Emphasis on cost savings | |
| Tax Strategy Implications | Aggressive tax planning | 1. Good Corporate Citizen perspective 2. May change by 2010 for Genentech | | 1. Good Corporate Citizen Perspective 2. Balanced tax benefits with risk | |
| Risk Strategy Implications | Contract Manufacturing | 1. Intensive capacity management 2. Collaborative manufacturing | | Multiple site, in country bulk manufacturing | Reliable infrastructure & supply |
| Infrastructure Implications | 1. Reliable cold chain infrastructure 2. Reliable supply chain & transportation 3. Uninterrupted supply of utilities | | | | |
| HR Strategy Implications | 1. Minimum education requirement 2. cGMP knowledge and compliance 3. Proximity to Western culture | | | | |
| Corporate History Implications | Predominantly Expansions | US Focused (Roche Holdings) | US/EU Centric | Global Expansion Commodity Mkt. | Predominantly Acquisitions |

Figure 11-24: Strategic Implications Based on Proposed Framework

late considerable reduction in Genentech’s effective tax rate. The effect of Roche’s 52% equity stake in Genentech, coupled with non-US marketing rights of Genentech’s products by Roche, the tax rates for this hypothetical case might be lower the current value for Genentech at 37.4%. Genentech has also secured an option to buy a plant being built by Lonza in Singapore that is expected to be commissioned by 2010. This marks a diversion from Genentech’s all-US manufacturing strategy and its implications are yet to be studied. However, in biologics it is very important to note that only microbial fermentation is usually relocated and mammalian cell synthesis is still closely operated in US Locations.

Table 11.4: Top Revenue Generating Biologics Companies of 2007

| | Amgen | Genentech | Novo Nordisk | Genzyme | Biogen Idec |
|---------------------------|--|--------------------------------------|---|----------------------------------|--|
| Product Revenues | \$14.31B | \$9.44B | \$6.35 B | \$3.46B | \$2.14B |
| % US Sales | 80% | 100% | 31% | 52% | 56% |
| Cost of Sales | 17.8% | 16.7% | 24.7% | 20.7% | 15.7% |
| Effective Tax Rate | 20.1% | 37.4% | 28.6% | 34.7% | 29.9% |
| Locations | US, Puerto Rico Netherlands Ireland ² | California Singapore ¹ | Denmark, US Brazil, Japan China, France | Belgium, US Ireland France | California North Carolina Netherlands ³ |

End of Table

¹Commissioning planned by 2010

²Discontinued in 2007

³Commissioning planned by 2009

The strategic implications based on the criteria proposed in the framework discussed in the previous section are shown in figure 11-24. The high margin nature of Amgen, Genentech, Biogen's products market proximity and access take precedence over cost efficiency. Novo Nordisk increasingly faces pressure in its insulin-based markets with the threat of price competition from rival Eli Lilly and local manufacturers of generic recombinant Human Insulin. At Genzyme, the orphan status of the top selling drug shifts the emphasis from cost efficient to timely delivery of the product to the patient. Therefore, the speculation is that cost of sales is a driving factor in determining the location for manufacturing and subsequently selling products at Novo and to a lesser level at Genzyme and at the least level at Amgen, Genentech and Biogen.

Tax strategies varied significantly between companies discussed here. Amgen aggressive pursuit of generating shareholder value out of tax savings has substantially paid off with its comparably low tax rates at 20%. Genentech and Biogen Idec seem to have a different view on tax savings and have predominantly US tax rates for all their sales. Genzyme, in spite of its presence in certain low tax locations, is yet to book lower tax rates. It is speculated that Genentech, Genzyme and Biogen consider tax as an integral fabric of reaching out to their consumers as a good corporate citizen. However, it should be duly noted that given Genentech and Biogen's new manufacturing facilities in Singapore and Netherlands, the tax strategy of these companies might be seeing some changes.

The perspectives of these companies on how technology transfer risk, undiversifiable country risk and supply chain risk should be mitigated vary from controlled utilization of contract manufacturers with active demand and capacity planning (e.g. Amgen), to Genentech and Biogen's collaborative manufacturing and sharing the risk of getting products to patients. Novo's disaggregation of its manufacturing into single bulk sourcing and multiple product formulation facilities essentially diversifies the risk of a single location being hit by some uncertain event. Genzyme's inclination to carry out operations close to the market with demand would let us to speculate that ensuring reliability in supply of products is an important aspect of Genzyme's risk

mitigation strategy.

The infrastructure and human resource strategies were found to be similar across these different companies. Technologically intense biologics manufacturing process demands well educated graduate and post-graduate work force unlike small molecule pharmaceutical manufacturing. Proximity to Western culture helps in securing expatriates willing to travel, live and train the local talent at their manufacturing locations. Knowledge and training in current Good Manufacturing Practices (cGMP) are critical in any company. Reliable infrastructure, utilities, land access, transportation and cold chain capabilities

Finally, historical perspectives of the current position of these companies clarifies the question of whether particular location decisions were strategically made and organically grown or whether an acquisition allowed the firm access to a new location that was not in the portfolio before. In addition, the global focus of Genzyme and Novo from early stages of product development is a differentiating feature from Amgen and Genentech where most initial sales and business was in US and EU.

11.7 Case Studies on Applying the Framework

Two case studies are shown below on the methodology of applying the proposed framework. One company, Amgen, has substantial revenues generated globally, but certain historic and product license constraints have not yet opened worldwide sales opportunities at the moment for Amgen. On the other hand, Novo Nordisk had been an international company with 99% of sales coming from outside of Denmark, the home country. It is hoped that these cases will show the usefulness and relevance of the Framework for organizing Global Manufacturing in Biologics. In pursuing this analysis, a set of five regions/countries have been examined - US/EU, Puerto Rico, Ireland, Singapore and India.

11.7.1 Location Decision for Amgen

Assuming US as the basis for factor costs, evidence points to at least 10% factor cost advantage in Singapore and India. However, given Singapore's growth in investments

in manufacturing, the expectations of rising factor costs makes it less favorable location than India with respect to factor costs of Amgen. However, the factor cost differences between Puerto Rico, Ireland and Singapore, are similar with very little differences and hence are found to have similar attractiveness as seen by the circles filled in figure 11-25.

Amgen's strategy of garnering tax savings to increase shareholder value would mean that Puerto Rico, Singapore and Ireland with very attractive tax rates ranging from 0% in Singapore to 12.5% in Ireland are equally attractive for manufacturing. However, country risk plays a mediating role in determining the better location of Ireland, Singapore and Puerto Rico. The added political risk and risk of IP infringements in India are undiversifiable by Amgen.

In country transportation and cold chain infrastructure is very well developed for pharmaceuticals and developing rapidly for generics at Singapore, Ireland and Puerto Rico. However, India is still playing catch-up in terms of country-wide infrastructure development. Finally, while India has a language advantage of English trained skilled labor, the Western proximity to Ireland and Puerto Rico by distance and Singapore by living standards make those locations more attractive.

11.7.2 Location Decision for Novo Nordisk

Similar to that seen for Amgen, US would be the basis for factor costs, and allevience points to at least 10% factor cost advantage in Singapore and India. However, given India's large diabetes population, market proximity for Novo might play a bigger role in entering India on contract fill-finish manufacturing basis. The factor cost differences between Singapore, Ireland and Puerto Rico were found to have similar attractiveness as seen by the circles filled in figure 11-26.

While Novo does not actively pursue tax saving strategy, its ability to arbitrage the gains from taxation in Special economic zones in India for example should not be lightly undermined. A careful review of the country risk factors indicates that supply disruptions, while manageable due to Novo's extensive distribution network, is still a risk. In that sense, Novo would prefer to minimize the risk of manufacturing location

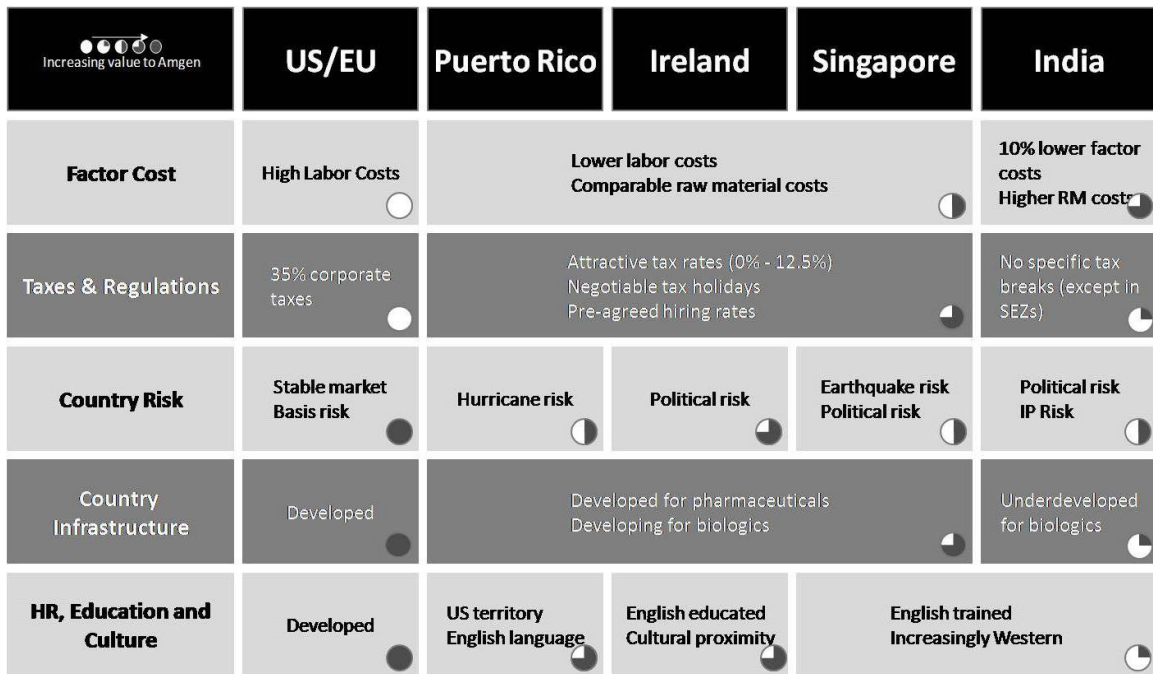


Figure 11-25: Application of the Proposed Framework for Amgen Inc.

disruption, by choosing to manufacture in close proximity to China and India - the two largest markets for Insulin.

In country transportation and cold chain infrastructure is very well developed for pharmaceuticals and developing rapidly for generics at Singapore, Ireland and Puerto Rico. However, India also has a strong supply chain to deliver Insulin related products which would play to India's advantage. Finally, while India's language advantage is expected to play at least an equal role with that of Singapore and Ireland however, proximity of the Western countries to Ireland and Puerto Rico by distance and Singapore by living standards increase the attractiveness of those locations tremendously when compared with India.

11.8 Impact and Summary

This work identifies the critical factors to be considered by country managers or international expansion teams while making decisions on which locations to expand manufacturing into. The framework places burden on a systematic cost-benefit-risk analysis on the planning manager while allowing for considering factors that may not

| Increasing value to Novo Nordisk | US/EU | Puerto Rico | Ireland | Singapore | India |
|----------------------------------|-----------------------------|---|--|---|---|
| Factor Cost | High Labor Costs | Lower labor costs Comparable raw material costs Significant transportation costs (Far away markets) | | | Proximity to market Lower labor cost |
| Taxes & Regulations | 35% corporate taxes | Attractive tax rates (0% - 12.5%) Negotiable tax holidays Pre-agreed hiring rates | | | No specific tax breaks except in SEZs |
| Country Risk | Stable market Basis risk | Hurricane risk | Political risk | Earthquake risk Political risk | Political risk |
| Country Infrastructure | Developed | Developing for Biologics Developed for Insulin | | | Developed for Insulin |
| HR, Education and Culture | Developed | US territory English language | English educated Cultural proximity | English trained Increasingly Western | |

Figure 11-26: Application of the Proposed Framework for Novo Nordisk A/S

directly enter into a financial model. The framework also provides a platform for risk assessment by planning managers that can be used as a continuous assessment tool to identify the potential problems and pitfalls in international manufacturing expansion. The strategy implications point out to two predominantly occurring patterns - tax and other incentives are heavily skewed towards attracting foreign investments into regions and that risk appetite, assessment and mitigation plays the second significant role in determining, or at least narrowing down location choices.

In summary, it is very important to note that while factor costs are given primary importance and attributed as the reason behind manufacturing shifting or expanding into newer locations outside of US and EU, it is definitely not the only criterion that firms must use in identifying the need to expand manufacturing globally. Tax incentives and other factors like legal and physical infrastructure and language also play critical roles in determining a successful location for pharmaceutical and biologics manufacturing. In biologics manufacturing, considerable history of expansion is absent both because of the recent nature of the industry and also because of technological and financial reasons of recouping investments from existing manufacturing

infrastructure. Application of the geographic level strategic decision framework increasingly pointed to locations where the risk benefit trade-off matched the expected returns of the firms. Finally, patent expirations in pharmaceuticals have facilitated the entry of newer generics companies that have sprung up in low cost countries in the past 10 years. The scenario is expected to push more towards an even lower cost base and drive margins further down. Pharmaceutical manufacturers will need a framework like the one presented here with which they can examine and make strategic location decisions.

11.9 Acknowledgments

I would like to express special thanks to Ms. Judy Lewent, Former CFO, Merck; Mr. Mark Bamforth, SVP of Operations, Genzyme; Mr. Bill Rich, GM of International Operations, Amgen; Mr. Brandon Smith, Director of Corporate Strategy, Amgen; Ms. Leslie Prince Rudolph, International Manufacturing Strategy Manager, Eli Lilly; Mr. Eric Cheslek, Manufacturing Strategy Manager, Eli Lilly; Dr. Mickey Koplove, Vice President, Wyeth Biopharma; Ms. Suzanne Sensabaugh, VP MDS Biopharma; Dr. Arun Chandavarkar, COO, Biocon India; Mr. Rakesh Bamzai, VP of Marketing, Biocon India; and Dr. Harish Iyer, GM of Research, Biocon India for their inputs, discussion and feedback on this chapter.

Chapter 12

Conclusion

Continuous manufacturing addresses some of the critical problems faced by secondary pharmaceutical manufacturing, around efficiency, scale-up, quality assurance and cycle-times. Instead of comparing the performance of continuous vs batch operations, continuous manufacturing should be viewed as an alternative design choice available for process design in pharmaceuticals. Blending was identified as the critical last step where variance can be altered to make or break the product by affecting product quality.

Investigation on continuous blending began by a thorough literature review in this area. The literature review revealed lack of experimental investigations on cohesive powders in continuous blending and an understanding of the effect of microscopic particle parameters on the performance of continuous powder blending processes. It was also shown in literature that the system comprising of the feeding (dispensing) system and continuous blender should be studied as one single entity as the performance of the continuous blender is strongly dependent on the efficacy of the feeding system.

A framework was created to understand phenomena in continuous blending and relate it to operational variables and material properties. Flow behavior of powders in blenders were studied by measuring residence time distributions of particles in continuous blenders. A process model based on integrating the flow behavior and disturbances introduced at the feeder was used in understanding the process operating variables.

Continuous blending at pilot plant scale was shown to achieve blend qualities that are mandated by FDA for safety and efficacy. Also, the effect of energy input through rotation rates of moving elements in the blender was shown to positively affect the blending process.

Mean residence time coupled with the disturbance frequency (or time period of feeder fluctuation) were the two most significant operational variables that affect blender performance. Most other independent operational variables like energy input, flow rates angles of incline and dependent operational variables like fill weight affect the blending process through mean residence.

Increase in particle size was shown to increase the axial dispersion coefficient of the material in the blender. Increased dispersion coefficients were shown to increase blender performance. A decrease in cohesive forces caused increased blender performance. This effect was evident when the particles of different cohesion and adhesion forces were mixed in the blender. Increased Cohesion and adhesion decreased the axial dispersion coefficient. Change in particle shape did not exhibit a strong effect on blender performance but did effect the fill weight in the blender considerably.

Multicomponent blending was demonstrated in the pilot-scale experiments. Addition of lubricant after mixing decreased the cohesion forces and caused the blend to segregate and blend quality to deteriorate. Lubricant coated the API and excipients with a fine layer of small particles that reduced the cohesion forces in the particles and increased the potential for segregation.

Identifying of an correct scale of scrutiny in powder blending leads to the correct assessments on continuous powder blending. Taking moving averages of process monitoring data was shown to be equivalent to offline sample collection and analysis. Theoretical predictions of blender performance were shown to be in agreement with experiments after taking into account the variation in the powder flow behavior in the blender.

This work advanced the knowledge on the behavior of particles in continuous mixing systems. The effects of particle parameters in continuous blenders were hitherto unknown and this thesis contributed to the scientific understanding of particle and

operational parameters on blending performance. This thesis also created a design framework for the pharmaceutical industry to investigate and implement continuous blending in particular and continuous processing in general in secondary pharmaceutical manufacturing.

Appendix A

Nomenclature

| | |
|-----------|--|
| API | Active Pharmaceutical Ingredient |
| VRR | Variance Reduction Ratio |
| RSD | Relative Standard Deviation |
| MRT | Mean Residence Time |
| RTD | Residence Time Distribution |
| FDA | Food and Drug Administration |
| PLS | Partial Least Squares Regression |
| MLR | Multiple Least squares Linear Regression |
| NIR | Near infra-red spectroscopy |
| LIF | Light Induced Fluorescence |
| DCL | Direct Compressible Lactose |
| MCC | Micro Crystalline Cellulose |
| RPM | Rotations per minute |
| NCE | New Chemical Entity |
| MgSt | Magnesium Stearate |
| A | Normalization Constant in Dispersion Model |
| A,B,C,D,E | Constants in Response Surface Model |
| a | Serial correlation coefficient |
| r | Time window of observation |
| E | Residence time distribution |

| | |
|------------------|---|
| I_o | Scale of segregation |
| G | Fourier transform of autocorrelation function |
| C | Concentration of API |
| t | Time |
| z | Axial distance |
| ν | Mean axial velocity |
| Bo | Bodenstein number (Peclet Number) |
| D, \mathcal{D} | Axial dispersion coefficient |
| Sig | LIF signal value |
| R | Correlation Coefficient |
| t_d, T_f | Time period of feeder fluctuation |
| W | Fill Weight in blender |
| F | Flow Rate in blender |
| p, q | Mass fractions of API and Excipient |
| n | # of particles in sample |
| τ | Space Time (Mean Residence Time) |
| τ_v | Residence time in V-section |
| τ_d | Residence time in Drum Section |
| μ | Mean residence time, Mean of particle sizes |
| Ψ | Dimensionless concentration of API |
| θ | Dimensionless time |
| ζ | Dimensionless axial distance |
| α, β | Calibration parameters |
| $sigma^2$ | Variance in concentration |
| m_p, m_q | Mean values of particle sizes |
| $rand$ | Random mixture |
| in | Input stream |
| out | Output stream |
| ss | At steady state |
| seg | Completely segregated |

Bibliography

- [1] A.Z.M.A. Abouzeid, T.S. Mika, K. V. Sastry, and D. W. Fuerstenau. The influence of operating variables on the residence time distribution for material transport in a continuous rotary drum. *Powder Technology*, 10(6):273–288, 1974.
- [2] The World Bank. World Development Indicators Online. <http://go.worldbank.org/3JU2HA60D0>, 2007.
- [3] C.A. Bartlett. Global competition and MNC managers. *ICCH Note No. 0-385-287*, 1985.
- [4] C.A. Bartlett and S. Ghoshal. The new global organization: differentiated roles and dispersed responsibilities. *Working Paper No. 9-786-013*, 1985.
- [5] J.P. Beaudry. Blender efficiency. *Chemical Engineering*, pages 112–113, July 1948.
- [6] H. Berthiaux, V. Mizonov, D. Ponomarev, and E. Barantzeva. Modeling continuous powder mixing by means of theory of markov chains. *Particulate Science and Technology*, 22:379–389, 2004.
- [7] H.R. Bjørsvik and H. Martens. Data analysis: Calibration of NIR instrument by pls regression. In D.A. Burns and E.W. Ciurczak, editors, *Handbook of Near-Infrared Analysis*, volume 27 of *Practical Spectroscopy Series*, chapter 6, pages 185–207. Marcel Dekker, 2 edition, 2001.
- [8] M.K. Boysworth and K.S. Booksh. Aspects of multivariate calibration applied to near-infrared spectroscopy. In D.A. Burns and E.W. Ciurczak, editors,

Handbook of Near-Infrared Analysis, volume 27 of *Practical Spectroscopy Series*, chapter 6, pages 209–239. Marcel Dekker, 2 edition, 2001.

- [9] J. Bridgwater. Fundamental powder mixing mechanisms. *Powder Technology*, 15:215–236, 1976.
- [10] J. Bridgwater. Particle technology. *Chemical Engineering Science*, 50(24):4081–4099, 1995.
- [11] J. Bridgwater, D.F. Bagster, S.F. Chen, and J.H. Hallam. Geometric and dynamic similarity in particle mixing. *Powder Technology*, 2(4):198–206, 1969.
- [12] C.J. Broadbent, J. Bridgwater, D.J. Parker, S.T. Keningley, and P. Knight. A phenomenological study of a batch mixer using a positron camera. *Powder Technology*, 76:317–329, 1994.
- [13] C. Chao and J. Lakshmikanthan. For biologics production, contract manufacturing organizations can bring real economic benefits. Deloitte Consulting LLP, 1993.
- [14] S.J. Chen, L.T. Fan, and C.A. Watson. Mixing of solid particles in motionless mixer: axial dispersed plug flow model. *Industrial and Engineering Chemistry: Process Design and Development*, 12(1):42–47, 1973.
- [15] P.W. Cleary. Dem simulation of industrial particle flows: case studies of dragline excavators, mixing in tumblers and centrifugal mills. *Powder Technology*, 109:83–104, 2000.
- [16] M.H. Cooke, D.J. Stephens, and J. Bridgwater. Powder mixing - a literature survey. *Powder Technology*, 15(1):1–20, 1976.
- [17] B. Cooker, F.R.G. Mitchell, and R.M. Nedderman. A radio pill and aerial system tracking the powder motion in a helical ribbon mixer. *Chemical Engineer*, 392:81–83, 1983.

- [18] B. Cooker and R.M. Nedderman. Circulation and power consumption in helical ribbon powder agitators. *Powder Technology*, 52(2):117–129, 1987.
- [19] B. Cooker and R.M. Nedderman. A theory of the mechanics of the helical ribbon powder agitator. *Powder Technology*, 50(1):1–13, 1987.
- [20] Asahi Kasei Corp. <http://www.ceolus.com/eng/product/celphere/index.html>, 2006.
- [21] P.V. Danckwerts. Continuous flow systems. *Chemical Engineering Science*, 2(1):1–13, 1953.
- [22] P.V. Danckwerts and S.M. Sellers. The effect of hold up and mixing on a stream of fluctuating composition. *Industrial Chemist*, 27:395+, 1951.
- [23] W.H. Davidson. The location of foreign direct investment activity: Country characteristics and experience effects. *Journal of International Business Studies*, 11(2):9–22, 1980.
- [24] DMV International Inc., Delhi, NY. *Product group overview: Pharmatose and DC Lactose*, 2006.
- [25] R.D. Domike. *Pharmaceutical powders in experiment and simulation: Towards a fundamental understanding*. Phd dissertation, Massachusetts Institute of Technology, Department of Chemical Engineering, September 2003.
- [26] Y.L. Doz, C.A. Bartlett, and C.K. Prahalad. Global competitive pressures and host country demands, managing tensions in MNCs. *California Management Review*, pages 63–74, 1981.
- [27] F.L. Dubois, B. Toyne, and M.D. Oliff. Manufacturing strategies of US multinationals: A conceptual framework based on a four industry study. *Journal of International Business Studies*, 24(2):307–333, 1993.
- [28] L.T. Fan, S.J. Chen, and C.A. Watson. Solids mixing. *Industrial and Engineering Chemistry*, 62(7):53–69, 1970.

- [29] L.T. Fan, Y.M. Chen, and F.S. Lai. Recent developments in solids mixing. *Powder Technology*, 61(3):255–287, 1990.
- [30] K. Ferdows. Making the most of foreign factories. *Harvard Business Review*, 3:73–88, 1997.
- [31] FMC Biopolymer Corporation, Philadelphia, PA. *Binders*, 2006.
- [32] H.S. Fogler. *Elements of Chemical Reaction Engineering*, chapter 14, pages 765–773. Prentice Hall NY, 2 edition, 1999.
- [33] FDA Center for Drug Evaluation and Research. Guidance for industry: Pat - a framework for innovative pharmaceutical manufacturing and quality assurance. url: <http://www.fda.gov/cder/OPS/PAT.htm/>, 2004.
- [34] A. Ghaderi. On characterization of continuous mixing of particular materials. *Particulate Science and Technology*, 21(3):271–282, 2003.
- [35] S. Ghoshal. Global strategy: An organizing framework. *Strategic Management Journal*, 8:425–440, 1987.
- [36] P.L. Goldsmith. The theoretical performance of a semi-continuous blending system. *The Statistician*, 16(3):227–251, 1966.
- [37] I.M. Grimsey, J.C. Feely, and P. York. Analysis of surface energies of pharmaceutical powders by inverse gas chromatography. *Journal of Pharmaceutical Sciences*, 91(2):571–583, 2002.
- [38] H. Grubert and J. Mutti. Taxes, tariffs and transfer pricing in multinational corporate decision making. *The Review of Economics and Statistics*, 73(2):285–293, 1991.
- [39] J. Gyenis. Motionless mixers in bulk solids treatment: A review. *Kona*, 20:9–23, 2002.

- [40] P.A. Hailey, P. Doherty, P. Tapsell, T. Oliver, and P.K. Aldridge. Automated system for the on-line monitoring of powder blending processes using near-infrared spectroscopy .1. system development and control. *Journal of Pharmaceutical and Biomedical Analysis*, 14(5):551–559, 1996.
- [41] C.F. Harwood, K. Walanski, B. Luebcke, and C. Swanstrom. The performance of continuous mixers for dry powders. *Powder Technology*, 11(3):289–296, 1975.
- [42] K.M. Hill, A. Caprihan, and J. Kakalios. Axial segregation of granular media rotated in a drum mixer: pattern evolution. *Physical Review E*, 56(4):4386–4393, 1997.
- [43] K.M. Hill, A. Caprihan, and J. Kakalios. Bulk segregation in rotated granular material measured by magnetic resonance imaging. *Physical Review Letters*, 78(1):50–53, 1997.
- [44] T. Horst. Firm and industry determinants of the decision to invest abroad: An empirical study. *The Review of Economics and Statistics*, 54(3):258–266, 1972.
- [45] B. Johnson. Personal communication. Axsun Technologies, 2006.
- [46] K.R. Jones and J. Bridgwater. A case study of particle mixing in a ploughshare mixer using positron emission particle tracking. *International Journal of Mineral Processes*, 53:29–38, 1998.
- [47] B.H. Kaye. *Powder Mixing*, chapter Monitoring mixing and mixers. Chapman and Hall, London, 1997.
- [48] V. Kehlenbeck and K. Sommer. Modeling of the mixing process of very fine powders in a continuous dynamic mixer. In *Fourth International Conference on Conveying and Handling of Particular Solids*, pages 9.26–9.31, Budapest, 2003.
- [49] P.C. Knight, J.P.K. Seville, A.B. Welln, and T. Instone. Prediction of impeller torque in high shear powder mixers. *Chemical Engineering Science*, 56(15):4457–4471, 2001.

- [50] S. Kocova and N. Pilpel. The tensile properties of mixtures and cohesive powders. *Powder Technology*, 7(1):51–67, 1973.
- [51] P.M.C. Lacey. The mixing of solids particles. *Transactions of the Institution of Chemical Engineers*, 51:53, 1943.
- [52] C.K. Lai, D. Holt, J.C. Leung, C.L. Cooney, G.K. Raju, and P. Hansen. Real time and noninvasive monitoring of dry powder blend homogeneity. *AIChE Journal*, 47(11):2618–2622, 2001.
- [53] B.F.C. Laurent and J. Bridgwater. Continuous mixing of solids. *Chemical Engineering Technology*, 22(1):16–18, 2000.
- [54] B.F.C. Laurent and J. Bridgwater. Dispersive granular flow in a horizontal drum stirred by a single blade. *AIChE Journal*, 48(1):50–58, 2002.
- [55] B.F.C. Laurent and J. Bridgwater. Influence of agitator design on powder flow. *Chemical Engineering Science*, 57:3781–3793, 2002.
- [56] B.F.C. Laurent and J. Bridgwater. Performance of single and six-bladed powder mixers. *Chemical Engineering Science*, 57(10):1695–1709, 2002.
- [57] B.F.C. Laurent, J. Bridgwater, and D.J. Parker. Motion in a particle bed agitated by a single blade. *AIChE Journal*, 48(9):1734+, 2000.
- [58] B.F.C. Laurent, J. Bridgwater, and D.J. Parker. Convection and segregation in a horizontal mixer. *Powder Technology*, 123(1):9–18, 2002.
- [59] D.R. Lessard. Frameworks for global strategic analysis. *Journal of Strategic Management Education*, 1(1):1–12, 2003.
- [60] D.R. Lide, editor. *CRC Handbook of Chemistry and Physics Internet Version*, chapter Physical Constants of Organic Compounds, page 3.298. Taylor and Francis, Boca Raton FL, 2006.

- [61] J.A. Lindley. Mixing processes for agricultural and food materials: 1. fundamentals of mixing. *Journal of Agricultural Engineering Research*, 48(3):153–170, 1991.
- [62] J.A. Lindley. Mixing processes for agricultural and food materials: 2. highly viscous-liquids and cohesive materials. *Journal of Agricultural Engineering Research*, 48(4):229–247, 1991.
- [63] J.A. Lindley. Mixing processes for agricultural and food materials: 3. powders and particulates. *Journal of Agricultural Engineering Research*, 49(1):1–19, 1991.
- [64] H. Mark. Data analysis: Multilinear regression and principal component analysis. In D.A. Burns and E.W. Ciurczak, editors, *Handbook of Near-Infrared Analysis*, volume 27 of *Practical Spectroscopy Series*, chapter 6, pages 129–183. Marcel Dekker, 2 edition, 2001.
- [65] A. Merz and R. Holtzmüller. Radionucleide investigations into the influence of the mixer chamber geometry on the mass transport in a continuous ploughshare mixer. In *Proceedings of the second Symposium on mixing of particulate solids*, number 65 in IChemE Symposium Series, pages S1/D1–S1/D6, London, 1981. Institution of Chemical Engineers.
- [66] A. Merz and R. Lücke. Einfluß der schaufelgeometrie auf axialdispersion und konvektiven transport beim kontinuierlichen feststoffmischen. *Chemie Technik*, 7(8):313–317, 1978.
- [67] O. Molerus. Über die axialvermischung bei transportprozessen in kontinuierlich betriebenen apparaturen. *Chemie Ingenieur Technik*, 38(2):137–145, 1966.
- [68] W. Müller. Untersuchungen zur pulvermischung. *Chemie Ingenieur Technik*, 39(14):851–858, 1967.
- [69] W. Müller. Methoden und derzeitiger kenntnisstand für auslegungen beim mischen von feststoffen. *Chemie Ingenieur Technik*, 53(11):831–844, 1981.

- [70] W. Müller and H. Rumpf. Das mischen von pulvern in mischern mit axialer mischbewegung. *Chemie Ingenieur Technik*, 39:365–373, 1967.
- [71] S.SH. Ngai. *Multiscale analysis and simulation of powder blending in pharmaceutical manufacturing*. Phd dissertation, Massachusetts Institute of Technology, Department of Chemical Engineering, August 2005.
- [72] K. Niranjani, D.L.O. Smith, C.D. Reilly, J.A. Lindley, and V.R. Phillips. Mixing processes for agricultural and food materials: 5. review of mixer types. *Journal of Agricultural Engineering Research*, 59(3):145–161, 1994.
- [73] J. Novosad. Studies on granular materials i. kinematics of granular materials mixed by a mechanical impeller. *Collections of Czechoslovak Chemical Communications*, 29:2681–2696, 1964.
- [74] J. Novosad. Studies on granular materials ii. apparatus for measuring the dynamic angle of internal and external friction of granular materials. *Collections of Czechoslovak Chemical Communications*, 29:2697–2701, 1964.
- [75] J. Novosad. Studies on granular materials iii. stress distribution in a granular material mixed by a mechanical impeller. *Collections of Czechoslovak Chemical Communications*, 29:2702–2709, 1964.
- [76] J. Novosad. Studies on granular materials v. experimental determination of movement of granular materials mixed by a mechanical impeller. *Collections of Czechoslovak Chemical Communications*, 33:4164–4171, 1968.
- [77] J. Novosad and G. Standart. Studies on granular materials iv. calculation of the shaft torque for mixing granular materials. *Collections of Czechoslovak Chemical Communications*, 30:3247–3264, 1965.
- [78] J.M. Olinger, P.R. Griffiths, and T. Burger. Theory of diffuse reflection in the NIR region. In D.A. Burns and E.W. Ciurczak, editors, *Handbook of Near-Infrared Analysis*, volume 27 of *Practical Spectroscopy Series*, chapter 3, pages 19–51. Marcel Dekker, 2 edition, 2001.

- [79] United Nations Industrial Development Organization. UNIDO Industrial Statistics Database - 3. <http://www.unido.org/index.php?id=o3533>, 2004.
- [80] D.J. Parker, A.E. Dijkstra, T.W. Martin, and J.P.K. Seville. Positron emission particle tracking studies of spherical particle motion in rotating drums. *Chemical Engineering Science*, 53:2011–2022, 1997.
- [81] L. Pernenkil and C.L. Cooney. A review on the continuous blending of powders. *Chemical Engineering Science*, 62(2):720–742, 2006.
- [82] K.R. Poole, R.F. Taylor, and G.P. Wall. Mixing powders to fine-scale homogeneity: Studies of batch mixing. *Transactions of the Institution of Chemical Engineers*, 42:T305–T315, 1964.
- [83] K.R. Poole, R.F. Taylor, and G.P. Wall. Mixing powders to fine-scale homogeneity: Studies of continuous mixing. *Transactions of the Institution of Chemical Engineers*, 43:T261–T271, 1965.
- [84] M. Porter. *The Competitive Advantage of Nations*. Free Press, 1990.
- [85] M. Poux, P. Fayolle, J. Bertrand, D. Bridoux, and J. Bousquet. Powder mixing: some practical rules applied to agitated systems. *Powder Technology*, 68(3):213–234, 1991.
- [86] M. Poux, J.O. Mouton, R. Faure, and D. Steimetz. Measurement of the voidage in a ploughshare mixer by a capacitive sensor. *Powder Technology*, 103(1):65–70, 1999.
- [87] C.K. Prahalad and Y.L. Doz. *The Multinational mission: Balancing Local Demands and Global Vision*. Free Press, 1987.
- [88] C.D. Rielly, D.L.O. Smith, and J.A. Lindley. Mixing processes for agricultural and food materials. *Journal of Agricultural Research*, 59(1):1–18, 1994.
- [89] H. Saftlas and W. Diller. Industry surveys healthcare: Pharmaceuticals. Standard and Poor’s Market Insight, 2007.

- [90] Y.P. Segonne, C.L. Briens, J.M. Chabagno, and J. Bousquet. Assessment of agitation and detection of deposits in mechanical solids mixers. *Powder Technology*, 116(1):69–75, 2001.
- [91] R.G. Sherritt, J. Chaouki, A.K. Mehrotra, and L.A. Behie. Axial dispersion in three-dimensional mixing of particles in a rotating drum reactor. *Chemical Engineering Science*, 58(2):401–415, 2003.
- [92] Y. Shi and M. Gregory. International manufacturing networks - to develop global competitive capabilities. *Journal of Operations Management*, 16:195–214, 1998.
- [93] K. Sommer. Mechanisms of powder mixing and demixing. *IChemE Symposium Series*, 65:S1/A/1–S1/A/19, 1981.
- [94] N. Sommier, P. Porion, P. Evesque, B. Leclerc, P. Tchoreloff, and G. Couarraze. Magnetic resonance imaging investigation of the mixing-segregation process in a pharmaceutical blender. *International Journal of Pharmaceutics*, 222(2):243–258, 2001.
- [95] K. Stange. Die mischgüte einer zufallsmischung als grundlage zur beurteilung von mischversuchen. *Chemie Ingenieur Technik*, 26(6):331–337, 1954.
- [96] O.S. Sudah, A.W. Chester, J.A. Kowalski, J.W. Beeckman, and F.J. Muzzio. Quantitative characterization of mixing processes in rotary calciners. *Powder Technology*, 126(2):166–173, 2002.
- [97] Datamonitor USA. Datamonitor industry profiles. Ref. Code. 0116-0372, 2007.
- [98] G.J. Vergote, T.R.M. DeBeer, C. Vervaet, J.P. Remon, W.R.G. Baeyens, N. Diericx, and F. Verpoort. In-line monitoring of a pharmaceutical blending process using ft-raman spectroscopy. *European Journal of Pharmaceutical Sciences*, 21(4):479–485, 2004.

- [99] R. Vernon. International investment and international trade in the product cycle. *Quarterly Journal of Economics*, 80(2):190–207, 1966.
- [100] R. Vernon. The product cycle hypothesis in a new international environment. *Oxford Bulletin of Economics and Statistics*, 41(4):255–267, 1979.
- [101] D. Weber, Y. Pu, and C.L. Cooney. Investigation of the interactions between magnesium stearate, microcrystalline cellulose and steel using atomic force microscopy. *submitted*, July 2005.
- [102] S.S. Weidenbaum. Mixing of solids. In T.B. Drew and J. W. Hoopes, editors, *Advances in Chemical Engineering*, pages 211–253. Academic Press, 1958.
- [103] R. Weinekötter and H. Gericke. *Mixing of solids*. Kluwer, 2000.
- [104] R. Weinekötter and L. Reh. Continuous mixing of fine particles. *Particle and Particle Systems Characterization*, 12(1):46–53, 1995.
- [105] J.C. Williams. Continuous mixing of solids. a review. *Powder Technology*, 15(2):237–243, 1976.
- [106] J.C. Williams and M.A. Rahman. Prediction of the performance of continuous mixers for particulate solids using residence time distributions. part i. theoretical. *Powder Technology*, 5(2):87–92, 1971.
- [107] J.C. Williams and M.A. Rahman. Prediction of the performance of continuous mixers for particulate solids. part ii. experimental. *Powder Technology*, 5(5):307–316, 1972.
- [108] J.J. Workman. NIR spectroscopy calibration basics. In D.A. Burns and E.W. Ciurczak, editors, *Handbook of Near-Infrared Analysis*, volume 27 of *Practical Spectroscopy Series*, chapter 6, pages 91–127. Marcel Dekker, 2 edition, 2001.
- [109] G.R. Ziegler and C.A. Aguilar. Residence time distribution in a co-rotating, twin-screw continuous mixer by the step change method. *Journal of Food Engineering*, 59(2-3):161–167, 2003.